Non-linear control and stabilization of VSC-HVDC transmission systems

Haitham Saad Mohamed Ramadan

THÈSE DE DOCTORAT

Présentée pour obtenir

Le GRADE de DOCTEUR EN SCIENCES
DE L'UNIVERSITE PARIS SUD XI

Spécialité : Génie Electrique - Automatique

Par

Haitham Saad MOHAMED RAMADAN

Sujet :

NON-LINEAR CONTROL AND STABILIZATION OF VSC-HVDC TRANSMISSION SYSTEMS

Commande Non Linéaire et Stabilisation des Systèmes
de Transmission VSC-HVDC

Soutenance le jeudi 15 mars 2012 à 14:00 devant les membres du jury :

M. Yvon BESANGER	GRENOBLE-INP	Professeur des universités (Rapporteur)
M. Demba DIALLO	LGEP	Professeur des universités (Président)
M. Xavier GUILLAUD	EC-LILLE	Professeur des universités (Rapporteur)
M. Robert KACZMAREK	SUPELEC	Professeur (Directeur de thèse)
M. Dimitri LEFEBVRE	Université du HAVRE	Professeur des universités (Examinateur)
M. Marc PETIT	SUPELEC	Professeur adjoint (Co-directeur de thèse)
Mme. Houria SIGUERDIDJANE	SUPELEC	Professeur (Co-directeur de thèse)

Dedication

I dedicate this dissertation to my wonderful family. Particularly to my loving mother, Amal, and my late father, Saad, who have helped so much and have given me their fullest support. I thank my understanding and patient wife, Asmaa, who has put up with these many years of research, and to our precious son, Saad, and our pretty daughter, Syrine, who are the joy of our lives. Finally, I dedicate this work to my brother, Hesham, my sisters, Rania, Rehan, Lamiaa and Manar, my grandmother, Fatma, my uncle, Shoukry all of whom believed in diligence, science, and the pursuit of academic excellence.

Acknowledgements

This dissertation contains the results attained during my PhD at SUPELEC during the years 2007-2011. Four years at SUPELEC have been the time of my life. In addition to the wonderful environment for pursuing advancement in engineering and technology, the professors and students are extraordinary. I am grateful for graduating from SUPELEC. There are of course a group of people who made this possible and I would like to express my thanks to them.

First of all, my thanks for the accomplishment of this study are directed to Prof. Jean-Claude VANNIER, Head of the Electrical Power and Energy Systems at SUPELEC, for his continuous and endless patience, extreme support and encouragement. I feel lucky to have landed in his department for about four years as a PhD student and I am looking forward to continuing our collaborations.

I am much in debt to Prof. Patrick BOUCHER, Head of the Automatic Control Department at SUPELEC, for hosting me in his teamwork and for his wonderful welcoming, his efforts keeping me on track and for giving me valuable advice.

My appreciation and thanks to the generosity of my advisor, Prof. Houria SIGUERDIDJANE, Professor in Automatic Control Department at SUPELEC, her constant encouragement has helped me to do lot of work which I would not have achieved otherwise. Her constant guidance, support and continuous interest in my work made me achieve this goal. This work would not have been possible without her vision and advice. I thank her for giving me enough space and freedom for exploring new things.

I am very grateful to my co-advisor, Dr. Marc PETIT, Associate Professor in Electrical Power and Energy Systems Department at SUPELEC.

His guidance helps me in strengthening my background of Electric Power Systems and directs me to the prominent research topic in this field. A major part of this work would not have been possible without his help, his guidance and support.

Prof. Robert KACZMAREK, Professor in Electrical Power and Energy Systems Department at SUPELEC, deserve particular recognition. He has also played a great role in shaping and supporting this research direction.

In addition, my appreciation are expressed to all the thesis committee members, including Prof. Demba DIALLO, Prof. Dimitri LEFEBVRE, Prof. Xavier GUILLAUD, and Prof. Yvon BESANGER, who provide me thoughtful questions, helpful comments and valuable advices.

I take this opportunity to convey my sincere thanks to Stephanie DOUESNARD, Josiane DARTRON, and all the administrative staff I have met in SUPELEC, ED-STITS and CESAL for their efforts, cooperation and friendly feelings.

I feel lucky being able to work with my colleagues in both Electrical Power and Energy Systems, and Automatic Control Departments at SUPELEC. Many friends and colleagues have helped me in the process, particularly Pierre LEFRANC for his valuable guidance, and encouragement in addition to Hicham BENLOUKLI, Adel BETTAYEB, Tamim CHALATI, Xavier JANNOT, Alaa DIB, Christophe GUTFRIND, Jing DAI, Benjamin DAGUSE, Nathalie SAKER, Ziyad FAROUH, Mohamed EBRAHEEM, Mohamed ELGOHARI, Amr ISMAIL, Mohamed TARAFAYA, Safaa MAHER and Ali JAAFAR for painstakingly proofreading my initial versions of this thesis specially in preparing the French Résumé of the thesis.

This research would not be possible without the generous scholarship from the Egyptian Government which offers me four years grant to accomplish my PhD research. Therefore, I would like to express my deep thanks for all the staff of the Egyptian cultural office in Paris especially Prof. Amal EL-SABBAN, Prof. Camelia SOBHI, Prof. Emad ELSHERBINY, Prof. Cherif KHATER, Mrs. Hanan ELSHARKAWY, Mrs. Mona ISMAIL, and Mrs. Marwa NAFEI for their attention, efforts, and kind communications.

List of Publications

Journal Papers:

[1] Ramadan H. S., Siguerdidjane H., Petit M., and Kaczmarek R., *"Performance enhancement and robustness assessment of VSC-HVDC transmission systems controllers under uncertainties"*, International Journal of Electrical Power and Energy Systems, IJEPES, Vol. 35 (1), pp. 34-46, February 2012.

[2] Ramadan H. S., Siguerdidjane H., Petit M., and Kaczmarek R., *"VSC-HVDC systems stabilization via robust nonlinear sliding mode control"*, Journal of Electric Power Systems Research, JEPSR, 2010. (Under Review)

Conference Papers:

[3] Ramadan H. S., Siguerdidjane H., Petit M., and Kaczmarek R., "Nonlinear control based sliding modes for HVDC Light system behavioral enhancement under parameters uncertainties", In Proc. of 7^{th} International Conference on Electrical Engineering, ICEENG-7, Cairo, Egypt, 2010.

[4] Ramadan H. S., Siguerdidjane H., Petit M., and Kaczmarek R., "VSC-HVDC systems stabilization and robustness realization using sliding mode controllers", In Proc. of International Conference on Renewable Energy: Generation and Applications, ICREGA'10, Al Ain, UAE, 2010.

[5] Ramadan H. S., Siguerdidjane H., and Petit M., "A robust stabilizing nonlinear control design for VSC-HVDC systems: a comparative study", In Proc. of IEEE International Conference of Industrial Technology, ICIT, Gippsland, Australia, 2009.

[6] Ramadan H. S., Siguerdidjane H., and Petit M., "Robust nonlinear control strategy for HVDC Light transmission systems technology", In Proc. of 34^{th} Annual Conference of the IEEE Industrial Electronics Society, IECON, Orlando, USA, 2008.

[7] Ramadan H. S., Siguerdidjane H., and Petit M., "Robust VSC-HVDC systems based on sliding mode control", In Proc. of 2^{nd} International Conference on Electrical Engineering Design and Technologies, ICEEDT, Hammamet, Tunis, 2008.

[8] Ramadan H. S., Siguerdidjane H., and Petit M., "On the robustness of VSC-HVDC systems controllers under parameters uncertainties", In Proc. of 40^{th} North American Power Symposium, NAPS, Calgary, Canada, 2008.

Nomenclature

AC: Alternating Current

AI: Artificial Intelligence

AOT: Asymptotic Output Tracking

BJT: Bipolar Junction Transistor

CSC: Current Source Converter

D: Load damping coefficient of the generator rotor in pu torque/(rad $\sec^{-1}$)

DC: Direct Current

$DFIG$: Doubly Fed Induction Generator

$D-Q$: Direct and Quadrature rotating frame

$d-q$: Direct and Quadrature rotating frame

DTC: Direct Torque Control

EMF: Electromagnetic Field

$E_q^{'}$: Transient EMF in the quadrature axis

FL: Feedback Linearization

FLC: Fuzzy Logic Control

FOC: Field Oriented Control

FRT: Fault Ride Through

GG: Generator-Generator

GL: Generator-Load

GTO: Gate Turn-off

H: Inertia constant of the generator rotor in sec

$HVAC$: High Voltage Alternating Current

$HVDC$: High Voltage Direct Current

IC: Initial Condition

$IGBT$: Isolated Gate Bipolar Transistor

NOMENCLATURE

IMC: Internal Model Control

i_d: Direct axis component of the armature current

i_f: Field current

i_{kd}: Current in the direct axis damper windings

i_{kq}: Current in the quadrature axis damper windings

i_q: Quadrature axis component of the armature current

LCC: Line Commutated Converter

LMI: Linear Matrix Inequality

LTI: Linear Time Invariant

NN: Neural Networks

$NorNed$: HVDC submarine cable between Norway and Netherlands

OHL: Over Head Lines

P: Active power in MW

PID: Proportional Integral Derivative

PLL: Phase Locked Loop

$PMSG$: Permanent Magnet Synchronous Generator

POD: Power Oscillation Damping

PWM: Pulse Width Modulation

Q: Reactive Power in MVars

RE: Renewable Energy

R_a: Armature windings resistance

R_f: Field windings resistance

R_{kd}: Direct axis damper windings resistance

R_{kq}: Quadrature axis damper windings resistance

R_{tl}: Transmission line series resistance

R_{tr}: the transformer windings resistance

SMC: Sliding Mode Control

$SMIB$: Single Machine Infinite Bus

STV: Stochastic Time Variation

T_{em}: Generator electromagnetic torque

TM: Trade Mark

TSO: Transmission System Operator

UGC: Under Ground Cable

V_{DC}: DC Voltage

VSC: Voltage Source Converter

VSS: Variable Structure System

V_{alt}: Generator terminal voltage

V_f: Field voltage

V_t: Terminal voltage of the busbar

V_d^{∞}: Direct axis component of the infinite bus voltage

V_q^{∞}: Quadrature axis component of the infinite bus voltage

WE: Wind Energy

WP: Wind Plant

WTG: Wind Turbine Generator

X_{ad}: Direct axis mutual inductive reactance

X_{aq}: Quadrature axis mutual inductive reactance

X_d: Direct axis self inductive reactance

X_{fd}: Field windings inductive reactance

X_{kd}: Direct axis damper windings inductive reactance

X_{kq}: Quadrature axis damper windings inductive reactance

X_q: Quadrature axis self inductive reactance

X_{tl}: Transmission line series inductive reactance

X_{tr}: Transformer windings leakage inductive reactance

$2DOF$: Two Degrees of Freedom

Δ: Variation of a signal

δ_{HVDC}: Angle of the generator rotor calculated in the VSC side

δ_r: Angle of the generator rotor mass in radians

ω_o: Synchronous angular frequency in rad/sec

ω_r: Slip angular frequency in rad/sec

©: CopyRight

Contents

List of Figures

List of Tables

Résumé

Introduction

LES besoins en énergie électrique sont en croissance constante, et les infrastructures – basées sur des réseaux de transport interconnectés et maillés – arrivent peu à peu en limite de leurs capacités. Le recours à de nouveaux moyens de production et le besoin de construire des infrastructures pour acheminer cette énergie permet de nouvelles opportunités.

L'énergie électrique est aujourd'hui produite, transportée et distribuée en courant alternatif (AC). Ce choix tient à quelques raisons majeures : la simplicité de production (les alternateurs sont plus simples et plus fiables que les générateurs à courant continu (DC)) ainsi que la facilité de changer de niveau de tension à l'aide de transformateurs.

Cependant, la maîtrise des transferts d'énergie en courant alternatif pose, dans les réseaux denses, des problèmes de plus en plus difficile à résoudre :

- la répartition des transits d'énergie dans les diverses branches des réseaux maillés se fait suivant des lois physiques et ne peuvent pas être maîtrisés facilement ;
- la puissance réactive doit être compensée au plus près de sa consommation afin de limiter les pertes et les chutes de tension ;
- les réglages de la fréquence des alternateurs interconnectés doivent être coordonnés.

Le courant continu pose aussi des problèmes : sa production nécessite le redressement des ondes de courant alternatif et le changement de tension ne peut se concevoir qu'au moyen de dispositifs complexes. Dans l'un et l'autre cas, le recours à une électronique de puissance très coûteuse s'avère nécessaire.

Le problème de la coupure du courant continu est techniquement résolu mais au prix de procédés sophistiqués et chers. Par ailleur, il y a des situations dans lesquelles le courant continu est plus intéressant que le courant alternatif.

HVDC

Un système de transmission à courant continu haute tension (HVDC) est un équipement d'électronique de puissance utilisé pour la transmission de l'électricité en courant continu haute tension.

Une liaison à courant continu est constituée d'une ligne à courant continu reliant au moins deux réseaux alternatifs par l'intermédiaire de stations de conversion. Une liaison HVDC est, la plupart du temps, insérée dans un système de transmission en courant alternatif. Elle est donc constituée de trois éléments :

1. un redresseur ;
2. une ligne de transmission ;
3. un onduleur.

Généralement, le redresseur et l'onduleur sont symétriques et réversibles (ils peuvent échanger leur rôle). Historiquement, le redresseur et l'onduleur ont d'abord été réalisés avec des soupapes à vapeur de mercure. Récemment, ils sont majoritairement réalisés avec des thyristors, quelques fois avec du transistor bipolaire à grille isolée (IGBT).

Ces systèmes de transmission de l'énergie électrique sont utilisés pour trois principales raisons :

- **Transporter des puissances sur de longues distances** :

  Le HVDC permet de transporter, sur de longues distances, des puissances souvent supérieures à 1000 MW. Il est dans ce cas technico-économiquement préférable d'utiliser du courant continu plutôt qu'alternatif classique (HVAC). Le coût élevé de l'électronique de puissance est compensé par deux avantages décisifs :

  – deux conducteurs sont nécessaires au lieu de trois en tension alternative (ou un conducteur seul, si l'on utilise la terre ou l'eau de mer comme deuxième conducteur), ce qui peut compenser le surcoût pour des liaisons longues ;

– au-delà d'une certaine distance, (50 à 100 km environ pour des liaisons sous-terraines ou sous-marines, 500 à 1000 km pour les lignes électriques aériennes), l'importance de courant capacitif rend peu intéressant le transport d'électricité en courant alternatif.

En 2012, la plus longue liaison HVDC du monde, sous le nom Rio Madeira (environ 2500 km), reliera l'Amazonas et la zone du Sao Paulo en Brésil.

La réalisation de liaisons sous-marines par câble sur de longues distances (typiquement plus de 50 km) en courant alternatif impose de compenser l'effet capacitif des câbles, faute de quoi la tension de ce câble est mal contrôlée. À cet effet, on installe dans les liaisons classiques des réactances de compensation à des points intermédiaires (postes électriques) de la liaison.

Dans une liaison sous-marine, on ne peut pas envisager un poste électrique à un point intermédiaire (sous la mer). En courant continu, cet effet capacitif n'existe pas, et justifie l'utilisation des HVDC pour ce type de liaison. De futures grandes installations offshore pourront ainsi mieux exporter leur courant électrique.

- **Transporter des puissances entre des reseaux électriques non synchrones :**

  Interconnecter des réseaux électriques non synchrones ou présentant des fréquences différentes (50 Hz ou 60 Hz dans la presque totalité des cas) nécessite un dispositif spécifique, et un HVDC est la réponse la plus courante. Par exemple, l'Arabie saoudite et le Japon utilisent les deux fréquences.

  Le projet d'interconnexion des pays du golfe Arabique, majoritairement en 50 Hz, prévoit une liaison HVDC de 1800 MW avec ce pays. C'est aussi le cas de la France et du Royaume-Uni, qui bien que tous deux à 50 Hz, ne sont pas considérés comme synchrones.

- **Contrôler du flux de puissance :**

  Le troisième intérêt des HVDC est le pilotage du flux de puissance entre deux parties d'un réseau électrique. Les équipements HVDC destinés à cette application ne comportent généralement pas de ligne de transmission, et les deux extrémités sont sur le même site : on parle du HVDC de type *back to back*. Dans certains cas ces équipements peuvent être en parallèle avec une liaison alternative.

En fait une grande partie des HVDC en service dans le monde sont des *back to back*. Des grands pays, comme la Chine, l'Inde, les États-Unis par exemple, présentent plusieurs ≪ régions électriques ≫ difficilement interconnectables entre elles, bien que à la même fréquence.

Contexte

La croissance continue de la demande d'électricité exige l'expansion continue des plans pour augmenter la capacité de production, la capacité de transport, et à promouvoir l'interconnexion des régions qui sont parfois séparées par de longues distances. La nécessité de transmettre l'énergie à travers la mer est très commun ainsi que l'interconnexion de systèmes asynchrones de différentes fréquences. Ceci suppose de trouver des systèmes techniquement et économiquement réalisables afin d'assurer la stabilité et de garantir un bon échange d'énergie. Dans un réseau de transport AC, les écarts angulaires entre les tensions aux extrémités d'un ligne influencent de la puissance transmise. Cet écart affecte la stabilité du réseau.

La transmission d'énergie électrique en utilisant des câbles sous-marins est limitée aux courtes distances dans le cas de HVAC en raison de la haute capacité diélectrique des câbles, et par conséquent, des reactances shunt de compensation sont nécessaires pour limiter la distance efficace de transmission [1, 2]. L'interconnexion directe des réseaux AC asynchrones est impossible via des liens HVAC.

Ces restrictions ont nécessité la recherche des solutions alternatives, qui, avec les développements technologiques et les progrès en électronique de puissance ont permis de progresser dans la transmission d'énergie électrique [1]. En conséquence, les systèmes de transmission HVDC ont émergé. En résultat, les actions économiques et technologiques pour revigorer le marché de l'énergie ont été fournies. Moins cher et plus des interconnexions efficaces ont été réalisées.

En outre, les systèmes de transmission HVDC ont permi d'interconnecter facilement des réseaux où la tension et la fréquence ne sont pas compatibles ou quand il y a des obstacles géographiques tel que les mers, ou les océans, ou les montagnes [1, 3, 4, 5, 6].

L'énergie renouvelable est constamment innovée dans le nouveau marché mondial. Bien que les centres de production d'électricité renouvelable soient souvent loin des points de consommation, la transmission d'énergie avec des pertes minimales doit être assurée. Dans le cas des sources de production renouvelables éolien offshore, il est nécessaire de transmettre de grandes quantités d'énergie avec un rendument satisfisant. A cet effet, plusieurs projets utilisant les technologies HVDC en combinaison avec des énergies renouvelables sont en cours de développement en particulier via des câbles sous-marins [7, 8, 9, 10].

Pour les raisons environnementales, techniques et économiques, l'installation de lignes HVDC est favorisée afin de maximiser l'efficacité de transmission d'électricité. Par conséquent, les cinq dernières décennies ont témoigné un développement significatif des systèmes de transmission HVDC. La technologie HVDC s'est notamment développée pour :

- Interconnecter les zones éloignées pour faciliter les échanges d'énergies (NorNed : le plus long câble HVDC sous-marin du monde opérationnel) ;
- Raccorder des parcs éolien offshore ;
- Acheminer de l'énergie hydro éloignée.

La plupart de ces systèmes sont basés sur les convertisseurs de source de courant (CSC) utilisant la technologie de thyristor. Les défauts de cette technologie de transmission sont l'absorption de la puissance réactive dans le système, l'existence des harmoniques ainsi que la valve, thyristor, ne peut pas être commuté en position ouverte en pilotant directement la grille. Cela limite la portée de son application [11].

Récemment, un avancement rapide et considerable est réalisé dans le domaine des dispositifs d'électroniques de puissance qui peuvent non seulement mettre active mais aussi désactive immédiatement, comme IGBT. Cela ouvre des possibilités pour l'industrie de l'énergie via l'utilisation du HVDC basé sur les convertisseurs de source de tension (VSC) avec la technologie IGBT qui est commercialisé sous le nom HVDC Light^{TM} par ABB. Siemens propose également la variante VSC-HVDC, proposé par le nom commercial HVDC Plus^{TM} [12, 13, 14, 15, 16]. Grâce aux valves électroniques IGBT, ces technologies innovantes montrent des avantages techniques et économiques plus considérables que les systèmes conventionnels de transmission CSC-HVDC.

RESUME

La technologie VSC-HVDC offre des avantages compétitifs pour les systèmes d'énergie actuels comme :

- L'échange des puissances active et réactive peut être contrôlée de manière flexible et indépendante ;
- Aucun problème de défaut de commutation ;
- Aucun communication est requise entre les stations interconnectées [11, 15].

Actuellement, le problème de la stabilisation des systèmes de transmission VSC-HVDC a attiré l'attention de la communauté d'énergie et aussi d'automatique. La conception de contrôleurs PI classique considère habituellement une condition de fonctionnement unique du système. Dans ce type de contrôleurs, le *feedback* est fixe et il amplifie l'erreur de contrôle qui détermine à son tour la valeur du signal d'entrée u (sortie du contrôleur) du système. La conception du contrôleur est traitée de la même manière pour les différentes conditions de fonctionnement. Ce contrôleur simple ne fonctionne souvent que dans une gamme de fonctionnement limité.

Les incertitudes paramétriques (principalement à cause d'une mauvaise précision des valeurs de paramètres ou des perturbations) font apparaitre un changement des conditions de fonctionnement. Donc, un faible amortissement indésirable ou même des oscillations instables peuvent être entraînées. Les paramètres de contrôleurs produisent un amortissement satisfaisant et améliorent la comportement dynamique des systèmes pour une condition de fonctionnement ne pouvant plus fournir l'amortissement suffisant pour les autres conditions.

Par conséquent, on peut considérer que les contrôleurs de type PI sont les plus simples pour les systèmes complexes non linéaires et dynamiques. Toutefois, dans certaines circonstances, les contrôleurs traditionnels PI avec des valeurs de gain fixe qui sont utilisés pour les systèmes de transmission VSC-HVDC produisent souvent une instabilité des systèmes [17, 18, 19, 20]. Ces contrôles de *feedback* classiques (celles qui sont facilement réglé manuellement) sont généralement appliqués aux systèmes sans incertitudes.

Bien que les contrôleurs réglés par les approches de conception conventionnelles soient simples, le manque de robustesse de ce type de contrôleurs n'est pas le seul problème rencontré.

Les procédures traditionnelles deviennent longues et difficiles à mettre en œuvre notamment dans les cas où : différents contrôleurs doivent être coordonnés, la coordination doit être réalisée pour une variété de conditions de fonctionnement, et pour des performances spécifiques à satisfaire. Par conséquent, pour surmonter les problèmes indésirables qui pourraient être rencontrées par les contrôleurs PI classiques mises au point avec le changement des conditions de fonctionnement et pour garantir la stabilité des systèmes, différentes approches pour la conception de contrôleurs robustes et les structures de contrôle adaptatif ont été proposées.

La présence des non-linéarités larges dans la dynamique du système VSC-HVDC rend les modèles linéarisés inadéquats pour la conception de contrôleur, une situation qui motive l'utilisation des techniques de commandes non linéaire [21]. Ainsi, un grand nombre de contrôleur pour des systèmes de transmission HVDC basé sur des techniques de contrôle différentes ont été proposées pour améliorer les systèmes transitoires et la stabilité dynamique [22, 23].

Des contrôleurs décentralisés, des structures de contrôle robuste, des lois de commandes adaptatives et des contrôleurs non-linéaires basés sur des techniques de contrôle intelligents tels que la logique floue et les réseaux de neurones (NN) ont été appliquées pour contrôler le HVDC [24, 25, 26].

Faire une revue de littérature disponible dans le contrôle DC adaptatif n'est pas très pertinent car il y a eu peu de travaux dans le cas de perturbations de grande amplitude. Ainsi, le contrôle adaptatif peut être non seulement inefficace, mais aussi peut dégrader la performance plutôt que l'améliorer [24, 25, 26].

En outre, les autres techniques de contrôle non linéaires tels que le linéarisation *feedback* [27, 28, 29], les techniques hamiltonien [30, 31], l'approache fondée sur la passivité [32], des perturbations singulières [33] ont été appliquées avec succès pour atteindre un niveau élevé de performance dynamique, en particulier en cas d'incertitudes paramétriques, ou les événements de contingences larges et inattendues [27].

De même, la commande par modes glissants (SMC) est une technique pour améliorer la robustesse du système sous des incertitudes paramétriques et/ou des perturbations exogènes [34, 35, 36]. Cette méthode de contrôle avancée (à base de modèle), agit efficacement sur les performances de contrôle de trajectoire pour les systèmes stochastiques (incertain ou mal défini).

La commande de type SMC représente un degré de stabilité raisonable. Elle a été démontré la capacité à amortir les oscillations en plus sa robustesse en présence des incertitudes paramétriques et/ou de bruit pour les systèmes non linéaires. Ainsi, ce type de commande, qui a attiré un certain nombre de recherches, est explicitement robuste en faveur de son insensibilité aux changements de topologie et/ou des paramètres. En outre, la méthode du suivi asymptotique d'une trajectoire de référence des sorties (AOT) est utilisée comme un contrôleur non-linéaire alternatif pour tels systèmes. La robustesse adéquate des contrôleurs AOT est vérifiée.

Etat de l'Art

Afin de surmonter les difficultés lors des conditions anormales de fonctionnement en particulier sous des incertitudes paramétriques, des perturbations et des défauts, l'utilisation des techniques de contrôle avancées telles que la commande robuste, adaptative, optimale et les commandes basées sur l'intelligence artificielle (AI) ont été élaborés pour améliorer la stabilité transitoire des systèmes énergétiques [27].

Ces approches non-linéaires ont été parmi des domaines les plus prometteurs d'applications de contrôle automatique [27]. Chacune de ces méthodes a été utilisée pour élaborer des contrôleurs non-linéaires pour les systèmes incertains, caractérisés par un manque de connaissance complète des caractéristiques dynamiques du système [37, 38, 39].

Dans [40], Reeve et al. (1994) ont proposé la commande adaptative par séquencement de gains pour les systèmes HVDC afin d'accommoder des perturbations larges. Dash et al. (1999) [24] ont étudié la performance de la liaison *point to point* HVDC en utilisant un tuner flou. Une méthode du tuner flou basé sur une fonction d'énergie pour le réglage des paramètres de contrôleurs d'un système de transmission HVDC a été présentée. Le lien DC a été exposé aux diverses perturbations (petites et grandes) pour examiner l'efficacité de la technique concernée. L'erreur de courant DC et sa dérivée ont été utilisés comme les deux signaux principaux pour générer le changement des gains PI du régulateur du courant du redresseur selon une base de règles floues. Les résultats des simulations ont confirmé la supériorité des régulateurs flous adaptatifs sur les contrôleurs classiques de gain fixe dans l'amortissement des oscillations transitoires du HVDC connectant des systèmes AC faibles.

Une fois de plus, comme expliqué dans [41], Dash et al. (1999) ont développé une stratégie de commande basée sur *Fuzzy Logic Control*(FLC) pour le système HVDC de type *point to point*. L'approche de FLC s'est élevée pour supprimer la non-linéarité dans le système de transmission non-linéaire HVDC, de sorte les dynamiques de la boucle fermée deviennent sous une forme linéaire. Avant l'application de cette commande, les paramètres basiques du modèle ont été identifiés par la formation d'un combineur adaptatif linéaire (adaline). Après l'élaboration du modèle mathématique d'une boucle fermée, l'action de contrôle peut être directement exprimée comme une fonction de l'erreur. En se basant sur les résultats obtenus, la supériorité de ces contrôleurs sur les commandes classiques a été affichée.

Thomas et al. (2001) [42] ont introduit une synthèse de contrôleurs non-linéaires pour les systèmes de transmission VSC-HVDC dans des conditions d'un réseau équilibré afin de mettre en évidence les dynamiques rapides et lentes respectivement associées aux boucles de contrôle de courant ainsi que la tension DC.

Durrant et al. (2003) ont proposé dans [43] une méthode basée sur un contrôleur de découplage à chaque station de conversion pour contrôler le système VSC. Cette méthode a utilisé le *feedback* rapide pour linéariser, découpler et simplifier la dynamique de *feedback* pour les courants (d-q). Les références des entrées de commande (courants d-q) ont été utilisées par la suite pour la mise en œuvre des stratégies de contrôle P-V (ou P-Q, ou V_{DC}-Q) au niveau supérieur de contrôle.

Ensuite, Durrant et al. (2004) ont décrit une conception de contrôleur basée sur l'inégalité matricielle linéaire (LMI) pour les systèmes VSC-HVDC a été robuste au cours d'une série de points de fonctionnement tel que démontré dans [44]. Toutefois, la conception de contrôleur non-linéaire basée sur LMI a été complexe. Ainsi, sa mise en œuvre est défavorable.

Ruan et al. (2007) [11] ont suggéré le contrôle *Feedback Linearization* (FL) pour le système VSC-HVDC. Un modèle d'espace d'état du système a été premièrement développé et ensuite a été transformé en axe (d-q) du châssis synchrone tournant. Selon ce modèle, la relation de correspondance entre les deux entrées de commande et les deux variables contrôlées de chaque station a été déterminée. En utilisant le contrôle FL, la tension de lien DC a été gouvernée et les puissances active et réactive ont été contrôlées. La validité du modèle d'espace d'état et de la stratégie de contrôle proposé a été vérifiée à amortir les oscillations du système et améliorer le niveau de sa stabilité.

Des meilleures performances ont été obtenues avec cette commande basée sur FL par rapport au contrôle traditionnel.

De nouveau, Ruan et al. (2007) [45] ont appliqué un contrôle adaptatif de *backstepping* dans le châssis synchrone pour améliorer les performances du comportement dynamique des systèmes VSC-HVDC. Les incertitudes paramétriques telles que le changement des impédances de la ligne AC ont été prises en compte dans le design. Pour un système d'ordre élevé, les lois finales de contrôle ont été dérivées, étape par étape via des fonctions de Lyapunov appropriées. Ainsi, le processus de design n'est pas si complexe. La performance de contrôle a été comparée avec celle du contrôle linéaire. L'efficacité des contrôleurs adaptatifs proposés a été démontrée par des études de simulation numérique sur un système de transmission VSC-HVDC. Ces contrôleurs contribuent de manière significative pour améliorer le comportement dynamique des systèmes VSC-HVDC sous une large gamme de conditions de fonctionnement.

Jovcic et al. (2007) ont examiné un système de contrôle approprié pour un système de transmission de courant continu basé sur VSC [46]. Chacun des deux convertisseurs VSC a deux entrées de contrôle et quatre canaux de contrôle sur un système de transmission VSC pour offrir un contrôle polyvalent. Toutefois, le défi principal a été l'interaction dynamique entre les boucles de régulation. La stabilité globale du système et sa robustesse satisfaisants ont été réalisées avec deux boucles fermées à gain élevé, un à chaque convertisseur.

Les deux boucles de contrôle peuvent être conçus en utilisant un modèle approprié MATLAB^{TM}, à la suite de la méthode du lieu des racines '*Root Locus*' et les indicateurs de robustesse. Le meilleur *feedback* rapide de stabilisation du côté redresseur a été trouvée à être une composante en quadrature de tension, qui complément le *feedback* de tension DC à gain élevé du côté onduleur.

Le contrôleur lent comporte trois boucles de contrôle de régulation PI utilisant comme signaux de retour : la tension AC du côté redresseur, la tension AC du côté onduleur et la puissance DC du côté redresseur. Le contrôle de transmission VSC en présence des conditions de défaut a été examiné avec un contrôleur indépendant jusqu'aux niveaux de courants de défaut. La commande de défaut contrôle les courants locaux de défaut DC à chaque convertisseur. Ce type de contrôleurs a été examiné pour des petits échelons en entrées et des scénarios de défaut typique des côtés AC et DC pour confirmer la performance de conception du contrôleur.

Pandey et al. (2009) ont présenté la conception des contrôleurs à auto-réglage pour des systèmes HVDC à deux extrémités [47]. Les contrôleurs ont été formulés en utilisant un nouveau model de convertisseur à temps discret basé sur l'échantillonnage à taux multiple. Le contrôleur du courant du côté de redresseur a été conçu pour traiter tout changement du courant du côté investisseur comme la perturbation déterministe agissante sur le système. Afin d'estimer le courant du côté d'investisseur, un observateur de suppression de bruit dynamique a été conçu qui nécessite seulement la mesure des paramètres au côté redresseur. Les dynamiques globales du système dépendent des dynamiques du contrôleur et d'observateur. L'investigation de la boucle fermée d'un contrôleur à autoréglage a été plutôt difficile, et l'inclusion des dynamiques d'observateur peuvent la rendre plus difficile. La performance de ces contrôleurs a été analysé à travers des simulations numériques détaillées sous une variété de perturbations larges. La modélisation adéquate des systèmes de transmission VSC-HVDC peut ouvrir la voie à leur utilisation efficace pour améliorer la stabilité transitoire, l'amortissement des oscillations de l'angle de puissance ainsi que la commande de la synchronisation de puissance [48, 49, 50].

Dans [48], Cole et al. (2008) ont proposé un modèle générique du VSC-HVDC afin d'étudier la stabilité de la tension et de l'angle du système. Le compromise nécessaire entre le respect de détail, de l'effort de modélisation, de la vitesse de simulation, et les données ont été considérées dans la modélisation des systèmes VSC-HVDC. Le modèle déduit a basé sur 'coupled current injectors' qui permettent l'implémentation facile dans la plupart des programmes commerciales de stabilité. Les simulations ont été exécutées pour montrer le comportement dynamique de la liaison HVDC dans un système simple.

De nouveau, Cole et al. (2011) ont conçu deux modèles dynamiques standards du VSC-HVDC pour étudier la stabilité du système [49]. Le modèle complet du système, composé du convertisseur et ses contrôleurs, les équations du circuit DC et les équations de couplage, a été dérivée mathématiquement. Le filtre AC et la boucle à verrouillage de phase (PLL), souvent négligé dans la modélisation du VSC-HVDC, ont été considérés. Par ailleurs, un modèle d'ordre réduit a été déduit du modèle complet en négligeant les constantes de temps les plus petites. Par conséquent, les auteurs ont présenté un ensemble réduit d'équations différentielles qui peuvent être intégrées avec une phase de temps plus grande.

Les modèles ont été mis en œuvre dans le programme de stabilité du MATLAB (MatDyn). Les résultats des simulations ont confirmé que le modèle complet répond de manière satisfaisante et que le modèle réduit peut être utilisé afin d'étudier des systèmes des dynamiques d'ordre inférieur.

Zhang et al. (2009) [50] ont vérifié que la commande de synchronisation de puissance est particulièrement applicable aux systèmes de transmission VSC-HVDC raccordés aux systèmes faibles de courant alternatif. Ils ont étudiés le contrôle de *feedback* multivariable afin de contrôler la synchronisation de puissance. Deux approches de conception différentes sont proposées : le contrôle des modèles internes (IMC) et la commande basée sur H^{∞}. Les deux approches ont été comparées par rapport à leurs performance dynamique, robustesse et simplicité.

Intégration des Eolienne dans les Réseaux Electriques

La proposition de la commission européenne d'atteindre 20% d'électricité d'origine renouvelable d'ici 2020 ouvre la voie à une expansion massive de la filière éolienne. Pour atteindre cet objectif, l'intégration des éoliennes à grande échelle devra se faire onshore, mais surtout offshore. La connexion de ces sites offshore représente alors des défis intéressants pour les gestionnaires de réseaux électriques nécessitant de nouvelles méthodes pour concevoir et exploiter le système [51, 52, 53]. Cela passe notamment par la mise en place de réseaux à technologie continu qui seront ensuite raccordés aux réseaux alternatifs.

Ce raccordement se fait par l'intermédiaire de convertisseurs utilisant la technologie VSC-HVDC. Cette technologie combine la flexibilité, la capacité de transmission, la contrôlabilité et l'opérabilité nécessaire par les exigences techniques et commerciales. L'éolien offshore favorise la technologie " machine synchrone à aimants permanents " pour laquelle le parc est connecté au réseau principal à l'aide d'un système de transmission VSC, Il n'y a alors pas de lien direct entre les machines et le réseau principal AC. Il en résulte plusieurs avantages techniques et économiques pour les gestionnaires du système de transport (TSOs), les développeurs et les fabricants de parc éolien.

Du point de vue des TSO, le convertisseur VSC coté réseau peut être directement relié à un centre de contrôle pour le pilotage des puissances active et réactive. En outre, le bus continu limite la propagation des perturbations du réseau vers l'éolienne (et vice-et-versa).

Par conséquent, il y a une réduction des contraintes mécaniques sur les éoliennes, ces contraintes étant reportées sur les convertisseurs de puissance. Les principales caractéristiques du système de transmission VSC-HVDC à grande échelle de l'énergie éolienne offshore sont :

- Le VSC-HVDC peut répondre aux recommandations du *grid code* ;
- Les éoliennes n'ont plus besoin d'être conçu pour satisfaire le *grid code*, l'optimisation peut se concentrer sur le coût, l'efficacité et la robustesse ;
- Le VSC-HVDC permet de découpler le parc éolien du réseau AC pour réduire la propagation des perturbations ;
- Le VSC-HVDC permet de contrôler la tension au point de raccordement et de éventuellement de participer au réglage de la fréquence. Ainsi, il peut être utilisé pour améliorer le niveau de la stabilité du réseau AC.

Ces dernières années, de nombreux travaux ont été dédiés au contrôle des parcs éoliens, et de leur intégration dans le réseau électrique. Deux situations sont rencontrées :

– Commande des convertisseurs VSC d'une éolienne asynchrone à double alimentation (DFIG) ;

– Commande des convertisseurs VSC d'une éolienne synchrone à aimants permanents (PMSG).

L'impact du contrôle du VSC-HVDC sur les performances dynamiques de parcs éoliens offshore pendant des régimes permanant et/ou des régimes transitoires ont été présentés dans la littérature.

Mahi et al. (2007) [54] ont proposée une stratégie de contrôle direct de couple (DTC) pour la machine de type DFIG d'une éolienne à vitesse variable. Les lois de commande non linéaires sont formulées pour fournir la référence de couple, et ainsi réduire l'erreur de la trajectoire de puissance électrique produite. L'approche DTC a été utilisée au lieu du contrôle classique à flux orienté (FOC). Cette technique de contrôle a montrée la dépendance plus faible vis-à-vis des paramètres du système, en plus sa simplicité relative d'implémentation.

La combinaison de la loi de contrôle multivariable puissante avec la commande de type DTC a garanti la bonne performance, ainsi que la robustesse contre les perturbations diverses.

Dans [55], Boukhezzar et al. (2009) ont conçu le contrôleur non linéaire en cascade pour une éolienne à vitesse variable de type DFIG. L'objectif principal de ce contrôleur est la capture optimale de l'énergie éolienne en dessous de la zone de puissance nominale. Des nouvelles structures de contrôle, même pour le DFIG et la partie mécanique (aeroturbine) ont été introduites afin d'éviter certains inconvénients des méthodes de contrôle existants. La commande globale a été composée de deux contrôleurs en cascade. Le premier concerne l'aeroturbine, tandis que le second concerne le DFIG. Ces contrôleurs ont été conçus en considérant l'aspect dynamique de la turbine éolienne, la non-linéarité du comportement de l'aérodynamique ainsi que la nature turbulente du vent. En utilisant la commande proposée, les résultats de simulation ont garanti l'amélioration de la performance du point de vue de l'efficacité avec des charges transitoires ainsi que son implémentation plus simple par rapport à certaines stratégies de contrôleur existantes.

Wang et al. (2011) [56] ont décrit l'utilisation de la technologie du VSC-HVDC pour atténuer les fluctuations de puissance crées par les parcs éoliens basé sur les machines de type DFIG. Un contrôle vectoriel à flux statorique orienté afin de capturer une énergie éolienne maximale a été présenté. Le contrôle indépendant de la puissance active et réactive a été réalisé. L'efficacité du contrôle de l'énergie éolienne en captant l'énergie maximale du vent a été également remplie. En outre, la stratégie de la coordination de contrôle entre les parcs éoliens et le système VSC-HVDC a été présentée. La régulation rapide de la puissance active et de la puissance réactive du système VSC-HVDC a maintenu la puissance d'injection du système AC une valeur stable, selon les besoins du système. Les résultats de simulation ont vérifié la pertinence de la stratégie de contrôle proposée afin d'atténuer les fluctuations de puissance de sortie [56].

Muyeen et al. (2010) [57] ont présenté les stratégies de fonctionnement et le contrôle du parc éolien offshore interconnecté aux systèmes HVDC. Le parc éolien offshore composé d'aérogénérateurs à vitesse variable avec de type PMSG a été considéré dans cette étude. Le système de transmission HVDC basée sur un point neutre à trois niveaux du VSC a été utilisé pour l'interconnexion entre le parc éolien offshore et le réseau onshore.

Une modélisation globale du système en proposant des stratégies de contrôle a été élaborée. Un contrôleur simple basé sur la logique floue a été adoptée dans la station offshore du VSC. Les réponses dynamique et transitoire du système ont été étudiées en considérant les données réelles de la vitesse du vent [56, 57, 58, 59, 60].

Zhao et al. (2011) [58] ont introduit la structure de raccordement DC du parc éolien basé sur le PMSG. Selon le système du VSC-HVDC, la topologie de type série-parallèle des unités de production DC a été proposée. La tension continue a été contrôlée au niveau du générateur afin d'atteindre l'objectif de la série-parallèle. Côté réseau, une méthode de découplage des puissances active et réactive a été appliquée pour suivre la puissance maximale en contrôlant les courants *d-q* du réseau. Les modèles du système de générateur unique, de connexion série et parallèle ont été établis. Les résultats des simulations ont mis en évidence l'efficacité de la stratégie de commande présentée [58].

Enfin, Nguyen et al. (2011) [60] ont étudié l'évaluation de la stabilité pour les systèmes de transmission VSC-HVDC lorsqu'ils sont appliqués à grande échelle. Des stratégies de contrôle ont été proposées pour permettre une intégration des grands parcs éoliens offshore dans le réseau électrique en minimisant les situations critiques et pour garantir la stabilité requise. Par conséquent, la capacité de ces systèmes complexes à supporter de défauts sur le réseau a été évaluée. Ainsi, différentes stratégies de contrôle ont été proposées pour le VSC-HVDC. Les résultats de simulation ont été évalués en analysant le temps de réponse et la fiabilité de la stratégie de contrôle [60].

Dans cette thèse, des contrôleurs conventionnels de type PI et des techniques de commandes non-linéaires avancées telles que AOT ou SMC ont été appliquées sur les systèmes de transmission VSC-HVDC. Les approches non-linéaires de type AOT et SMC, simples et robustes, fournissent explicitement une amélioration des performances du comportement dynamique et d'une élévation du niveau de la stabilité du système même en présence des incertitudes paramétriques et/ou des perturbations.

Ainsi, une étude intéressante afin d'améliorer la performance dynamique du système nommé *Single Machine via VSC-HVDC* (SM via VSC-HVDC) et d'amortir les oscillations de l'angle de puissance en utilisant la commande classique PI est introduite en présence des défauts. Le principal avantage de ce type du contrôle est sa simplicité.

Objectifs de la Thèse

L'objectif de cette thèse est d'étudier la stabilisation, les commandes non-linéaires et l'amélioration des performances dynamiques des systèmes de transmission VSC-HVDC sous les incertitudes paramétriques, telles que les fluctuations des paramètres de câbles DC ou de lignes AC, et/ou des perturbations (défauts).

D'une part, les contrôleurs à *feedback* non-linéaires basés sur les techniques AOT et SMC sont respectivement utilisés pour atteindre ce but grâce à leur robustesse aux incertitudes paramétriques et les perturbations exogènes. Ces approches de commandes avancées, basés sur des systèmes de structures variables (VSS), ont la capacité à contrôler un système non-linéaire en présence des incertitudes associées à l'estimation des paramètres et la modélisation des erreurs. Ils fournissent, avant tout, la robustesse de performance ainsi que la simplicité des procédures de conception de commandes.

Premièrement, les modèles mathématiques d'espace d'états du système de transmission VSC-HVDC, qui relient soit générateur-charge (GL) or générateur-générateur (GG) où le flux de puissance est unidirectionnel ou bidirectionnel respectivement, sont développés. Pour les systèmes GL VSC-HVDC, les contrôleurs conventionnels PI sont appliqués. Puis, des signaux non-linéaires de commandes basés sur AOT et SMC sont formulés pour les systèmes GG VSC-HVDC. Les puissances réactives aux côtés AC des deux VSCs sont contrôlées vers leurs valeurs de référence spécifiées. Les valeurs favorables de consigne sont nulles afin d'atteindre un facteur de puissance d'unité. En outre, la puissance active au coté AC d'un VSC et la tension DC sur l'autre convertisseur sont régies à leurs valeurs nominales. Par conséquent, la puissance transmise est contrôlée adéquatement. La chute de tension et la perte de puissance dans le lien DC sont prises en considération. En conséquence, la stabilisation globale et l'amélioration de performance des systèmes en présence des incertitudes paramétriques, sont effectués. La robustesse de commandes conventionnelle et non-linéaire proposées est évaluée.

En utilisant MATLAB®, les résultats vérifient d'une manière significative que les commandes robustes désirées basées sur AOT et SMC peuvent fournir une performance favorable de trajectoire, et contribuent efficacement à l'amélioration du comportement dynamique des systèmes, dans les conditions normaux de fonctionnement ou en présence des incertitudes paramétriques telle que la variation de paramètres de câble DC pour différent longueurs de liens DC.

De ce fait, les commandes non-linéaires robustes proposées peuvent constituer un bon candidat pour résoudre une variété de problèmes pratiques des systèmes VSC-HVDC notamment en présence des variations de paramètres de liens DC.

D'autre part, le système de transmission GG VSC-HVDC est remplacé par un nouveau système équivalent nommé SM via VSC-HVDC. Après la modélisation analytique du système, le contrôleur conventionnel PI est appliqué au niveau du convertisseur afin d'améliorer la stabilité transitoire du système et pour amortir les oscillations de l'angle de rotor du générateur synchrone.

Contributions de la Thèse

Cette thèse comporte deux parties principales. Dans la première, les contrôleurs conventionnel et non-linéaire ainsi la stabilisation de systèmes de transmissions VSC-HVDC sont réalisées. Deux systèmes différents, GL VSC-HVDC et GG VSC-HVDC, sont étudiés. Quant à l'existence d'incertitudes paramétriques, le modèle physique du système de transmission VSC-HVDC est explicitement discuté. Ensuite, les modèles mathématiques d'espace d'états des deux systèmes de transmission, dont le flux de puissance est respectivement unidirectionnel et bidirectionnel, sont élaborés selon des expressions relativement simples pour évaluer la réponse du système en régime permanent et transitoire dans les réseaux d'énergie. Puisque les incertitudes paramétriques sont associées au fonctionnement du système, des différentes méthodologies de commandes non-linéaires sont appliquées afin de contourner des situations anormales.

Pour les système GL VSC-HVDC, les contrôleurs conventionnel PID sont conçus pour réduire l'impact des incertitudes paramétriques et perturbations sur les performances dynamiques du système. Les actions de commandes générées sont directement exprimées comme une fonction de l'erreur, ses dérivés ou intégrales. Les commandes conventionnelles proposées garantissent une performance acceptable de trajectoire quand les paramètres du régulateur PID sont choisies de manière appropriée. Après le choix convenable des gains de réglage afin d'obtenir une réponse adéquate, les commandes classiques sont vérifiées afin d'être efficaces en gérant la tension DC ainsi en contrôlent les puissances réactive indépendamment et d'une manière flexible.

La puissance réactive est contrôlée vers sa valeur de reference à l'extrémité AC de VSC du système GL VSC-HVDC. Pour obtenir un facteur de puissance d'unité, la valeur de référence de la puissance réactive est fixée à zéro. En contrôlant les puissances réactives Q dans le cas de N convertisseurs connectés à un même réseau DC, (N-1) convertisseurs sont pilotés en puissance active P et le N^{eme} pilote la tension de bus DC.

Les résultats de simulation confirment que les contrôleurs traditionnels proposés fournissent des niveaux adéquates de stabilité dans certains points de fonctionnement. Le temps de réponse et le comportement dynamique du système peuvent encore être améliorées par l'optimisation des gains de réglage. L'évaluation de la robustesse des contrôleurs est misee en évidence en présence d'incertitudes paramétriques telles que des variations de résistance de câble DC et des changements de réactance de ligne AC. Ainsi, le comportement dynamique et les performances de trajectoire sont obtenus même avec des changements de consigne. Une robustesse acceptable et une performance suffisante sont réalisées. L'analyse du système avec un PID est très simple mais sa conception peut être délicate, car il n'existe pas de méthode unique pour résoudre ce problème. Il faut trouver des compromis, le régulateur idéal n'existe pas. En général on se fixe un cahier des charges à respecter sur la robustesse, le dépassement et le temps d'établissement du régime stationnaire. Parfois, les performances d'un PID peuvent devenir insuffisantes en raison de la présence du non-linéarité du système ou d'un retard trop important dans le modèle, on fait alors appel à d'autres algorithmes de réglage.

Pour les systèmes de transmission GG VSC-HVDC, les commandes de *feedback* basées sur différentes commandes telles que AOT et SMC sont déduites. L'élaboration des deux contrôleurs AOT et SMC est relativement simple et claire parce que les lois non-linéaires des commandes résultantes sont dérivées étape par étape. La technique de commande basée sur SMC appliquée au système garantie la réalisation de robustesse et la performance de trajectoire en utilisant la théorie de Lyapunov.

En considérant les commandes basées sur la theorie de VSS, les puissances active et réactive d'une extrimettees AC du VSC sont contrôlées en utilisant directement leurs signaux de référence. Egalement, la tension DC et la puissance réactive de l'autre convertisseur VSC sont gérées. En effet, la chute de tension dans le lien DC, les pertes et la direction de flux de puissances sont prises en compte. Par conséquent, la commande non-linéaire SMC est capable d'atteindre le but désiré.

Considérant les incertitudes paramétriques des réseaux électriques telles que les fluctuations de resistance du câble DC, les variations de réactance de ligne AC et les changements de signaux de référence, la robustesse du contrôleur conçu et sa performance dynamique sont évaluées.

Les résultats de simulation montrent explicitement la robustesse inhérente des contrôleurs sous les incertitudes paramétriques pour différent longueurs de câbles DC. En plus, la stabilité du système et son comportement dynamique sont renforcés en utilisant les contrôleurs non-linéaires proposés notamment en présence des variations de résistance du câble DC.

Le problème de *chattering* est un inconvénient majeur des commandes de type AOT et SMC. Donc, la nécessité d'avoir des transitions douces significatives ainsi un comportement dynamique sans *chattering* est prise en considération notamment pour l'élaboration de la commande non-linéaire SMC. Par conséquent, le phénomène de *chattering* qui apparait en utilisant la commande SMC peut être surmonté en proposant des fonctions continues telles que la fonction saturation ou la fonction hyperbolique au lieu de la fonction sigmoïde discontinu.

Dans le cas d'un système GG VSC-HVDC dans lequel les deux réseaux AC sont interconnectés par des liens de courant continu, des commandes basées sur AOT et SMC sont utilisées afin de contrôler les puissances réactives sur les côtés AC de deux convertisseurs du HVDC, pour maintenir la puissance active au terminal envoyant AC du VSC à sa valeur de consigne, et pour gouverner les tensions continues sur le ligne DC raccordant les deux stations AC. En considérant les différentes distances séparant les postes AC ainsi que les variations de la référence de puissance active de $\pm 20\%$ chacun, ces commandes non-linéaires garantient efficacement d'erreur statique du trajectoire égale à zéro même en présence de variation de la référence de puissance active notamment avec des incertitudes paramétriques telles que les variations de résistance du câble DC.

Les figures (1) et (2) illustrent la capacité de la commande basée sur SMC en considerant ces perturbations. Dans la figure (1), bien que les longueurs de liaison DC varient, le comportement des puissances réactives rest toujours à zéro. Un facteur de puissance d'unité sur les côtés AC des convertisseurs VSC sont obtenus sous la variation de la référence de la puissance active envoyée et avec l'incertitudes paramétriques de l'impédance de la liaison DC.

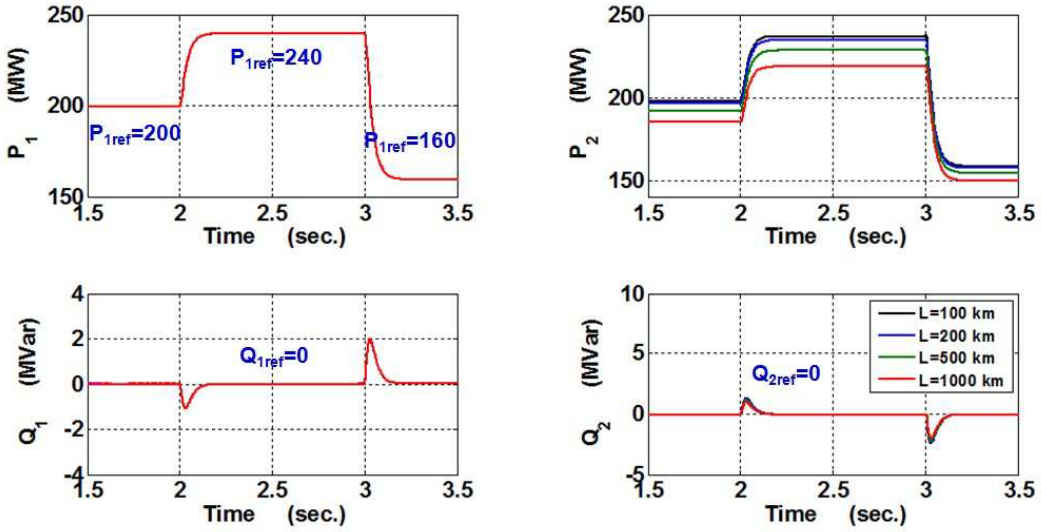

Figure 1: Les comportements dynamiques des puissances active et réactive sur les cotées AC des convertisseurs en utilisant la commande basée sur SMC.

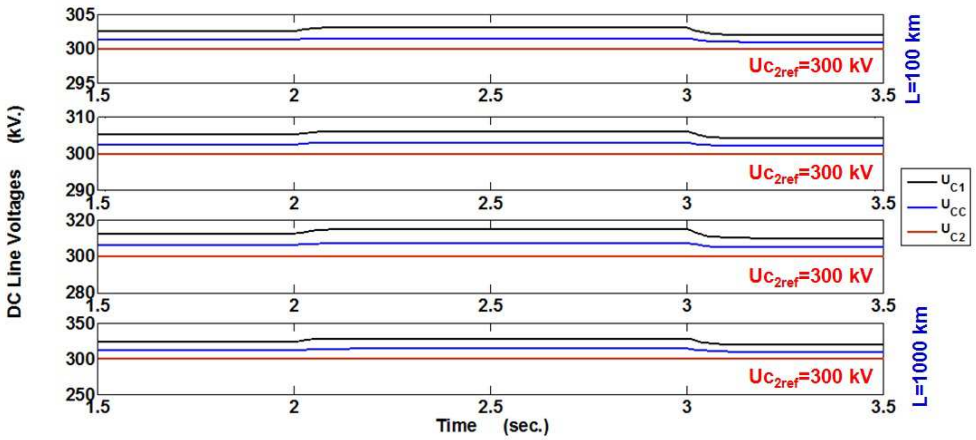

Figure 2: Les comportements des tensions DC en considèrant des différentes longueurs de liaison DCen utilisant la commande basée sur SMC.

La puissance active à la borne d'envoi AC suit parfaitement sa valeur nominale pour la première periode pour toutes les longueurs considérées. Des écarts acceptables résultent par rapport à la puissance nominale dans les periodes suivantes. Le temps de stabilisation peut être géré en augmentant les gains de réglage des contrôleurs jusqu'à la réalisation d'un temps de réponse adéquat avec un niveau de dépassement convenable inférieur à 15%.

Dans la figure (2), des tensions admissibles de courant continues (U_{C1}, U_{C2} et U_{CC}) sont atteints pour les différentes longueurs de liaison DC. U_{C2} est à sa valeur nominale de 300 kV pour toutes les longueurs proposées de liaison DC. Pour ces longueurs de liaison DC, les valeurs estimées des U_{CC} et U_{C1} sont effectées en raison de la chute de tension du lien qui ne reste pas constant. Simplement, la résistance de la liaison DC varie proportionnelle à sa longueur. La plus longe des liaisons DC voient les chutes de tension plus élevées. Par conséquent, les valeurs supérieures de U_{CC} et U_{C1} sont révélées.

Explicitement, l'approche de la commande non linéaire basée sur SMC peut être considérée comme une méthode de contrôle efficace et sans *chattering* surtout avec la sélection appropriée des gains de réglage.

Elle fournit l'amortissement signifiant d'oscillations et diminue le temps de convergence. Par conséquent, elle peut être avantageusement utilisé non seulement lors de conditions normales d'exploitation, mais aussi pour de longueurs différentes de liaison DC afin d'améliorer les performances dynamiques du système.

La deuxième partie fournit une contribution substantielle pour ma thèse. Elle vise à étudier l'influence de la commande du VSC-HVDC sur l'amélioration de la performance dynamique du réseau de courant alternatif au cours de défauts. Le modèle mathématique du système SM via VSC-HVDC proposé est initialement réalisé. Ensuite, le contrôleur conventionnel PI est appliqué au niveau du convertisseur du système pour agir sur les oscillations de l'angle de puissance (POD) de la machine synchrone ; puis pour améliorer son comportement dynamique lors de défauts.

Les résultats de simulation vérifient la possibilité de l'utilisation de la commande classique PI, qui sont relativement simples à mettre en œuvre, pour asservir la tension ou l'angle au niveau du convertisseur afin de garantir une amélioration acceptable des performances dynamiques du système ; ainsi pour l'amortissement des oscillations de l'angle de puissance de la machine synchrone.

Pour l'amortissement des oscillations de l'angle du rotor de la machine synchrone dans le système SM via VSC-HVDC, le système peut-être contrôlé en ajustant l'angle ou l'amplitude de la tension au niveau de convertisseur VSC. Puis, les composantes *d-q* de la tension sur le côté VSC sont asservies. Par conséquent, deux approches basées sur les contrôleurs PI sont proposées :

- La première approche consiste à ajuster d'une manière continue la valeur du $V_{d_{(ref)}}^{\infty}$ en considérant une référence constante de la puissance active sur le côté du convertisseur. On calcule alors la quantité du ΔV_d^{∞} qui permet l'asservissement de la valeur du $V_{d_{(ref)}}^{\infty}$. Le cas d'étude de base est réalisé pour ΔV_d^{∞}=0 ;
- La deuxième approche a basée sur le control de la valeur du $V_{d_{(ref)}}^{\infty}$ en cas de la variation du $P_{HVDC(ref)}$. En effet, la valeur du ΔP_{HVDC} estimée à partir du $\Delta\delta_{HVDC}$ est considérée dans la boucle de régulateur PI.

La Figure (3) représente le comportement dynamique des angles de puissance au niveau du convertisseur et de la machine asynchrone (δ_{HVDC} et δ_r) dans le cas de base de SM via VSC-HVDC en présence du défaut. Les gains du contrôleur PI (K_p et K_i) utilisés pour la régulation de la référence de la composant directe de la tension au niveau de convertisseur $V_{d_{(ref)}}^{\infty}$ sont choisis comme ($0,005$ et 4), respectivement. Il est intéressant de comparer les réponses des δ_{HVDC} et δ_r. Le temps de stabilisation du δ_{HVDC} est plus court et son amplitude est plus faible comparé au temps de réponse du δ_r. En régime permanent, δ_r=δ_{HVDC}.

La figure (4) illustre l'impact du contrôle du $V_{d_{(ref)}}^{\infty}$ sur les performances dynamiques de l'angle du rotor du générateur synchrone δ_r. L'angle du rotor est estimé par l'intégration de la vitesse du rotor de la machine. Le comportement dynamique est étudié avec et sans considération de l'effet du ΔV_d^{∞} en asserviront $V_{d_{(ref)}}^{\infty}$.

La figure (5) montre l'impact de contrôler la valeur du $P_{HVDC(ref)}$ sur l'amélioration de la réponse dynamique de l'angle du rotor de la machine. En augmentant la valeur du K_p, on obtient un comportement dynamique plus stable, mieux amorti et avec de temps de stabilisation plus court par rapport au scénario du cas de base.

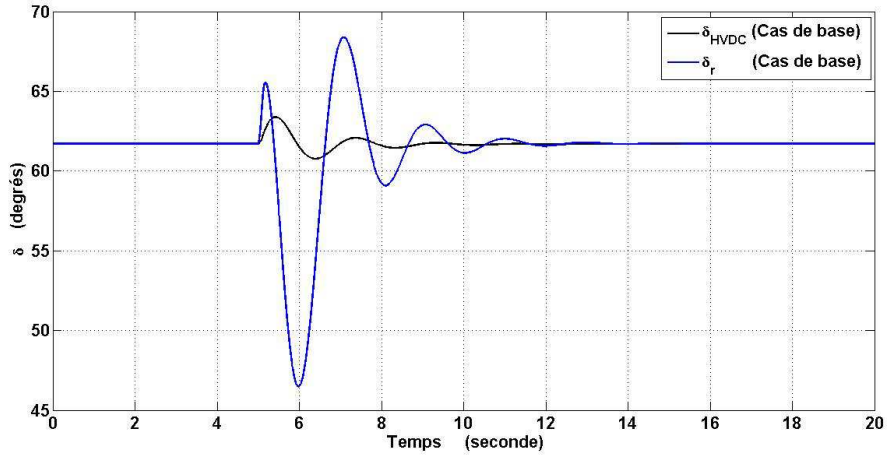

Figure 3: Le comportement dynamique des angles δ_r et δ_{HVDC} dans le cas de base du système SM via VSC-HVDC en présence d'un défaut à t=5 secondes (R_{fault}=10 Ω et t_{fault}=120 msecondes).

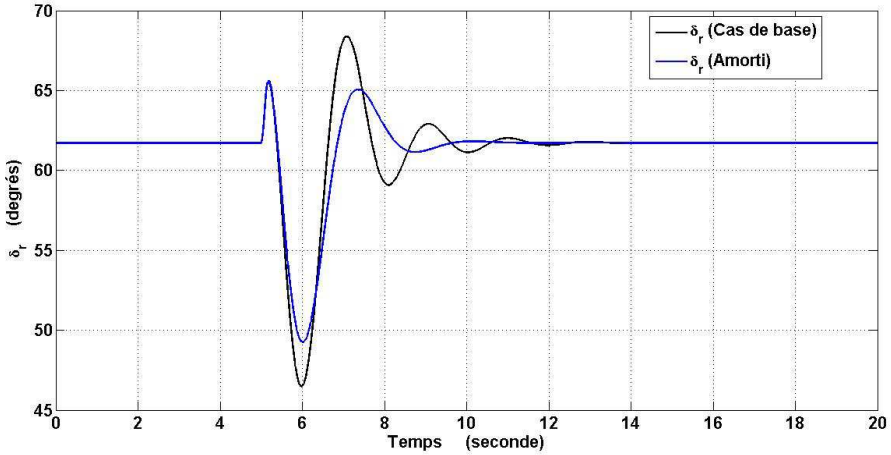

Figure 4: La réponse dynamique de l'angle du rotor de la machine synchrone δ_r en contrôlant $V_{d(ref)}^{\infty}$ avec une commande classique PI (K_p = 0.005, K_i = 4) en présence d'un défaut à t=5 secondes (R_{fault}=10 Ω et t_{fault}=120 msecondes).

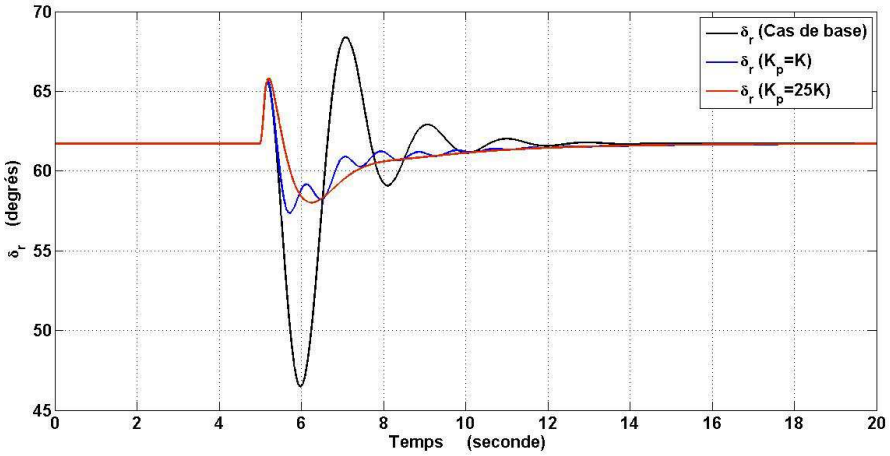

Figure 5: Le comportement dynamique de l'angle du rotor de la machine synchrone δ_r en contrôlant $P_{HVDC_{(ref)}}$ avec une commande classique PI ($K_p = 0.005$, $K_i = 4$) en présence d'un défaut à t=5 secondes (R_{fault}=10 Ω et t_{fault}=120 msecondes).

Donc, on peut constater l'efficacité du contrôle du fonctionnement du générateur synchrone, l'amélioration de sa performance dynamique et l'amortissement des oscillations de l'angle de puissance en ajustant la valeur et l'angle de la tension au niveau du convertisseur avec un contrôle classique PI intégré dans les deux approches proposées.

Grandes Lignes de Thèse

Après l'introduction, le chapitre 1 introduit brièvement un aperçu des systèmes de transmissions HVDC où un arrière-plan historique des principaux types des systèmes de transmissions d'énergie est présenté. Les aspects environnementaux, techniques et économiques des systèmes de transmissions HVDC sont explicités. Les avantages de la mise en œuvre des systèmes HVDC plutôt qu'utiliser des systèmes de transmissions HVAC sont exposés. Les configurations HVDC les plus récentes selon la technologie d'électronique de puissance et la catégorie de transmission sont montrées. Ensuite, l'intégration des éoliennes dans les réseaux électriques est introduite.

Le chapitre 2 fournie une brève définition des commandes non-linéaires robustes et adaptatives. Alors, un sommaire des différentes techniques modernes de ces commandes utilisées pour la stabilisation des systèmes est présenté.

Les raisons principales d'incertitudes paramétriques qui existaient dans les réseaux électriques sont clairement exposées. Ensuite, les concepts de base derrière l'élaboration de commandes non-linéaires SMC et AOT, basées sur la théorie de Lyapunov appliquées aux systèmes VSC-HVDC, sont mises en évidence par des dérivations mathématiques simples.

Dans le chapitre 3, le modèle mathématique du système de transmission VSC-HVDC, qui interconnecte le générateur-charge (GL) où le flux de puissance est unidirectionnel, est déduit. Pour les systèmes GL VSC-HVDC, la puissance est livrée du générateur vers la charge. En conséquence, les équations de l'espace d'états du système sont clairement développées. Les commandes conventionnelles linéaires de type PI sont introduites. Les résultats de simulation présentent l'efficacité de ces contrôleurs pour améliorer le comportement dynamique du système GL VSC-HVDC et pour renforcer son stabilité. D'ailleurs, la robustesse de ces commandes traditionnelles est interprétée en présence des incertitudes paramétriques telles que les variations de charge et/ou la réactance de ligne AC.

Ensuite, le modèle mathématique d'espace d'états du système VSC-HVDC, qui interconnecte le générateur-générateur (GG) où la puissance peut être transmise dans les deux sens, est développé. Les commandes non-linéaires basées sur AOT et SMC sont formulées et largement démontré. Pour les systèmes de transmissions VSC-HVDC des puissances élevées, les résultats de simulation et l'analyse qui mettent en évidence la robustesse des commandes non-linéaires proposées envers à la présence d'incertitudes paramétriques sont illustrés. Egalement, le comportement dynamique du système et son niveau de stabilité, en utilisant ces contrôleurs relativement simples, sont étudiés.

Le chapitre 5 présente un réseau AC piloté par un convertisseur VSC-HVDC pour un système de transmission GG VSC-HVDC. Pour une extrémité du réseau, le modèle mathématique du générateur synchrone est considéré au septième ordre afin de prendre en compte la dynamique du système. De l'autre extrémité, le réseau AC est représenté par un bus mais avec une tension fixe et un angle variable. Nous étudions l'influence de l'utilisation d'un régulateur PI conventionnel sur la puissance active ou la composante directe de la tension du terminal AC du convertisseur VSC afin d'amortir les oscillations de l'angle de puissance. Pour illustrer l'effet de ce contrôleur sur la stabilité globale, différentes conditions de fonctionnement du réseau sont étudiées notamment avec la présence de défauts.

Les résultats des simulations vérifient que la commande classique proposée du coté du convertisseur est capable d'amortir les oscillations de l'angle de puissance de la machine et d'améliorer le comportement dynamique du système, même sous les défauts.

Finalement, les conclusions principales et les contributions de cette thèse ainsi que les suggestions pour les directions de recherche dans le futur et les perspectives sont fournies.

Introduction

MODERN human society needs an ever-increasing supply of electrical power. Electrical power systems, which are very complex in nature, have been built to satisfy this increasing demand. The trend in electric power production is toward an interconnected network of transmission lines linking generators and loads into large integrated systems. Successful operation of a power system depends largely on its ability to provide reliable and uninterrupted service to the loads. Ideally, the loads must be continuously fed at constant voltage and frequency. A reliable service is to keep synchronous generators running in parallel and with adequate capacity to meet the load demand, and to maintain the power network's integrity. If a generator loses synchronism with the rest of the system, significant voltage and current fluctuations may occur. Then, transmission lines may be automatically tripped by their relays at undesired locations [21]. A major system's shock may lead to a loss of synchronism for one or more machines.

Context

The continued growth in electricity demand requires ongoing expansion plans to increase the generation capacity, transmission capability, and to promote the interconnection of regions that sometimes are separated by long distances. The need to transmit energy across the sea is very common as well as to interconnect asynchronous systems of different frequencies. This implies finding technically and economically feasible systems that ensure stability and provide proper exchange of energy. The power transfer in AC lines commonly depends on the angular difference between voltage phasors at both ends of the line. This angular difference varies with the AC line length and affects the system's stability.

The power transmission using submarine cables is limited to short distances in case of High Voltage Alternative Current (HVAC) due to high dielectric capacity cables. Therefore, compensating inductors are required for limiting the effective transmission distance [1, 2]. Direct interconnection of asynchronous AC systems is impossible via HVAC links. The foregoing limitations have been forced to seek alternative solutions, which with technological developments and advances in power electronics have enabled progress in power transmission [1]. Accordingly, the globalization process based on High Voltage Direct Current (HVDC) transmission systems has been emerged. As a consequence, economic and technological actions to invigorate the trade of energy have been provided. Cheaper and more efficient interconnections have been performed. Furthermore, HVDC transmission systems have assisted to overcome instability problems and to easily interconnect systems where voltage and frequency are not compatible or when there are geographic obstacles such as seas, or oceans, or mountains [1, 3, 4, 5, 6].

VSC-HVDC Technology Challenges

Due to environmental, technical and economical reasons, the installation of HVDC lines is favored in order to maximize the electric power transmission efficiency. As a result, the past five decades witnessed significant development in HVDC transmission systems. Most of these systems are based on Current Source Converters (CSC) utilizing thyristor technology. The shortcomings of this transmission technology are the system's reactive power absorbtion, the harmonic existence besides that its valve or thyristor cannot be turned off with gate signal directly. These drawbacks limit the range of its application [11].

Recently, rapid advancement is achieved in the field of power electronic devices which can not only switch on but also switch off immediately, such as Insulated Gate Bipolar Transistor (IGBT). That opens opportunities for the power industry via the utilization of HVDC based on Voltage Sourced Converters (VSC) with IGBT technology which is commercially known as HVDC Light^{TM} by ABB. Siemens also offers VSC-HVDC variant, commercialized as HVDC Plus^{TM} [12, 13, 14, 15, 16].

Owing to IGBT valves, this new innovative technology exhibits substantial technical and economical advantages over conventional CSC-based HVDC systems. VSC-HVDC transmission technology offers competitive benefits to today's power systems such as:

(i) Active and reactive power exchange can be controlled flexibly and independently;

(ii) No commutation failure problem;

(iii) No communication required between two interconnected stations [11, 15].

Lately, the problem of VSC-HVDC transmission system's stabilization has attracted renewed attention in both power systems and control communities. The design of conventional PI controllers usually considers a system's single operating condition. In this type of controllers, feedback is fixed and amplifies the control error which in turn determines the value of the input signal u (controller output) to the system. The controller design is processed in the same manner for different operating conditions. This simple controller often works only within a limited operating range.

In case of parameter uncertainties (mainly due to poor precision of parameters' values or disturbances), changed operating conditions, and/or faults, undesirable poorly damped or even unstable oscillations may result. More clearly, controller parameters yielding satisfactory damping and enhancing system's dynamic behavior for one operating condition may no longer provide sufficient damping for others. Therefore, it can be considered that the simplest yet controllers for complex nonlinear and dynamic systems are PI types. However, under certain circumstances, traditional PI controllers with fixed gain values which are used for VSC-HVDC transmission systems often cause system's instability [17, 18, 19, 20].

These classical feedback controls (those which are readily tuned manually) are usually applied to systems without uncertainties. Although controllers tuned by conventional design approach are simple, lack of robustness of that kind of controllers is not the only problem encountered.

Conventional procedures become time consuming and difficult to implement especially for cases in which: different controllers are to be coordinated, the coordination must be conducted for a variety of operating conditions, and certain performance specifications have to be satisfied. Consequently, to overcome the undesired problems probably encountered by PI conventionally tuned controllers under operating conditions' variations and to guarantee system stability, different robust controllers design and adaptive control structures have been proposed.

The presence of large nonlinearities in VSC-HVDC system dynamics make the linearized models inadequate for controller design, a situation that motivates the use of nonlinear control techniques [21]. This inherent non-linearity causes the design of appropriate controllers difficult under different normal and abnormal situations. Thus, a large number of HVDC controller schemes based on various control techniques have been proposed to improve the systems' transient and dynamic stability [22, 23]. Decentralized controllers, robust control structures, adaptive control laws, and nonlinear controllers based on Artificial Intelligent (AI) control techniques such as fuzzy logic and neural networks have been applied to HVDC control.

Elaborate literature available in DC adaptive control are not very conclusive for all practical situations because of the absence of insight into performance with large disturbances. Hence, the adaptive control not only may be ineffective, but also may degrade the performance rather than enhancing it [24, 25, 26]. In addition, other nonlinear control techniques such as Feedback Linearization (FL) [27, 28, 29], Hamiltonian techniques [30, 31], passivity-based approach [32], singular perturbations [33] have been successfully applied to achieve high dynamic performance especially under parameter uncertainties, or large and unexpected contingencies [27].

Likewise, Sliding Mode Control (SMC) is a technique for improving robustness under parameter uncertainties and exogenous disturbances [34, 35, 36]. SMC, an advanced (model-based) control method, efficiently acts if high performance motion control (such as trajectory tracking or model following) is required on stochastic (uncertain or ill defined) systems.

SMC performs better degree of stability and is capable to damp out the oscillations besides its robustness with respect to parameter variations and/or noise for nonlinear systems. In addition, SMC controller, which has attracted a number of researches, is explicitly robust in favor of its insensitivity to changes in both topology and parameters.

Furthermore, Asymptotic Output Tracking (AOT) approach has been used as an alternative nonlinear controller for such systems. The robustness of AOT controllers has been verified.

HVDC Nonlinear Control: State of the Art

To get rid of the difficulties during abnormal operating conditions particularly under parameter uncertainties, disturbances and faults, the use of advanced control techniques such as robust, adaptive, optimal, and artificial intelligence-based methods of control design to improve power systems transient stability has been of the most promising areas of automatic control applications [27]. Each of these methods has been used to design nonlinear controllers for uncertain systems, characterized by a lack of complete knowledge of systems' dynamic features [37, 38, 39].

In [40], Reeve et al. (1994) have tried gain scheduling adaptive control for HVDC systems to accommodate large disturbances.

Dash et al. (1999) [24] have studied the point to point HVDC link performance using a fuzzy tuner. An energy function based fuzzy tuning method for the controller parameters of an HVDC transmission link has been presented. The DC link was subjected to various small and large disturbances to examine the concerned technique effectiveness. The DC current error and its derivative have been used as the two principal signals to generate the change in the PI gains of the rectifier current regulator according to a fuzzy rule base. Computer simulation results have confirmed the adaptive fuzzy controllers superiority over the conventional fixed gain ones in damping out transient oscillations in HVDC links connected to weak AC systems.

Once more as explained in [41], Dash et al. (1999) have developed a simplified Fuzzy Logic Control (FLC) strategy for a point to point HVDC link. FLC approach has amounted to canceling the non-linearities in HVDC transmission systems. Thus, the closed-loop dynamics becomes in a linear form. Prior to the control application; the basic model parameters have been identified by training an adaptive linear combiner (adaline). After developing the closed loop mathematical model, the control action can directly be expressed as any function of the error. Based on the results, the superiority of such controllers over conventional ones has been displayed.

Thomas et al. (2001) [42] have introduced a nonlinear controller synthesis for VSC-HVDC systems under balanced network conditions to highlight fast and slow dynamics respectively associated with current control loops and DC bus voltage control loop.

Durrant et al. (2003) have proposed in [43] a method for controlling VSC transmission based on a decoupling controller at each converter station.

This method has used fast-feedback to linearize, decouple and simplify feedback dynamics for direct and quadrature (d-q) currents. The d-q current control reference inputs have been further used for implementing P-V (or P-Q, or V_{DC}-Q) control strategies at higher control level.

Yet again, Durrant et al. (2004) have designed a nonlinear controller design based on Linear Matrix Inequality (LMI) for VSC-HVDC. The controller was robust over a range of operating points [44]. However, LMI based nonlinear controller design was complex and complicated. Thus, its implementation is unfavorable.

Ruan et al. (2007) [11] have suggested Feedback Linearization (FL) control for VSC-HVDC transmission systems. A steady-state model of VSC-HVDC system has been initially developed, and then it has been transformed into d-q axis of the rotating synchronous frame. According to this model, the corresponding relationship between the two control inputs and the two controlled variables of each station has been determined. Using the FL control, DC link voltage has been governed and both active and reactive powers have been controlled. The proposed control strategy has been verified to damp system oscillations and to enhance system stability. Better performance has been attained compared to traditional control.

Again, Ruan et al. (2007) [45] have applied an adaptive backstepping control in synchronous frame to improve the dynamic behavior of VSC-HVDC systems. Parameter uncertainties such as the change of AC line impedances have been considered for controller's design. For the high-order system, feedback control laws have been derived step by step through suitable Lyapunov functions. Thus, the design process was not so complex. The control performance has been compared to those of linear control. The effectiveness of the proposed adaptive controller has been demonstrated for VSC-HVDC systems through digital simulation studies. These controllers significantly contribute to improve VSC-HVDC system dynamic behavior under wide range of operating conditions.

Jovcic et al. (2007) have investigated a suitable nonlinear control system for DC transmission systems based on VSC [46]. Each of the two VSC converters has two control inputs and four control channels on a VSC transmission system to offer potential for a versatile control. However, the main challenge has been the dynamic interaction among the control loops. The overall system stability and its satisfactory robustness have been verified with two high-gain feedback loops, one at each converter.

Both control loops can be designed using suitable MATLAB model, following the root locus rules and robustness indicators. The best fast stabilizing feedback at rectifier side has been found to be AC voltage quadrature component, which complements the high-gain DC voltage feedback at inverter side. The slow controller has consisted of three PI regulating control loops using the following feedback signals: AC voltage at rectifier side, AC voltage at inverter side, and DC power at rectifier side. VSC transmission control under fault conditions has been considered with a separate controller that takes over system control for fault-level currents. The fault controller regulates the local DC currents at each converter. This type of controllers has been tested for a wide range of small-signal step inputs and typical fault scenarios on AC and DC side to confirm the controller performance.

Pandey et al. (2009) have presented self-tuning controllers design for a two terminal HVDC link [47]. The controllers have been formulated utilizing a novel discrete-time converter model based on multi-rate sampling. The current controller at the rectifier terminal has been designed treating any change in the inverter end current as deterministic disturbance acting on the system. To estimate the inverter end current, a dynamic noise rejecting observer has been designed which requires the measurement of rectifier end quantities only. Overall system dynamics have depended on both controller and observer dynamics.

The closed loop investigation of a self-tuning controller was rather difficult, and the inclusion of the observer dynamics may further add to this difficulty. The controller performance has been tested through detailed nonlinear digital simulation under a variety of large disturbances.

Adequate modeling of VSC-HVDC transmission systems can pave the way for their effective utilization for enhancing the transient stability, damping power angle oscillations as well as power-synchronisation control [48, 49, 50].

In [48], Cole et al. (2008) have proposed a generic VSC-HVDC model for voltage and angle stability studies. The required trade-off between respect of detail, modeling effort, simulation speed, and data requirements has been considered in the modeling of VSC-HVDC systems. The deduced model has based on coupled current injectors which allow easy implementation in most commercial stability programs. Simulations have been performed to show the dynamic behavior of the modeled HVDC link in a simple system.

Then in [49], Cole et al. (2011) have designed two standard VSC-HVDC dynamic models for stability studies. The full system model, consisting of the converter and its controllers, DC circuit equations, and coupling equations, has been derived mathematically. The AC filter and Phase Locked Loop (PLL), often neglected in VSC-HVDC modeling, have been accounted. Furthermore, a reduced order model has been deduced from the full model by neglecting the smallest time constants. Consequently, a reduced set of differential equations that can be integrated with a larger time step has been presented. The models have been implemented in the MATLAB based stability program (MatDyn). Simulations have confirmed that the full model responds satisfactorily and that the reduced model can be used for lower order dynamics studies.

Zhang et al. (2009) [50] have verified that power-synchronization control is particularly applicable to VSC-HVDC systems connected to weak AC systems. The multivariable feedback design aspect of the power synchronization control has been investigated by two different design approaches: Internal Model Control (IMC) and H^{∞} control. Both approaches have been compared regarding their dynamic performance, robustness and simplicity.

Wind Energy Challenges

Global environmental concerns associated with conventional energy generation have led to the rapid growth of Wind Energy (WE) in power systems [61]. WE, a source of Renewable Energy (RE), comes from air current flowing across the earth's surface. Wind turbines harvest this kinetic energy and convert it into power. The electricity is sent through transmission and distribution lines to customers [61].

WE has numerous and clear advantages. Thus, its technology has taken a leap forward in recent years. Wind power is the most mature and cost-effective RE technologies available today. It is competitive with traditional power plants.

The electricity from fossil-fuel-powered sources depends on fuels whose prices are costly and may vary considerably. However, the cost of wind power is relatively stable. Wind power is inexhaustible and requires no 'fuel'. Additionally, Wind Turbine Generators (WTGs) do not produce Greenhouse Gases (GHGs) that may cause global warming [62].

Nevertheless, convenient WTG sites may require significant infrastructure improvement to deliver the wind power to the load center. Wind power plants have relatively little impact on the environment compared to other conventional power plants. There is some concern over the noise, visual impacts, and, sometimes, birds have been killed by flying into the rotor blades. These problems can been greatly reduced by technologically improving or properly siting wind plants [62].

WTGs integration into the electric power system exhibits challenges to power-system planners and operators. These challenges stem primarily from the natural characteristics of wind plants. Rapid expansion of wind power in the electricity sector is raising questions about how wind resource variability might affect the capacity of wind farms at high levels of penetration [61, 62].

Large wind farms are being developed in many countries. These wind farms may present a significant power contribution to the grids, and therefore, play an important role on the power quality and the control of power systems. Consequently, high technical demands are expected to be met by these generation units, such as to perform frequency and voltage control, regulation of active and reactive power, quick responses under power system transient and dynamic situations, for example, it may be required to reduce the power from the nominal power to 20% power within 2 seconds.

The power electronic technology is an important part in both the system configurations and the control of the wind farms in order to fulfill these demands [63].

The European Commission proposal for 20% RE by 2020 paves the way for a massive expansion of WE and a new energy future for Europe. To reach the goal, WE is a key technology and large scale integration is required both onshore and offshore. This represents interesting challenges to the power system requiring new ways of designing and operating the system. Especially large scale offshore wind power – usually located on the continental shelves, far from coastlines – will require attention to new focus areas [51, 52, 53].

Consequently, certain researchers have recently studied the grid integration of offshore wind farms using VSC-HVDC transmission system. In addition, the impact of VSC-HVDC control on the dynamic performance of the offshore wind farms during steady state and transient conditions have been presented in literature [57]. Two different situations have been adressed:

– VSC control for the Doubly Fed Induction Generation (DFIG) of WTGs;

– VSC control for the Permanent Magnet Synchronous Generation (PMSG) of WTGs.

In [54], Mahi et al. (2007) have presented a Direct Torque Control (DTC) strategy for DFIG of a variable speed wind turbine. Nonlinear state feedback control laws are formulated to provide the torque reference so as to reduce the produced electrical power tacking error. DTC has been used as an alternative to the classical Field Oriented Control (FOC) method . This control technique has shown lower parameter dependency in addition to its relative structure simplicity because neither torque nor flux estimators is needed. The combination of both powerful multivariable control law and the DTC strategy has guaranteed good performance besides increasing the robustness against different perturbations.

In [55], Boukhezzar et al. (2009) have designed a cascaded nonlinear controller for a variable speed wind turbine equipped with a DFIG. The main objective of the proposed controller has been wind energy capture optimization below the rated power area. New control structures for both the DFIG and the mechanical part (aeroturbine) have been introduced in order to overcome some of the drawbacks of the existing control methods. The global controller has composed of two cascaded ones. The first one concerns the aeroturbine, while the second one is for the DFIG. These controllers have been designed while accounting for the dynamic aspects of the wind turbine and its aerodynamic behavior nonlinearity in addition to the turbulent nature of the wind. Simulation results have verified that the proposed controller ensures enhanced performance in terms of efficiency with an acceptable drive train transient loads and significant implementation simplicity compared to some existing control strategies.

In [56], Wang et al. (2011) have described the use of VSC-HVDC technology to mitigate power output fluctuation caused by wind farms based on DFIGs which dominate in large capability WTGs. Stator flux oriented vector control technology and capturing maximal wind energy have been adopted. The independent control of active and reactive power has been realized and wind generation by capturing maximal wind energy with efficiency has been also fulfilled. Additionally, the coordinated control strategy between wind farms and VSC-HVDC system has been presented. Both active and reactive power fast regulation of VSC-HVDC system have maintained the injection power of the AC system stable according to the system needs.

Simulation results have verified the suitability of the proposed control strategy towards mitigating the power output fluctuations [56].

In [57], Muyeen et al. (2010) have presented the operation and control strategies of an offshore wind farm interconnected to HVDC systems. The offshore wind farm composed of variable speed wind turbines driving PMSGs has been considered in this study, based on DC-bus concept. The HVDC transmission system based on a three-level neutral point clamped VSC has been used for the interconnection between the offshore wind farm and onshore grid. Detailed modeling and control strategies are developed for the individual component of the overall system. A simple fuzzy logic controller has been adopted in the offshore VSC station. Real wind speed data has been used in the simulation study to obtain realistic responses. Both dynamic and transient analyses of the proposed system have been demonstrated [56, 57, 58, 59, 60].

In [58], Zhao et al. (2011) have introduced the DC connection structure of wind farm based on PMSG. According to VSC-HVDC transmission, the topology of series-parallel DC generation units has been proposed. Regarding to the control strategy of the power generation and transmission system, the DC voltage has been controlled on the generator-side for achieving the purpose of series-parallel, and on the grid-side active and reactive power decoupling method has been applied to track maximum wind power by controlling the *d-q* currents of the grid. The models of single generator, series connection and parallel connection system have been established. Simulation results have proved the validity of the topology scheme and the corresponding control strategy as presented in [58].

According to [60], Nguyen et al. (2011) have studied the stability assessment for the VSC-HVDC transmission systems when applied to a large scale. Appropriate control strategies have been investigated for the VSC-HVDC transmission to reach a full integration of large offshore wind farms into the power system operation while minimizing the critical situations for the power system operation and guaranteeing the required stability level. Therefore, the Fault Ride Through (FRT) capabilities of such complex systems have been evaluated. Thus, different emergency control strategies have been proposed for VSC-HVDC. Among them, the reduction of power generation by wind turbines using a voltage based information carrier has been analyzed. Simulation results have been assessed regarding aspects such as the time response and the reliability of the control strategy [60].

Thesis Objectives

The objective of this thesis deals with the stabilization, nonlinear control and dynamics performance enhancement of VSC-HVDC transmission systems under parameter uncertainties, such as load resistance, DC cable parameter and/or AC line reactance variations. Furthermore, the AC network control and stabilization through VSC-HVDC systems are illustrated. The impact of controlling the VSC side on enhancing the dynamic behavior of the synchronous generator and damping its rotor angle oscillations are studied in presence of faults.

Nonlinear feedback controllers based on both SMC and AOT techniques are respectively used for accomplishing this purpose in favor of their robustness with respect to parameter uncertainties and exogenous disturbances. These advanced control approaches, based on Variable Structure Systems (VSS), have the capability of controlling nonlinear plants in presence of uncertainties associated with parameter estimation and modeling errors. They provide, foremost, performance robustness as well as control design simplicity.

The steady state mathematical models of generator-load (GL) and generator-generator (GG) VSC-HVDC transmission systems, where the power flow is unidirectional and bidirectional respectively, are developed. The GL VSC-HVDC transmission system is initially controlled via the classical PI controllers, with fixed tuning gains, supposing different operating conditions. Then, the system dynamic response and the controller robustness are assessed. For GG VSC-HVDC systems, appropriate nonlinear feedback control signals based on AOT and SMC are formulated. The active power at the AC terminal of either converters and the DC voltage at the DC side of the other VSC are regulated to their prescribed reference values. Additionally, the reactive powers at the AC sides of both converters are controlled towards their specified set-point values. Zero reactive power set-point is considered at both VSCs' AC sides to attain desirable unity power factor. Therefore, the transmitted power is adequately regulated. Obviously, the DC link voltage drop and power losses are taken into account. Accordingly, overall systems' stabilization and performance improvement, under parameter uncertainties, are studied. The robustness of the proposed control techniques, for both VSC-HVDC systems under study, is then evaluated.

Using MATLAB®, the results significantly verify that the desired robust controllers based on both AOT and SMC can achieve favorable tracking performance, and contribute efficiently towards improving the system dynamic behavior, supposing DC cable parameters variations, for different DC link lengths. The chattering behavior resulted using AOT is avoided using continuous functions for SMC design. The proposed nonlinear controllers, which are verified to be robust against DC cable parameter variations, can constitute a good candidate against this type of uncertainty. However, these controllers are not robust to AC line reactance variations.

Finally, GG VSC-HVDC transmission system is replaced by a new equivalent system named Single Machine via VSC-HVDC (SM via VSC-HVDC) systems. After the mathematical modeling of such system, the conventional PI controller is applied at the converter's side in order to improve the the system transient stability and to damp the power angle oscillations of the synchronous generator.

Thesis Contributions

This thesis comprises two main parts. In the first one, nonlinear control and stabilization of VSC-HVDC transmission systems are performed. Two different systems, GL VSC-HVDC and GG VSC-HVDC, are studied. Regarding parameter uncertainty existence, the physical model of VSC-HVDC transmission system is explicitly discussed.

The steady state mathematical models of both GL VSC-HVDC and GG VSC-HVDC transmission systems, whose power flow are respectively unidirectional and bidirectional, are developed based on relatively simple expressions to assess systems' steady state responses in upgraded power networks. As parameter uncertainties are involved in systems' operation, different nonlinear control methodologies are applied to circumvent these abnormal situations.

The design of GL VSC-HVDC transmission system controllers, to reduce the influences of the parameter uncertainties interference with system dynamic performance, is employed. Therefore, conventional PID controllers are proposed. The control actions are directly expressed as a function of the error, it's derivative or integral. After the appropriate choice of tuning gains, the proposed controllers are verified to be effective on both governing DC bus voltage and controlling the reactive power flexibly and rapidly.

The reactive power is controlled towards their pre-specified set-point value at the VSC's AC-side of GL VSC-HVDC system. To ensure unity power factor, reactive power reference value is set to zero.

Simulation results confirm that the classical PI controllers (either without or with an internal current control loop) provide reasonable stability levels and dynamic performance. The responses may be further enhanced via tuning gains optimization. However, the PI controllers -with fixed gains- are not robust enough against different parameter uncertainties (i.e., load resistance changes and AC reactance variations).

For GG VSC-HVDC transmission systems, nonlinear feedback control laws based on different nonlinear control systems such as AOT and SMC are deduced. The necessity of significant smooth transitions and chattering-free behavior are highlighted especially for nonlinear SMC design. Thus, chattering phenomena that appear in AOT control are treated proposing SMC with continuous functions such as saturation and hyperbolic ones instead of the discontinuous sigmoid function. Both AOT and SMC controller design processes are relatively simple because feedback laws are derived step by step. The control technique based on SMC guarantee robustness realization and tracking performance making use of Lyapunov theory. SMC is used to control active and reactive powers of either converters and to govern the DC link voltage and the reactive power of the other. Indeed, DC link voltage drop, power losses and power flow direction are accounted for. Considering networks' parameter uncertainties such as AC line and DC cable parameter variations besides reference signal variations, the designed controller robustness is evaluated and the system's dynamic performance is illustrated.

Simulation results explicit a leap forward in controllers inherent robustness under DC cable resistance uncertainties for different DC link lengths. Moreover, overall system's stability and its dynamic behavior are enhanced using the proposed nonlinear controllers. On the other hand, it is verified that the same controller is not robust against the AC line reactance variations.

The second part of the thesis aims at studying the influence of VSC-HVDC control on enhancing the AC network dynamic performance during faults. After the mathematical modeling of the proposed SM via VSC-HVDC system, the conventional PI controller is applied on the converters side of the system to act on Power Oscillations Damping (POD) of the synchronous machine even under a fault as an important contribution of this study.

Simulation results verify that the use of the conventional PI control, which are simple to be implemented, for governing the voltage or the angle on the converter side can guarantee acceptable dynamic performance enhancement as well as power angle oscillations improvement inside the synchronous machine in presence of faults.

Thesis Outline

Following the Introduction, Chapter 1 briefly introduces an overview of HVDC transmission systems in which a historical background of main types of electrical transmission systems is presented. The environmental, technical and economical aspects of HVDC transmission systems are explicitly demonstrated. The advantages of using HVDC transmission systems rather than HVAC are argued. The latest HVDC configurations according to both power electronics technology and transmission category are shown. Then, the integration of WE to the grid via VSC-HVDC technology is introduced.

Chapter 2 gives a brief definition for both robust and adaptive control. It offers a synopsis of different modern robust and adaptive control techniques used for nonlinear system's stabilization. The main reasons of parametric uncertainties existed in electrical power systems are clearly exhibited. Then, the basic concepts behind both SMC and AOT control design, applied to VSC-HVDC systems, are displayed with the provision of minimal mathematical derivations.

In Chapter 3, the steady state mathematical model of the generator-load (GL) and generator-generator (GG) VSC-HVDC systems, where the power flow is unidirectional and directional respectively, are deduced. For GL VSC-HVDC systems, the power is delivered from the generator to the load. As a consequence, the overall system state space equation representation is developed. Thereafter, conventional PI controllers, which are simple to be implemented, are explicitly introduced. The controller tuning gains are chosen using automated tuning simulink PID controller. Simulation results that illustrate the proposed PI controller effectiveness (either without or with an internal current control loop) are revealed. Their flexibility towards enhancing GL VSC-HVDC system's dynamic behavior and stability are attentively interpreted. However, the system dynamic performance is influenced by parameter uncertainties using fixed gains conventional controllers. Unfavorable overshoots result in the system dynamic behavior.

Nonlinear feedback controllers based on either AOT or SMC are then formulated and extensively demonstrated for GG VSC-HVDC systems. Simulation results verifies the robustness of the proposed nonlinear controllers against parameter uncertainties such as DC cable resistance variations. Their enhanced dynamic behavior and stability level as well as their relative structural simplicity are explicitly illustrated. However, lack of robustness of these nonlinear controllers against AC line reactance variations is encountered.

To clarify the SMC superiority, the system dynamic behavior in case of using two-terms SMC is compared to its corresponding performance attained from using conventional cascaded PI controller with internal currwnt control.

Chapter 5 explores the AC network control via VSC-HVDC for GG VSC-HVDC transmission systems. The full nonlinear seventh order generator mathematical model is considered for one of both AC networks in order to present its detailed dynamics. The other AC network equipped with the DC link is represented as a bus with constant voltage and variable angle. Then, the impact of using the conventional PI controller for controlling either the active power or the direct component of the voltage at the VSC's AC side on the generator's power angle oscillations is studied. Simulation results verify that the proposed controllers preserve system stability with guaranteed power angle oscillations damping and dynamic behavior enhancement particularly in presence of external perturbations such as faults.

Finally, the main conclusions and contributions of this thesis in addition to several suggestions for future work research directions and perspectives are drawn.

Chapter 1

Overview of HVDC Transmission Systems

THIS chapter briefly introduces a historical background of the main types of electrical transmission systems. It focuses on the general environmental, technical and economical aspects of HVDC transmission systems. The advantages of using of HVDC transmission systems rather than HVAC ones are stated. Then, the latest HVDC technologies are introduced. HVDC types according to power electronics technology as conventional LCC-HVDC transmission systems and recent VSC-HVDCs respectively are extensively explained. Additionally, HVDC configurations due to transmission category; back to back, point to point and multi-terminal HVDC systems are discussed. Moreover, VSC-HVDC worldwide most modern installations, providing the main reasons and comments on each installation, are pointed out. Finally, the conclusions concerning VSC-HVDC systems utilization are drawn.

1.1 Introduction

High Voltage Direct Current (HVDC) technology has characteristics that make it especially attractive for certain transmission applications. HVDC transmission has been widely recognized as being advantageous for long-distance bulk-power delivery, asynchronous interconnections, and long submarine cable crossings [64]. Therefore, HVDC has been in use for more than 50 years and has remained a niche technology.

HVDC has proved to be a reliable and valuable transmission media for electrical energy in favor of its technical superiority compared with HVAC transmission. Nonetheless, a comprehensive HVDC/HVAC system planning approach is not commonly found within utilities, and therefore full HVDC technology's advantage is not being taken. HVDC projects often provide strategically important enhancements and cost effective additions to AC networks. However, HVDC transmission is perceived to be expensive, difficult to integrate in an AC network, to require highly skilled personnel to operate and maintain, and to have high power losses [64, 65].

Recent developments in energy policies and stronger environmental lobbies have a significant impact on the design and construction of electrical power transmission networks, and could provide a number of opportunities for HVDC transmission. The number of HVDC projects committed or under consideration globally has increased in recent years reflecting a renewed interest in this mature technology. This new converter design has broadened the potential range of HVDC transmission to include applications for underground, offshore, economic replacement of reliability-must-run generation, and voltage stabilization. This broader range of applications has contributed to the recent growth of HVDC transmission [64, 65].

1.2 Historical Background

Power transmission utilized with DC is not a new idea. The first commercially generated electricity by Thomas Edison in the 1880s was DC at low voltage levels [64, 66]. The first electricity transmission system was also DC, but because of the low voltage levels the electric energy had to be generated close to its consumers to avoid too large losses. The AC system by Nikola Tesla made it possible to easily transform the voltage to higher voltage levels, suitable for electric power transmission over long distances. The generation of power no longer needed to be close to its customers; instead it could be placed where the energy source was located. For this reason, the winner in the "*war of currents*" in the late 1880s was the AC technology. It has been the dominating technology for power transmission ever since. HVAC is very good for transforming the voltage and thereby reduce the losses in transmission over longer distances. As the current passes zero each cycle in HVAC breakers, it is possible to construct big meshed AC grids that can connect large number of generators and consumers [67, 68].

History may have looked different if there had been a technology earlier that was able to step up the DC voltage to a higher level, as transformers do with AC. In 1901, such a component made it possible when Hewitt's mercury-vapor rectifier was presented. This high voltage valve made it possible, at least in theory, to transmit DC power at high voltage levels and for long distances. Hence, HVDC technology was born. The development of mercury arc valves in the 1930s improved the technology and in 1945 a commercial HVDC system in Berlin was commissioned. This system was never put into operation [66, 69]. In 1954, the first commercial HVDC transmission connected the Swedish island of Gotland to the mainland via 96 km, 20 MW submarine cables has been put into service. The converter stations at that time used mercury arc valves as key element, the filtering was done with single tuned filters, with oil-immersed components. The control was strictly analogue, and with essential functions only. HVDC technology makes it possible to connect AC networks that are not synchronous or have large differences in phase angle [68]. HVDC is also more economical when large amounts of power shall be transmitted long distances on Over Head Lines (OHL). The most important advancements since then, especially in power electronics and semiconductors domain, lead to the present VSC-HVDC [70].

The development of power electronics and semiconductors in the late 1960s led to the thyristor based valve technology, first tested in Gotland transmission in 1967, and later introduced on a larger scale in Canada 1972 with a rating of 320 MW. Today the thyristor based current source Line Commutated Converter (LCC) technology is used in the majority of HVDC transmissions in the world. One of the largest HVDCs is the Three Gorges-Shanghai link with a rating of 3000 MW and ±500 kV [71, 72]. The LCC-HVDC technology is also known as HVDC Classic, conventional HVDC or even HVDC. During the late 1990s, the semiconductor development for power electronics, such as IGBTs and Gate Turn-Off (GTO) thyristors, had reached the point where their ratings made it possible to be used for VSCs. The first commercial VSC-based HVDC transmission was first commissioned in 1999 on Gotland island with an underground cable (UGC) of 50 MW. ABB refers to LCC-HVDC and VSC-HVDC technologies as HVDC Classic and HVDC Light^{TM} respectively. Siemens also offers VSC-HVDC variant, commercialized as HVDC Plus^{TM}. VSC technology has been improved in recent years due to continuous semiconductor development[66, 71, 72].

1.3 Electrical Transmission Systems

Traditionally, a transmission grid is a network of power stations, transmission circuits, and substations [68]. Energy is usually transmitted within the grid with three-phase AC. High-voltage grid in Europe uses alternating current at 50 Hz. A hundred years ago, the transformer and the three-phase system made it possible to transmit AC power efficiently and economically over vast distances and to distribute the power to a multitude of users [15].

For over a century, electrical transmission systems have been based mainly on OHL. The main reason for this has been its cost advantage when compared to high-voltage UGC transmission [73]. In general, it is getting increasingly difficult to build OHL. It changes the landscape. The construction of new lines is often met by public resentment and political resistance. People are often concerned about possible health hazards of living close to OHL. In addition, a right-of-way for a high voltage line occupies valuable land. The process of obtaining permissions for building new OHL is also becoming time-consuming and expensive.

Yet, laying a new UGC is administratively much easier and quicker than for an OHL [15, 73]. Moreover, UGCs can assist the transmission of power across: densely populated urban areas, areas where land is unavailable or planning consent is difficult, rivers and other natural obstacles, land with outstanding natural or environmental heritage, areas of significant or prestigious infrastructural development, and land whose value must be maintained for future urban expansion and rural development [68].

Advantages of AC transmission using UGC compared to OHL [68]:

- Less subject to damage from severe weather conditions;
- UGCs suffer interruptions and faults much less frequently than OHLs;
- Greatly reduced emission of electromagnetic fields (EMF);
- Narrower surrounding strip of about 1-10 meters is required to install, and to be kept permanently clear for safety, maintenance and repair;
- UGCs pose no hazard to low flying aircraft or to wildlife, and are significantly safer as they pose no shock hazard;

- Much less subject to conductor theft, illegal connections, sabotage, and damage from armed conflict.

On the other hand, the disadvantages of AC UGCs compared to OHLs [68]:

- Capital costs for UGCs are clearly higher than for OHLs of the same transmission capacity;
- Easier and quicker to repair;
- UGCs, due to their proximity to earth, cannot be maintained live, whereas OHLs can be;
- Operations are more difficult since the UGC's high reactive power produces large charging currents and so makes voltage control more difficult especially at high voltages.

The advantages of the transmission system can in some cases outweigh its disadvantages of higher investment, maintenance and management costs. Recent studies suggest the cost premium of UGC's transmission is in the range of 5-15 times the traditional OHL alternative. But this comparison is already dated.

Two main factors are affecting the paradigm [73]:

- Environmental restrictions are increasing the costs and implementation time for overhead transmission;
- Technological development significantly reduces the cost of underground transmission.

However, today's AC transmission and distribution systems are, at least in principle, based on ideas that have not changed so much as: to generate power, step up the voltage with transformers, transmit power, step down the voltage and distribute power. Despite their proven advantages, it is difficult and expensive to adapt AC transmission and distribution systems either to numerous small scale generating plants or to other complex and variable generation units recently established. Environmental concerns and regulations also put heavy restrictions on building new right-of-ways and on small-scale, fossil-fueled generating plants, such as diesel generating plants [15]. Therefore, HVDC transmission systems have lately replaced overhead HVAC ones due to environmental, technical, and economical aspects.

1.3.1 Environmental Aspects of HVDC

An HVDC transmission system is basically environment-friendly because improved energy transmission possibilities contribute to a more efficient utilization of existing power plants [69].

1. **Visual impact and space requirements:**
   An HVDC cable uses significantly less land than an HVAC OHL [66]. An HVDC transmission with an OHL requires less space per MW than traditional AC solutions. The tower's visual impact is therefore reduced. If a cable is used, the only visual impact is the converter stations. However, the size of these stations in comparison with traditional AC stations may have larger visual impact to be dealt with [66, 69].

2. **Electric and magnetic fields:**
   The magnetic field produced by a DC line is stationary while in the AC case it is alternating, which can cause inducing body currents. This results in fewer restrictions for the magnetic field in the HVDC line [74]. The electric field is less severe in DC lines compared to AC ones since there is no steady state displacement current in the DC case [66, 75]. VSC-HVDC cables' magnetic fields are almost eliminated with the bipolar system. However, an undersea HVDC line can cause disturbances to magnetic compass systems on vessels crossing the cable [66, 69].

3. **Radio interference:**
   The harmonics created in switching processes by converters cause disturbances in the kHz and MHz regions. An appropriate shielding of valves minimizes this problem. This makes the radio interference comparable with AC solutions [74, 75, 76]. Radio interference is normally a minor problem in transmission systems.

4. **Audible noise:**
   An underground DC cable naturally has no audible noise emission. Audible noise from transmission line corona is most noticeable when OHL conductors are wet in foggy weather conditions. Consequently, buildings construction close to OHLs might be restricted. Audible noise mostly depends on line's voltage and its design specifications [73].

Furthermore, underground HVDC cables have better environmental profile than overhead HVAC lines in favor of these additional reasons:

- **Right-of-way as a loss of CO_2 sink:** growing forests are considered CO_2 sinks because trees convert carbon dioxide from the atmosphere into carbon stored in the form of wood and organic soil matter. A forest can absorb 9.2 tons of CO_2 per hectare per year. For example, building a 400 km, 400 kV OHL through an area that is 75 percent forest represents a loss of a carbon sink of 16,780 tons of CO_2 per year [73];
- **Material use:** AC OHL's material weight is higher than for a DC cable. The material used in a DC cable has only 17.6 percent the environmental impact of AC OHL [73].

1.3.2 Technical Merits of HVDC

The DC link technical advantages over an AC one are [69]:

- A DC link allows power transmission between AC networks with different frequencies, or systems which can not be synchronized for other reasons;
- Inductive and capacitive parameters do not limit either the transmission capacity or the maximum length of a DC OHL or DC cable. Additionally, the conductor cross section is fully utilized because there is no skin effect;
- There is no phase shift between current and voltage. With AC, this flaw has to be eliminated using controlling elements in an energy-intensive process [77];
- HVDC solutions may have lower power losses especially for large distances. The power loss in a HVDC converter station is higher than that in an AC substation because of the conversion between AC and DC and the harmonics produced by this process. However, the total power loss in a HVDC transmission line can be 50% to 70% of that in an equivalent HVAC one. Moreover, when VSC-HVDC underground transmission is used inside an AC-grid, the transmission system can be more optimally operated that leads to lower electrical losses;
- Fast modulation of DC transmission power can be used for power oscillations damping in an AC grid and thus improving system's stability;

- A digital control system provides accurate and fast active power flow control. Thus, HVDC helps stabilize the existing three-phase current networks that it connects.

Attention should be taken to harmonics produced by all power electronic converters as a byproduct of conversion process. In order to prevent these harmonics spreading into AC network, where they could cause problems, AC harmonic filters are used at AC terminals of the HVDC scheme. AC harmonic filters and any shunt capacitor banks used for reactive power compensation can actually cause magnification of the distortion produced by other remote harmonic sources. Therefore, HVDC manufacturers need to consider new converter topologies and commercialization of low-cost active AC harmonic filters, which would provide adaptable filtering of harmonics over a broad range.

1.3.3 Economical Merits of HVDC

As world energy resources are normally decentralized from the ever increasing energy consumption, long HVDC transmissions are a particularly interesting area for the future. A key characteristic of HVDC transmissions is higher power transfers in fewer lines than an equivalent AC solution [78]. Furthermore, a major constraint when designing traditional AC transmission lines over long distances is the significant inductance such a line will have. The effects of both the line inductance and capacitance have to be compensated along the AC line and this adds costs for long distances. The frequency is zero for DC; hence the inductance is irrelevant. Subsequently, an overhead DC line with its towers can be designed to be less costly per km than an equivalent AC solution, if both the investment and capitalization of total energy losses are considered.

Whenever long-distance transmission is discussed, the concept of "*break-even distance*" frequently arises. This is where the savings in line costs offset the higher converter station costs. Bipolar HVDC lines use only two insulated sets of conductors rather than three. This results in narrower rights-of-way, smaller transmission towers, and lower line losses than with AC lines of comparable capacity. A rough approximation of savings in line construction is about 30%. Furthermore, long-distance AC lines usually require intermediate switching stations and reactive power compensation which increases the overall AC transmission cost [64].

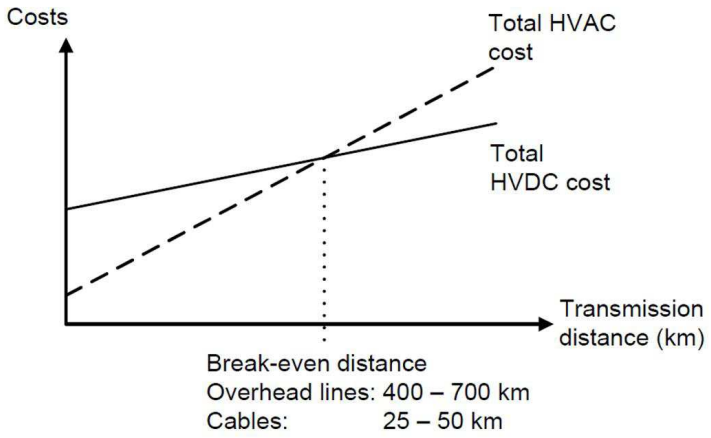

Figure 1.1: Cost against transmission distance for HVDC and HVAC systems.

HVDC converter stations at both ends are more costly than equivalent AC terminals, thus, an economical break-even distance arises, as illustrated in Figure (1.1) [66]. The break-even distance, where the HVDC solution becomes more economical than an equivalent AC, greatly depends on land conditions and project specifications [79].

The reasons for choosing HVDC are generally economic and not technical. Power system stability improvements and environmental circumstances may, however, also be reasons for using this technology. Favorable economics of bulk power transmission with HVDC together with its controllability make it an interesting alternative or complement to AC transmission. Therefore, thanks to HVDC transmission's economical, technical, and environmental merits, the strategies for future transmission infrastructure development go clearly towards HVDC applications.

1.4 HVDC Applications

HVDC transmission applications can be broken down into different basic categories. Although the rationale for selection of HVDC is often economic, there may be other reasons for its selection.

HVDC may be the only feasible way to interconnect two asynchronous networks, reduce fault currents, utilize long UGC circuits, bypass network congestion, share utility rights of-way without degradation of reliability, and to mitigate environmental concerns. HVDC nicely complements AC transmission systems as explicitly demonstrated in [64] and the references within in. Therefore, the following HVDC applications are presented:

Long-distance bulk power transmission

HVDC transmission systems often provide a more economical alternative to AC transmission for long-distance bulk power delivery from remote resources such as hydroelectric developments, mine-mouth power plants, or large-scale wind farms. Higher power transfers are possible over longer distances using fewer lines with HVDC than with AC transmission. Typical HVDC lines utilize a bipolar configuration with two independent poles, one at a positive voltage and the other at a negative voltage with respect to ground. Bipolar HVDC lines are comparable to a double circuit AC line since they can operate at half power with one pole out of service but require only one-third the number of insulated sets of conductors as for double circuit AC line [64].

Underground and submarine cable transmission

The charging current in HVAC cables makes transmissions over long distances impractical. In order to keep voltage levels and power losses within reasonable limits, HVAC transmission requires reactive power compensation equipment along the cable. Such equipment adds cost to the link, and in some cases can not be implemented. If however the cable is fed with HVDC, the large capacitance is irrelevant since the charging current is frequency dependent [80].

Nonetheless, there is no physical restriction limiting the distance or power level for HVDC underground or submarine cables. For these types of HVDC transmission cables, considerable savings in both installation and losses costs are yielded. For a given cable conductor, HVDC cable's losses can be about half those of AC ones. AC cables clearly require more conductors (three phases), carry the reactive current component, present skin-effect, and carry induced currents in the cable sheath and armor. With this cable system, the need to balance unequal loadings or the risk of post contingency overloads often requires the use of series-connected reactors or phase shifting transformers. These potential problems do not exist with a controlled HVDC cable system.

Extruded HVDC cables with prefabricated joints used with VSC-based transmission are lighter, more flexible, and easier to splice than the mass-impregnated oil-paper cables MINDs used for conventional HVDC, thus making them more conducive for land cable applications where transport limitations and extra splicing costs can drive up installation costs. Thus, long distance underground with DC VSC-based transmission is comparatively economically feasible for use in areas with rights-of-way constraints, or subjected to licence difficulties or delays compared with OHLs [64].

Asynchronous ties

With HVDC transmission systems, interconnections can be performed between asynchronous networks for more economic or reliable system operation. Asynchronous systems' interconnections allow mutual benefit while providing a buffer between both AC systems. These interconnections often use back to back converters with no transmission line. Asynchronous HVDC links act as an effective "*firewall*" against propagation of cascading outages in any network from passing to another one.

In August 2003, Northeast blackout of North America gave an example of "*firewall*" against cascading outages of asynchronous interconnections. As the outage expanded and propagated around the lower Great Lakes and through Ontario and New York, it stopped at the asynchronous interface with Quebec. Quebec was unaffected; the weak AC interconnections between New York and New England tripped. However, HVDC links from Quebec continued to deliver power to New England [64].

Offshore transmission

Self-commutation, dynamic voltage control, and black-start capability allow compact VSC-HVDC transmission to serve isolated loads on islands or offshore production platforms over long-distance submarine cables. This capability can eliminate the need for running expensive local generation or provide an outlet for offshore generation such as that from wind.

VSCs can operate at variable frequency to efficiently drive large compressor or pumping loads using high-voltage motors. Therefore, VSC-based HVDC transmission allows efficient use of either long-distance land or submarine cables. It also provides reactive support to the wind generation complex unit [64].

Multi-terminal systems

Most HVDC systems are of point to point HVDC transmission type with a converter station at each end. The use of intermediate taps is rare. Conventional HVDC transmission uses voltage polarity reversal to change the power flow direction. Polarity reversal requires no special switching arrangement for two terminal system where both terminals reverse polarity by a control action with no switching. However, special DC side switching arrangements are required for polarity reversal in multi-terminal systems where they may be desired to reverse the power direction at a tap while maintaining the same power direction on remaining terminals. For a bipolar system, this can be done by connecting the converter to the opposite pole. Notably, VSC-HVDC reverses power through the reversal of current direction rather than voltage polarity [64].

Power delivery to large urban areas

Power supply to large cities depends on local generation and power import capability. Local generation is often older and less efficient than newer units located remotely. However, older less-efficient units located near the city center must often be dispatched out-of merit because they must be run for voltage support or reliability due to inadequate transmission. Air quality regulations may limit the availability of these units. New transmission into large cities is difficult to site due to right-of-way limitations and land-use constraints [64].

Compact VSC-based underground transmission circuits can be placed on existing dual-use rights-of-way to bring in power as well as to provide voltage support allowing a more economical power supply without compromising reliability. The receiving terminal acts as a virtual generator delivering power, supplying voltage regulation and reserving dynamic reactive power. Stations are compact and housed mainly indoors, making siting in urban areas somewhat easier. Furthermore, dynamic voltage support offered by VSCs can often increase the adjacent AC transmission capability [64].

Stabilization in power systems

HVDC links can be used within synchronous AC systems to improve the power flow control from one part of the system to another, and consequently, to prevent large cascading failures or even blackouts in the grid. System stability can be improved since the HVDC link provides damping torque [66, 75].

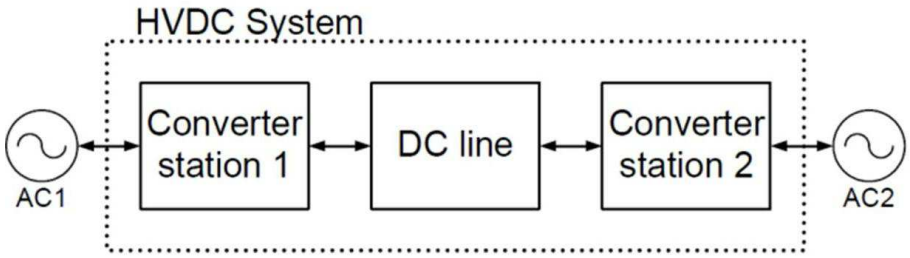

Figure 1.2: Simplified schematic of overall HVDC system configuration.

1.5 HVDC System Configuration

Figure (1.2) shows a simplified schematic diagram of an HVDC system configuration, with the basic principle of transferring electric energy from an AC system or node to another, in any direction. The system consists of three blocks: two converter stations and a DC line. Within each station block there are several components involved in the conversion of AC to DC and vice versa.

1.6 HVDC Classifications

HVDC systems can be classified according to either power electronics technology used or their power transmission categories as follow [64]:

1.6.1 HVDC Types according to Power Electronics Technology used:

Modern HVDC transmission systems are practically available in two basic types according to the converter power electronics technology. These are conventional current source line-commutated converters based-HVDC (LCC-HVDC) and self-commutated voltage source converters based-HVDC (VSC-HVDC).

HVDC based on line-commutated converters

Conventional HVDC transmission employs current source LCCs with thyristor valves. Such converters require a synchronous voltage source in order to operate. Figure (1.3) shows a conventional HVDC converter station with LCCs. The basic building block used for HVDC conversion is the three phase full-wave bridge named as a six-pulse or Graetz bridge.

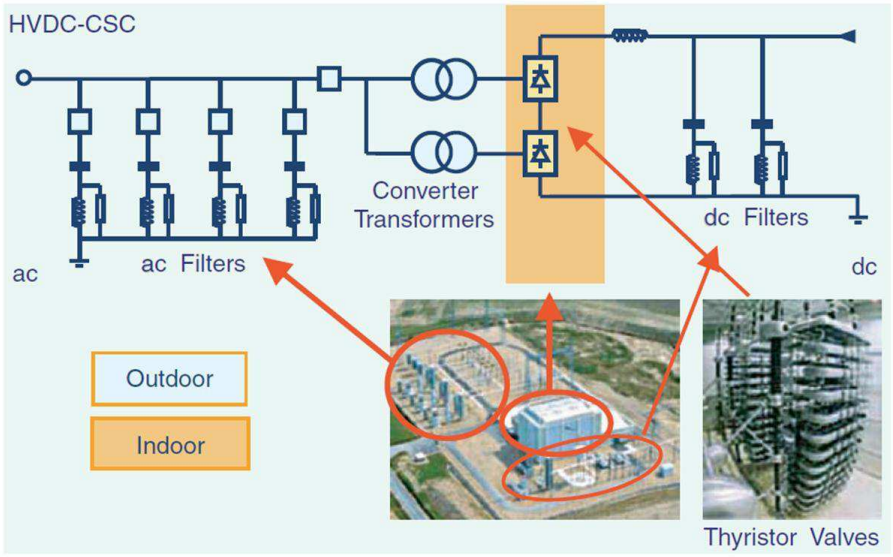

Figure 1.3: Conventional HVDC with current source converters (LCC-HVDC).

The term six-pulse is due to six commutations or switching operations per period resulting in a characteristic harmonic ripple of six times the fundamental frequency in the DC output voltage. Each six-pulse bridge comprise six controlled switching elements or thyristor valves. Each valve consists of a number of series-connected thyristors to reveal desired DC voltage ratings [64].

The DC terminals of two six-pulse bridges with AC voltage sources phase displaced by 30° can be connected in series to increase the DC voltage and eliminate some of the characteristic AC current and DC voltage harmonics. The 30° phase displacement is achieved by feeding one bridge through a transformer with a wye-connected secondary and the other bridge through a transformer with a delta-connected secondary. Operation in this manner is referred to as 12-pulse operation.

Most modern HVDC transmission schemes utilize 12-pulse converters to reduce harmonic filtering requirements needed for six-pulse operation (e.g., fifth and seventh harmonics on the AC side and sixth on the DC side). Although these harmonic currents still flow through the valves and transformer windings, they are 180° out of phase and are cancelled out on the primary side of the converter's transformer.

LCCs require a relatively strong synchronous voltage source in order to commutate. Commutation is the transfer of current from one phase to another in a synchronized firing sequence of thyristor valves. The three-phase symmetrical short circuit capacity available from the network at the converter connection point should be at least twice the converter rating for converter operation. LCCs can only operate with AC current lagging the voltage, so the conversion process requires reactive power. Reactive power is supplied from the AC filters, which seem capacitive at fundamental frequency, shunt banks, or series capacitors that are an integral part of converter stations. Any surplus or deficit in reactive power from these local sources must be accommodated by AC systems. This difference in reactive power needs to always be within a given band to keep the AC voltage within the desired tolerance.

The weaker the AC system or the further the converter is away from generation, the tighter the reactive power exchange must be to keep within the desired voltage tolerance. Figure (1.4) illustrates the reactive power demand, compensation, and exchange with the AC network as a function of DC load current [64].

Because of the following drawbacks, LCC-HVDC system is considered inefficient and its application range is therefore limited [15, 81]:

- A distortion of AC voltage can lead to commutation failures, with an interruption of power flow as a result. Thus, both the rectifier and the inverter of conventional HVDC systems require sufficiently strong AC grids for valve commutation. Simply, LCC requires a receiving network of a strength exceeding the HVDC link's power;

- Higher degree of complexity for a multi-terminal system, for at least two reasons: Firstly, the reversal of active power flow is only performed by reversing the DC polarity. Secondly, high-speed communication between all terminals will be required for control purposes;

- The reactive power must be supplied externally. This is usually done in steps with switched filters and other capacitive elements;

- There is no inherent black start capability in a LCC-HVDC system. It can not deliver power to the network without other generation sources;

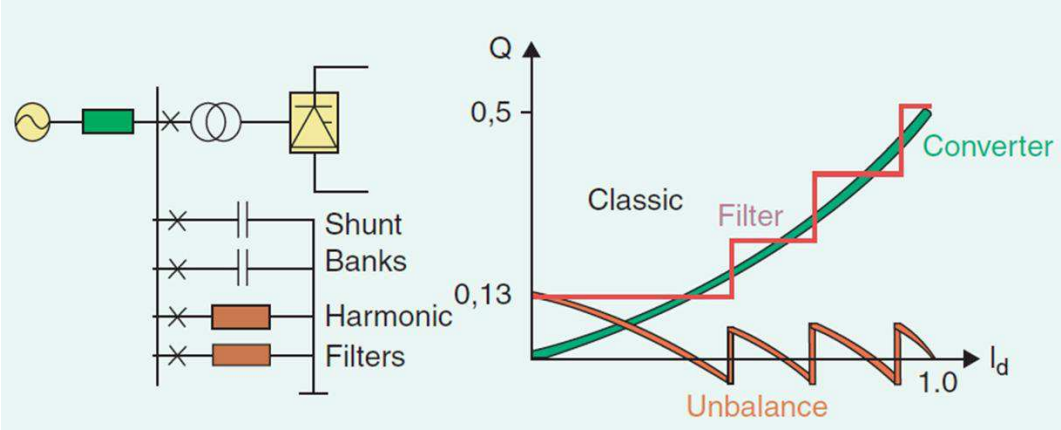

Figure 1.4: Reactive power compensation for LCC-HVDC station.

- Moderate control bandwidth for AC voltage and reactive power, which may cause problems for stable wind turbine generators (WTGs) operation and grid code compliance;
- Continuous operation of active power below 5% may not be possible, which complicates wind plant (WP) energization and operation at low wind speeds.

Therefore, converters with series capacitors connected between valves and transformers were introduced in the late 1990s for weak-system back to back applications. These converters are called capacitor-commutated converters based-HVDC (CCC-HVDC). The series capacitor provides some of the converter reactive power compensation requirements automatically with load current. It provides part of the commutation voltage in order to improve voltage stability. Overvoltage protection of series capacitors is simple since the capacitor is not exposed to line faults. The fault current for internal converter faults is limited by the impedance of converter transformers. The CCC-HVDC configuration allows higher power ratings in areas were the AC network is close to its voltage stability limit [64].

HVDC based on voltage source converters

HVDC transmission using VSCs with Pulse Width Modulation (PWM), commercially known as HVDC Light^{TM} by ABB, was introduced in the late 1990s. Siemens also offers a VSC-HVDC variant, commercialized as HVDC plus^{TM}.

Since then, the progression to higher voltage and power ratings for these converters has roughly paralleled that for thyristor valve converters in the 1970s. VSC-HVDC based on IGBT valves are self-commutated. An IGBT is a combination of PNP Bipolar Junction Transistor (BJT) and a MOSFET. Thus, it has the BJT's low conduction losses advantage besides the MOSFET's fast commutation merit. IGBT cells have a small size (around $1cm^2$). Many IGBT cells are, thus, connected in parallel in IGBT chips and then in modules capable to handle current up to 2.4 kA with blocking voltage up to 6.5 kV.

The design of both HVDC Light and HVDC plus is very close to each other. A module concept is used to provide flexibility in the building. The size (volume and weight) is very small for both. However, the HVDC Light concept has a lower weight whereas the HVDC Plus concept can have a smaller volume by using SF6 insulated device to shrink the converter down as minimum as possible. Those criteria are very important for offshore construction. Converter stations require little maintenance. They are designed to be unmanned and can be operated remotely.

The main difference between both is on the number of level in the converter. HVDC Light converters are based on PWM. However, HVDC Plus uses a new multi-level approach, individual module capacitors are uniformly distributed throughout the topology, and each level is individually controlled to generate a small voltage step. In this way, each module within the multi-level converter is a discrete voltage source in itself, with a local capacitor to define its voltage step without creating ripple voltage distortion across the converters' other phases. By incrementally controlling each step, an almost sinusoidal voltage is generated at the AC outputs of multi-valves. To allow the use of modular IGBTs, Siemens has developed an economical and fail-safe short-circuit mechanism within the multi-level module.

Figure (1.5) shows a VSC-HVDC converter station. It mainly consists of:

- High voltage valves with series-connected IGBTs;
- Compact, dry, high-voltage DC capacitors;
- High capacity control system;
- Solid dielectric DC cable.

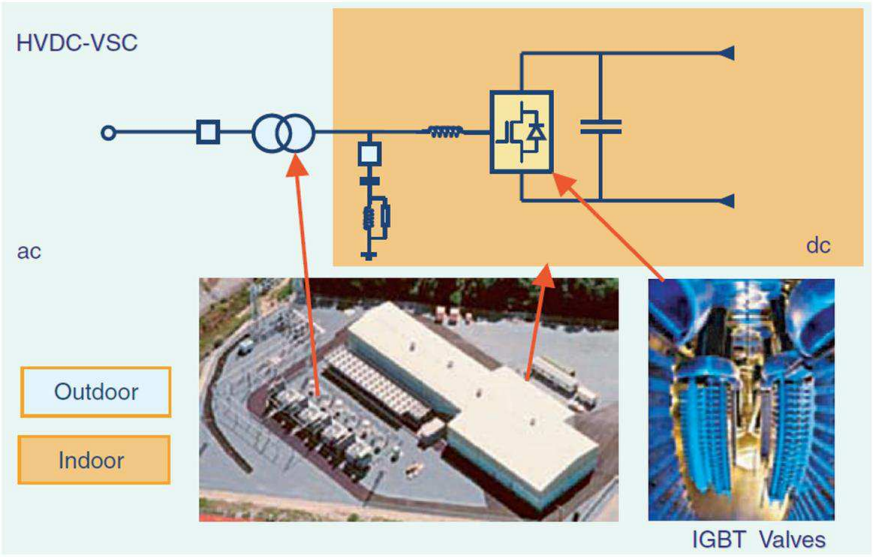

Figure 1.5: HVDC with voltage source converters.

VSC-based systems are self-commutated with IGBT valves and solid-dielectric extruded HVDC cables. Instead of a stiff current, a stiff voltage is used in VSC-HVDC systems. Thus, the converter creates an AC voltage electronically which can be rapidly changed in amplitude and phase. The power direction can be accordingly reversed by changing the current direction and not by DC voltage polarity changement. Figure (1.6) depicts solid-state converter development for both types of converter technologies using thyristor and IGBT valves [64].

HVDC transmission with VSCs can be beneficial to overall system performance. It can rapidly control both active and reactive power independently. Reactive power can also be controlled at each terminal independent of the DC transmission voltage level. This control capability gives total flexibility to place converters anywhere in the AC network since there is no restrictions on minimum network short-circuit capacity.

Self-commutation with VSC even permits black start; i.e., the converter can be used to synthesize a balanced set of three phase voltages like a virtual synchronous generator. The dynamic support of AC voltage at each converter terminal improves the voltage stability. The power transfer capability of both sending and receiving ends of the AC systems can be increased, thereby, the DC link's transfer capability is leveraged.

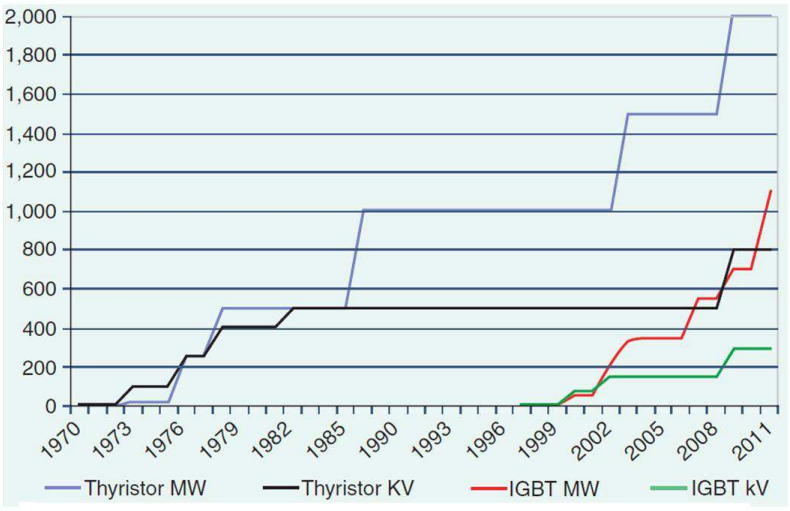

Figure 1.6: Solid-state converter development.

Figure (1.7) shows the active and reactive power operating range for a converter station with a VSC. Unlike conventional HVDC transmission, the converters themselves have no reactive power demand. Their reactive power can be actually controlled to regulate AC system voltage just like a generator.

VSC-HVDC is explicitly attractive in favor of the following features [82, 83]:

- Independent control of reactive and active power;
- Reactive control independent of other terminal(s);
- No communication between stations during normal operation is required;
- Simpler interface with AC system;
- No need of transformers for the conversion process for DC transmission;
- Compact filters;
- Continuous AC voltage regulation;
- No minimum power restriction;

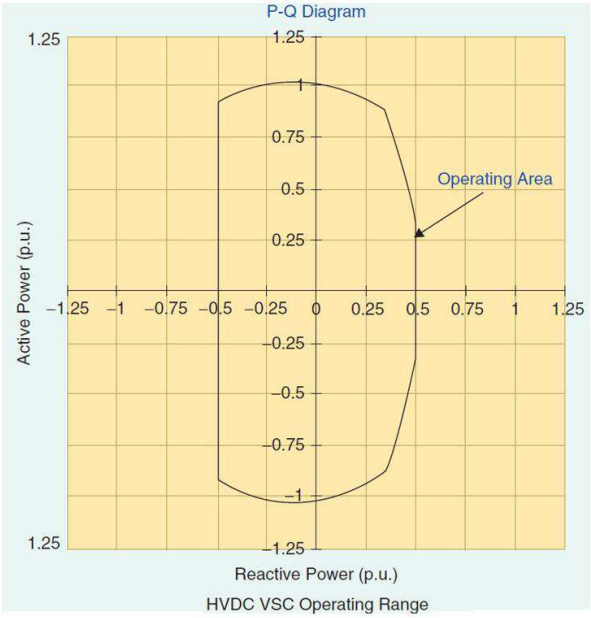

Figure 1.7: Operating range for VSC-HVDC transmission.

- Operation in extremely weak systems;
- No commutation failures;
- No restriction on multiple infeeds;
- No polarity reversal required to reverse power;
- Black-start capability;
- Variable frequency.

Consequently, VSC-HVDC transmission technology is economically feasible to connect small scale or renewable power generation plants to the main AC grid. Vice versa, using the same technology, remote locations as islands, mining districts and drilling platforms can be supplied with power from the main grid. Thus, the need for inefficient, polluting local generation such as diesel units is eliminated. This technology also relies on a new type of UGC which can replace OHL at no cost penalty [15].

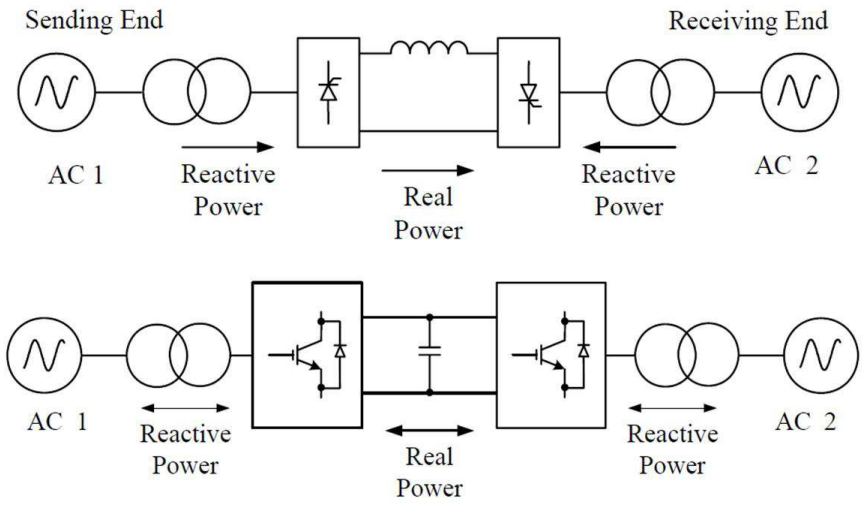

Figure 1.8: Simplified schematic diagram for different HVDC types according to power electronics technology for (a) LCC-HVDC; (b) VSC-HVDC.

Simplified schematic diagram for different HVDC types according to power electronics technology, LCC-HVDC and VSC-HVDC systems, are illustrated in Figure (1.8). Notably, VSC-HVDCs have the ability of bidirectionally transmitting electric energy from an AC system to another.

1.6.2 HVDC Types According to Power Transmission Category

Depending upon the function and location of converter stations, various classifications of HVDC systems can be identified. The ones drawn in this section involve LCC-HVDC configurations but similar forms exist for VSC-HVDC with or without transformers depending upon the project in question [83, 84].

- **Back to back HVDC system**

  In this case, the two converter stations are located at the same site. There is no power transmission for a DC link over a long distance. The back to back LCC-HVDC system with 12-pulse converters is shown in Figure (1.9). Clearly, two AC systems of similar or different frequency can be connected.

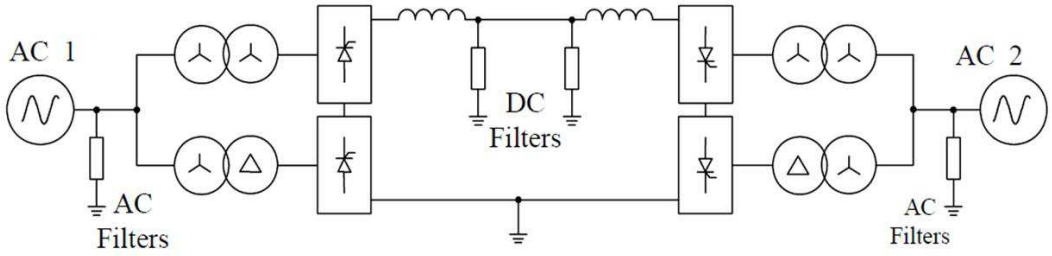

Figure 1.9: Back to back LCC-HVDC system with 12-pulse converters.

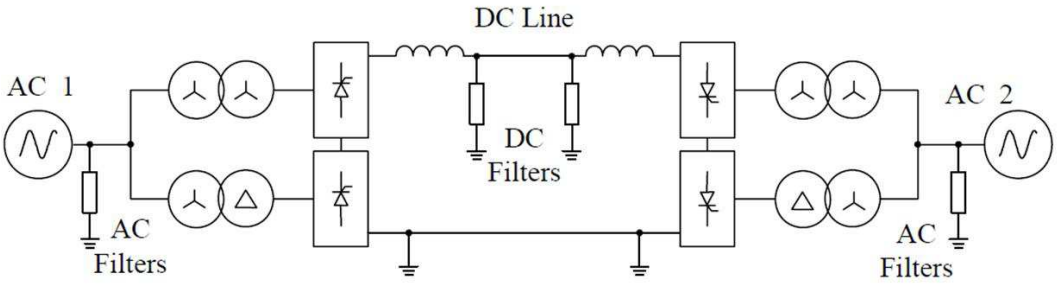

Figure 1.10: Monopolar LCC-HVDC system with 12-pulse converters.

- **Point to point HVDC system**

  OHLs or submarine cables are used in this type of transmission systems to connect the converter stations. These systems can be either monopolar or bipolar.

  - **Monopolar HVDC system**

    In a monopolar HVDC system, two converters which are separated by a single pole line and a positive or a negative DC voltage is used. Many of cable transmissions with submarine connections use monopolar system. The ground is used for returning current. Figure (1.10) shows a block diagram of a monopolar LCC-HVDC system with 12-pulse converters.

  - **Bipolar HVDC system**

    Bipolar HVDC systems, depicted in Figure (1.11), are the most common LCC-HVDC system configuration in applications where OHLs are used to transmit power.

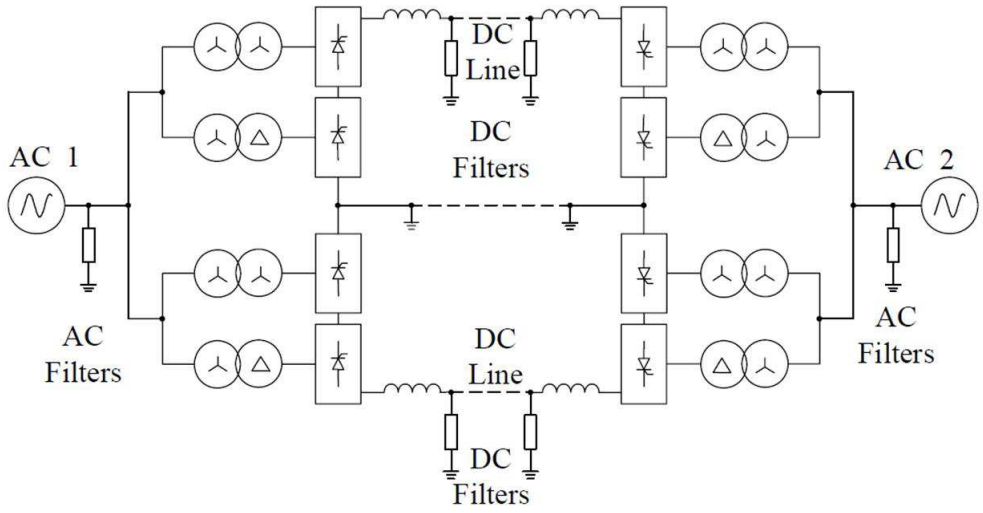

Figure 1.11: Bipolar LCC-HVDC system with one 12-pulse converter per pole.

A bipolar system comprises two monopolar ones. The advantage of such system is that one pole can continue to transmit power while the other is out of service. In other words, each system can operate on its own as an independent system with the earth return. Since one is positive and the other is negative, in case that both poles have equal currents, the ground current is theoretically zero, or in practice within a 1% difference.

- **Multi-terminal HVDC system**

  A multi-terminal LCC-HVDC system with 12-pulse converters per pole is shown in Figure (1.12). Explicitly, converters 1 and 3 act as rectifiers while converter 2 operates as an inverter. Otherwise, converter 2 acts as a rectifier when both converters 1 and 3 operate as inverters. By mechanically switching the connections of a given converter other combinations can be achieved.

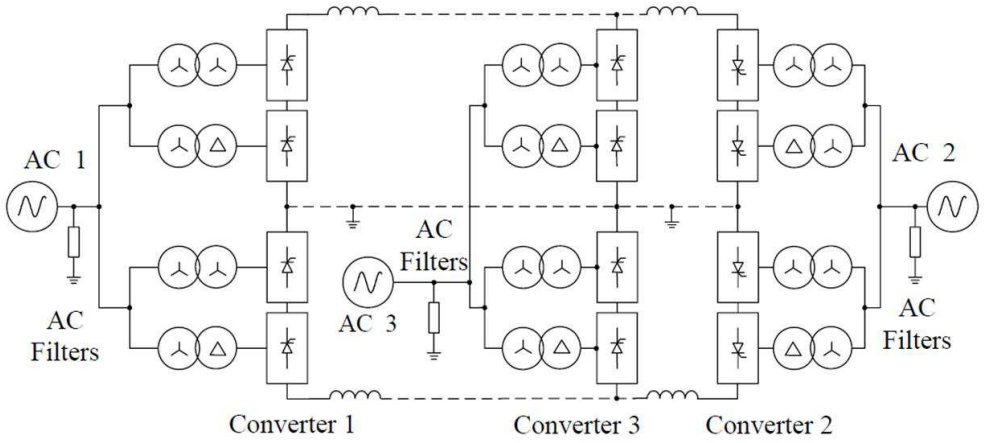

Figure 1.12: Multi-terminal CSC-HVDC system–parallel connected.

1.7 VSC-HVDC Recent Installations

Table 1.1 shows various projects worldwide where VSC-HVDC systems have been successfully exploited [83, 85]. For each project, the reasons of choosing VSC-HVDC are clearly summarized. VSC technology has been selected as the basis of these recent projects in favor of its controllability, compact modular design, ease of system interference and low environmental impact. VSC-HVDC transmission systems can practically transmit power underground and underwater over long distances. It offers numerous environmental benefits, including "*invisible*" power lines, neutral electromagnetic fields, oil-free cables and compact converter stations. Therefore, the experiences gained from the projects so far ensure that VSC-HVDC technology remains competitive and assists utilities worldwide in order to deliver efficient, reliable and economic energy to customers no matter how challenging the applications are.

Table 1.1: Summary of recent VSC-HVDC projects

Project Name	Year	P (MW)	V_{AC} (kV)	V_{DC} (kV)	DC link (km)	Comments and Reasons for VSC-HVDC Choice
Gotland, *Sweden*	1999	50	80	±80	(2×70)*	Wind power voltage support.
Eagle Pass, *USA*	2000	36	132	±15.9	B2B	Controlled asynchronous connection for trading. Voltage control.
Tjaereborg, *Denmark*	2000	7.2	10.5	±9	(4×4.3)*	Wind power (Demonstration project).
DirectLink, *Australia*	2000	180	$110^{(Bungalora)}$_ $132^{(Mullumbimby)}$	±80	(6×59)†	Controlled asynchronous connection for trading.
MurrayLink, *Australia*	2002	220	$132^{(Berri)}$_ $220^{(RedCliffs)}$	±150	(2×180)†	Controlled asynchronous connection for trading.
CrossSound, *USA*	2002	330	$345^{(NewHeaven)}$_ $138^{(Shoreham)}$	±150	(2×40)*	Controlled connections for power enhancement.
Troll offshore, *Norway*	2005	84	$132^{(Kollsnes)}$_ $56^{(Troll)}$	±60	(4×70)*	Environmental merit; Compactness of converter on platform.
Estlink, *Estonia-Finland*	2006	350	$330^{(Estonia)}$_ $400^{(Finland)}$	±150	(2×31)† (2×74)*	Connection of asynchronous AC systems.
Valhall offshore, *Norway*	2009	78	$300^{(Lista)}$_ $11^{(Valhall)}$	±150	292*	Cost reduction; Efficiency improvement; GHG emission Minimization.

*Submarine Cable
†Underground Cable

1.8 WE Integration via VSC-HVDC Technology

RE is continuously innovated in new global markets. Although the renewable electricity generation centers are often far from consumption points, it is necessary to transmit large energy amounts with minimal losses. For this purpose, several projects using HVDC technologies in combination with RE are currently being developed especially via submarine cables [7, 8, 9, 10].

The wind may be more stable offshore, but there will be less geographical smoothing effect, so wind variations will still be a key issue. Power transmission and grid connection represent other main challenges for realization of large scale wind power, and especially for offshore wind farms [53]. In addition, reactive power can be supplied at the offshore station for the WTGs, and it can also be supplied at the onshore stations to regulate the voltage. Furthermore, active power can be used to control the grid frequency, in case it is weak.

To be profitable, large-scale development of WE production will require state-of-the-art HVDC technology as previously mentioned. This technology combines the flexibility, transmission capacity, controllability and operability required both by technical and commercial requirements [86]. By using HVDC, transmission grids can be optimized and controlled to support the introduction of renewable generation into the grid [86].

The offshore network may act as a power pool where power may be injected to and extracted from the network at different nodes. Thus, flexibility to control direction of power in the network is required while governing the voltage. For such a situation, implementation of VSC-HVDC technology is favorable [87]. VSC-HVDC transmission systems may be preferred compared to the conventional HVDC technology for certain power levels [63]. Moreover, a general control strategy would be required in order to regulate the power flows in the offshore network and the exchange of power with onshore power systems [87].

When connecting a wind park to the main grid by means of a VSC transmission system, the wind park is disconnected from the main grid. This results in several technical and economical benefits for Transmission System Operators (TSOs), wind park developers and WTG's manufacturers.

From TSOs point of view, a VSC-connected wind park becomes comparable to a normal power plant (although a generation with intermittent operation). The main grid-side of the VSC converter can be directly connected to a control or power dispatch center [86]. Additionally, AC faults appearing in a wind park or main grid will not be propagated by the VSC transmission system, thus, less mechanical stress on WTGs is provided. Furthermore, the inherent VSC voltage and frequency control capability simplifies wind park black starts and its energization transients will not transfer to the main grid [88]. The following summarizes the main features of VSC-HVDC transmission for large-scale offshore wind power evacuation [88]:

- VSC-HVDC can fully cope with grid code;
- WTGs no longer need to be designed for fulfilling the grid code, and the optimization can focus on cost, efficiency and robustness;
- VSC-HVDC can separate the wind farm from the AC network. Thus, faults in the AC grid will not give stress or disturbances on the wind turbine. Moreover, faults in the wind farm will not affect the AC network;
- VSC-HVDC provides voltage and frequency control, and it can be used for enhancing the stability of the AC network.

The planned France-Spain interconnection line is a clear example where the implementation of a VSC-HVDC interconnection is chosen as a technically and environmentally feasible solution [89]. The aim is to address cross-border congestions (frequently occurring in both directions), enhancing the net transfer capacity and avoiding overloading of the transmission line, with a clear environmental advantage over conventional HVAC transmission [89].

1.9 Conclusions

HVDC today is a very mature technology that is still developing rapidly into higher voltages and higher power and more flexibility. The world faces tremendous challenges on energy supply to growing population.

If this energy should be supplied without damage to the environment; new types of generation will be required such as distant hydro, wind at sea and solar generation in the deserts. All this require transmission of huge electric energy amounts over long distances. HVDC is the most suitable technology for this task [68]. Thus, HVDC will have a great and considerable role in the future to create a more sustainable world.

Furthermore, VSC-HVDC technology is now emerging as a robust and economical alternative for future transmission grid expansion. Thus, well-controlled VSC-HVDC applications could significantly improve overall system performance, enabling smart operation of transmission grids with improved security and efficiency.

In addition, VSC-HVDC transmission also offers a superior solution for many challenging technical issues associated with integration of large-scale RE sources such as offshore wind power.

Consequently, for VSC-HVDC transmission links, where parameters uncertainties are involved in the plant operation. These uncertainties result from either poor modeling or abnormal situations. Therefore, nonlinear control design which is robust under all possible normal and abnormal situations is a must. Thus, nonlinear control and stabilization of VSC-HVDC transmission systems in presence of parameter uncertainties will be extensively shown and explained in the rest of the thesis.

Chapter 2

Nonlinear Control Systems

THIS chapter provides an overview of both robust and adaptive nonlinear control used for VSC-HVDC transmission system's stabilization and performance enhancement. Then, the main reasons of parametric uncertainties existed in electrical power systems are clearly stated. Moreover, the basic concepts of variable structure systems control theory comprising both SMC and AOT control, with the provision of minimal mathematical derivations, are surveyed. An extended explanation for SMC theory and design are pointed out. The features and drawbacks of SMC are discussed. Finally, the state-of-the-art techniques for solving the problem of chattering are explicated.

2.1 Introduction

The control of uncertain nonlinear systems has become an important subject of research. Accordingly, considerable progresses in both nonlinear adaptive and robust control techniques have been attained. Among these techniques, the design approaches based on Lyapunov's direct method or the phase plane one have offered analysis tools for nonlinear controllers construction. Since they are not systematic, their application to complex systems often fails. In absence of parameters uncertainties, backstepping approach can be used to force a nonlinear system to behave like a linear one in a new set of coordinates. However, backstepping and other forms of FL control require cancelation of nonlinearities, even those which are helpful for stabilization and tracking.

A major advantage of backstepping is its flexibility to avoid cancelations of useful nonlinearities and to pursue the stabilization and tracking objectives, rather than that of linearization. Intuitively, FL approaches, including the backstepping approach [90, 91] do not guarantee robustness under parameter uncertainties or unmodeled dynamics.

Recently, great attention has been paid to control design for nonlinear and uncertain plants by using the theory of Variable Structure Systems (VSS) [92]. A central feature of VSS's control is sliding mode, which occurs when the system state repeatedly crosses certain subspaces, or sliding surfaces, in the state or error vector space. The design of the sliding surface completely determines the closed-loop system performance [93, 94]. When a certain matching criterion holds, nonlinear VSS's control can yield invariance to parameter uncertainties and external disturbances [92, 95]. A difficulty in applying the VSS's control approach is the need of full state knowledge [94]. Practically, it is neither possible nor feasible to have full information regarding the state. Thus, when the state cannot be measured, the output is measured instead. Moreover, the use of state observers is a natural step towards the relaxation of this condition. However, the system implementation complexity is increased, and only asymptotic tending of the state to the sliding surface can be achieved. In order to simplify the system control implementation, the output feedback or Asymptotic Output Tracking (AOT) control can be applied instead of the state feedback [96, 97].

SMC [98, 99] based on VSS theory, that explicitly accounts for an imprecise description of the controlled plant model, guarantees the control targets attainment in the presence of modeling errors, parameter uncertainties, and/or external disturbances. SMC approach has been proved efficient technique to provide high-fidelity performance for different control problems. Theoretically, ideal sliding modes are of infinite-frequency switching. However, real conventional sliding modes feature high finite frequency switching of the input signal (control) due to switching element imperfections, discrete-time control implementation or unmodeled plant dynamics. During the sliding mode, the system possesses high robustness against various kinds of uncertainties [100]. In spite of robustness properties, high frequency oscillations of the state trajectories around the sliding manifold, known as chattering phenomena [101, 102], are found. Chattering is considered as the major SMC implementation obstacle. Different methods have been proposed to reliably prevent it such as boundary layer solution [103], observer-based solution [102], and either higher order or integral SMC [104, 105].

An appropriate control law modification via using continuous high-gain saturation functions, or hyperbolic tangent functions instead of the sigmoid ones can be employed to eliminate chattering [102, 106, 107].

2.2 Theoretical Background

Feedback has often had revolutionary consequences with drastic improvements in control performance. The Proportional—Integral—Derivative (PID) controller, which involves three separate parameters: the integral (I), proportional (P) and derivative (D) that are respectively based on the past, present and future control error, is the generic control loop feedback mechanism (controller) widely used in industrial control systems [108, 109]. The weighted sum of these three actions is used to adjust the process via a control element. The error, the difference between the measured process variable and the desired set-point, is minimized by adjusting the process control inputs. To attain significant performance, the PID parameters used in the calculation must be tuned according to the nature of the system, its parameters and operating conditions. The controller response can be described in terms of how it is responsiveness to an error, the degree to which the controller overshoots the set-point, and the degree of system oscillation. The PID control algorithm guarantee neither system's optimal control nor stability. Some applications may require only one or two modes to provide appropriate system control. This is achieved by setting the gain of undesired control outputs to zero. Thus, the PID controller will be called a PI, PD, P or I controller in the absence of the corresponding control actions. PI controllers are fairly common, since derivative action is sensitive to measurement noise, whereas the absence of an integral value may prevent the system from reaching its target value due to the control action.

While PID controllers are applicable to many control problems, and often perform satisfactorily. However, they can act poorly in some applications, and do not in general provide optimal control. The fundamental difficulty with PID control is that it is a constant parameter feedback system with no direct knowledge of the process [108]. The most significant improvement here is to incorporate feed-forward control with knowledge on the system, and to use the PID only to error control.

Alternatively, PIDs can be modified in other ways like changing the parameters (either gain scheduling in different use cases or adaptively modifying them based on performance), improving measurement (higher sampling rate, precision, accuracy, and low-pass filtering if necessary), or cascading multiple PID controllers.

PID controllers, when used alone, can give poor performance or even cause instability. When the PID loop gains must be reduced, the control system does not overshoot, oscillate or hunt about the control set-point value. They also have difficulties in presence of non-linearities, may trade-off regulation versus response time, do not react to changing process behavior, and delay in responding to large disturbances [108, 109]. To overcome the risk of either system's performance degradation or system instability when using PID controllers; adaptive or robust nonlinear controllers have been used instead to gain considerable system performance particularly in presence of process dynamics, nonlinearities, parameter uncertainties and/or external disturbance [108, 109].

2.3 Adaptive versus Robust Nonlinear Control

Two nonlinear control approaches principally account for system models' uncertainties and/or external disturbances. Adaptive controller, the first approach, is a controller with adjustable parameters and a mechanism for adjustment (fine-tuning) which is used to deal with plant uncertainty and/or time-varying parameters. Its basic idea is to have a controller which tunes itself with respect to the plant being controlled. Self-tuning devices are appreciably successful, but they involve on-line design computations and therefore are not as simple to be implemented as a fixed controller. The ideal adaptive control would be a dual control, in which the control signal is optimal for both plant estimation and control. However, dual control is computationally prohibitive.

Robust control, the second approach, can deal with uncertainties in fixed controller design. It is insensitive to parameter uncertainties and/or external disturbances [110, 111, 112, 113].

2.3.1 Adaptive Control

Adaptive control for nonlinear systems is defined as nonlinear dynamic (state or output feedback) compensators capable of guaranteeing asymptotic tracking of an output reference signal for any unknown parameter vector and any closed loop system initial

condition when time varying disturbances are absent [110, 111, 112, 113]. Adaptive controllers typically consist of a Linear Time Invariant (LTI) compensator together with an identifier (or tuner) used for compensator parameters adjustment.

Most adaptive controllers up to date, unfortunately, have several major drawbacks: (a) they do not track very well time-varying parameters; (b) only asymptotic results are typically proved, however, the transients may be poor; (c) they are nonlinear, so the effect of the Initial Conditions (ICs) and the exogenous input are coupled; and finally (d) the control signal can become quite large (in comparison to what the control signal would be if the plant parameters were known and the "*correct*" LTI compensator were applied) [110, 111, 112, 113].

2.3.2 Robust Control

Robust control deals generally with the nonlinear controller design in presence of plant uncertainties. This can simultaneously cover: parameter variations (affecting low- and medium-frequency ranges) and unstructured model uncertainties (often located in the high-frequency range). Although the control adaptation will handle the parameter variations, conversely, the problem of managing unstructured model uncertainties may remain [110, 111, 112, 113].

Until recently, robust control and adaptive control have been viewed as two techniques that compete with each other to cope with plant model uncertainties. However, the latest developments indicate that both techniques complement each other, thus, an adaptive control can be built on top of a robust one in order to marry the both controls' advantages [110, 111, 112, 113].

Forcing mechanical and electrical structures to follow a desired trajectory is emphatically a fundamental task for various applications and products particularly electrical power systems. These systems are governed by a set of nonlinear and strongly coupled differential equations. Accordingly, they pose a challenge when designing control algorithms to meet the highly appreciated demands of precision and fast response time especially in the presence of system parameter uncertainties.

2.4 Power System Uncertainty

There are many causes of power system's operating conditions' variations. For instance, the most common uncertainties which are a matter of great concern to design robust controllers for power systems are [114]:

- Variation of operating conditions of the generation units as well as the continual changes in the load power consumption;
- Variation of the power system's structure, primarily due to changes in the network configuration and the generation unit's number;
- Uncertain parameters of the power system elements, which are mainly caused by parameter's variation due to either climate changes, alteration of the power system operation mode, or simply erroneous parameter assessment;
- Bad approximations in power system modeling, resulting in unstructured uncertainties mostly caused by the physical or topological model reduction, or, by the linearization of power systems' nonlinear models.

VSC-HVDC transmission systems can be influenced by either external or internal interference of uncertainties. Attention is thus paid to both power system uncertainty and operating conditions' variations especially due to either changes in the network configuration, erroneous parameter assessment, alteration of power system operation modes, or bad approximations in power system modeling.

Indeed, parametric uncertainties such as: load power consumption variation (load impedance value), either DC or AC line impedance stochastic fluctuations caused by the thermal effects on the line resulted from high currents flow though the cable reasoned of online switching or faults, in addition to frequencies' disadjustments due to the unexpected unbalance between the power system generation and demand, are taken into consideration.

2.5 Variable Structure System Control

The nonlinear system's trajectory control requires control schemes that take into account system nonlinearities, modeling uncertainties as well as disturbances. Various VSS control algorithms have been successfully used for trajectory tracking problems because they leads to an explicit high performance systems that are robust to parameter uncertainties and noise.

VSSs often exhibit a peculiar behavior (called "*sliding mode behavior*" or "*sliding motion*"), characterized by the fact that the commutation between different system structures takes place at infinite frequency. The control laws based on VSSs are designed so that the system trajectory always reaches the sliding surface. This is known as the reaching phase. Once on the sliding surface, the control structure is changed discontinuously to maintain the system on the sliding surface. At this stage, the system is in the sliding phase. Linear or nonlinear control laws may be supposed during either the control's whole mission or parts of it. Their structures change according to a preselected switching logic that depends on the system state along the trajectory [95, 115, 116].

Popular VSS control approaches for trajectory tracking problems are based on Lyapunov method which yields multivariable designs to produce sliding mode on the intersection of several switching surfaces.

Principally, VSSs can be represented by the parallel connection of several different continuous subsystems (called structures) that act one at a time in the input-output path as shown in Figure 2.1.

2.6 Sliding Mode Control

SMC, developed in early 1950s by V. Utkin, has been proved successful in control problems. It has been recognized as an efficient tool for robust controllers design in complex high-order nonlinear dynamic plants operating under various uncertainty conditions. SMC, based on VSS control theory, provides means to overcome poor performance or instability problems and to guarantee robustness under parameter uncertainties resulted when PID controllers are used [117, 118]. SMC's major advantage is its low sensitivity to parameter variations and disturbances which relaxes the necessity of the system's exact modeling [119].

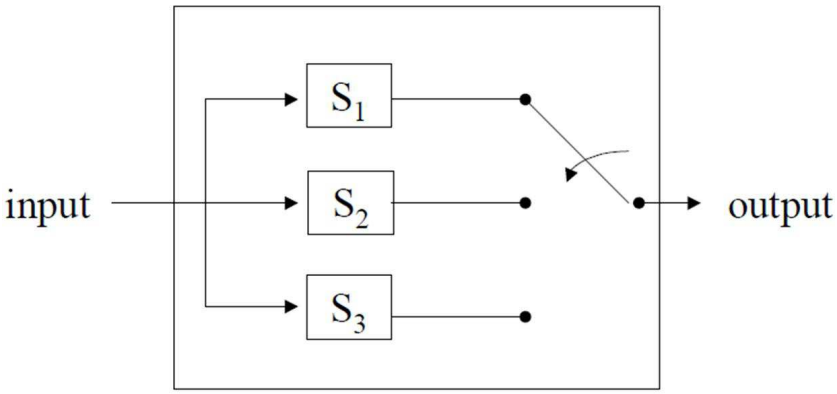

Figure 2.1: The controlled VSS representation.

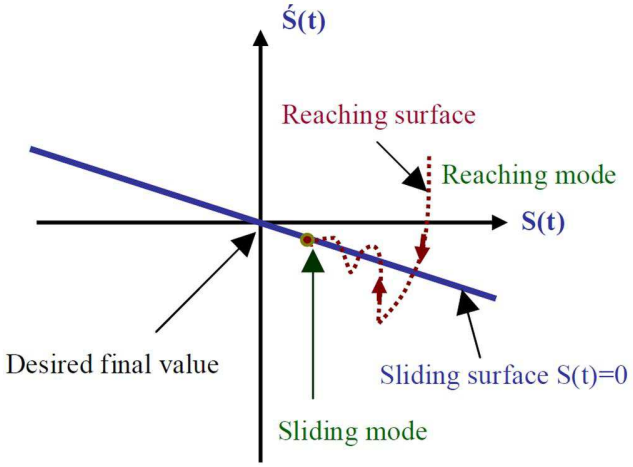

Figure 2.2: Graphical interpretation of SMC.

The SMC approach consists of two steps: The **first step** is the choice of a manifold in the state space. Once the state trajectory is constrained on it, the controlled plant exhibits the desired performance. The **second step** is represented by the design of a discontinuous state-feedback capable of forcing the system state to reach, in finite time, such a manifold (accordingly called "*sliding manifold*").

As depicted in Figure 2.2, it is clear that the idea behind the SMC is to derive the system state trajectory and to force the error signal to approach the sliding surface, $S(t) = 0$, and then slide along it until reaching the desired final value.

During the sliding motion, if the so-called "*invariance principle*" can be invoked; any system belonging to a certain set behaves in the same way (semigroup property). Consequently, different systems performing a sliding mode on the same manifold may exhibit the same behavior, which depends only on the manifold on which the sliding mode occurs. In certain sense, the sliding mode erases the original system's dynamics, and replaces it with the one specific for the sliding manifold [95].

To clarify, the class of nonlinear time-invariant systems, which is linear with respect to the control, is algebraically expressed in the form [90]:

$$\begin{aligned} &\dot{x} = f(x) + G(x)\,u + z(x) \\ &\dot{x} = f(x) + \sum_{i=1}^{m} g_i(x)\,u_i \;+\; z(x) \qquad with\ x(t_0) = x_0 \end{aligned} \tag{2.1}$$

where $x \in \mathbb{R}^{\mathrm{n}}$ is the system state and $u \in \mathbb{R}^{\mathrm{m}}$ represents the control input. The vector functions $f,\ g : \mathbb{R}^n \longmapsto \mathbb{R}^n$ and the matrix $G(x) = (g_1 \;\; g_2 \;\cdots\; g_m)$ are assumed to be continuously differentiable. The vector function $z : \mathbb{R}^n \longmapsto \mathbb{R}^n$ summarizes the unknown parameter uncertainties and external disturbances. SMC theory deals with the state feedback control schemes that use switching control actions. The control input $u(x)$ is therefore chosen as a discontinuous function of the system state, thus:

$$u(x) = \begin{cases} u^+(x) & \text{for} \quad s(x) > 0 \\ u^-(x) & \text{for} \quad s(x) < 0 \end{cases} \tag{2.2}$$

where $s \;:\; \mathbb{R}^n \longmapsto \mathbb{R}^m$ is a continuously differentiable function. The feedback signal $u(x)$, which is not a continuous function of time, exhibits a discontinuity point at $s(x) = 0$ as:

$$\lim_{s(x)\to 0} u^+(x) \neq \lim_{s(x)\to 0} u^-(x)$$

Due to its robustness, SMC has been successfully applied in different trajectory tracking applications of electrical power systems structures particularly for the stabilization and performance enhancement of VSC-HVDC transmission systems as will be shown later in the thesis.

2.7 Lyapunov Stability Theorems

For SMC design, a number of approaches can be employed, in particular, the method based on the selection of Lyapunov function [90].

Consider a Lyapunov function $V(x) : \mathbb{R}^{n} \longmapsto \mathbb{R}^{m}$ such that $V(0) = 0$. In the sense of Lyapunov, the system is asymptotically stable for:

- $V(x) > 0$: positive definite
- $\dot{V}(x) < 0$: negative definite

In order to conclude global asymptotic stability, an additional condition called "*properness*" or "*radial unboundedness*" is essentially required.

For fulfilling asymptotic stability condition, the control input should be chosen such that the Lyapunov function candidate satisfies Lyapunov stability criteria, then:

$$V\left(x\right) = \frac{1}{2} s^{2}\left(x\right) \tag{2.3}$$

Its derivative $\dot{V}(x) = s(x)\dot{s}(x) < 0$ should be negative definite. Thus, one of the following single term formula or two-terms formula can be supposed for $s(x)$ while allowing positive values for the tuning gains K, K_1, and K_2.

Single term formula:

$$\dot{s}\left(x\right) = -K \ func(s\left(x\right))$$

Two-terms formula:

$$\dot{s}\left(x\right) = -K_1 \ s\left(x\right) - K_2 \ func(s\left(x\right))$$

$func(s(x))$ can be either the *sign*, *sat*, and tanh functions that respectively refers to the sigmoid, saturation and hyperbolic tangent functions that are defined as:
Sigmoid function:

$$sign(s(x)) = \begin{cases} 1 & s(x) > 0 \\ 0 & s(x) = 0 \\ -1 & s(x) < 0 \end{cases}$$

Saturation function:

$$sat(s(x)) = \begin{cases} 1 & s(x) \geq 0 \\ s(x) & -1 \leq s(x) \leq 1 \\ -1 & s(x) \leq 0 \end{cases}$$

Hyperbolic tangent function:

$$\tanh(s(x)) \ = \frac{e^{2s(x)} - 1}{e^{2s(x)} + 1}$$

On the other hand, for AOT control:

$$\dot{s}\,(x) = -K\ s(x)$$

Either *sat* or *tanh* function can be used instead of the *sign* function in order to avoid the discontinuity point 'singularity' at the zero point. Making use of these continuous functions guarantee the avoidance or reduction of highly undesirable chattering which is caused by the imperfect switching that results from the impossible achievement of infinitely fast switching control via AOT or single term SMC.

2.8 Existence Conditions and Control Design

To ensure that the system state remains in sliding mode after reaching it, the existence conditions stated in Equation (2.4) have to be fulfilled [102].

$$\lim_{s(x)\to 0^+} \dot{s}\ (x) < 0 \qquad \text{and} \qquad \lim_{s(x)\to 0^-} \dot{s}\ (x) > 0 \tag{2.4}$$

To guarantee that the manifold is reached after a finite period of time and independent of the systems' ICs, the sufficient reaching condition expressed in Equation (2.5) should also be satisfied in addition to Equation (2.4) .

$$\dot{s}s < 0,\ \forall\ s \neq 0 \tag{2.5}$$

In terms of Lyapunov's theory, the existence and reaching conditions for sliding mode can be summarized as follows:
If there exists a Lyapunov function

$$V\,(s) \in\ \mathbb{R}^+ : \begin{cases} V\,(s) = 0 & \text{for } s = 0 \\ V\,(s) > 0 & \text{for } s \neq 0 \end{cases} \tag{2.6}$$

and a constant $\varepsilon > 0$ satisfying the condition

$$\dot{V}(s) \leq -\varepsilon\sqrt{V} \tag{2.7}$$

Sliding mode exists on the manifold $s = 0$ and is reached within finite time after starting from any initial state. Condition stated in Equation (2.7) guarantees finite transient time. If only $\dot{V}(s) < 0$ were fulfilled for all $s \neq 0$ with $\lim_{s\to 0} \dot{V}(s) = 0$, then the points of attraction defined by $s = 0$ would only be asymptotically stable and would not be reached in finite periods of time. This situation is common for differential equations with the right-hand side satisfying the Lipschitz condition. Domains of attraction for sliding mode controllers may be found due to nonlinear control theory. The reaching condition provides a design rule for sliding mode controller. Two approaches for possible SMC design methods for systems with vector control input can be used, i.e., the component-wise control approach and the unit control one.

2.9 Chattering Issue

SMC applied to nonlinear systems frequently shows an undesired effect, known as chattering, which results from the control's discontinuous nature. Chattering is the main SMC design's obstacle. This undesirable effect is caused by: high bandwidth dynamics which are often neglected in the open-loop plant model used for control design. In SMC implementations, this dynamics is excited by the switched control input. Furthermore, the infinitely high switching frequencies assumed in SMC theory cannot be realized in practice. Assuming that the control unit can switch ideally, chattering may also be caused by unmodeled dynamics in the plant. Subsequently, unacceptable finite-amplitude high-frequency oscillations to the controlled system behavior result.

This chattering phenomenon can cause undesirable audible noise, poor control accuracy, high wear of moving mechanical parts, and high heat losses in power circuits. As there is usually a trade-off between chattering reduction and robustness, chattering can be reduced without sacrificing robustness in the control design [90].

Obviously, the reasons of chattering may be assigned to different components of the electromechanical system, as illustrated in Figure 2.3.

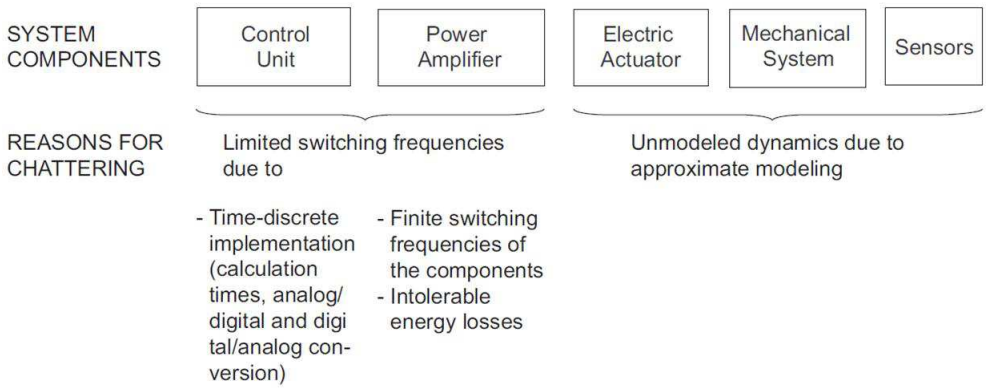

Figure 2.3: Reasons for chattering in sliding mode controlled electromechanical systems.

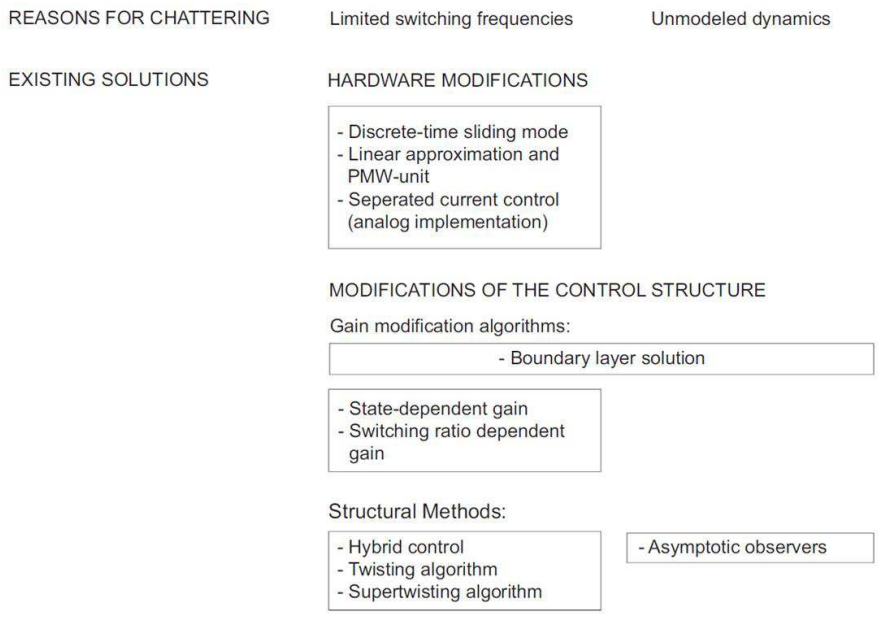

Figure 2.4: Chattering reduction methods.

2.10 Chattering Reduction Concepts

For chattering reduction, different concepts exist. They can be categorized as methods that modify the hardware or the control structure as displayed in Figure 2.4. Schemes that change the control structure can be classified in gain modification algorithms and structural methods. Some methods offer a trade-off between chattering reduction and robustness. Others are quite effective but hard to implement.

To reduce chattering, an integrator to smooth the switching function can be considered. Boundary layer solution, observer-based solution and higher order SMC can be proposed. Additionally, linear approximations of the discontinuous control input can be used. Alternatively, fuzzy or neural networks merged with SMC theory are supposed [102, 103, 104, 105, 106, 107].

In this thesis, the sigmoid function is replaced by either continuous high-gain saturation function, or hyperbolic tangent one to reduce chattering and to achieve considerable control robustness.

2.11 Conclusions

The difference between both robust and adaptive control of nonlinear systems have been presented. The vital causes of electrical power systems uncertainties are noticeably demonstrated. Then, SMC theory and its control design methodology are summarized.

The main characteristics, features and drawbacks of SMC methodologies are highlighted. Explicitly, the principle advantages of the SMC approach are its simplicity (of both design and implementation) as well as its efficient performance and significant robustness. Chattering problem is the main reason of generalized criticism towards SMC. This later presumes that the controlled system model is known exactly and the switching frequency of the control input is infinite. As a result, SMC schemes real-life applications often show some chattering effects in presence of parameter uncertainties.

In recent years, semiconductor technologies have rapidly improved. Solid state switches that allow high switching frequencies together with minor energy losses are available. These modern devices make pure SMC algorithms a viable option for control problems involving nonlinearities and/or parameter uncertainties. Hence, the superb and simple theoretical properties of SMC design are provided with minimal algebraic derivations and explanations.

The thesis target is to develop a robust nonlinear control for VSC-HVDC transmission system stabilization and performance improvement. The chattering reduction while maintaining the controller's robustness properties besides keeping the control design process simple is taken into account. For this purpose, nonlinear control techniques, based on VSS theory such as both SMC and AOT control that account for an imprecise description of the controlled plant model and guarantee the control targets attainment, will be explicitly applied to provide high-fidelity performance for the system in the presence of modeling errors and parameter uncertainties. The use of both SMC and AOT control methodologies, as will be shown later in the thesis, will yield a smooth control and considerable performance in the control implementation. Consequently, less chattering and better convergence accuracy while preserving the controller's robustness properties will be demonstrated.

Chapter 3

VSC-HVDC Modeling, Control and Stabilization

This chapter deals with the control, stabilization and performance enhancement of VSC-HVDC transmission systems under parameter uncertainties. For this purpose, the simplest yet conventional PI control is applied to the generator-load (GL) VSC-HVDC transmission system. Moreover, the generator-generator (GG) VSC-HVDC transmission one -that exhibits a nonlinear character- is then controlled via Lyapunov theory based nonlinear control methodologies such as AOT or SMC approaches in order to enhance the system performance and improve its stability.

For the GL VSC-HVDC system with unidirectional power flow, the steady state mathematical model is comprehensively described and deduced. Then, the feedback conventional PI controllers are proposed in order to govern the DC link voltage and to control the reactive power while observing the active power dynamic performance. The system's dynamic behavior is explicitly demonstrated and analyzed in presence of load resistance variations, AC reactance changes and step in the reference signals.

For the GG VSC-HVDC systems with directional power flow, the overall system state space representation is developed. Appropriate feedback control signals, as a combination of state space variables and outputs, are hence formulated to control the active and reactive powers at the AC terminal of either VSCs via Lyapunov theory based nonlinear control such as AOT or SMC. Furthermore, the DC voltage and the reactive power are governed to their desired reference values for the other converter.

Desirable unity power factor is revealed for zero reactive power reference. The DC link power losses and voltage drop are considered. The results are introduced to evaluate the robustness of the nonlinear controllers and their flexibility towards acquiring favorable tracking performance, improving the system's dynamic behavior and enhancing its stability for different DC link lengths considering parameter uncertainties such as DC cable and AC line parameter variations.

3.1 Introduction

VSC-HVDC is a newly developed HVDC transmission technology in favor of the ever increasing penetration of the power electronics technologies into power systems mainly due to the continuous progress of high-voltage high-power fully controlled semiconductors. It is mostly based on extruded DC cables and VSCs with IGBT technology. The high power IGBT development allows the use of VSCs in HVDC systems in a frequency range of 1-2 kHz [7, 120] with much lower harmonic distortion than in the conventional HVDC systems. The VSC-HVDC transmission system connects AC networks and includes converters at each AC side. The control of DC voltages and power flows is of primary necessity and importance.

Under strict environmental and economical constraints due to the deregulation, the VSC-HVDC system provides a significant promising solution to power transmission and distribution thanks to its unique features [16, 121, 122, 123]:

- The active and reactive power exchange can be controlled flexibly and independently;
- The power quality and system stability can be improved via continuously adjustable active and reactive powers supported with AC voltage feedback control;
- The ability of feeding AC systems with low short circuit power or even passive networks with no local power generation.

Since an electrical power system is a disturbed network, its global information is not available real time, and the system's parameters and topology often change [124, 125].

The VSC-HVDC transmission system, which is one of these nonlinear electrical power systems, is accordingly characterized by parameter uncertainties, neglected dynamics, as well as time dependence. The control of such systems has been a serious challenge to the control community [102, 126]. Advanced nonlinear control techniques has consequently become a must to improve the power system stability. This later is defined as the power system ability to attain an acceptable steady-state behavior under operating conditions' variations and/or after an unexpected disturbance [27, 127].

Contrary to the design of classic control systems, where linearized models depend on a certain operating point, the advanced control techniques allow the controlled system to face parameter uncertainties and/or large disturbances due to the use of the whole structural properties.

In this chapter, the load quantity and the AC reactance variations are considered as system parameter uncertainties in case of GL VSC-HVDC systems. Other uncertainties such as the change in the DC cable or AC line impedance will be proposed for the GG VSC-HVDC systems. These uncertainties are often caused by the thermal effects entailing the flow of high currents in the cable in consequence of faults or on-load switching, or reasoned by the variation of the system topology, or due to the unbalance between the system's power generation and the demand.

After the development of both VSC-HVDC systems' mathematical model, conventional PI control besides AOT and SMC are applied for the system's control design. For these nonlinear approaches, the final control laws are derived step by step through VSS theory. Thus, the design process is not complex. Considering various parameter uncertainties, such as DC cable and AC line parameter variations, the controllers' robustness, their dynamic performance and system stability are hence assessed.

3.2 D-Q transformation theory

The substitutions which replace the synchronous machine variables associated with the stator windings (currents, voltages, and flux linkages) with another variables related to fictitious windings rotating with the rotor was first investigated by Park [128]. Therefore, a polyphase winding can be reduced to a set of two phase windings with their magnetic axes aligned in quadrature as depicted in Figure (3.1).

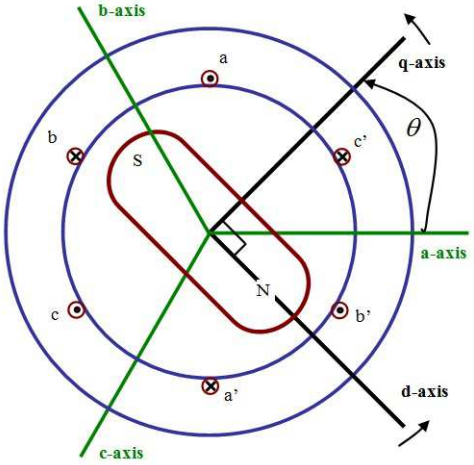

Figure 3.1: *d-q* representation in synchronous machines.

The *d-q* axis transformation eliminates the phase-winding's mutual magnetic coupling. Consequently, the magnetic flux linkage of one winding becomes independent of the current in the other winding. This transformation system allows both polyphase windings in the machine's stator and rotor to be viewed from a common reference frame, which may rotate at any angular speed or remain fixed to the stator. The reference frame can be assumed to be rotating at any arbitrary angular speed.

For explicitly, let S represents any of the synchronous machine variables (current, voltage, or flux linkage) that to be transformed from the *a-b-c* frame to *d-q* frame, therefore, the relation $S_{dq0} = [P]S_{abc}$ is used.

Under balanced 3-phase systems, the zero sequence component S_0 is always zero. The Park transformation equation is given by:

$$\begin{bmatrix} S_d \\ S_q \\ S_0 \end{bmatrix} = \underbrace{\frac{1}{3}\begin{bmatrix} \sin\theta & \sin\left(\theta - \frac{2\pi}{3}\right) & \sin\left(\theta - \frac{4\pi}{3}\right) \\ \cos\theta & \cos\left(\theta - \frac{2\pi}{3}\right) & \cos\left(\theta - \frac{4\pi}{3}\right) \\ 1 & 1 & 1 \end{bmatrix}}_{[P]} \begin{bmatrix} S_a \\ S_b \\ S_c \end{bmatrix} \tag{3.1}$$

3.3 Mathematical Modeling of GL VSC-HVDC systems

The converter substation of the GL VSC-HVDC system scheme shown in Figure (3.2) is coupled with an AC network via an equivalent impedance $R_{L1} + jX_{L1}$. The AC generator is directly connected to the load with unidirectional power flow.

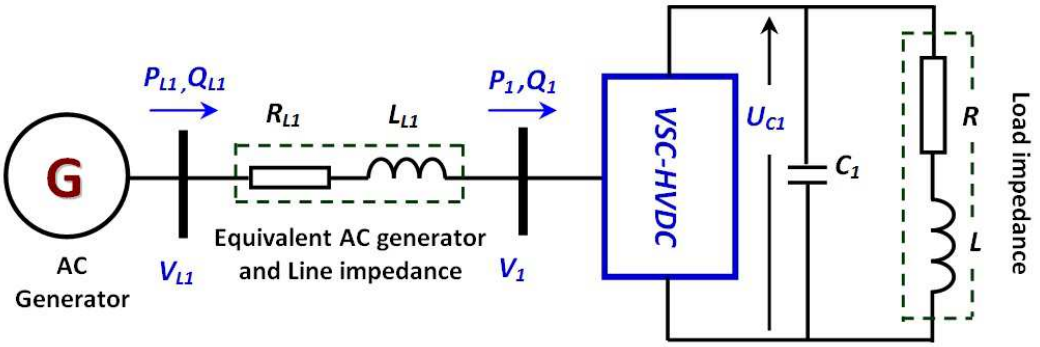

Figure 3.2: Physical model of GL VSC-HVDC system.

The DC capacitor C_1 is used across the VSC's DC side during feeding a load of an equivalent impedance $R + jX$. Both R and L respectively refer to the load equivalent resistance and its equivalent inductance.

For transmission applications, DC filters and zero-sequence blocking reactors can be used to mitigate interference on any metallic telephone circuits existed adjacent to the DC cables.

The AC network at the terminal is assumed very strong. Hence, the AC network can be modeled as an AC voltage source due to the relatively small capacities of most of VSC-HVDC systems compared to that of power systems [42].

The rectifier substation is devoted to control the reactive power Q_1 and to govern the DC bus voltage U_{C1} while noticing the active power P_1 performance in the VSC-HVDC continuous-time equivalent model depicted in Figure (3.3) [42, 44, 129, 130, 131]. From this model, the voltage drop in each phase 'ph' is given by:

$$L_{L1}\frac{di_{L1_{ph}}}{dt} + R_{L1}i_{L1_{ph}} = v_{L1_{ph}} - v_{1_{ph}} \tag{3.2}$$

According to the d-q phasor diagram illustrated in Figure (3.4) and for a duty cycle r_1, the following set of equations is demonstrated considering a balanced three phase system rotating at a pulsation ω_1 with $\theta = \omega_1 \times t$, and d-q rotating frame initially oriented on θ:

$$\begin{cases} \overrightarrow{v_{L1}} = V_{L1}\ e^{j\gamma_1} = V_{L1}\cos(\gamma_1)\ + jV_{L1}\sin(\gamma_1)\ = V_{L1_d} + jV_{L1_q} \\ \overrightarrow{v_1} = V_1\ e^{j\psi_1} = V_1\cos(\psi_1)\ + jV_1\sin(\psi_1)\ = V_{1_d} + jV_{1_q} \\ \overrightarrow{i_{L1}} = I_{L1}\ e^{j\varphi_1} = I_{L1}\cos(\varphi_1)\ + jI_{L1}\sin(\varphi_1)\ = I_{L1_d} + jI_{L1_q} \end{cases} \tag{3.3}$$

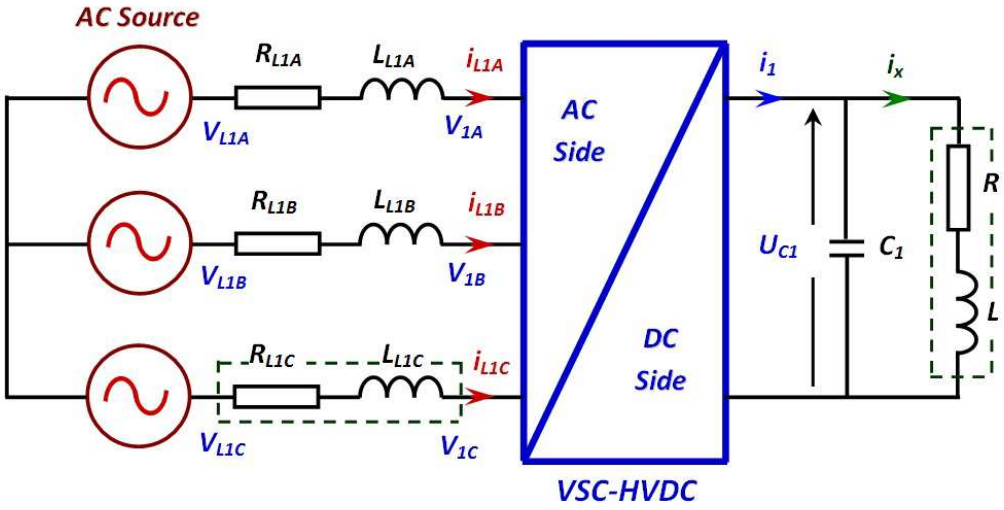

Figure 3.3: Continuous–time GL VSC-HVDC model.

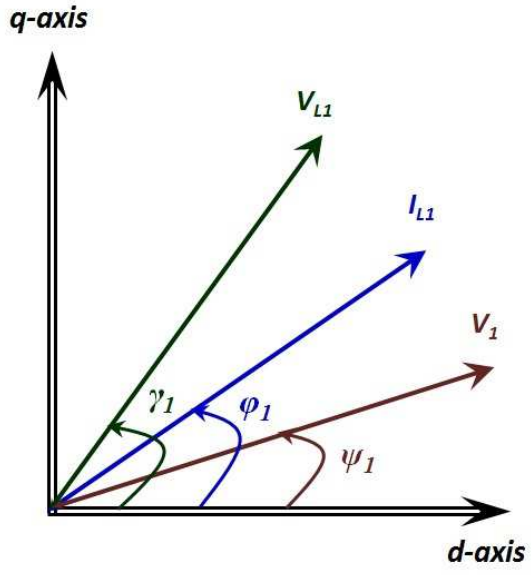

Figure 3.4: d-q phasor diagram.

where v_{L1_d} and v_{L1_q} are the constant *d-q* voltage components of the AC source estimated using Park transformation. i_{L1_d} and i_{L1_q} are the *d-q* current components flowing in the AC line. v_{1_d} and v_{1_q} are the *d-q* voltage components on the AC side of the VSC-HVDC transmission system.

Furthermore,

$$\overrightarrow{v_1} = r_1 \frac{U_{C1}}{2} e^{j\psi_{\omega 1}} \tag{3.4}$$

Taking into account that,

$$\overrightarrow{r_1} = r_1 e^{j\psi_{\omega 1}} = V_{1_{d\omega}} + jV_{1_{q\omega}} \tag{3.5}$$

then,

$$\overrightarrow{v_1} = V_{1_{d\omega}} \frac{U_{C1}}{2} + jV_{1_{q\omega}} \frac{U_{C1}}{2} \tag{3.6}$$

where,

$$\begin{cases} V_{1_{d\omega}} = 2\frac{v_{1_d}}{U_{C1}} \\ V_{1_{q\omega}} = 2\frac{v_{1_q}}{U_{C1}} \end{cases} \tag{3.7}$$

$V_{1_{d\omega}}$ and $V_{1_{q\omega}}$ are the dimensionless *d-q* components that show the relation between the *d-q* voltage components on the AC side of the VSC-HVDC transmission system, v_{1_d} and v_{1_q} respectively, and the DC bus voltage U_{C1}. They present the converter duty cycles.

From the GL VSC-HVDC system illustrated in Figure (3.3):

$$L_{L1} \frac{\overrightarrow{di_{L1}}}{dt} + R_{L1} \overrightarrow{i_{L1}} + j\omega_1 L_{L1} \overrightarrow{i_{L1}} = \overrightarrow{v_{L1}} - \overrightarrow{v_1} \tag{3.8}$$

Substituting from Equation (3.3) into Equation (3.8), the following equations are deduced:

$$L_{L1} \frac{di_{L1_d}}{dt} + R_{L1} i_{L1_d} - \omega_1 L_{L1} i_{L1_q} = v_{L1_d} - v_{1_d} \tag{3.9}$$

$$L_{L1} \frac{di_{L1_q}}{dt} + R_{L1} i_{L1_q} + \omega_1 L_{L1} i_{L1_d} = v_{L1_q} - v_{1_q} \tag{3.10}$$

Applying the loop and node equations for the DC side of the VSC HVDC system, thus:

$$C_1 \frac{du_{C_1}}{dt} = i_1 - i_x \tag{3.11}$$

$$u_{C_1} = L \frac{di_x}{dt} + Ri_x \tag{3.12}$$

Additionally, to derive the active and reactive power equations, the power equality on both sides of the ideal lossless rectifier is applied for a balanced three phase generation, then:

$$U_{C1}I_1 = 3V_1 I_{L1}\cos\left(\psi_1 - \varphi_1\right) \tag{3.13}$$

therefore,

$$I_1 = \frac{3}{4}(v_{1_{d\omega}} i_{L1_d} + v_{1_{q\omega}} i_{L1_q}) \tag{3.14}$$

$$U_{C1}I_1 = \frac{3}{4}U_{C1}(v_{1_{d\omega}} i_{L1_d} + v_{1_{q\omega}} i_{L1_q}) \tag{3.15}$$

Using Equations (3.7) and (3.15), the active and reactive powers entering the rectifier, P_1 and Q_1 respectively, are derived as [42, 129, 130, 131, 132]:

$$\begin{cases} P_1 = \frac{3}{2}(v_{1_d} i_{L1_d} + v_{1_q} i_{L1_q}) \\ Q_1 = \frac{3}{2}(v_{1_q} i_{L1_d} - v_{1_d} i_{L1_q}) \end{cases} \tag{3.16}$$

Similarly, the active and reactive powers supplied by the generator, P_{L1} and Q_{L1} respectively, are estimated by:

$$\begin{cases} P_{L1} = \frac{3}{2}(v_{L1_d} i_{L1_d} + v_{L1_q} i_{L1_q}) \\ Q_{L1} = \frac{3}{2}(v_{L1_q} i_{L1_d} - v_{L1_d} i_{L1_q}) \end{cases} \tag{3.17}$$

The global continuous-time equivalent VSC-HVDC system mathematical model, that indicates the relationships among the systems' different variables, is thus exhibited by the following state space equation form:

$$\begin{cases} \dot{x} = [A]\, x + g(x)u + [R]\, z \\ y = h\left(x, u, z\right) x \end{cases} \tag{3.18}$$

where,

$$\begin{aligned} x_{1,\ldots 4} &= [i_{L1_d},\ i_{L1_q}, u_{C1},\ i_x]^T \\ u_{1,2} &= [v_{1_{d\omega}}, v_{1_{q\omega}}]^T \\ z_{1,2} &= [v_{L1_d}, v_{L1q}]^T \\ y_{1,2} &= [P_1, Q_1]^T \end{aligned}$$

x, u, z and y respectively refer to the state variables, control signals, constant d-q voltage components of the AC source calculated using Park transformation and the output power signals [131, 132].

Explicitly, the system is of fourth order with two control inputs and two outputs. The $[A]$, $g(x)$, $[R]$ and $h(x,u,z)$ matrices are defined as:

$$[A] = \begin{bmatrix} \left(\frac{-R_{L1}}{L_{L1}}\right) & \omega_1 & 0 & 0 \\ -\omega_1 & \left(\frac{-R_{L1}}{L_{L1}}\right) & 0 & 0 \\ 0 & 0 & 0 & \left(\frac{-1}{C_1}\right) \\ 0 & 0 & \left(\frac{1}{L}\right) & \left(\frac{-R}{L}\right) \end{bmatrix}_{4*4}$$

$$g(x) = \begin{bmatrix} \left(\frac{-1}{2L_{L1}}\right) x_3 & 0 \\ 0 & \left(\frac{-1}{2L_{L1}}\right) x_3 \\ \left(\frac{3}{4C_1}\right) x_1 & \left(\frac{3}{4C_1}\right) x_2 \\ 0 & 0 \end{bmatrix}_{4*2}$$

$$[R] = \begin{bmatrix} \left(\frac{1}{L_{L1}}\right) & 0 \\ 0 & \left(\frac{1}{L_{L1}}\right) \\ 0 & 0 \\ 0 & 0 \end{bmatrix}_{4*2}$$

$$h(x,u,z) = \frac{3}{2}\begin{bmatrix} v_{1_d} & v_{1_q} & 0 & 0 \\ v_{1_q} & -v_{1_d} & 0 & 0 \end{bmatrix}_{2*4}$$

The outputs of the state space representation differ according to the objective of the controller. Therefore, $h(x,u,z)$ will be consequently changed. For example, in case of controlling (U_{C1} and Q_1) instead of (P_1 and Q_1), the new matrix $h(x,u,z)$ will be:

$$h(x,u,z) = \begin{bmatrix} 0 & 0 & 1 & 0 \\ \frac{3}{2}v_{1_q} & \frac{-3}{2}v_{1_d} & 0 & 0 \end{bmatrix}_{2*4}$$

The simplified overall VSC-HVDC system block diagram together with its controller (i.e., the conventional PI controller or the Lyapunov (LPV) theory based nonlinear controller) is presented in Figure (3.5). It is mandatory to find out the control inputs u_1 and u_2 with which U_{C1} and Q_1 tracked their reference values.

The following system hypotheses are assumed: (i) Balanced three phase AC networks which are modeled as AC voltage sources; (ii) Synchronized rotation reference frame (d,q); (iii) Ideal lossless VSC of neglected dynamics; (iv) No internal current control loop; (v) Parameters uncertainties as: Load impedance besides the DC and AC line parameter variations.

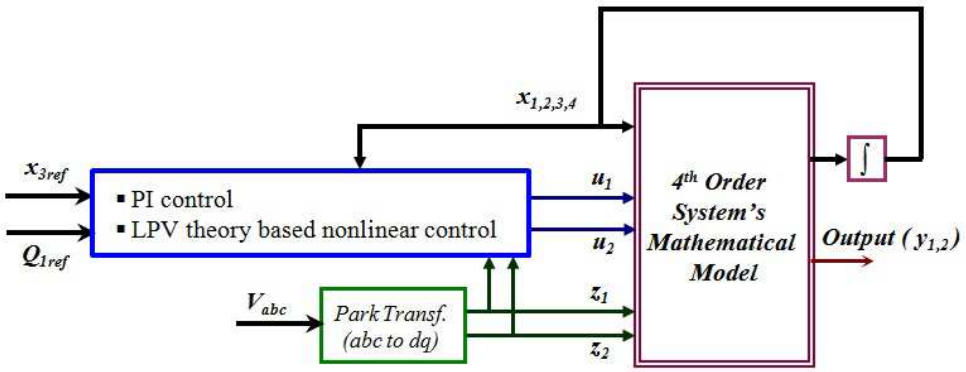

Figure 3.5: Simplified overall system's block diagram together with its controller.

3.4 VSC-HVDC Systems Control via PI Controllers

Due to their simplicity, conventional PI controllers are first proposed to control the reactive power Q_1 on the VSC's AC side and to govern the DC voltage U_{C1} to their corresponding reference values. Unity power factor is attained for zero reference value of Q_1. For GL VSC-HVDC systems, the flow of the active power P_1 is unidirectional.

For this purpose, automated tuning Simulink PID controller blocks are used. This PID tuner provides fast and widely applicable PID tuning method for the controller blocks. Therefore, PID parameters can be tuned for attaining reasonable robust design with acceptable response time.

A typical design of the PID tuner involves the following tasks:

- Launching the PID tuner. Hence, the software automatically identifies the system input and output. Then, it uses the current operating point for the system linearization. Therefore, a linearized system model is found out and an initial controller is designed to achieve a reasonable tradeoff between performance and robustness;

- Tuning the controller in the PID tuner by manually adjusting the design criteria in two design modes. These modes are simply the system stability margins (i.e., phase margin and gain margin).

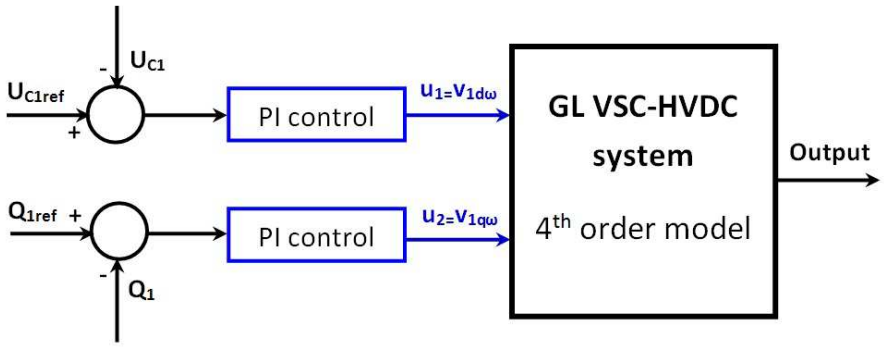

Figure 3.6: PI control for VSC-HVDC systems.

A compromise between the controller performance (measured by settling time) and robustness (measured by overshoot) should be accounted. Larger gain margins result in faster responses. Greater phase margins lead to smaller overshoot. Therefore, the PID parameters that can robustly stabilize the system are designed.

After tuning the conventional PID controller parameters, the system dynamic performance and stability are studied regarding the step response of any of the controlled signals. Alternatively, ramp variations can be also supposed to ensure slow and smooth variations of the reference signals. Hence, the robustness of the such PID controller is evaluated under parameter variations and/or perturbation.

As illustrated in Figure (3.6), two PI controllers -with either fast or slow responses- are used for controlling U_{C1} and Q_1 on the VSC terminals. The system dynamic behaviors are compared for different operating conditions while using both PI controllers. The designed fast PI controller provides a time response of settling time of about 30 mseconds. To govern U_{C1} and Q_1, two fast PI controllers with ($K_p = 0$, $K_i = 1.6919E{-}4$) and ($K_p = 1.4264E{-}9$, $K_i = 3.9179E{-}6$) are respectively considered.

On the other hand, the proposed slow PI controller has a settling time of about 200 mseconds. Slow PI controllers with ($K_p = 0$, $K_i = 3.3775E{-}5$) and ($K_p = 1.9393E{-}10$, $K_i = 1.8486E{-}8$) are supposed to control U_{C1} and Q_1 respectively. Practically, slow PI controllers of settling time above 150 mseconds is more acceptable for power system applications due to implementation constraints.

Step in Q_{1ref}

In Figure (3.7), the states and outputs dynamic behavior of the system are presented considering a step in the reactive power reference Q_{1ref}. It drops from 40 MVar to 0 MVar at t=2 seconds. One second later, it becomes -40 MVar. These variations in Q_{1ref} present different system operating conditions (i.e., lagging, unity and leading power factor respectively at the converter's AC terminal).

As shown in Figure (3.7a), the states' time responses are stable even when considering a step in Q_{1ref}. Obviously, U_{C1} is governed to its 300 kV reference value. Due to the step, U_{C1} increases to 312 kV before reaching again its steady state value after 88.2 mseconds using the fast PI controller. However if the slow PI controller is proposed, U_{C1} increases to 307 kV before reaching again its reference value after about 250 mseconds. Additionally, the currents dynamic behavior is stable if either PI controllers is used. Better overshoot and more reasonable settling time are depicted for i_{L1_d}, and i_x time responses following the mentioned step if slow PI controllers are used.

On the other hand, i_{L1_q} dynamic behavior reaches new steady state values after the mentioned step. Unlike the i_{L1_d} and i_x behavior, i_{L1_q} time response is more influenced by Q_{1ref} variation. As Q_{1ref} decreases from 40 MVar to 0 MVar, i_{L1_q} varies from -450 A to -200 A Then, it increases to 50 A when Q_{1ref} becomes -40 MVar. The dynamic behavior of i_{L1_q} confirms the mutual relation between this current component and the Q_1 dynamic performance.

Figures (3.7b) and (3.7c) demonstrate the active and reactive power behavior of the system after Q_{1ref} step. Obviously, P_1 perfectly reaches its 200 MW steady state value. The overshoot and the settling time depend on the PI controller's gain tuning. For fast PI controllers, the overshoot and the settling time are about 15% and 50 mseconds respectively in the P_1 dynamic performance. However, their corresponding values become 6% and 200 mseconds for slow PI controllers. Moreover, the Q_1 time response tracks their stepped reference values when either fast or slow PI controllers is used. Clearly, better overshoot and more practical time responses are attained in case of slow PI controllers. After the mentioned step, Q_1 behavior needs about 25 mseconds to reach again its desired reference value while using a fast PI controller. However, implementing this fast controller that provides very short settling time may be practically impossible especially for high rated power systems.

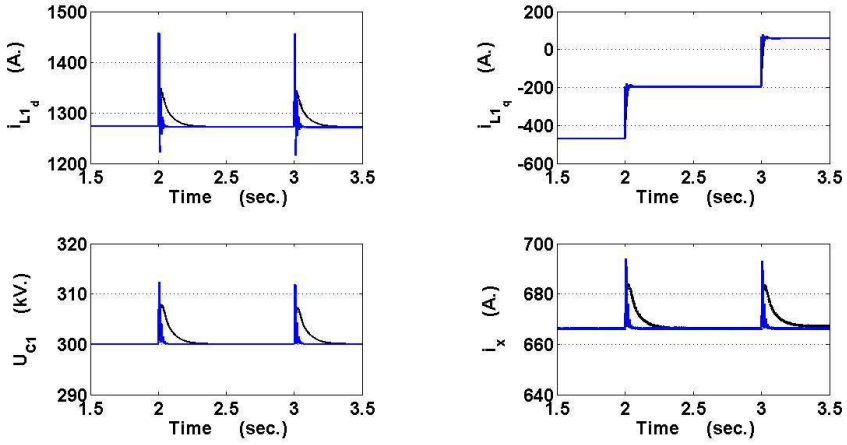

(a) i_{L1_d}, i_{L1_q}, U_{C1} and i_x time responses

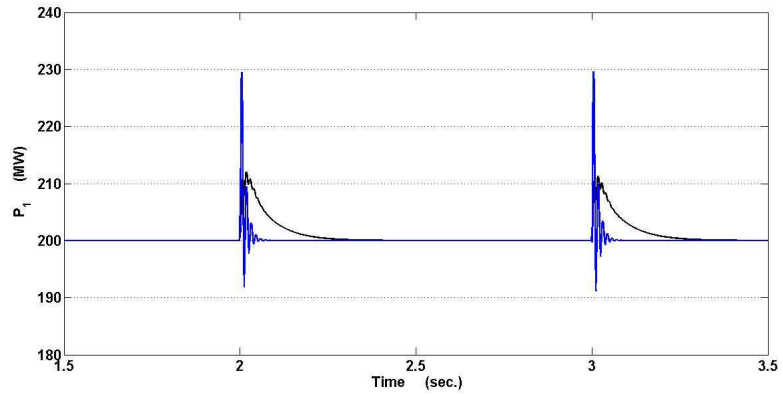

(b) P_1 time response

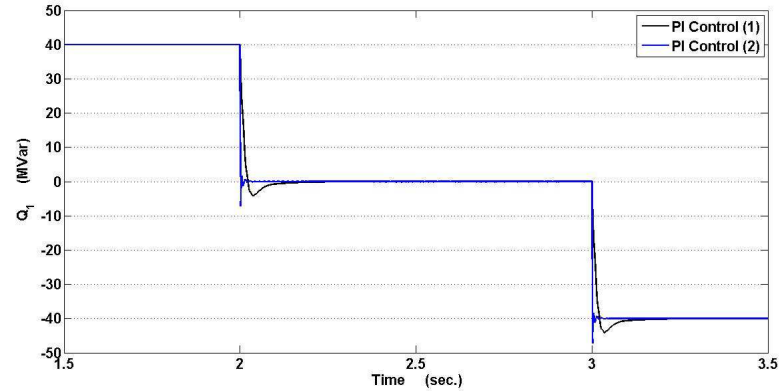

(c) Q_1 time response

Figure 3.7: States and outputs dynamic behavior via PI control:
(a) $Q_{1ref} = 40$ MVar for (t=0 to 2 sec.);
(b) $Q_{1ref} = 0$ MVar for (t=2 to 3 sec.);
(c) $Q_{1ref} = -40$ MVar for (t=3 to 4.5 sec.).

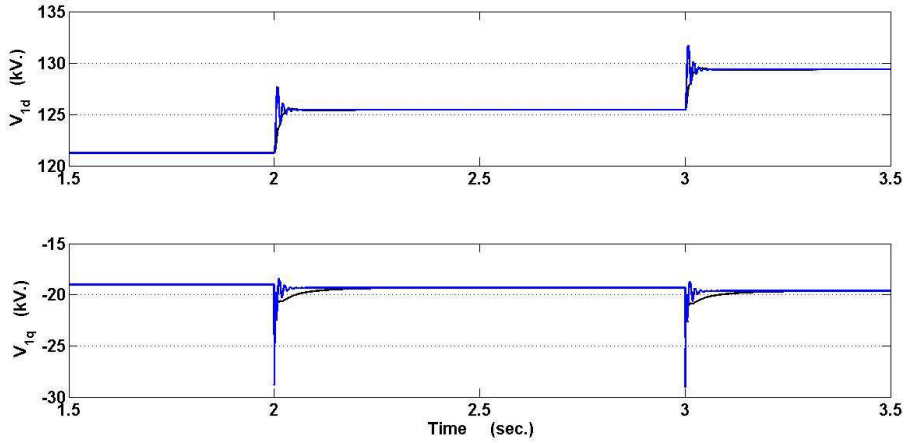

Figure 3.8: v_{1_d} and v_{1_q} time responses.

Figure (3.8) depicts the dynamic performance of the *d-q* voltage components on the AC side of the VSC. V_{1d} behavior is greatly influenced by Q_{1ref} variation rather than V_{1q}. The variation of both V_{1d} and i_{L1q} behaviors guarantee the trajectory tracking of Q_1 behavior in accordance to Q_{1ref} variation.

Indeed, the control signals ($V_{1_{d\omega}}$ and $V_{1_{q\omega}}$) have the same waveform shape of the dynamic performance of (V_{1d} and V_{1q}) respectively due to their proportional relationships presented in Equation (3.7).

Uncertainty in Load Resistance

The GL VSC-HVDC transmission system states and outputs dynamic behavior is illustrated in Figure (3.9). The fast and slow PI controllers, with the same tuning gains previously stated, are used for controlling U_{C1} and Q_1 respectively to their corresponding reference values of 300 kV and zero. The load resistance is instantaneously increased by 20% and 100% of its base value at t=2 seconds and t=3 seconds respectively. Stable states and power flows dynamic performance are attained even under load resistance variations.

In Figure (3.9a), the *d-q* current components' behavior are clearly affected by the variation of load resistance. i_{L1_d} and i_{L1_q} time responses reach new stable steady state values in consequence of each load resistance variation.

For the *d-q* current components behavior, shorter settling time and smaller overshoot are shown if using the fast PI controller. Due to i_{L1_q} time response, an overshoot of about 200 A for a duration of approximately 150 mseconds is noticed if the load resistance is increased by 20%. Additionally, the overshoot rises to 500 A if the load resistance is doubled.

The U_{C1} dynamic behavior is controlled to its 300 kV reference value considering this type of uncertainty. However in case of using fast PI controller, its behavior depicts overshoots of 10 kV and 25 kV that last about 30 mseconds each.

According to the inversely proportional relation between the load current i_x and the load impedance, the load current decreases by 20% and then halved with respect to load resistance variation.

Figures (3.9b) and (3.9c) illustrate the power flows time responses using PI controllers (fast and slow) considering load resistance uncertainties. The active power behavior decreases with the increase of the load resistance due to their inverse proportional relation. On the other side, the reactive power is always zero.

If the slow PI controller is used considering load resistance variation, unfavorable high overshoots of about -45 MVar and -90 MVar with reasonable settling time of about 150 mseconds duration each are presented. Still, the fast PI controller provides faster time response with negligible overshoot that may be impossibly implemented due to physical limitations as illustrated in Figure (3.9c).

Figure (3.10) shows the *d-q* voltage components time responses. These components are stabilized using the fast and slow PI controllers even considering load resistance variation. Following the resistance change, new steady state values of the *d-q* voltage behavior are attained. These values together with the *d-q* current components behavior act on controlling Q_1 as demonstrated in Equation (3.16).

Uncertainty in AC Line Reactance

Figure (3.11) illustrates the system states and outputs dynamic behavior considering AC line reactance variation while using the conventional PI control for governing U_{C1} to 300 kV and controlling Q_1 to zero. It is assumed that the AC line reactance is increased by 20 % at t=2 seconds. From Figure (3.11a), the system is stable when controlled using either fast or slow PI controller. The DC voltage U_{C1} reaches its trajectory reference value of 300 kV.

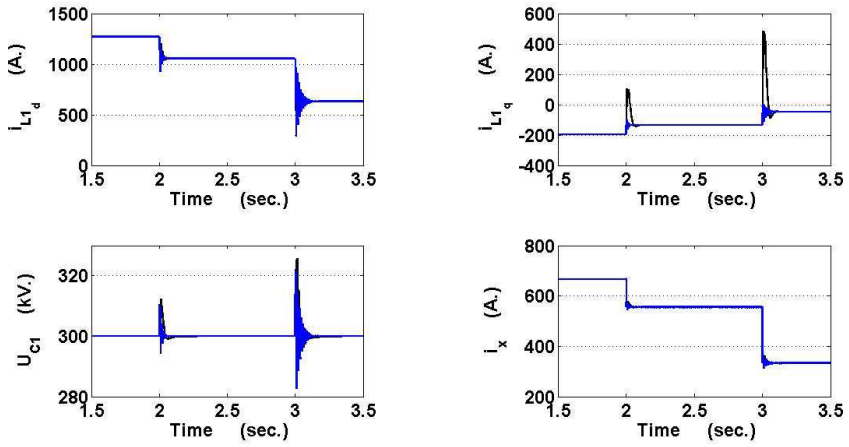

(a) i_{L1_d}, i_{L1_q}, U_{C1} and i_x time responses

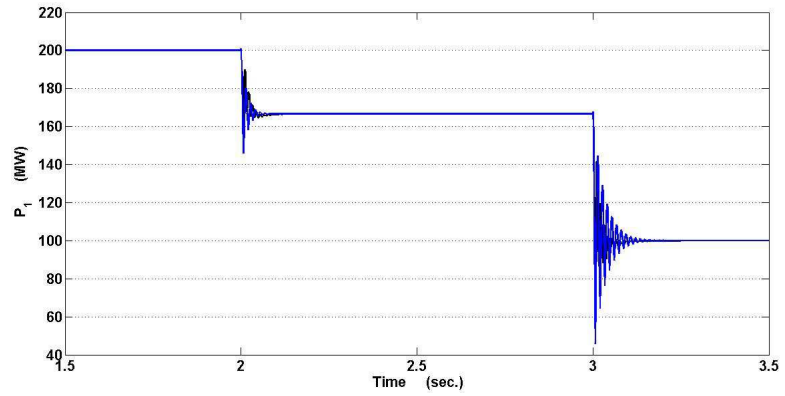

(b) P_1 time response

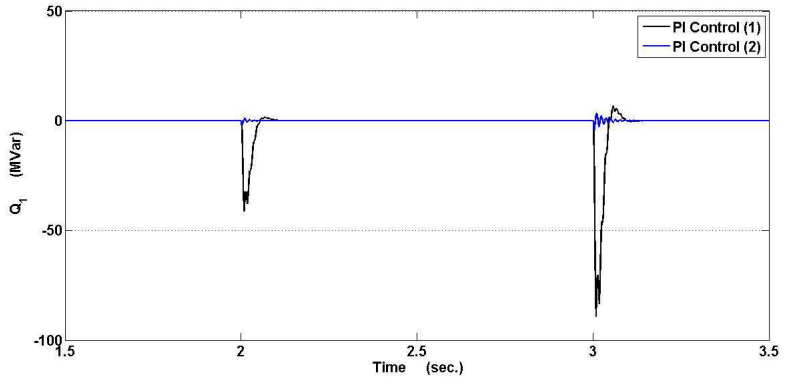

(c) Q_1 time response

Figure 3.9: VSC-HVDC system states and outputs dynamic behavior via PI control considering load resistance variation.

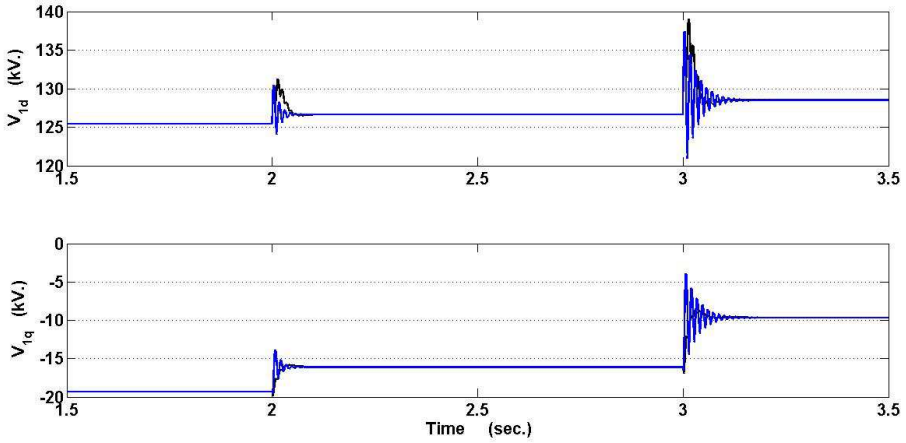

Figure 3.10: v_{1_d} and v_{1_q} time responses.

In case of fast PI controller, negligible overshoot and settling time of about 25 mseconds are attained. Supposing slow PI controller, U_{C1} drops to 288 kV before reaching again its steady state value with an acceptable settling time of 150 mseconds.

Stable dynamic behavior of i_{L1_d} is depicted in presence of this type of uncertainty. Although fast PI control provides better dynamic performance than the slow one, it can not be implemented due to physical restrictions. After the AC line reactance rise, slow PI control renders acceptable settling time of about 200 mseconds for i_{L1_d} time response. i_{L1_d} decreases from 1266 A to 1120 A before reaching its steady state value. In addition, i_{L1_q} time response decreases from -200 A to its new steady state value of -250 A. However, an undesired drop to -450 A that lasts about 150 mseconds is yielded following the AC line reactance variation.

Figure (3.11b) shows that the active power dynamic behavior remains stable even in presence of AC line reactance variation in favor of conventional PI controllers. For fast PI control, the overshoot and settling time are approximately -10 MW and 50 mseconds respectively. Their corresponding values become about -24 MW and 150 mseconds in case of slow PI control. Figure (3.11c) demonstrates the reactive power dynamic behavior following the change in AC line reactance. Using slow PI controller, Q_1 undesirably increases to 38 MVar due to this variation with a settling time of about 150 mseconds.

For fast PI control, better response with smaller overshoot and shorter settling time is obtained.

Figure (3.12) explicit the stable *d-q* voltage components' time responses. These components are stabilized using either fast or slow PI controller in presence of AC line reactance variation. New steady state values of the *d-q* voltage behavior are attained due to this variation in order to guarantee that Q_1 tracks its desired reference value.

The system dynamic behavior in presence of step variations or uncertainties are presented in Figures (3.7)–(3.12). Although the system is stabilized via the traditional PI controller, it is stated that:

- The system dynamic behavior greatly depends on the choice of the controllers' tuning gains;
- The system dynamic performance is influenced supposing the same tuning gains for different operating conditions;

The conventional PI control is not robust enough against all possible uncertainties encountering the system. Adequate dynamic behavior can be attained for limited range of uncertainties only. However for other operating conditions, poor performance may be yielded. To meet that, the gains should be retuned. Alternatively, internal PI current control loops can be added for enhancing the system's dynamic behavior.

3.5 VSC-HVDC Control via Cascaded PI Controllers

Internal PI current control loops can be used in cascade to other outer conventional PI controllers as proposed in Figure (3.13). The inputs of the internal PI controllers are the *d-q* current components flowing in the AC line (i_{L1_d} and i_{L1_q}). Their outputs are the overall system control signals ($V_{1_{d\omega}}$ and $V_{1_{q\omega}}$) required for enhancing the system performance. Hence, more PI controllers are designed.

The gains of the inner current control loops should be initially tuned. Then, the outer loop PI controllers' gains are to be attentively chosen to guarantee controlling the reactive power Q_1 and governing the voltage on the converter's DC side U_{C1}. Step by step, the desired gains are selected when reaching acceptable trade-off between controller robustness and system performance. The PI controllers' gains are listed in Appendix A.

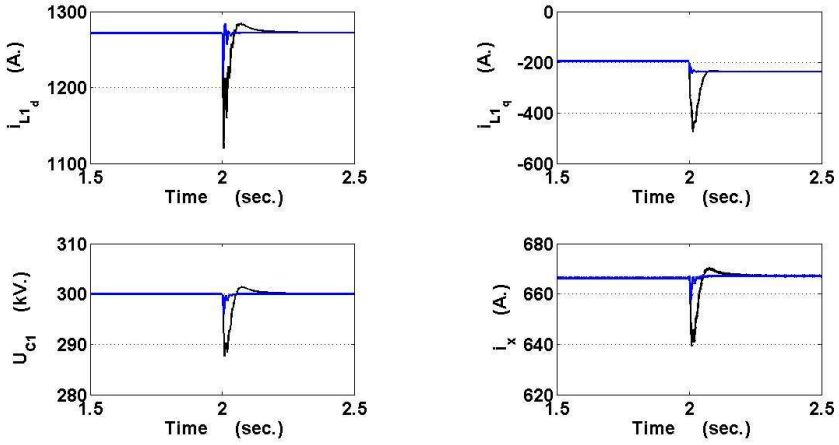

(a) i_{L1_d}, i_{L1_q}, U_{C1} and i_x time responses

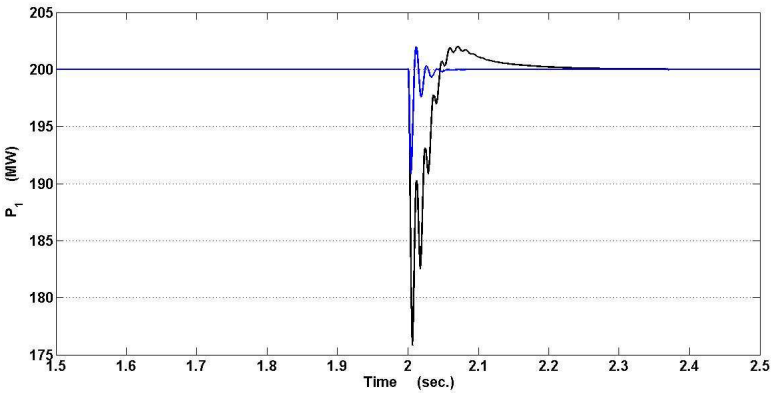

(b) P_1 time response

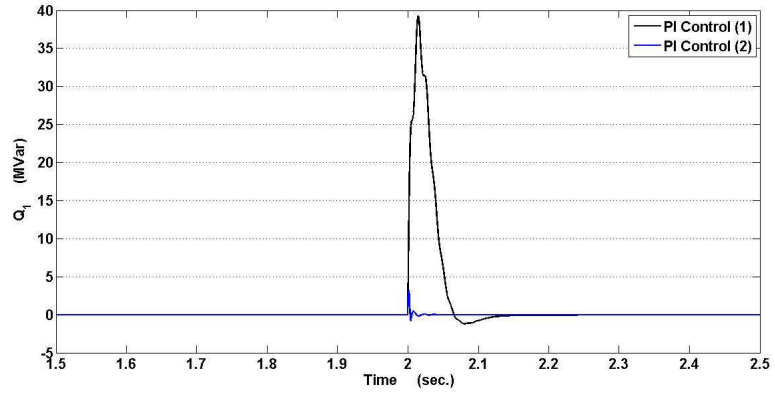

(c) Q_1 time response

Figure 3.11: VSC-HVDC system states and outputs dynamic behavior via PI control considering AC line reactance variation.

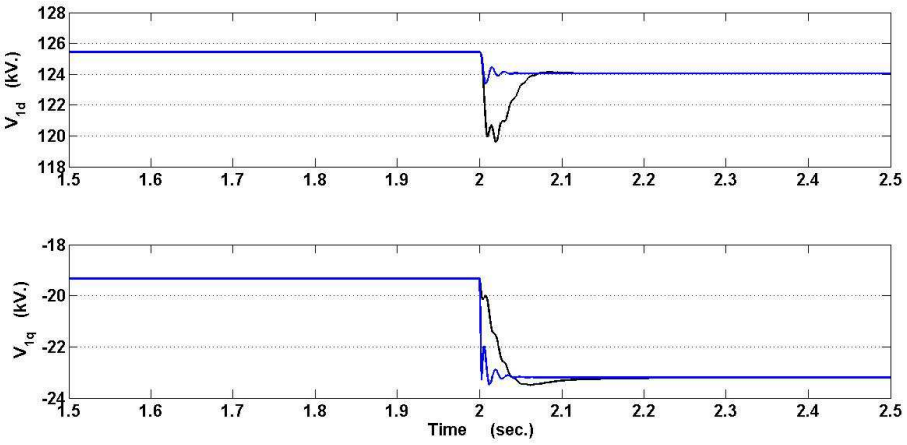

Figure 3.12: v_{1_d} and v_{1_q} time responses.

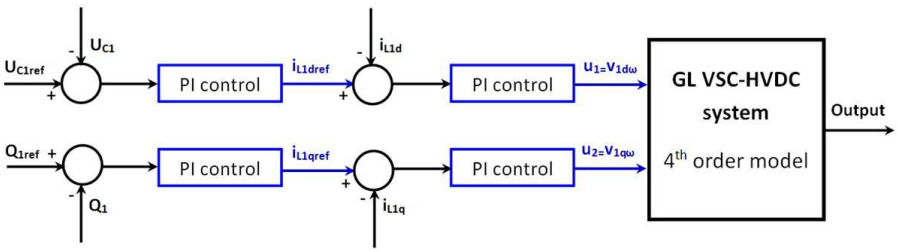

Figure 3.13: GL VSC-HVDC system controlled via PI control with internal current control loop.

Because of the use of multiple PI controllers for controlling the system, more complexity are encountered choosing the most appropriate tuning gains because of the mutual interaction and coordination among them especially when accounting for physical constraints (i.e., current behavior are faster than voltage responses). Therefore, procedures become difficult to implement for coordinating different controllers. The coordination must be conducted for a variety of operating conditions in order to satisfy certain performance specifications.

Step in Q_{1ref}

The system states and outputs dynamic behavior considering a step in the reactive power reference Q_{1ref} are illustrated in Figure (3.14). These variations in Q_{1ref} present different system operating conditions (i.e., lagging, unity and leading power factor respectively at the converter's AC terminal).

In Figure (3.14a), the states' time responses are stable even when considering a step in Q_{1ref}. Obviously, U_{C1} is governed to its 300 kV reference value. Due to the step, U_{C1} increases to 301.2 kV before reaching again its steady state value after about 300 mseconds using the conventional PI controller with a cascaded internal current control. Therefore, U_{C1} increases to 301.1 kV before reaching again its reference value after about 300 mseconds. The U_{C1} variations are considered negligible and the overshoot is about 0.3%. Moreover, the currents dynamic behavior is stable. Acceptable overshoots and reasonable settling time ($\approx$ 200 mseconds) are shown for i_{L1_d}, and i_x time responses following the mentioned steps.

Unlike the i_{L1_d} and i_x behavior, i_{L1_q} time response is significantly impacted by Q_{1ref} variation. As Q_{1ref} decreases from 40 MVar to 0 MVar, i_{L1_q} varies from -469 A to -196 A. Then, it increases to 59 A when Q_{1ref} becomes -40 MVar. The dynamic behavior of i_{L1_q} confirms the mutual relation between this current component and the Q_1 dynamic performance.

The active and reactive power dynamic behavior considering Q_{1ref} step are respectively demonstrated in Figures (3.14b) and (3.14c). P_1 performance perfectly reaches its 200 MW steady state value. Acceptable overshoots and settling times of about 0.6% and 500 mseconds respectively are shown. In addition, the Q_1 time response desirably tracks its stepped reference values. Practical time responses with settling time approximately 300 mseconds are attained in case of using cascaded PI controllers.

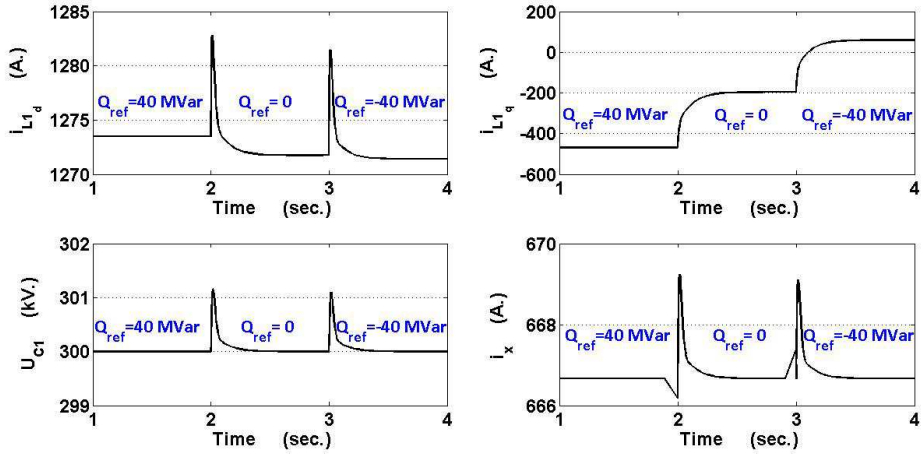

(a) i_{L1_d}, i_{L1_q}, U_{C1} and i_x time responses

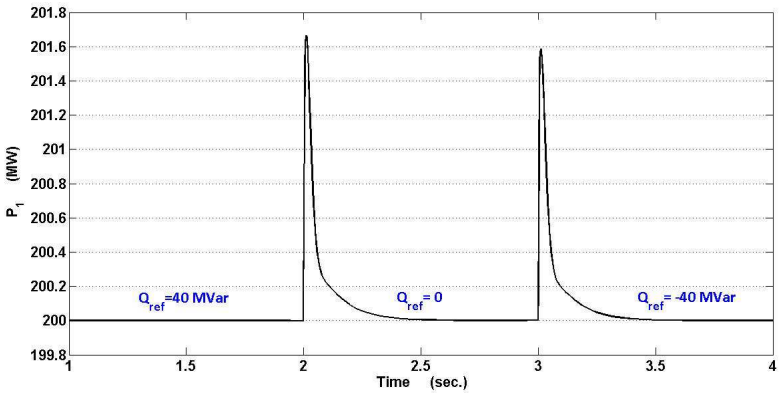

(b) P_1 time response

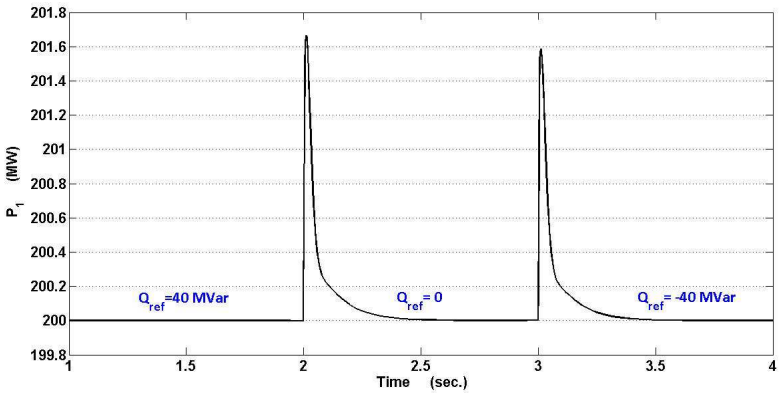

(c) Q_1 time response

Figure 3.14: States and outputs dynamic behavior via cascaded PI control:
(a) $Q_{1ref} = 40$ MVar for (t=0 to 2 sec.);
(b) $Q_{1ref} = 0$ MVar for (t=2 to 3 sec.);
(c) $Q_{1ref} = -40$ MVar for (t=3 to 4.5 sec.).

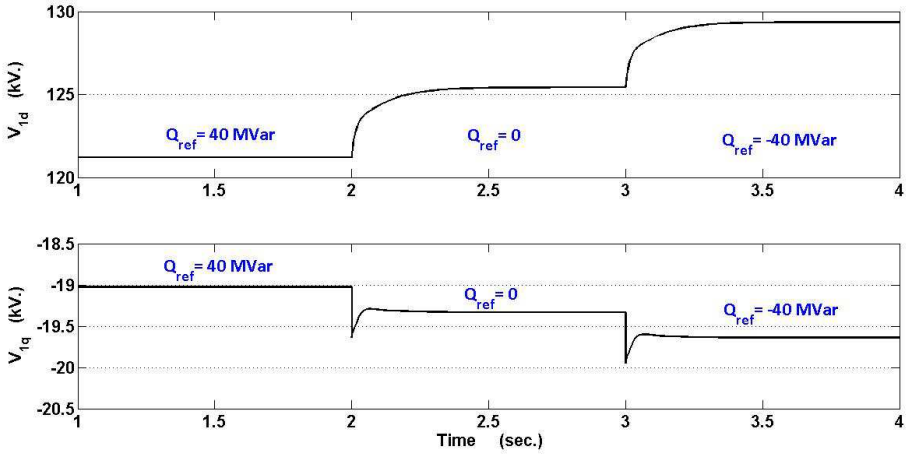

Figure 3.15: v_{1_d} and v_{1_q} time responses.

The dynamic performance of the *d-q* voltage components on the AC side of the VSC are depicted in Figure (3.15). V_{1d} behavior is more affected by Q_{1ref} variation rather than V_{1q}. The variation of both V_{1d} and i_{L1q} behaviors ensures the trajectory tracking of Q_1 behavior in consequence of Q_{1ref} variation. Obviously, the control signals ($V_{1_{d\omega}}$ and $V_{1_{q\omega}}$) have the same waveform shape of the dynamic performance of (V_{1d} and V_{1q}) respectively due to their proportional relationships presented in Equation (3.7).

Uncertainty in Load Resistance

In Figure (3.16), the system states and outputs dynamic behavior is shown. The internal and outer PI controllers in cascaded, with the unchanged tuning gains previously, are used for controlling U_{C1} and Q_1 respectively to their corresponding reference values of 300 kV and -16 MVar. The load resistance is instantaneously increased by 20% and 100% at t=2 seconds and t=3 seconds respectively. Stable states and power flows dynamic performance are attained even under load resistance variations.

The *d-q* current components' behavior are influenced by load resistance variations as depicted in Figure (3.16a). i_{L1_d} and i_{L1_q} time responses reach new stable steady state values in consequence of each load resistance variation. For i_{L1_q} time response, it unfavorably increases from -92 A to 413 A, then, reaches its new steady state value of -26 A if the load is increased by 20%. The settling time is about 300 mseconds.

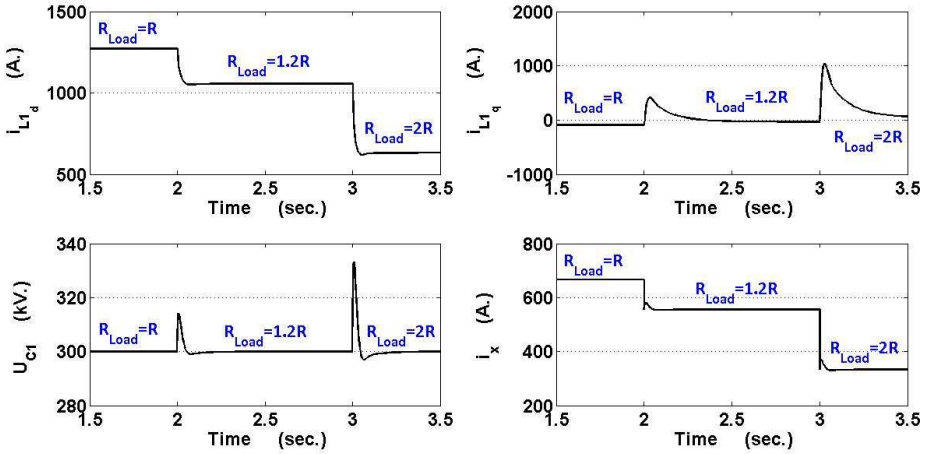

(a) i_{L1_d}, i_{L1_q}, U_{C1} and i_x time responses

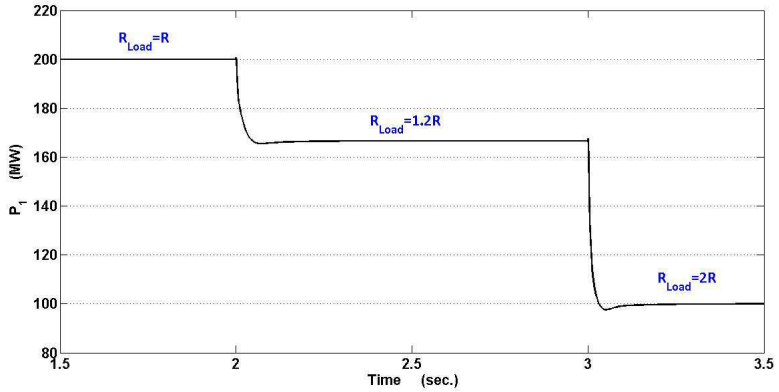

(b) P_1 time response

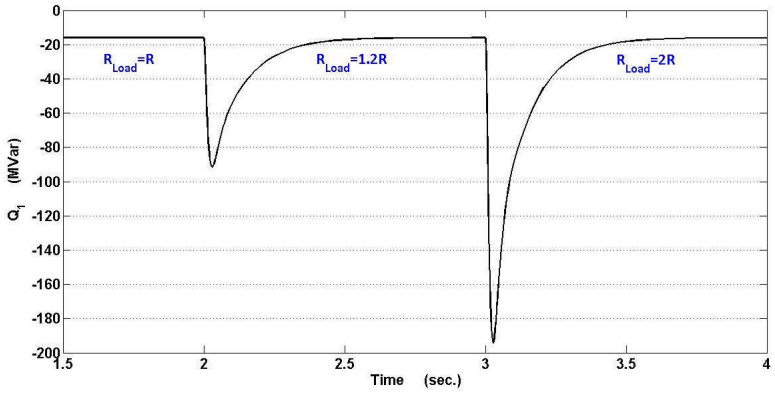

(c) Q_1 time response

Figure 3.16: VSC-HVDC system states and outputs dynamic behavior via cascaded PI control considering load resistance variation.

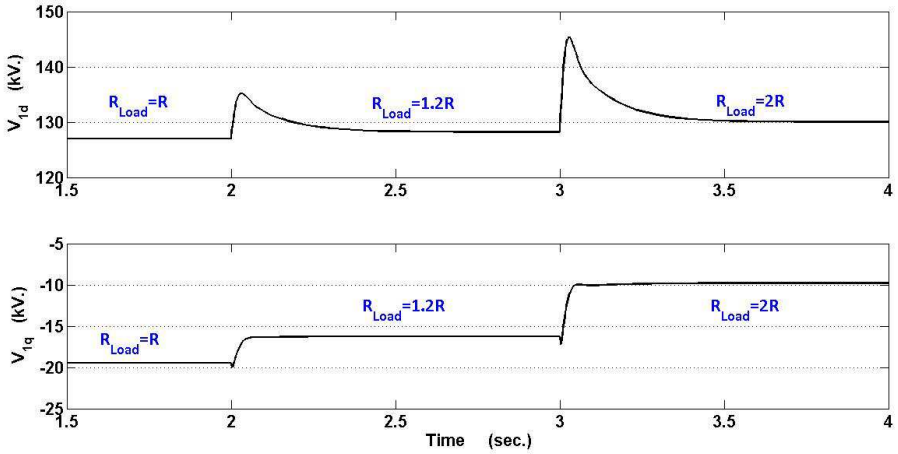

Figure 3.17: v_{1_d} and v_{1_q} time responses.

Additionally, the response undesirably rises from -26 A to 1037 A if the load resistance is doubled before attainting again its 68 A steady state value at a settling time of 300 mseconds.

The U_{C1} dynamic behavior is controlled to its 300 kV reference value considering this type of uncertainty. However, its behavior depicts overshoots of 4.7% and 11.1% that last about 100 mseconds each.

According to the inversely proportional relation between the load current i_x and the load impedance, the load current decreases by 20% and then halved with respect to proposed load resistance variation.

Figures (3.16b) and (3.16c) illustrate the power flows time responses considering load resistance uncertainties. The active power behavior decreases with the increase of the load resistance due to their inverse proportional relation. On the other side, the reactive power is always zero with unfavorable high overshoots of about -75 MVar and -177 MVar and reasonable settling time of about 400 mseconds duration each.

The *d-q* voltage components time responses are shown in Figure (3.17). These components are stabilized using the proposed cascaded PI controllers in presence of load resistance variation. Following the resistance change, new steady state values of the *d-q* voltage behavior are attained. These values together with the *d-q* current components behavior act on controlling Q_1 as demonstrated in Equation (3.16).

Uncertainty in AC Line Reactance

The system states and outputs dynamic behavior considering AC line reactance variation while using the cascaded conventional PI control for governing U_{C1} to 300 kV and controlling Q_1 to zero are illustrated in Figure (3.18). It is assumed that the AC line reactance is increased by 20% at t=2 seconds. From Figure (3.18a), the system is stable and the DC voltage U_{C1} reaches its trajectory reference value of 300 kV. U_{C1} behavior drops to 294 kV before reaching again its steady state value after about 250 mseconds.

Stable dynamic behavior of i_{L1_d} is depicted in presence of this type of uncertainty. After the AC line reactance rise, the proposed PI control renders acceptable settling time of about 400 mseconds for i_{L1_d} time response. i_{L1_d} decreases from 1270 A to 1215 A before reaching its steady state value. In addition, i_{L1_q} time response decreases from -92 A to its new steady state value of -132 A after about 400 mseconds. However, an undesired drop to -695 A that is yielded following the AC line reactance variation.

Figure (3.18b) shows that the active power dynamic behavior remains stable even in presence of AC line reactance variation in favor of the proposed cascased PI controllers. The overshoot and settling time are approximately -10 MW and 400 mseconds respectively. Figure (3.18c) demonstrates the reactive power dynamic behavior following the change in AC line reactance. Using the cascaded PI controllers, Q_1 undesirably increases to 64.7 MVar due to this variation with a settling time of about 400 mseconds.

Figure (3.19) explicit the stable *d-q* voltage time responses. These components are stabilized in presence of AC line reactance variation. New steady state values of the *d-q* voltage behavior are attained due to this variation in order to guarantee that Q_1 tracks its desired reference value.

It can be stated that the PI controllers have the following disadvantages:

- Lack of robustness and poor performance under certain operating conditions;
- Difficulty of tuning their gains in case of multiple PI controllers because of interaction and coordination constraints;

To ameliorate the system stability and to enhance its dynamic behavior, the conventional PI control is replaced by Lyapunov theory based nonlinear control technique.

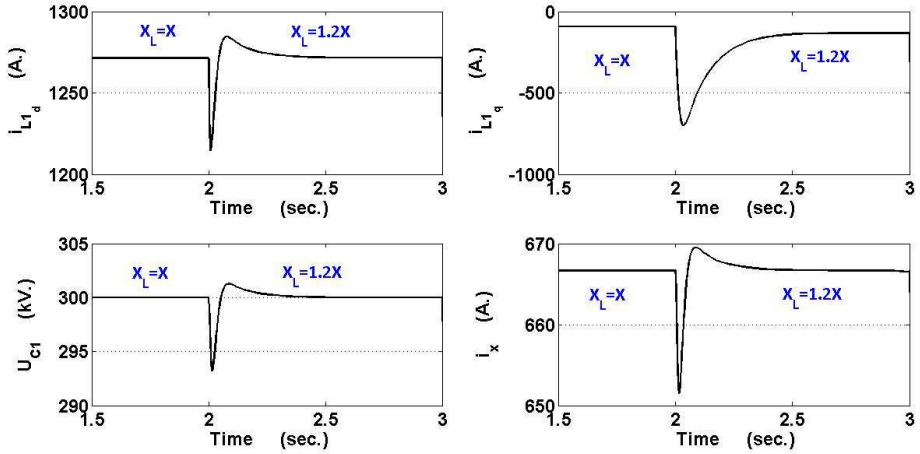

(a) i_{L1_d}, i_{L1_q}, U_{C1} and i_x time responses

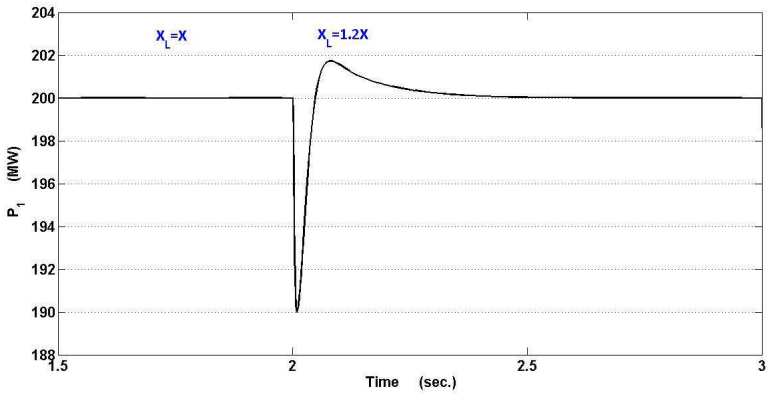

(b) P_1 time response

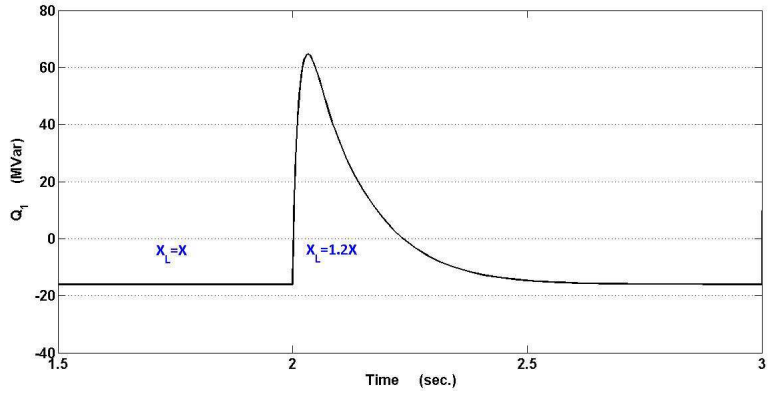

(c) Q_1 time response

Figure 3.18: VSC-HVDC system states and outputs dynamic via cascaded PI control considering AC line reactance variation.

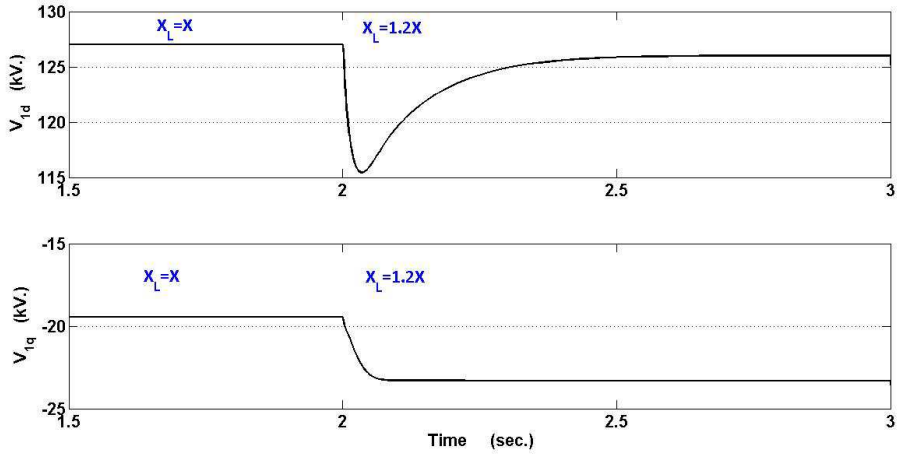

Figure 3.19: v_{1_d} and v_{1_q} time responses.

In favor of the robustness feature of the VSS theory-based controllers against uncertainties besides their relative simplicity, AOT and SMC approaches are then proposed for GG VSC-HVDC transmission systems.

3.6 Mathematical Model of GG VSC-HVDC Systems

VSC-HVDC links connect mostly asynchronous AC networks, therefore, including converters at each AC side. The steady state analysis of VSC-HVDC systems is significantly simplified assuming that: (i) AC networks are strong enough to be modeled as AC voltage sources that deliver balanced sinusoidal voltage with constant amplitude and frequency; (ii) All voltage and current harmonics produced by the converters are filtered out; (iii) The converter transformers' resistance and magnetizing impedance are negligible; (iv) The converter is lossless with neglected dynamics since the valves are ideal with no arc voltage drop; (v) The DC voltage and current have no ripples.

GG VSC-HVDC transmission system controller design is mainly based on its mathematical model. However, its actual physical system may be influenced by external or internal uncertainties. Among these uncertainties, we will consider the DC cable resistance fluctuations caused by thermal effects resulted of high currents flow due to on-line switching or faults, besides the variations of the AC line reactance influenced by the change in the network topology or continuous change in the shunt capacitances.

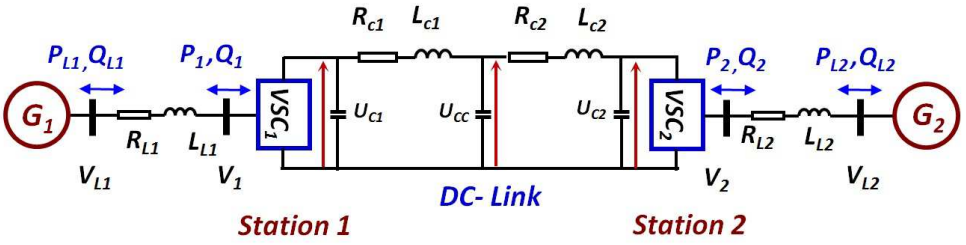

Figure 3.20: GG VSC-HVDC transmission system's scheme.

Accordingly, GG VSC-HVDC controller design becomes a must to reduce the influence of parameter uncertainties on the system's dynamic performance.

The schematic representation of the GG VSC-HVDC link is shown in Figure (3.20) [42, 43, 44, 130, 131, 132, 133, 134]. The system's main components are: load Tap Changing (LTC) transformers, VSC-HVDC converter stations to perform the AC/DC/AC conversion process, AC and DC filters, DC current filtering reactance and DC transmission cable.

In Figure (3.20), reactive powers (Q_1 and Q_2) on both VSCs' AC sides are controlled to their desired values with the goal of attaining unity power factor. Moreover, the active power and the DC voltage (P_1 and U_{C2}) are maintained at their rated values. The DC link power losses and voltage drop as well as directional active power flow control are obviously considered.

The continuous–time equivalent model of the GG VSC-HVDC transmission system is depicted in Figure (3.21) [42, 130, 131, 132, 133, 134]. The VSCs are coupled with AC generation stations via equivalent impedances $R_{L1} + jX_{L1}$ and $R_{L2} + jX_{L2}$. Two shunt DC capacitors (C_1 and C_2) are connected across the VSCs' DC sides to mitigate the impulse current impacts, and attenuate the harmonics on the DC side.

According to Figure (3.21), the voltage drops in each phase for both sides are expressed by the following:

$$L_{L1_{ph}} \frac{di_{L1_{ph}}}{dt} + R_{L1_{ph}} i_{L1_{ph}} = v_{L1_{ph}} - v_{1_{ph}} \tag{3.19}$$

$$L_{L2_{ph}} \frac{di_{L2_{ph}}}{dt} + R_{L2_{ph}} i_{L2_{ph}} = v_{2_{ph}} - v_{L2_{ph}} \tag{3.20}$$

where, 'ph' denotes to phase A, B or C respectively.

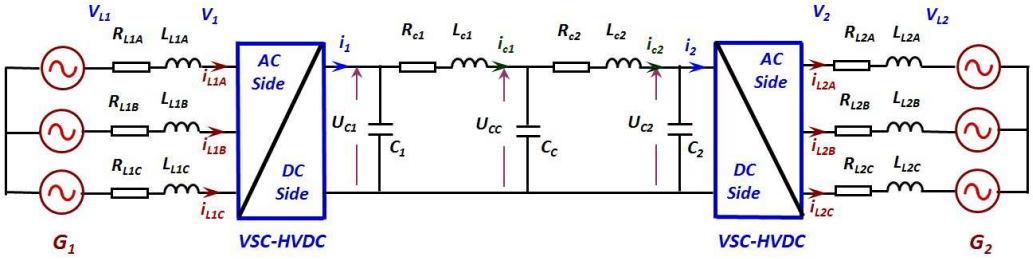

Figure 3.21: Continuous–time GG VSC-HVDC model.

As previously deduced in Section 3.3:

$$\begin{cases} V_{1_{d\omega}} = 2\frac{v_{1_d}}{U_{C1}} \\ V_{1_{q\omega}} = 2\frac{v_{1_q}}{U_{C1}} \end{cases} \tag{3.21}$$

and,

$$\begin{cases} V_{2_{d\omega}} = 2\frac{v_{2_d}}{U_{C2}} \\ V_{2_{q\omega}} = 2\frac{v_{2_q}}{U_{C2}} \end{cases} \tag{3.22}$$

where, ($V_{1_{d\omega}}$ and $V_{1_{q\omega}}$) and ($V_{2_{d\omega}}$ and $V_{2_{q\omega}}$) are the dimensionless d-q components expressing relations between the d-q voltage components on VSC-HVDC transmission system AC sides –(v_{1_d} and v_{1_q}) and (v_{2_d} and v_{2_q}) respectively– and the DC bus voltages on both DC link sides (U_{C1} and U_{C2}).

By analogy, the equations of both converter sides are deduced. Thus, from the GG VSC-HVDC system illustrated in Figure (3.21):

$$L_{L1}\frac{\overrightarrow{di_{L1}}}{dt} + R_{L1}\overrightarrow{i_{L1}} + j\omega_1 L_{L1}\overrightarrow{i_{L1}} = \overrightarrow{v_{L1}} - \overrightarrow{v_1} \tag{3.23}$$

$$L_{L2}\frac{\overrightarrow{di_{L2}}}{dt} + R_{L2}\overrightarrow{i_{L2}} + j\omega_2 L_{L2}\overrightarrow{i_{L2}} = \overrightarrow{v_2} - \overrightarrow{v_{L2}} \tag{3.24}$$

where, ω_1 and ω_2 refer to the angular frequency of both interconnected AC generation stations in (rad/sec).

The current and voltage vectors exhibited in Equations (3.23) and (3.24) are replaced by their d-q components, so that:

$$\overrightarrow{i_{L1}} = i_{L1_d} + j i_{L1_q} \tag{3.25}$$

$$\overrightarrow{v_{L1}} = v_{L1_d} + jv_{L1_q} \tag{3.26}$$

$$\overrightarrow{v_1} = v_{1_d} + jv_{1_q} \tag{3.27}$$

$$\overrightarrow{i_{L2}} = i_{L2_d} + ji_{L2_q} \tag{3.28}$$

$$\overrightarrow{v_{L2}} = v_{L2_d} + jv_{L2_q} \tag{3.29}$$

$$\overrightarrow{v_2} = v_{2_d} + jv_{2_q} \tag{3.30}$$

Therefore,

$$L_{L1}\frac{di_{L1_d}}{dt} + R_{L1}i_{L1_d} - \omega_1 L_{L1}i_{L1_q} = v_{L1_d} - v_{1_d} \tag{3.31}$$

$$L_{L1}\frac{di_{L1_q}}{dt} + R_{L1}i_{L1_q} + \omega_1 L_{L1}i_{L1_d} = v_{L1_q} - v_{1_q} \tag{3.32}$$

$$L_{L2}\frac{di_{L2_d}}{dt} + R_{L2}i_{L2_d} - \omega_2 L_{L2}i_{L2_q} = v_{2_d} - v_{L2_d} \tag{3.33}$$

$$L_{L2}\frac{di_{L2_q}}{dt} + R_{L2}i_{L2_q} + \omega_2 L_{L2}i_{L2_d} = v_{2_q} - v_{L2_q} \tag{3.34}$$

Applying the loop and node equations along the GG VSC-HVDC system's DC link, we have:

$$C_1\frac{du_{C1}}{dt} = i_1 - i_{c1} \tag{3.35}$$

$$u_{C1} - u_{CC} = L_{c1}\frac{di_{c1}}{dt} + R_{c1}i_{c1} \tag{3.36}$$

$$C_C\frac{du_{CC}}{dt} = i_{c1} - i_{c2} \tag{3.37}$$

$$u_{CC} - u_{C2} = L_{c2}\frac{di_{c2}}{dt} + R_{c2}i_{c2} \tag{3.38}$$

$$C_2\frac{du_{C2}}{dt} = i_{c2} - i_2 \tag{3.39}$$

From Equations (3.21) and (3.22), the *d-q* voltage components on VSCs' AC sides (v_{1_d}, v_{1_q}, v_{2_d} and v_{2_q}) are functions of the required control feedback signals.

As introduced in Equations (3.7) and (3.15), the active and reactive powers entering both converters, (P_1 and Q_1) and (P_2 and Q_2), are derived as:

$$\begin{cases} P_1 = \dfrac{3}{2}(v_{1_d} i_{L1_d} + v_{1_q} i_{L1_q}) \\ Q_1 = \dfrac{3}{2}(v_{1_q} i_{L1_d} - v_{1_d} i_{L1_q}) \end{cases} \tag{3.40}$$

and,

$$\begin{cases} P_2 = \dfrac{3}{2}(v_{2_d} i_{L2_d} + v_{2_q} i_{L2_q}) \\ Q_2 = \dfrac{3}{2}(v_{2_q} i_{L2_d} - v_{2_d} i_{L2_q}) \end{cases} \tag{3.41}$$

Furthermore, the active and reactive powers delivered by both generators, (P_{L1} and Q_{L1}) and (P_{L2} and Q_{L2}), are expressed by:

$$\begin{cases} P_{L1} = \dfrac{3}{2}(v_{L1_d} i_{L1_d} + v_{L1_q} i_{L1_q}) \\ Q_{L1} = \dfrac{3}{2}(v_{L1_q} i_{L1_d} - v_{L1_d} i_{L1_q}) \end{cases} \tag{3.42}$$

and,

$$\begin{cases} P_{L2} = \dfrac{3}{2}(v_{L2_d} i_{L2_d} + v_{L2_q} i_{L2_q}) \\ Q_{L2} = \dfrac{3}{2}(v_{L2_q} i_{L2_d} - v_{L2_d} i_{L2_q}) \end{cases} \tag{3.43}$$

Equations (3.31)–(3.41) that illustrate the overall VSC-HVDC system's global mathematical model are then reformulated into the state space representation form:

$$\begin{cases} \dot{x} = [A]\, x + g(x)u + [R]\, z \\ y = h\,(x, u, z)\, x \end{cases} \tag{3.44}$$

where, x, u, z and y respectively refer to the state variables, control signals, *d-q* components of the AC source voltage calculated using Park transformation, and output power signals (*active and reactive*).

The overall system is of ninth order. It comprises four control inputs and four outputs, as follows:

$$\begin{aligned} x_{1,\ldots 9} &= [i_{L1_d}, i_{L1_q}, u_{C1}, i_{c1}, u_{CC}, i_{c2}, u_{C2}, i_{L2_d}, i_{L2_q}]^T \\ u_{1,\ldots 4} &= [v_{1_{d\omega}}, v_{1_{q\omega}}, v_{2_{d\omega}}, v_{2_{q\omega}}]^T \\ z_{1,\ldots 4} &= [v_{L1_d}, v_{L1q}, v_{L2_d}, v_{L2q}]^T \\ y_{1,\ldots 4} &= [P_1, Q_1, P_2, Q_2]^T \end{aligned}$$

The $[A]$, $g(x)$, $[R]$ and $h(x,u,z)$ matrices are printed out as::

$$[A] = \begin{bmatrix} \left(\frac{-R_{L1}}{L_{L1}}\right) & \omega_1 & 0 & 0 & 0 & 0 & 0 & 0 & 0 \\ -\omega_1 & \left(\frac{-R_{L1}}{L_{L1}}\right) & 0 & 0 & 0 & 0 & 0 & 0 & 0 \\ 0 & 0 & 0 & \left(\frac{-1}{C_1}\right) & 0 & 0 & 0 & 0 & 0 \\ 0 & 0 & \left(\frac{1}{L_{c1}}\right) & \left(\frac{-R_{c1}}{L_{c1}}\right) & \left(\frac{-1}{L_{c1}}\right) & 0 & 0 & 0 & 0 \\ 0 & 0 & 0 & \left(\frac{1}{C_C}\right) & 0 & \left(\frac{-1}{C_C}\right) & 0 & 0 & 0 \\ 0 & 0 & 0 & 0 & \left(\frac{1}{L_{c2}}\right) & \left(\frac{-R_{c2}}{L_{c2}}\right) & \left(\frac{-1}{L_{c2}}\right) & 0 & 0 \\ 0 & 0 & 0 & 0 & 0 & \left(\frac{1}{C_2}\right) & 0 & 0 & 0 \\ 0 & 0 & 0 & 0 & 0 & 0 & 0 & \left(\frac{-R_{L2}}{L_{L2}}\right) & \omega_2 \\ 0 & 0 & 0 & 0 & 0 & 0 & 0 & -\omega_2 & \left(\frac{-R_{L2}}{L_{L2}}\right) \end{bmatrix}$$

$$g(x) = \begin{bmatrix} (\frac{-1}{2L_{L1}})x_3 & 0 & 0 & 0 \\ 0 & (\frac{-1}{2L_{L1}})x_3 & 0 & 0 \\ (\frac{3}{4C_1})x_1 & (\frac{3}{4C_1})x_2 & 0 & 0 \\ 0 & 0 & 0 & 0 \\ 0 & 0 & 0 & 0 \\ 0 & 0 & 0 & 0 \\ 0 & 0 & (\frac{-3}{4C_2})x_8 & (\frac{-3}{4C_2})x_9 \\ 0 & 0 & (\frac{1}{2L_{L2}})x_7 & 0 \\ 0 & 0 & 0 & (\frac{1}{2L_{L2}})x_7 \end{bmatrix}$$

$$[R] = \begin{bmatrix} (\frac{1}{L_{L1}}) & 0 & 0 & 0 \\ 0 & (\frac{1}{L_{L1}}) & 0 & 0 \\ 0 & 0 & 0 & 0 \\ 0 & 0 & 0 & 0 \\ 0 & 0 & 0 & 0 \\ 0 & 0 & 0 & 0 \\ 0 & 0 & 0 & 0 \\ 0 & 0 & (\frac{-1}{L_{L2}}) & 0 \\ 0 & 0 & 0 & (\frac{-1}{L_{L2}}) \end{bmatrix}$$

$$h(x,u,z) = \begin{bmatrix} v_{1_d} & v_{1_q} & 0 & 0 & 0 & 0 & 0 & 0 & 0 \\ v_{1_q} & -v_{1_d} & 0 & 0 & 0 & 0 & 0 & 0 & 0 \\ 0 & 0 & 0 & 0 & 0 & 0 & 0 & v_{2_d} & v_{2_q} \\ 0 & 0 & 0 & 0 & 0 & 0 & 0 & v_{2_q} & -v_{2_d} \end{bmatrix}$$

To provide practical and realistic conditions, AOT and SMC –based nonlinear controllers are used to control (P_1 and Q_1) for side 1 and (U_{C2} and Q_2) for side 2 of GG VSC-HVDC systems. The overall system's mathematical model remains the same.

However, the outputs equations are changed to comprise (P_1, Q_1, U_{C2}, and Q_2) instead of (P_1, Q_1, P_2, and Q_2) [135].

Therefore, $h(x, u, z)$ become:

$$h(x,u,z) = \begin{bmatrix} v_{1_d} & v_{1_q} & 0 & 0 & 0 & 0 & 0 & 0 & 0 \\ v_{1_q} & -v_{1_d} & 0 & 0 & 0 & 0 & 0 & 0 & 0 \\ 0 & 0 & 0 & 0 & 0 & 0 & 1 & 0 & 0 \\ 0 & 0 & 0 & 0 & 0 & 0 & 0 & v_{2_q} & -v_{2_d} \end{bmatrix}$$

Indeed, the voltage drop and the power losses in the DC link are taken into account according to the power flow direction (flow from station 1 to station 2 or vice versa).

Subsequently, our goal will be the design of robust nonlinear controllers under parameters uncertainties and for different DC links lengths.

3.7 Lyapunov Theory–based Nonlinear Control

For nonlinear GG VSC-HVDC transmission systems, the design of feedback controllers to cope with a wide range of model uncertainties leads either to robust or to adaptive control problem. Hereby, the robust Lyapuvov theory–based nonlinear control such as AOT and SMC are applied for system's in which the model uncertainty is characterized as imposed perturbations.

The basic target is to design the control input so that the control output y_i tracks its reference value y_{iref}. Accordingly, the tracking error ε_i approaches zero when time tends to infinity. To validate that, two different controllers based on AOT and SMC are proposed.

After developing the system's mathematical model, the design of robust nonlinear controllers based on AOT and SMC is illustrated. The actual VSC-HVDC physical system is often influenced by external or internal uncertainties' interferences. Despite parameter uncertainty and nonlinear dynamics, appropriate nonlinear feedback laws –based on AOT and SMC– are consequently deduced so that the actual trajectory tracks the desired trajectories. Therefore, both active and reactive powers of the first converter (P_1 and Q_1) besides the DC voltage and reactive power of the other (U_{C2} and Q_2) are controlled [135].

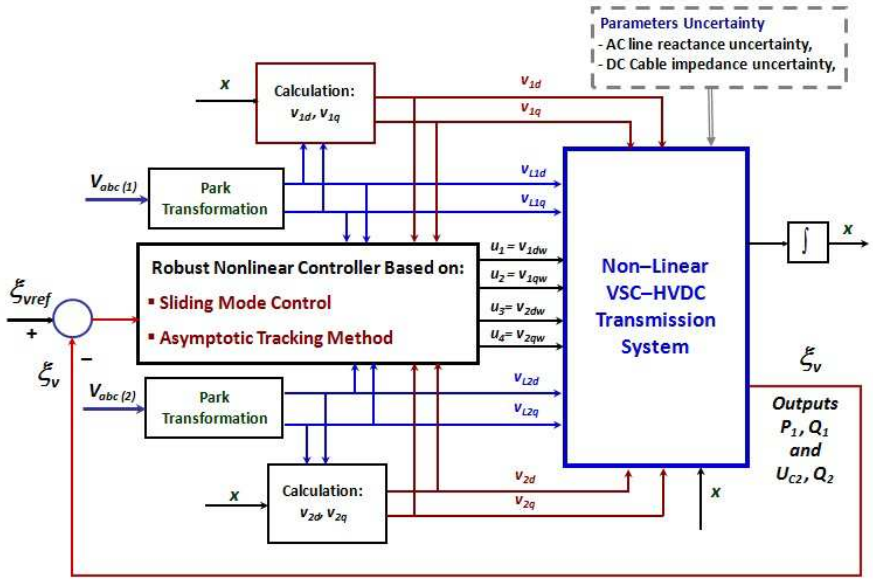

Figure 3.22: Overall GG VSC-HVDC system schematic diagram with nonlinear controller based on AOT and SMC.

Unity power factors are realized at both converters' AC sides through zero reactive powers tracking [135]. The receiving converter DC voltage, U_{C2}, is to be governed to its rated value. The DC link losses and voltage drop are taken into account. Bidirectional control of active power flow is performed [135].

AOT and SMC–based nonlinear controllers are examined to perform reference trajectory tracking or stabilization of nonlinear VSC-HVDC system. A proof of stability is given when the system exhibits finite time convergence to the origin in case of stabilization problem, or to reference trajectory for tracking problem in presence of parameter uncertainties [94].

The overall GG VSC-HVDC system block diagram together with its nonlinear control is shown in Figure (3.22).

For this purpose, the references of outputs and states (P_1, Q_1, U_{C2} and Q_2) supposing the power delivered to station 2 are [135]:

$$\xi_{1ref}=200 \text{ MW}, \xi_{2ref}=0 \text{ MVar}, \xi_{3ref}=300 \text{ kV}, \text{ and } \xi_{4ref}=0 \text{ MVar}$$

where, ξ_{1ref}, ξ_{2ref}, and ξ_{4ref} respectively refer to the reference values of the ouputs P_1, Q_1, and Q_2. ξ_{3ref} denotes the reference value of the DC voltage state U_{C2}.

As the reference values are constant, their derivatives are zeros.

In order to formulate nonlinear controller based on AOT and sliding modes, these steps should be pursued:

Step 1: Assume the sliding surfaces as error functions for the signals to be tracked, then: $\varepsilon_v(\xi) = \xi_{vref} - \xi_v$. Obviously, ξ_v can be either an output or a state signal.

Step 2: To ensure stability in accordance with Lyapunov stability theorem, an appropriate mandatory positive definite Lyapunov energy function candidate such as $V(\xi) = 0.5\varepsilon^2(\xi) > 0$ is considered. Then, the negative definiteness of its time derivative $\dot{V}(\xi) = \varepsilon(\xi)\dot{\varepsilon}(\xi) < 0$ has to be ensured.

Step 3: The negative definiteness ($\dot{V}(\xi) < 0$) is validated by suitably selecting positive tuning gains using:

- ***AOT approach:*** $\dot{\varepsilon}(\xi) = -K\varepsilon(\xi)$

  Despite choosing a positive value for the tuning gain K leads to system's stability, undesirable chattering may be expected in the system dynamic behavior. Accordingly, the nonlinear AOT approach may be unfavorable compared to the SMC one.

- ***SMC approach:*** $\dot{\varepsilon}(\xi) = -K_1\varepsilon(\xi) - K_2 func(\varepsilon(\xi))$

  Any two-terms SMC formula among the set of equations in Section 2.7 can be proposed for $\dot{\varepsilon}(\xi)$. Positive tuning gains K_1 and K_2 are selected to ensure $\dot{V}(\xi)$ to be always negative. The choice of two-terms formula sliding surface with a hyperbolic tangent function can adequately amend the chattering problem probably caused by single-term SMC (K_1=0).

For simplicity, equal positive tuning gains are assumed (K_1=K_2=K). Therefore, $\dot{\varepsilon}(\xi) = -K(\varepsilon(\xi) + \tanh(\varepsilon(\xi)))$.

The rate at which the tracking error converges to zero is governed by the proper selection of tuning gains using a simple trial and error approach. Therefore, system's behavior with shorter settling time, reasonable overshoot and acceptable steady-state error will be revealed.

Step 4: Any positive tuning gains selection guarantees the attainment of the previously mentioned stability conditions of Lyapunov candidate and its derivatives. These tuning gains affects the convergence speed.

Higher positive values of tuning gains leads to more negative definite $\dot{V}(\xi)$. Consequently, the system's behavior in catching up its input's variation is faster. Thus, shorter time response is accomplished.

Selecting K=100 results in two to three cycles of transient response if the frequency is 50 or 60 Hz which is acceptable for power system applications [136, 137].

Step 5: The robustness of the nonlinear controllers based on AOT and sliding modes is realized and evaluated in case of different DC link lengths up to 1000 km (i.e., *10 times the typical DC link length*).

It should be noted that the Lyapunov function and its derivative can be functions of either the system state variables, outputs or both.

3.7.1 Nonlinear Feedback Control Laws Deduction

To deduce feedback AOT and SMC signals, these error signals and their derivations are assumed:

$$\varepsilon_v(\xi) = \xi_{vref} - \xi_v \qquad v = 1, \dots 4 \tag{3.45}$$

$$\dot{\varepsilon}_v(\xi) = \dot{\xi}_{vref} - \dot{\xi}_v \qquad v = 1, \dots 4 \tag{3.46}$$

For AOT:

$$\dot{\varepsilon}_v(\xi) = -K(\varepsilon_v(\xi)) \qquad v = 1, \dots 4 \tag{3.47}$$

For two-terms SMC:

$$\dot{\varepsilon}_v(\xi) = -K(\varepsilon_v(\xi) + \tanh(\varepsilon_v(\xi))) \qquad v = 1, \dots 4 \tag{3.48}$$

$$\dot{\xi}_v = -\dot{\varepsilon}_v(\xi) \qquad v = 1, \dots 4 \tag{3.49}$$

Therefore, ($\dot{P}_1$ and $\dot{Q}_1$) and ($\dot{U}_{C2}$ and $\dot{Q}_2$) respectively are expressed as:

$$\begin{cases} \dot{\xi}_1 = \dot{P}_1 = \dfrac{3}{2}(v_{1_d}\dot{i}_{L1_d} + v_{1_q}\dot{i}_{L1_q}) \\ \dot{\xi}_2 = \dot{Q}_1 = \dfrac{3}{2}(v_{1_q}\dot{i}_{L1_d} - v_{1_d}\dot{i}_{L1_q}) \end{cases} \tag{3.50}$$

and,

$$\begin{cases} \dot{\xi}_3 = \dot{U}_{C2} = \dfrac{-1}{C_2} i_{c2} + \dfrac{3}{4C_2} i_{L2_d} u_3 + \dfrac{3}{4C_2} i_{L2_q} u_4 \\ \dot{\xi}_4 = \dot{Q}_2 = \dfrac{3}{2}(v_{2_q} \dot{i}_{L2_d} - v_{2_d} \dot{i}_{L2_q}) \end{cases} \tag{3.51}$$

The currents' state derivatives ($\dot{i}_{L1_d}$, $\dot{i}_{L1_q}$, $\dot{i}_{L2_d}$, and $\dot{i}_{L2_q}$) in Equations (3.50)-(3.51) are replaced by their corresponding equations listed in the state space expressions of Equation (3.44).

Both equations stated in (3.50) are then simultaneously solved to deduce the control inputs related to the first converter, then:

$$\begin{cases} u_1 = \dfrac{v_{1_d}(\frac{2}{3}\dot{\xi}_1 - \alpha_1) + v_{1_q}(\frac{2}{3}\dot{\xi}_2 - \alpha_2)}{(\frac{-1}{2L_{L1}}) x_3 (v_{1_d}^2 + v_{1_q}^2)} \\ u_2 = \dfrac{v_{1_q}(\frac{2}{3}\dot{\xi}_1 - \alpha_1) - v_{1_d}(\frac{2}{3}\dot{\xi}_2 - \alpha_2)}{(\frac{-1}{2L_{L1}}) x_3 (v_{1_d}^2 + v_{1_q}^2)} \end{cases} \tag{3.52}$$

Similarly, the other couple of equations in (3.51) are simultaneously solved to formulate the second converter control signals, therefore:

$$\begin{cases} u_3 = \dfrac{\frac{1}{2L_{L2}} x_7 v_{2d} [\dot{\xi}_3 + \frac{1}{C_2} x_6] - \frac{3}{4C_2} x_9 [\frac{2\dot{\xi}_4}{3} - \alpha_3]}{(\frac{1}{2L_{L2}})(\frac{-3}{4C_2}) x_7 [x_8 v_{2d} + x_9 v_{2q}]} \\ u_4 = \dfrac{\frac{1}{2L_{L2}} x_7 v_{2q} [\dot{\xi}_3 + \frac{1}{C_2} x_6] + \frac{3}{4C_2} x_8 [\frac{2\dot{\xi}_4}{3} - \alpha_3]}{(\frac{1}{2L_{L2}})(\frac{-3}{4C_2}) x_7 [x_8 v_{2d} + x_9 v_{2q}]} \end{cases} \tag{3.53}$$

where,

$$\begin{aligned} \alpha_1 &= v_{1_d}(-\frac{R_{L1}}{L_{L1}} x_1 + \omega_1 x_2 + \frac{1}{L_{L1}} z_1) + v_{1_q}(-\omega_1 x_1 - \frac{R_{L1}}{L_{L1}} x_2 + \frac{1}{L_{L1}} z_2) \\ \alpha_2 &= v_{1_q}(-\frac{R_{L1}}{L_{L1}} x_1 + \omega_1 x_2 + \frac{1}{L_{L1}} z_1) - v_{1_d}(-\omega_1 x_1 - \frac{R_{L1}}{L_{L1}} x_2 + \frac{1}{L_{L1}} z_2) \\ \alpha_3 &= v_{2_q}(-\frac{R_{L2}}{L_{L2}} x_8 + \omega_2 x_9 - \frac{1}{L_{L2}} z_3) - v_{2_d}(-\omega_2 x_8 - \frac{R_{L2}}{L_{L2}} x_9 - \frac{1}{L_{L2}} z_4) \end{aligned}$$

Noticeably, the control inputs of both converters are decoupled as given in Equations (3.52) and (3.53) respectively.

3.7.2 Stability Analysis and Robustness Assessment

Different nonlinear approaches based on Lyapunov theory such as AOT and SMC are therefore used for performing the required control objectives. The system states and output powers' time responses are pointed out to investigate the effectiveness of the proposed controllers. When these controllers are employed to VSC-HVDC systems shown in Figure (3.20) under different operating conditions, the dynamic behaviors are compared in order to verify which control methodology is better adopted to deal with GG VSC-HVDC systems. The robustness of the proposed controllers are assessed under parameter uncertainties such as DC cable resistance and AC line reactance variations.

Simulations are performed using two-terms SMC controller with $K_1 = K_2 = 100$ under parameter uncertainties. It is assumed that DC link's resistance is increased up to 25% of its rated value (i.e., *worst possible realistic value due to uncertainties caused by high currents flow*). Different DC link distances up to 10 times its typical length of 100 km are studied.

Simulations are done for 200 km, 500 km and 1000 km DC link lengths. Therefore, the DC link parameters as resistances, inductances and shunt capacitances are increased to 2, 5 and 10 times their typical values respectively

The controllers robustness are examined for different DC link lengths (200, 500 and 1000 km) where the length variation is assumed by changes of link's resistance (*changing the resistance is enough as the line inductance is negligible because the rate of change of d-q currents are zeros and the capacitive reactance is vanished in DC*).

The designated controller, with fixed tuning gains, can be therefore used to provide better dynamic stability and enhanced system's performance if:
(i) An identical VSC-HVDC transmission system is used to interconnect two AC networks separated by higher distances up to 1000 km;
(ii) Uncertainties in the VSC-HVDC's DC link impedance up to 25%.

As shown in Figure (3.23), the power flows of both sides and the DC line voltage dynamic behavior depicts the system's stability with different DC link lengths up to 1000 km considering a step in P_{1ref}. P_{1ref} was initially adjusted to 200 MW rated value. At t=2 seconds, it increases by 20% to be 240 MW. A second later, it decreases to 160 MW.

From Figure (3.23a), the reactive powers Q_1 and Q_2 successfully tracks their zero reference values. Therefore, unity power factor is attained for both sides. Very small overshoots with setting time of about 150 mseconds are yielded in the reactive powers behavior. The active power of the sending side VSC's AC terminal P_1 is perfectly controlled to its 200 MW, 240 MW and 160 MW rated values (i.e., *the value to be tracked*). After the step, no active power overshoot reveals. Setting time of about 150 mseconds is required for tracking the new active power reference. The active power on the receiving side VSC's AC terminal P_2 becomes less than P_1 with a value equivalent to the power losses in the DC line. The losses are directly proportional to the DC link's length. Longer DC line leads to higher power loss. Hence, smaller P_2 is attained.

From Figure (3.23b), admissible DC voltages (U_{C1}, U_{CC} and U_{C2}) result for different DC link lengths. U_{C2} is perfectly governed to its rated 300 kV for all proposed DC link lengths. For different DC link lengths, U_{CC} and U_{C1} values are altered because the DC line voltage drop does not remain constant. The DC line length varies proportionally to its resistance. Thus, longer DC links result in greater voltage drops. Therefore, higher values of U_{CC} and U_{C1} are revealed.

Figure (3.24) illustrate the proposed AOT controller's capability to control the active and reactive power at the sending VSC's AC terminal to their set-point values of 200 MW and zero respectively considering DC line resistance uncertainties up to 25%. In addition, the reactive power at receiving HVDCs' AC side is successfully maintained to its reference value. Q_{2ref} was initially adjusted at 40 MVar that represents a lagging power factor case. Then at t=2 seconds, it decreases to zero for a duration of one second in which the unity power factor is yielded. Finally, Q_{2ref} drops to -40 MVar and the power factor becomes leading. AOT control efficiently guarantees zero steady state tracking error under this kind of parameter uncertainties. However, undesired chattering in the P_2 behavior is demonstrated. This problem is considered as the major AOT implementation obstacle.

From Figure (3.24b) confirms that the DC voltage on the receiving DC terminal of the GG VSC-HVDC is perfectly governed to its rated 300 kV using nonlinear control based AOT. The DC voltage on the sending DC terminal exceeds 300 kV with an amount equivalent to the DC line voltage drop. Explicitly, unfavorable high frequency oscillations appear in the U_{CC} and U_{C1} dynamic performance if AOT control is used.

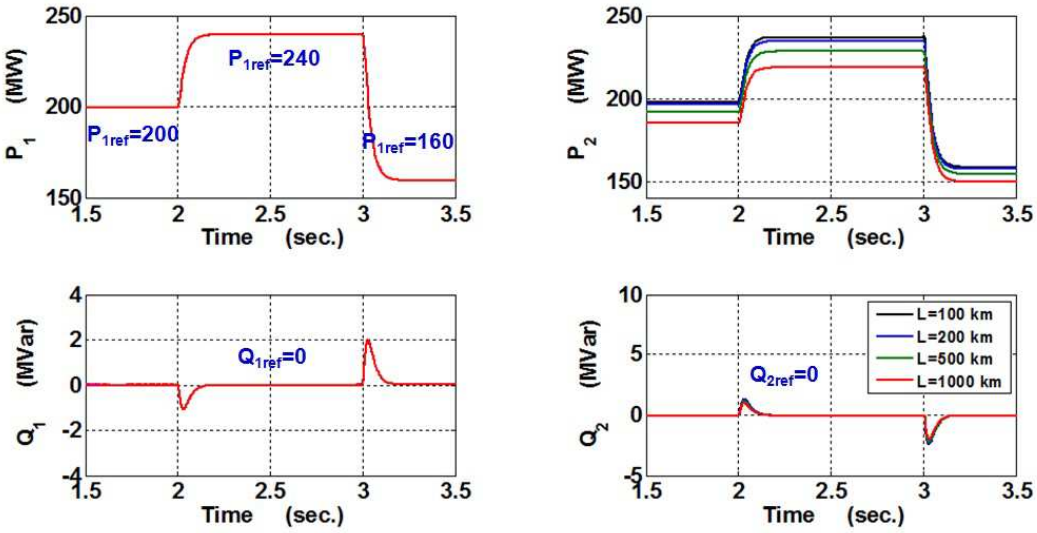

(a) Active and reactive powers time responses

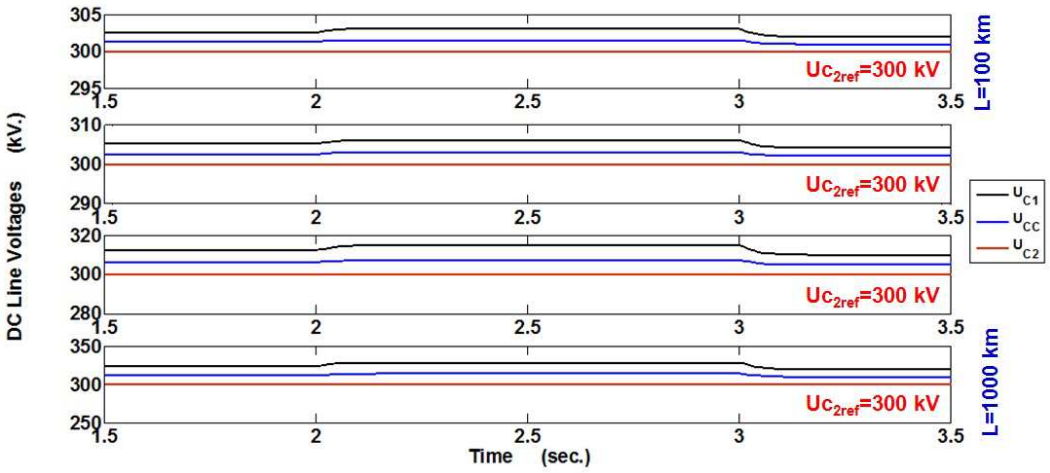

(b) DC line voltages time responses

Figure 3.23: System dynamic behavior using two-terms SMC (Step: P_{1ref}).

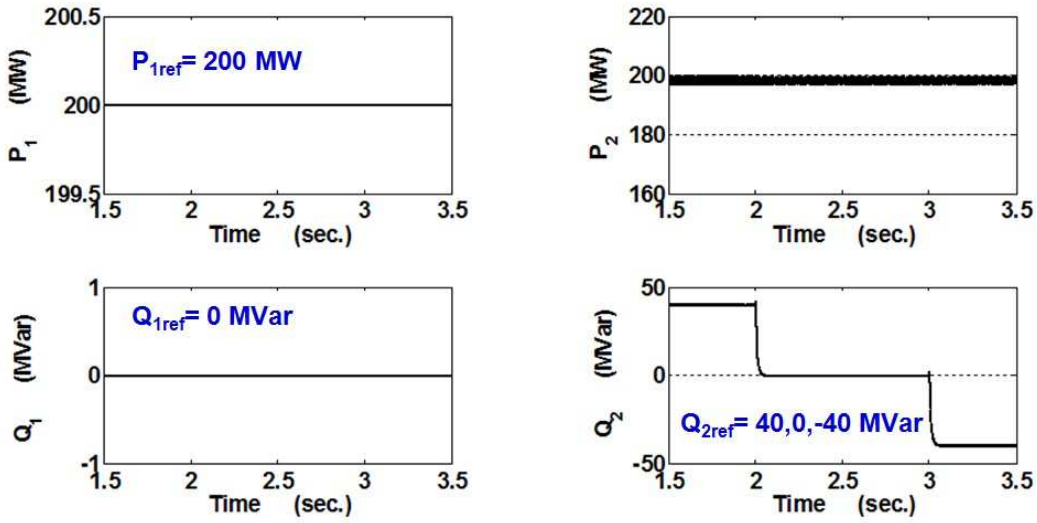

(a) Active and reactive powers time responses

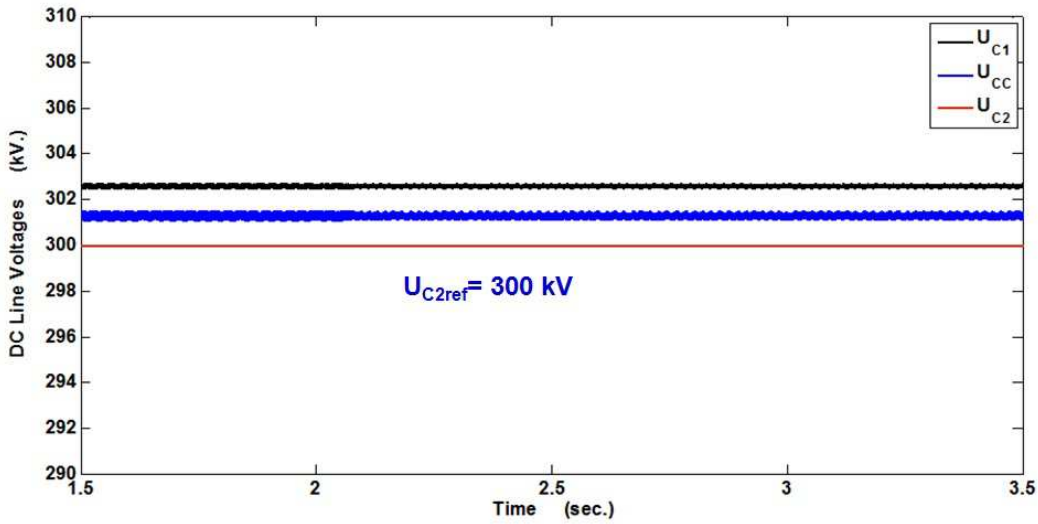

(b) DC line voltages time responses

Figure 3.24: System dynamic behavior using AOT control (Step: Q_{2ref}).

Figure (3.25) depicts the system's active, reactive powers and the DC line voltages dynamic behavior considering nonlinear controller based two-terms SMC in presence of variations in the DC line resistance until 25% and a step in Q_{2ref}. The SMC successful operation toward stabilizing the system is verified. Desirable chattering-free behavior result in case of using a two-terms SMC with a continuous hyperbolic function.

Considering AC line reactance variations, the system dynamic behavior is presented in Figure (3.26). The AC line reactance X_{L1} is increase by 20% of its typical value at t=2 seconds due to a sudden variation in the topology of the network. Initially, the P_1, Q_1, U_{C2} and Q_2 perfectly tracks their reference values of 200 MW, zero MVar, 300 kV and zero MVar respectively. Unity power factor is attained at the AC sides of both converters. Due to the AC line reactance rise, U_{C2} and Q_2 time responses track their reference values. A very small overshoot of about 150 mseconds settling time result in Q_2 behavior. Although their stable dynamic behavior, P_1 and Q_1 -on the side where the AC line reactance varies- are not controlled to their expected values previously mentioned. Consequently, P_2 performance is influenced. High steady state error appears in their behaviors. This undesired error could not be eliminated either by using an integral part in the SMC or by retuning the controller gains.

Using the proposed two-terms SMC controller, Figure (3.27) illustrates the percentage error result in P_1 behavior in case of AC line reactance variations. When X_{L1} changes by -20%, -10%, +10% and +20% of its nominal value, the error in P_1 is always positive. Increasing or decreasing X_{L1} by the same percentage leads to equal steady state errors. Obviously, the percentage error in P_1 behavior is about 9% if X_{L1} changes by $\pm$10%. This error increases to 28.3% for X_{L1} variation of $\pm$20%. The relation between $\Delta P_1\%$ and $\Delta X_{L1}\%$ is not linear.

Similarly, Figure (3.28) demonstrates the error in Q_1 behavior while changing X_{L1}. In consequence of X_{L1} variation, the reactive power behavior no longer tracks its reference zero value. Accordingly, the power factor differs than unity. Q_1 behavior increases to +57.19 MVar and +90.1 MVar if X_{L1} rises by +10% and +20% respectively. However, the decrease of X_{L1} by the latter percentages leads to negative Q_1 behavior. Nonlinear relation between the error in Q_1 behavior and X_{L1} variation is shown.

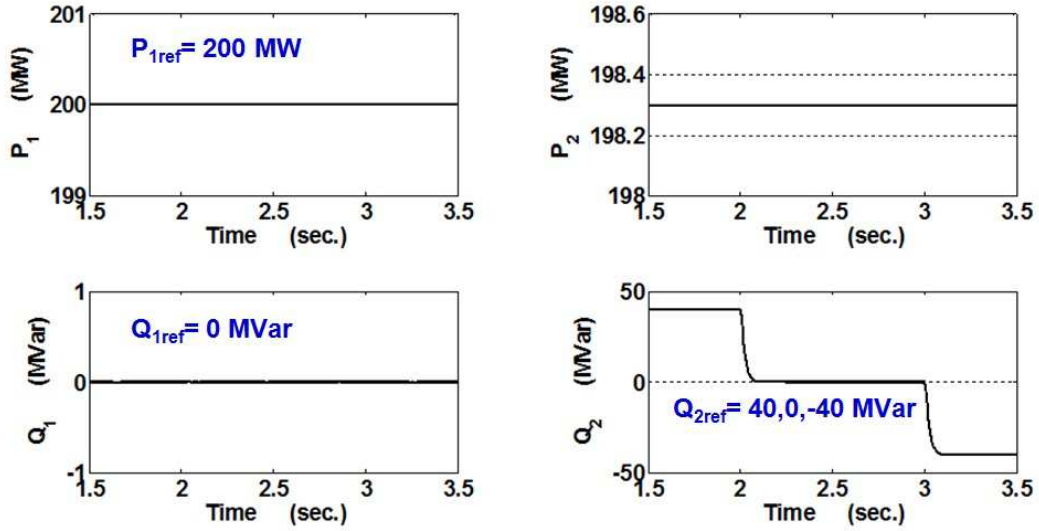

(a) Active and reactive powers time responses

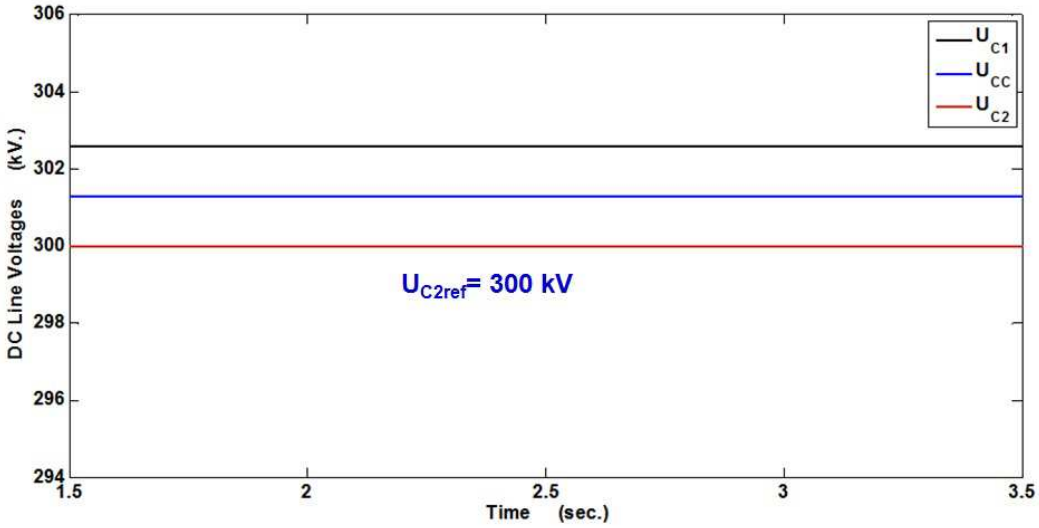

(b) DC line voltages time responses

Figure 3.25: System dynamic behavior using the two-terms SMC (Step: Q_{2ref}).

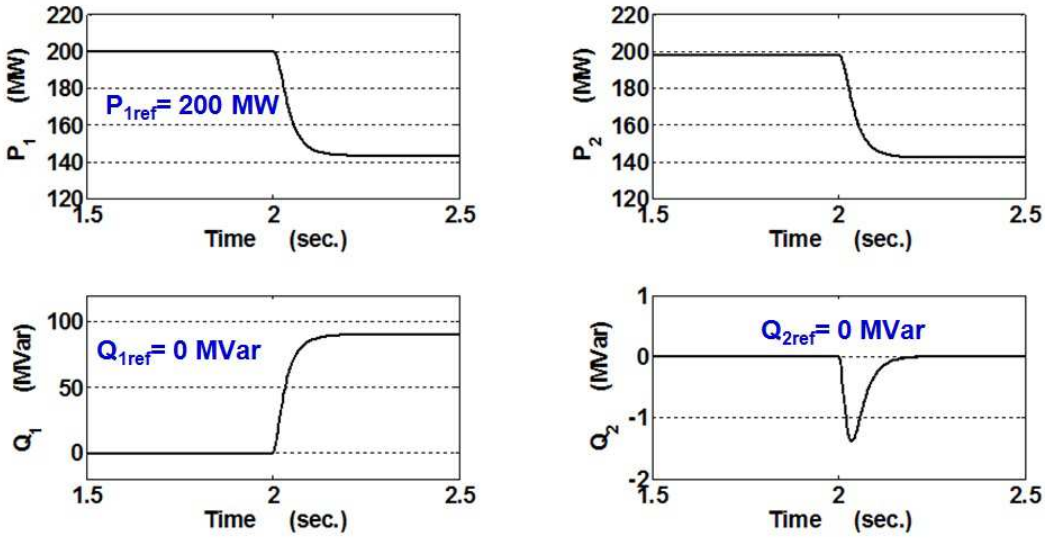

(a) Active and reactive powers time responses

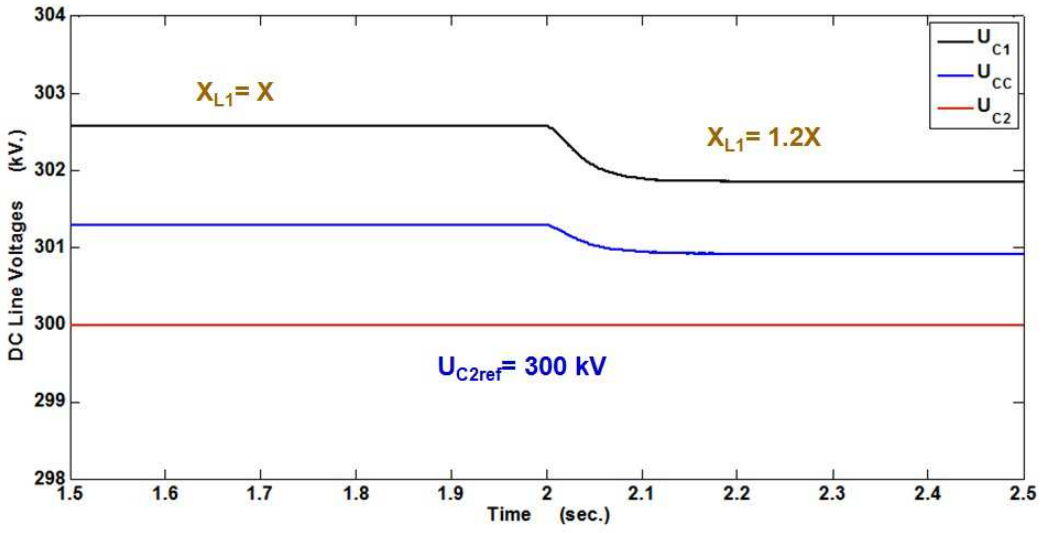

(b) DC line voltages time responses

Figure 3.26: System dynamic behavior using the two-terms SMC considering AC line reactance variations.

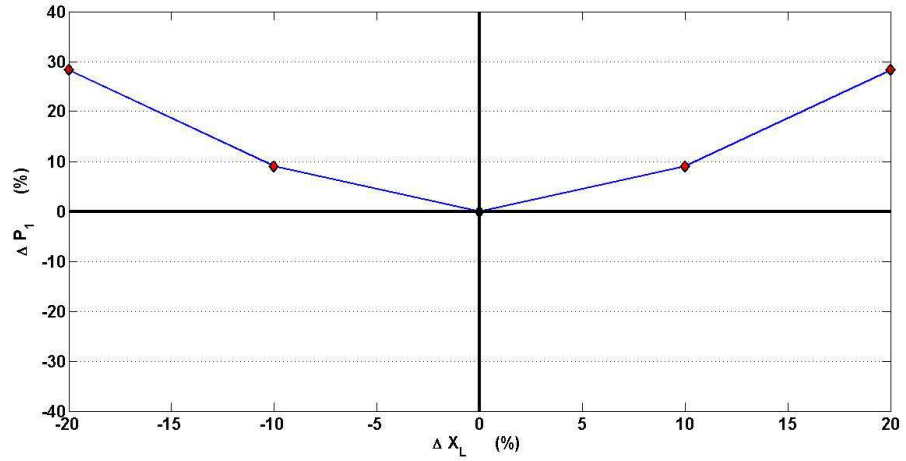

Figure 3.27: $\Delta P_1\%$ versus $\Delta X_{L1}\%$.

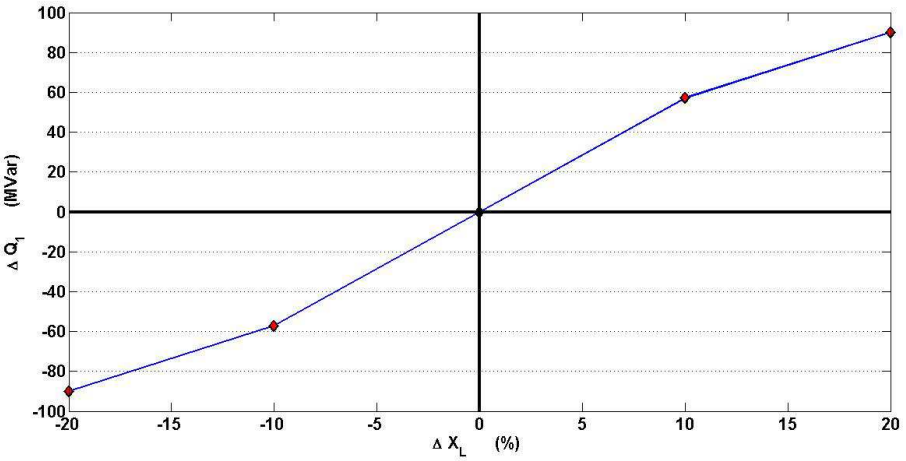

Figure 3.28: ΔQ_1 versus $\Delta X_{L1}\%$.

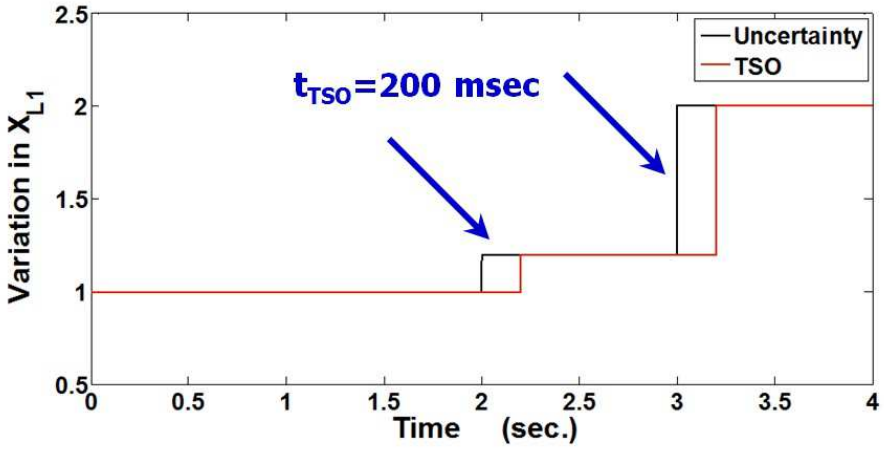

Figure 3.29: Correction of the AC line reactance through TSO.

It is concluded that the system dynamic performance is negatively influenced by the variation of the AC line reactance. Therefore, neither the AOT nor two-terms SMC is robust for this type of uncertainty as the control signals defined in Equations (3.52) and (3.53) are greatly affected by the AC line parameters.

In order to avoid this problem, it is supposed the new value of AC line reactance will be received from the TSO a certain time after the reactance variation. As shown in Figure (3.29), the time required until providing the controller with this new value is taken as 200 mseconds. The AC line reactance increases by 20% and 100% at t=2 and t=3 seconds respectively.

In Figure (3.30), the GG VSC-HVDC dynamic behavior is demonstrated in presence of AC line reactance variation and its correction via TSO.

During the first interval that terminates at t=2 seconds, $X_{L1} = X$. The two-terms SMC perfectly stabilizes the system. The controller acts perfectly towards controlling P_1, Q_1, U_{C2} and Q_2 to their corresponding reference values because $X_{L1} = X$ in the control signal expressions stated in Equations (3.52) and (3.53).

During the second interval (from t=2 seconds to t=2.5 seconds), $X_{L1} = 1.2X$. The steady state errors appear in the dynamic behavior of P_1, Q_1, and P_2. These error last 200 mseconds as still $X_{L1} = X$ in Equations (3.52) and (3.53).

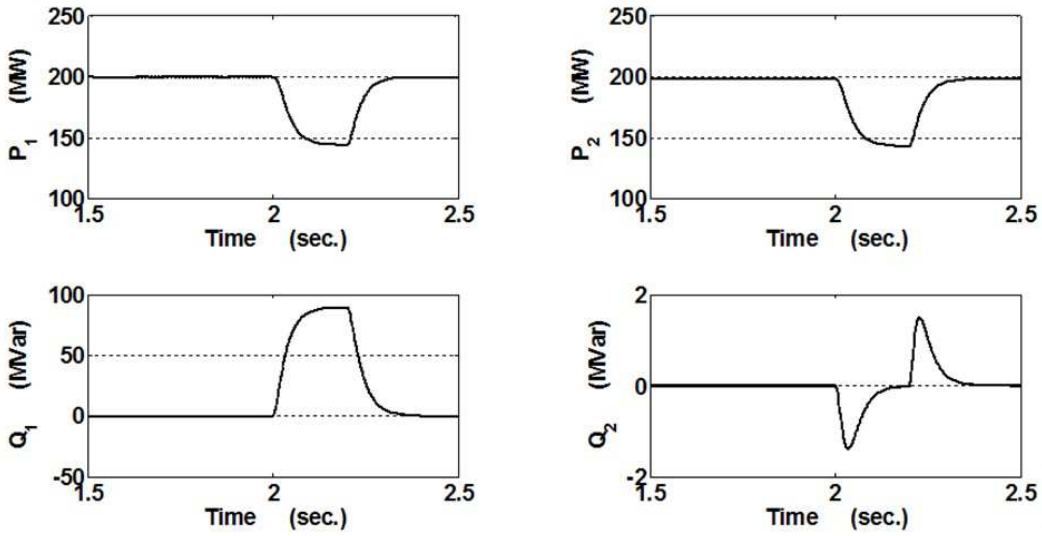

(a) Active and reactive powers time responses

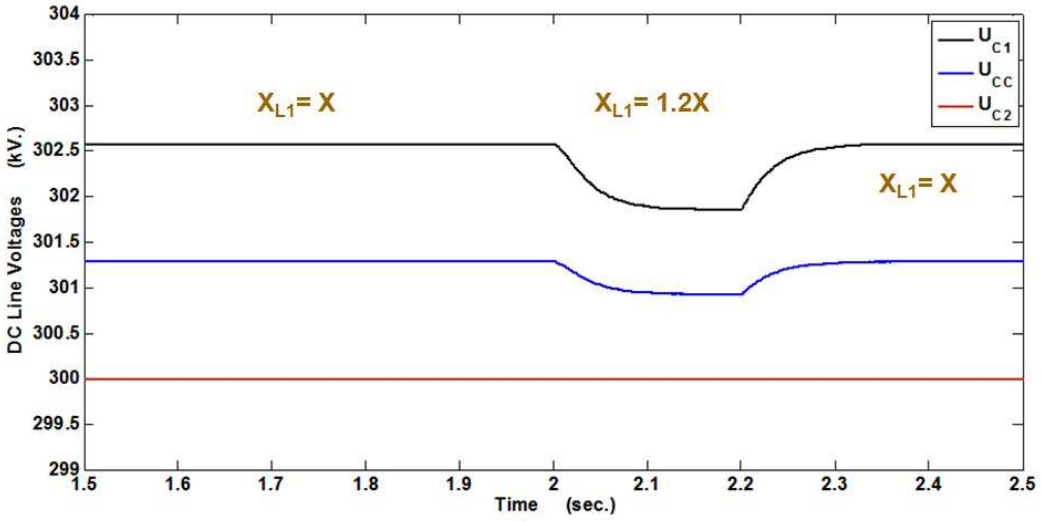

(b) DC line voltages time responses

Figure 3.30: System dynamic behavior using the two-terms SMC considering AC line reactance variation and correction via TSO.

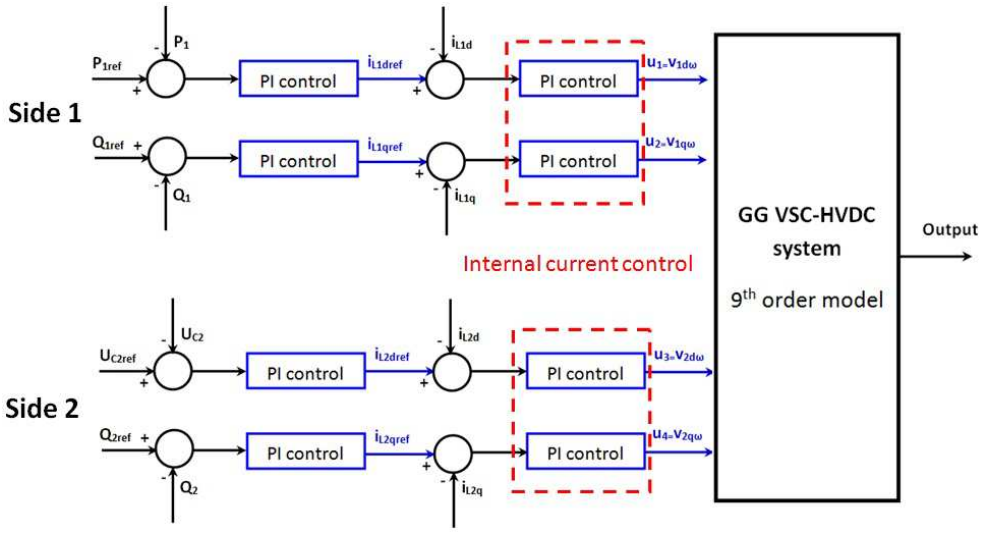

Figure 3.31: GG VSC-HVDC system controlled via PI control with internal current control loop.

However at 2.2 seconds, the TSO informs the control center with the new value X_{L1}. Then, a modification in calculating the control signals is accomplished. Therefore, $X_{L1} = 1.2X$ in Equations (3.52) and (3.53). Thereafter, the capability of the two-terms SMC towards maintaining again P_1, Q_1, U_{C2} and Q_2 at their corresponding reference values is verified.

Explicitly, nonlinear chattering-free two-terms SMC approach can be considered as a successful control methodology against DC link parameter variations especially with the proper selection of tuning gains. It can be favorably used not only during normal operating conditions but also for different DC link lengths to enhance the system performance.

To confirm the feasibility of using the two-terms SMC for GG VSC-HVDC transmission systems, the system's dynamic behavior and controller robustness are compared with the case of applying conventional PI control with cascaded internal current control in presence of uncertainties.

For this purpose, the overall system is controlled via PI control with internal current control loop as demonstrated in Figure (3.31. Four controllers are required for each converter. Two among them are used in the current control loop.

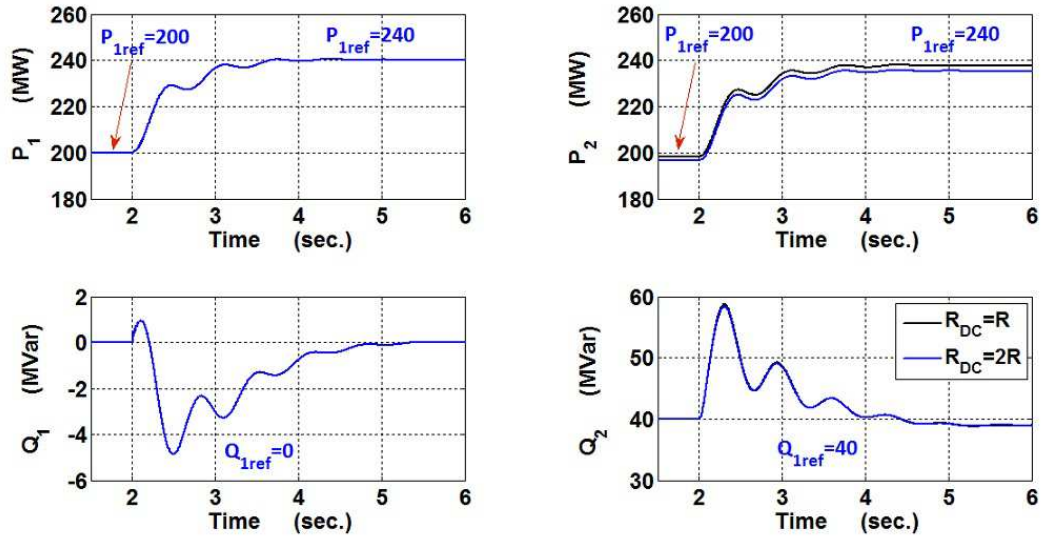

(a) Active and reactive powers time responses

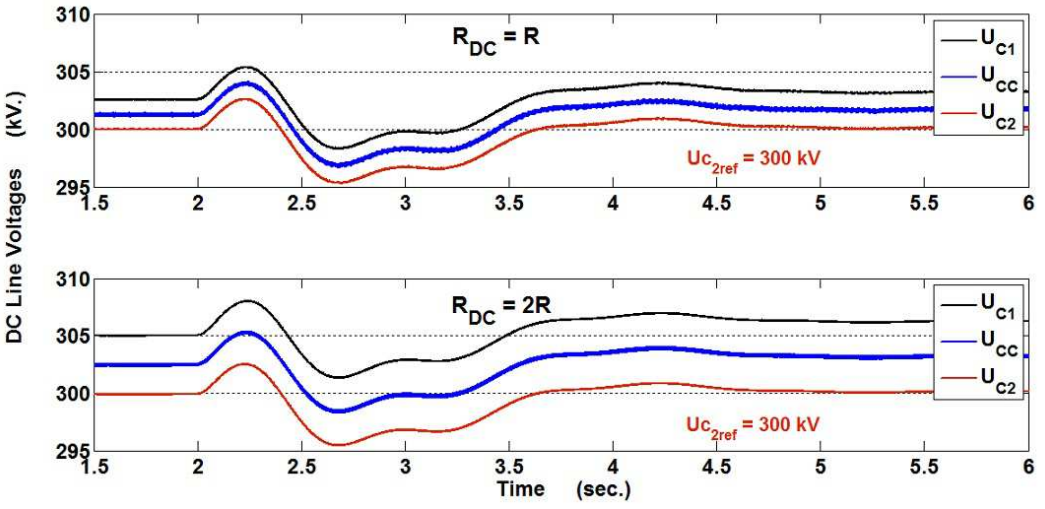

(b) DC line voltages time responses

Figure 3.32: System dynamic behavior using conventional PI controllers with cascaded internal current control (Step in P_{1ref} for two different DC line resistances).

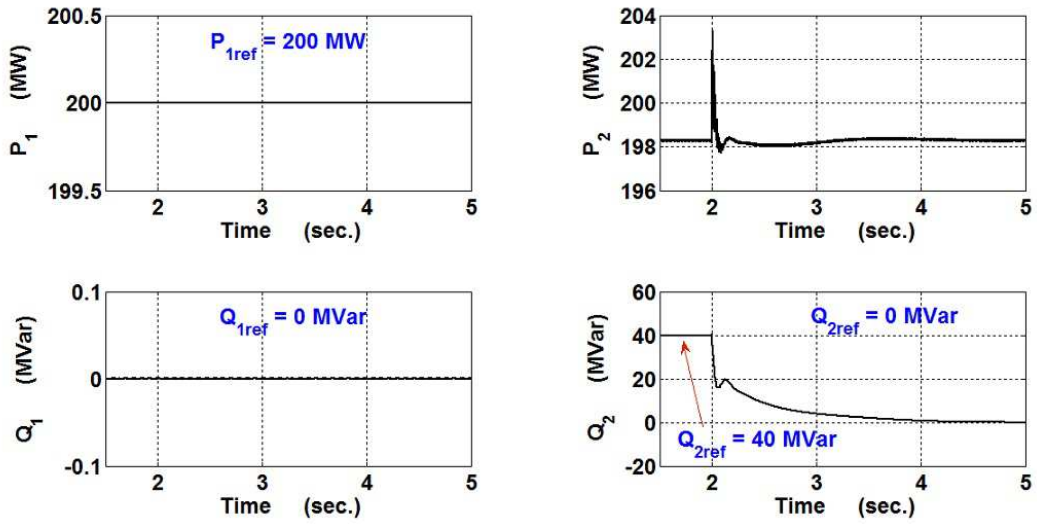

(a) Active and reactive powers time responses

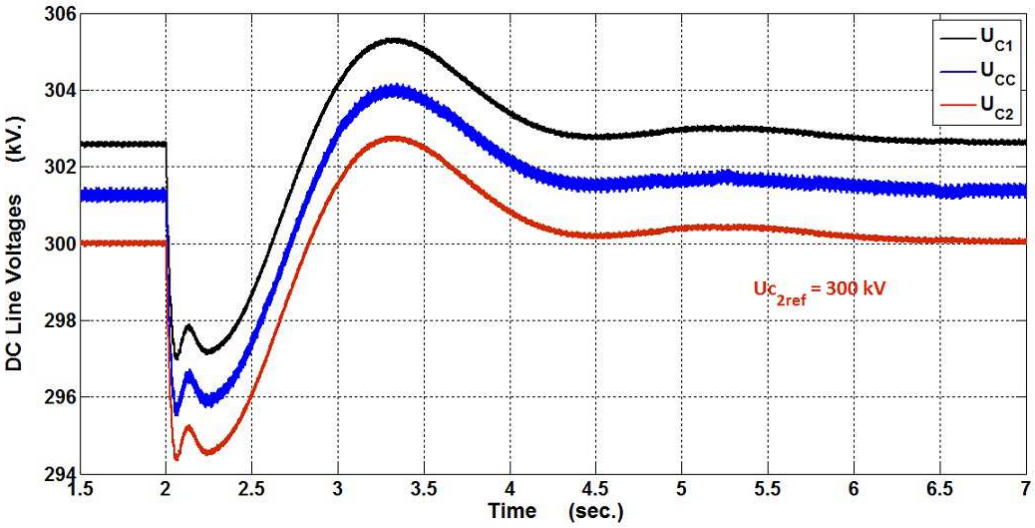

(b) DC line voltages time responses

Figure 3.33: System dynamic behavior using conventional PI controllers with cascaded internal current control (Step: Q_{2ref}).

Indeed, more PI controllers lead to more difficulty in tuning the controllers. Hence, the PI controller gains for both sides are tuned, step by step, to guarantee zero tracking errors and to ensure stability. However, attaining adequate compromise between the system performance and the controller robustness becomes more complex because of the mutual interaction and coordination of the controllers. The controllers parameters are listed in Appendix A.

Figure (3.32) demonstrates the system performance when controlled using cascaded conventional PI control with internal current loops. It is considered that P_{1ref} rises suddenly by 20% at t=2 seconds and the DC resistance is doubled (i.e., the DC link length is increased by 100%). In Figure (3.33), the system dynamic behavior is illustrated when controlled using cascaded conventional PI control with internal current loops in case of changing the reactive power reference Q_{2ref}. Initially, Q_{2ref}=40 MVar. At t=2 seconds, Q_{2ref} decreases to zero.

As shown in Figure (3.33a), (P_1 and Q_1) time responses perfectly track their corresponding (200 MW and zero MVar) reference values respectively. Reasonable behavior with settling time of about 1.5 seconds reveal in the Q_1 dynamic behavior. Moreover, stable DC line voltage dynamic behavior with acceptable overshoot and settling time of about 1.5 seconds are presented in Figure (3.33b).

The dynamic behavior shown in Figures (3.32) and (3.33) is less acceptable than that previously depicted in Figures (3.23) and (3.25) respectively where the two-terms SMC is used. Oscillated behavior with more overshoot and higher settling time of about 1.5 seconds is attained with cascaded conventional PI controllers.

3.8 Conclusions

Conventional PI controllers are applied to control GL VSC-HVDC transmission systems. The main purpose of governing the DC link voltage and controlling reactive power is attained. Thus, unity power factor is maintained. However, the system dynamic behavior is influenced by certain uncertainties. Therefore, conventional PI controllers are not robust enough against them.

For GG VSC-HVDC transmission systems, the system states and output powers' time responses investigate the effectiveness of various nonlinear control based AOT and SMC controllers under normal operating conditions and DC line parameter variations.

The dynamic behaviors are compared in order to verify which nonlinear control methodology is better adopted to deal with these systems. Furthermore, the proposed nonlinear controllers robustness are examined under parameter uncertainties such as DC line parameter variations, AC line reactance and reference signal variations.

For GG VSC-HVDC system, the results clarify that AOT control and two-terms SMC are robust to DC link parameter variations, for different DC link lengths up to 10 times. The controller's capability towards tracking the reference variations, improving the overall system's dynamic behavior and enhancing its stability are verified. In addition, these robust nonlinear controllers can be easily derived and implemented.

However, AOT controller's dynamic behavior comprises undesirable chattering. Thus, this nonlinear approach is less efficient towards the VSC-HVDC stabilization. Its dynamic performance is less attractive compared to that revealed when nonlinear two-terms SMC controllers are used.

The use of nonlinear controller based on two-terms SMC is significantly effective and a relatively successful control methodology especially when proper tuning gains are considered. Distinguished chattering-free dynamic behavior and satisfied stability level are performed in presence of DC link parameter variations. Hence, two-terms SMC can be profitably used to enhance system behavior not only during normal operating conditions but also in presence of this type of uncertainties and reference variation conditions.

However, this type of controllers is not robust against AC line reactance variations as the control signals are highly dependent on the AC line parameters. The AC line reactance value should be continually replaced by its new value in the controllers design. An additional adaptive parameter could be provided in the controller to remedy this problem.

Two-terms SMC provides enhanced behavior and relative simple gain tuning compared to the cascaded conventional PI controllers with internal current control.

Chapter 4

AC Network Control via VSC-HVDC Systems

THIS chapter aims illustrating the AC network control and stabilization through VSC-HVDC transmission systems. The overall GG VSC-HVDC system is replaced by a new equivalent model named SM via VSC-HVDC system. One of the ideal AC sources of the GG VSC-HVDC system is replaced by a nonlinear generator of seventh order mathematical model. The rest of the system, the DC link and the other ideal voltage source, is represented by a bus of constant voltage and variable angle. This bus is located at the converter side. After modeling the overall system, the conventional PI controller is employed at the converter's side to control the AC network, to damp the power angle oscillations and to enhance the system dynamic performance in presence of faults. Simulation results verify the controller capability towards desirably damping the power angle oscillations and enhancing the AC network's dynamic behavior.

4.1 Introduction

Power systems are nonlinear large-scale systems. Their modeling is a trade-off between respect of detail, modeling effort, simulation speed and data requirements. A detailed modeling is often necessary particularly when studying electromagnetic transients. For planning studies, when the details of the equipment are not yet known, standard models can be used. In order to obtain more acceptable results, quite detailed models '*full models*' should be used instead [49].

Additionally, if the equipment is located far away from the part of the system under study, the equipment can be modeled with less of details '*reduced model*'. Only for a detailed study of a part of the system where the equipment plays a prominent role, full models that closely mimic the behavior of the actual system are needed [19, 48, 49].

Standard models exist for numerous power system equipments, such as excitation systems [138], and steam and hydro turbines [139]. However, to our knowledge, no standard models for VSC-HVDC have been proposed in literature as stated in [49]. Recently, VSC-HVDC has an increasingly wide range of application in the power system [140]. Therefore, it is clearly an area of interest and receives a lot of attention. The power system engineer needs models of VSC-HVDC systems. In most stability and electromagnetic transients programs, such models are not yet available because the technology is relatively new, and hence not yet widespread [48, 49].

In order to study the impact of the VSC-HVDC control on damping the power angle oscillations of the synchronous generator in case of considerable disturbances such as faults, the GG VSC-HVDC transmission system is equivalently modeled by another simplified system of a single machine via VSC-HVDC system (SM via VSC-HVDC). For the SM VSC-HVDC system, synchronous machine is mathematically described by its full 7^{th} order model, wheras the VSC-HVDC is replaced by a less detailed model. Regardless of power electronics topologies, it is considered as a bus of constant voltage magnitude and variable angle . Hereby, the continuous adjustment of the d-component of the converter's voltage or the angle on its side becomes necessary to enhance the power angle oscillations of the synchronous machine's rotor.

The frequently occurring transient stability issues make studying the impact of VSC-HVDC systems on synchronous machines an essential pre-requisite. In addition, linking HVDC transmission systems with synchronous generators requires effective control strategy to improve the power angle oscillations as well as the overall system's transient stability [141].

Power system controllers design are mightily used to damp power system electromechanical oscillations. There are many approaches to damp these oscillations. Still, classical methods are not robust in presence of noise and system uncertainties mainly come from parameter variations, varying network topology (i.e., mainly from faults and/or sudden load variations) and dynamic variations [142].

Certain researchers design robust high order dynamic controllers which are relatively difficult to be implemented in practice [143, 144].

Due to its simplicity and ease to be practically implemented, a conventional PI controller is applied on the converters side of the SM via VSC-HVDC system to act on Power Oscillations Damping (POD) of the synchronous machine even under a fault as an important contribution of this study.

4.2 System Under Study

Synchronous generators play an important role in power system stability studies. An adequate model for synchronous generators is essential for a valid analysis of stability and dynamic performance. Hence, one of the AC generators in the GG VSC-HVDC tranmission system sketched and explicitly modeled in Section 3.6 is replaced by its detailed full seventh order nonlinear generator mathematical model [19, 145, 146, 147]. This model mainly accounts for the generator dynamics. It is quite accurate for studying low-frequency oscillations and transient stability of power systems [148]. However, the other AC source equipped with the DC link is equivalently replaced by a bus with a voltage of constant magnitude V^{∞} and variable angle. Before demonstrating the criteria proposed for enhancing the power angle oscillations of the SM via VSC-HVDC system, the full order mathematical model of the single machine infinite bus (SMIB) system is presented.

4.2.1 SMIB system

The extended synchronous generator, shown in the SMIB diagram of Figure (4.1), is mathematically expressed by the following equations with the state space vector $x^t = [i_d, i_q, i_f, i_{kd}, i_{kq}, \omega_r, \delta_r]$ [19, 145, 146, 147]:

$$\frac{1}{\omega_o}(-X_{dt}\dot{i}_d + X_{ad}\dot{i}_f + X_{ad}\dot{i}_{kd}) = R_{eq}i_d + \frac{\omega_r}{\omega_o}(-X_{qt}i_q + X_{aq}i_{kq}) + V_d^{\infty} \tag{4.1}$$

$$\frac{1}{\omega_o}(-X_{qt}\dot{i}_q + X_{aq}\dot{i}_{kq}) = R_{eq}i_q - \frac{\omega_r}{\omega_o}(-X_{dt}i_d + X_{ad}i_f + X_{ad}i_{kd}) + V_q^{\infty} \tag{4.2}$$

$$\frac{1}{\omega_o}(-X_{ad}\dot{i}_d + X_f\dot{i}_f + X_{ad}\dot{i}_{kd}) = -R_f i_f + V_f \tag{4.3}$$

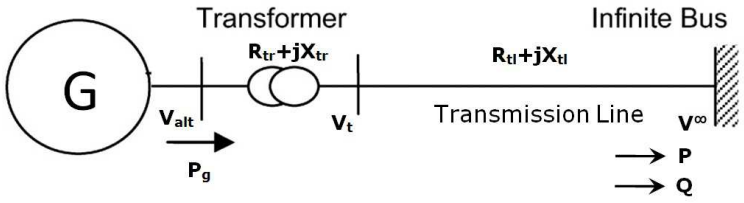

Figure 4.1: Single machine infinite bus system.

$$\frac{1}{\omega_o}(-X_{aq}\dot{i}_q + X_{kq}\dot{i}_{kq}) = -R_{kq}i_{kq} \tag{4.4}$$

$$(\frac{2H}{\omega_o})\dot{\omega_r} = T_m - T_{em} - (\frac{D}{\omega_o})\omega_r \tag{4.5}$$

where,

$$T_{em} = \psi_d i_q - \psi_q i_d \tag{4.6}$$

thus,

$$T_{em} = -(X_d - X_q)i_d i_q + X_{ad}i_f i_q + X_{ad}i_{kd}i_q - X_{aq}i_{kq}i_d \tag{4.7}$$

$$\dot{\delta_r} = \omega_r \tag{4.8}$$

where,

$X_{dt} = (X_d + X_{tr} + X_{tl})$;

$X_{qt} = (X_q + X_{tr} + X_{tl})$;

$R_{eq} = (R_a + R_{tr} + R_{tl})$; and

$X = (X_d - X_q)$

The *d-q* components of the infinite bus voltage can be estimated by:

$$V_d^{\infty} = V^{\infty}\sin(\delta_r) \tag{4.9}$$

$$V_q^{\infty} = V^{\infty}\cos(\delta_r) \tag{4.10}$$

Equations (4.1)–(4.10) are gathered together to form the 7^{th} order synchronous generator block diagram with both V_f and T_m as inputs and all the system states as outputs. The parameters and variables in these equations are in (pu) values as listed in Appendix A, unless otherwise stated. They are defined as:

X_d: direct axis self inductive reactance

X_q: quadrature axis self inductive reactance

X_{ad}: direct axis mutual inductive reactance

X_{aq}: quadrature axis mutual inductive reactance

X_{fd}: field windings inductive reactance

X_{kd}: direct axis damper windings inductive reactance

X_{kq}: quadrature axis damper windings inductive reactance

R_a: armature windings resistance

R_f: field windings resistance

R_{kd}: direct axis damper windings resistance

R_{kq}: quadrature axis damper windings resistance

R_{tr}: transformer windings resistance

X_{tr}: transformer windings leakage inductive reactance

R_{tl}: transmission line series resistance

X_{tl}: transmission line series inductive reactance

H: inertia constant of the generator rotor in sec

D: load damping coefficient of the generator rotor in pu torque/(rad sec^{-1})

T_{em}: generator electromagnetic torque

ω_o: synchronous angular frequency in rad/sec

ω_r: slip angular frequency in rad/sec

δ_r: angle of the generator rotor mass in radians

i_d: direct axis component of the armature current

i_q: quadrature axis component of the armature current

i_f: field current

i_{kd}: current in the direct axis damper windings

i_{kq}: current in the quadrature axis damper windings

V_{alt}: generator terminal voltage

V_t: terminal voltage of the bus connected the transformer with the line

V_d^{∞}: direct axis component of the infinite bus voltage

V_q^{∞}: quadrature axis component of the infinite bus voltage

V_f: field voltage

$E_q^{'}$: transient EMF in the quadrature axis

P: steady state active power flow at the infinite bus

Q: steady state reactive power flow at the infinite bus

The mathematical model deduction and the initial conditions' calculations of this new equivalent system are fulfilled using Equations (4.1)–(4.8). Additionally, the steady state machine equation is derived from the former equations by assuming: (i) the derivation of the state variables = 0; (ii) the per unit slip ratio $(\omega_r/\omega_o) = 1$; and (iii) the steady state damper currents $i_{kdo} = i_{kq_o} = 0$.

Assuming an apparent power $(P + jQ)$ delivered to the the infinite bus (i.e., lagging power factor), then, the current flow can be calculated as:

$$i = I\angle{-\phi} = (P - jQ)/(V^{\infty})^{*} \tag{4.11}$$

Due to the phasor diagram representation depicted in Figure (4.2), $E_q^{'}$ can be deduced.

As the angle of the infinite bus voltage is always zeros, the initial rotor angle (δ_r=δ) is the angle of $E_q^{'}$ (i.e., the phase angle between the q-axis with respect to the infinite bus voltage).

Hence, the d-q components of the current can be calculated as:

$$I_{do} = I\sin(\delta_{ro} + \phi) \tag{4.12}$$

$$I_{qo} = I\cos(\delta_{ro} + \phi) \tag{4.13}$$

Then, the d-q components of the terminal voltage V_t are expressed by:

$$V_{tdo} = V_d^{\infty} + (R_{tr} + R_{tl})I_{do} - (X_{tr} + X_{tl})I_{qo} \tag{4.14}$$

$$V_{tqo} = V_q^{\infty} + (R_{tr} + R_{tl})I_{qo} + (X_{tr} + X_{tl})I_{do} \tag{4.15}$$

Therefore,

$$V_{to} = \sqrt{V_t^2{}_{do} + V_t^2{}_{qo}} \tag{4.16}$$

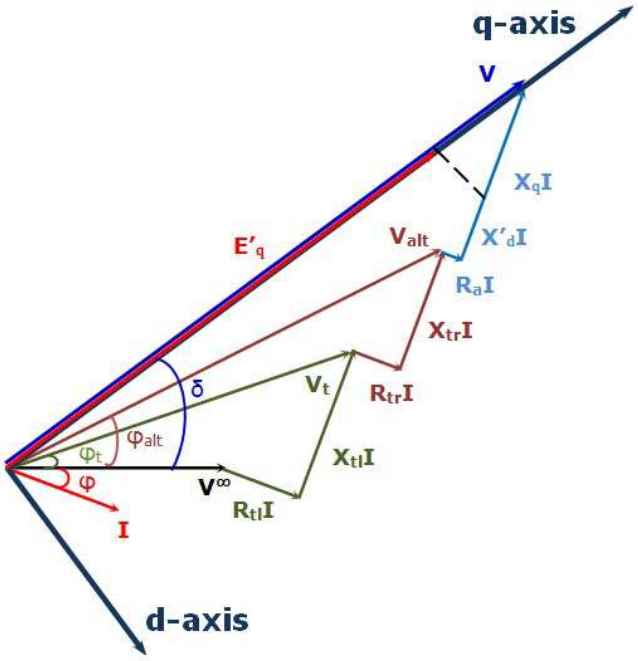

Figure 4.2: Voltages and currents phasor diagram representation.

The field current and voltage initial steady state values are:

$$I_{fo} = (R_{eq}I_{qo} + X_{dt}I_{do} + V_q^{\infty})/X_{ad} \tag{4.17}$$

$$V_{fo} = R_f I_{fo} \tag{4.18}$$

The initial steady state power delivered by the synchronous machine is:

$$P_g = V_{altdo}I_{do} + V_{altqo}I_{qo} \tag{4.19}$$

If a fault of a resistance R_{fault} and duration t_{fault} is supposed at the bus between the transformer and the transmission line in the SMIB system, then:

$$I_{fault} = \frac{V_t}{R_{fault}} \tag{4.20}$$

In case of fault, the current delivered by the generator is the sum of both the transmission line and the fault path currents. Before the fault occurrence and after its clearance, the fault resistance is considered as an open circuit. Thus, it can be modeled by a very high resistance of 1 MΩ.

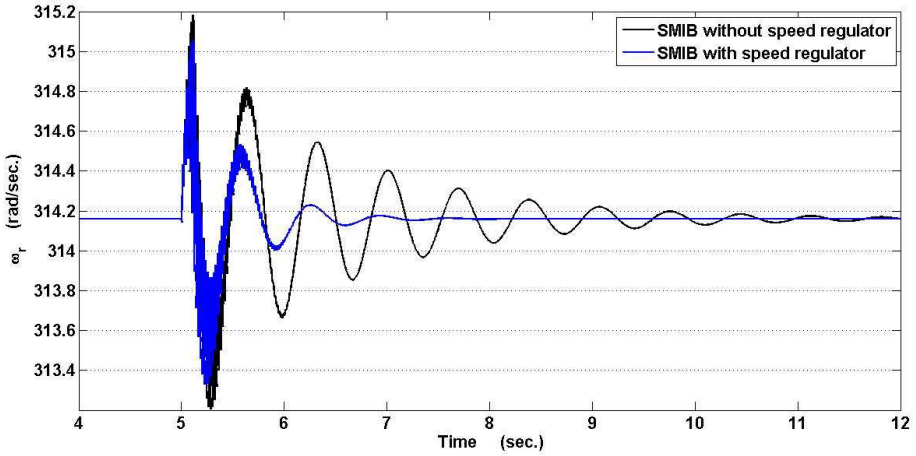

Figure 4.3: Rotor angular velocity time response for SMIB system in presence of a fault at t=5 seconds (R_{fault}=10 Ω and t_{fault}=120 mseconds).

However during the fault, small resistance of less than 10Ω is to be assumed. To reduce the risk of the generator's loss of synchronism in consequence of load variation or a fault, a PI controller (with $K_p \approx 0.0497$ and $K_i \approx 0.1034$) acts as a rotor speed regulator in order to keep the frequency near its scheduled value (50 Hz). Thus, the system's mechanical torque is adjusted.

In case of SM via VSC-HVDC systems, this PI regulator will act on guaranteeing the equilibrium between the system generation and its demand.

Figure (4.3) demonstrates the rotor speed time response in a SMIB system with and without a speed control considering a fault. Improved rotor speed time response result if the speed in regulated. Better performance with reduced overshoot and shorter settling time is obtained.

However, explicit oscillations of 50 Hz frequency appear in the rotor speed dynamic behavior. These oscillations mainly result due to the DC component of the fault current during the fault. The oscillations last less than 1 second after the fault.

Figure (4.4) shows that the rotor angle oscillations is damped when using a speed regulator despite the fault occurrence in the SMIB system. The dynamic response has lower overshoot and goes faster towards the steady state value compared to the case without using the speed regulator.

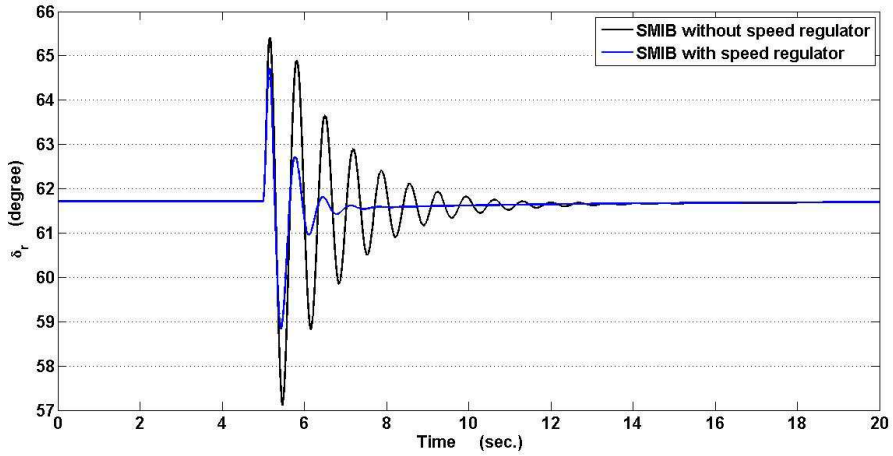

Figure 4.4: Rotor angle dynamic behavior for SMIB system in presence of a fault at t=5 seconds (R_{fault}=10 Ω and t_{fault}=120 mseconds).

4.2.2 SM via VSC-HVDC Model

The updated GG VSC-HVDC transmission system can be sketched as in Figure (4.5). In order to formulate the modified equivalent system of the GG VSC-HVDC transmission system as illustrated in Figure (4.6), the AC source of the first side -which is considered as the sending unit- is replaced by the seventh order synchronous generator model. The second side, the DC link grouped with the other AC source, is modeled as a bus which has a voltage of constant magnitude and variable angle. Both sides are connected through a transformer of an impedance ($R_{tr} + jX_{tr}$) and an AC transmission line of an impedance ($R_{tl} + jX_{tl}$) as explicitly demonstrated in Figure (4.6). Thus, R_{L1} and X_{L1} are equivalent to ($R_{tr} + R_{tl}$) and ($X_{tr} + X_{tl}$) respectively. (P_{L1} and Q_{L1}) correspond to (P_g and Q_g). Additionally, V_{L1} and V_1 shown in Figure (4.5) are respectively similar to V_{alt} and V^{∞} of Figure (4.6).

4.2.2.1 POD for SM via VSC-HVDC System for constant P_{HVDC} reference

In order to damp the power angle oscillations of the machine's rotor for SM via VSC-HVDC system in case of constant P_{HVDC} reference, two different approaches are considered. The first, the base case, aims at governing the reference of V_d^{∞} through a PI controller. For base case simulations, ΔV_d^{∞} is supposed to be always zero.

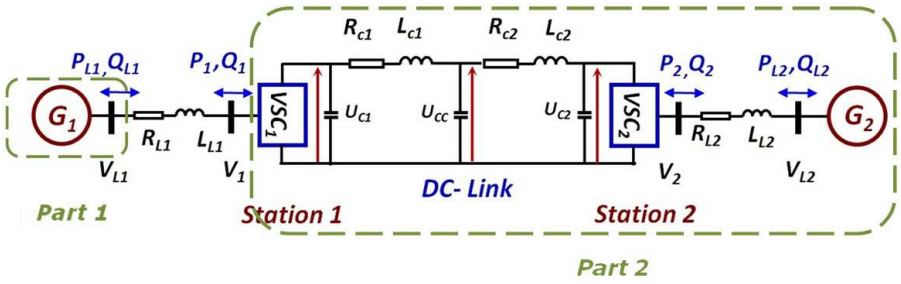

Figure 4.5: Physical model for the GG VSC-HVDC system under study.

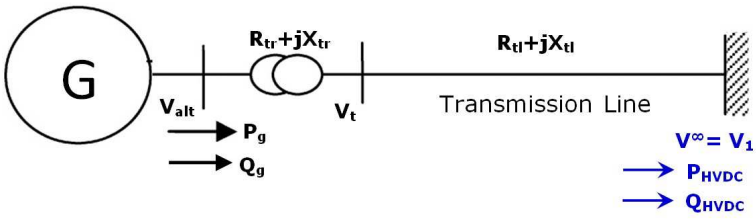

Figure 4.6: Equivalent physical scheme of GG VSC-HVDC system.

On the other hand, the second approach deals with taking into account the effect of ΔV_d^∞ on adjusting $V_{d_{(ref)}}^\infty$. The dynamic performance related to this method is represented as the damped case behavior afterward.

Figure (4.7) presents the phasor diagram of the SM via VSC-HVDC system quantities in which the (d,q) reference frame rotates at rotor synchronous speed ω_o.

The angles δ_r and δ_{HVDC}, plotted in the following figures, are defined as: $\delta_r = \angle(\overline{OV_0^\infty}, \overline{Oq})$, $\delta_{HVDC} = \angle(\overline{OV^\infty}, \overline{Oq})$, where, OV_0^∞ and OV^∞ respectively refer to the initial steady state and the instantaneous infinite bus voltage phasors. Obviously, $\delta_{HVDC} = \delta_r$ at steady state.

Base Case: ΔV_d^∞=0

For the SM via VSC-HVDC system, the voltage at the converter's side is always constant (i.e., 1 pu) as an infinite bus, however its angle is variable. The rotor angle oscillations in the generator side can be damped by governing the reference of V_d^∞ with the use of PI controller. Therefore, $V_{d_{(ref)}}^\infty$ can be estimated through a PI controller as shown in Figure (4.9a).

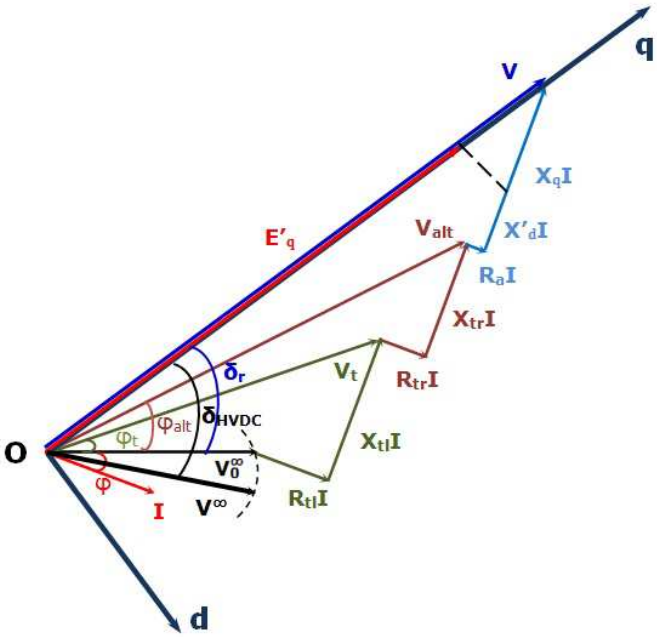

Figure 4.7: Phasor diagram representation of SM via VSC-HVDC system.

$P_{HVDC_{(ref)}}$ and $P_{HVDC_{(mes)}}$ are respectively the active power reference and measured values on the converter terminal. Supposing unity power factor, $P_{HVDC_{(ref)}} = 1$ pu while $P_{HVDC_{(mes)}}$ is calculated by:

$$P_{HVDC_{(mes)}} = V_d^{\infty} i_d + V_q^{\infty} i_q \tag{4.21}$$

where,

$$V_q^{\infty} = \sqrt{(1 - (V_d^{\infty})^2)} \tag{4.22}$$

At steady state conditions, δ_{HVDC} and δ_r have similar values. However, δ_{HVDC} estimated at the converter's side is given by:

$$\delta_{HVDC} = tan^{-1}(\frac{V_d^{\infty}}{V_q^{\infty}}) \tag{4.23}$$

Figure (4.8) presents a comparison between the rotor angle dynamic behavior for both SMIB and the proposed SM via VSC-HVDC system (base case depicted in Figure (4.9a)). A fault of resistance 10Ω and duration 120 mseconds is considered at t=5 seconds. At steady state, the rotor angle time responses are approximately the same.

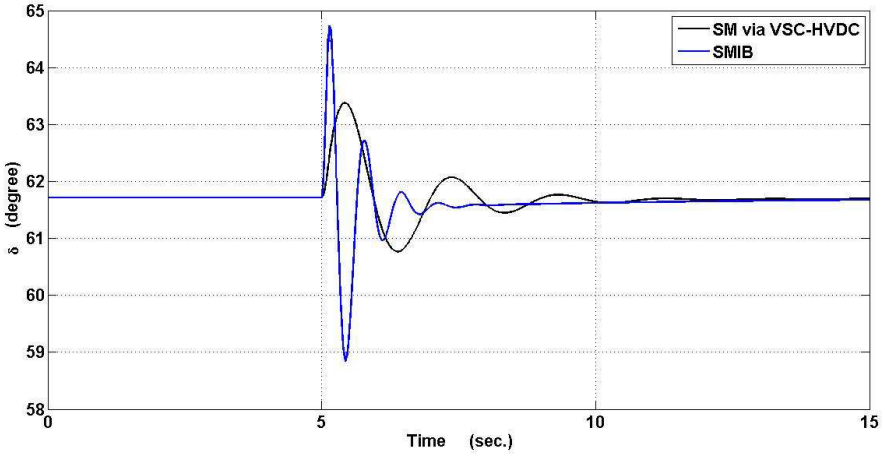

Figure 4.8: Comparison between the rotor angle dynamic performance of the SMIB system with speed regulator and the equivalent SM via VSC-HVDC one (base case) in presence of a fault at t=5 seconds (R_{fault}=10 Ω and t_{fault}=120 mseconds).

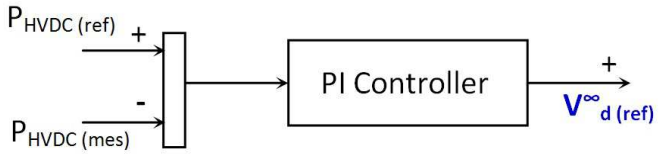

(a) PI controller for governing $V_{d_{(ref)}}^{\infty}$ (base case).

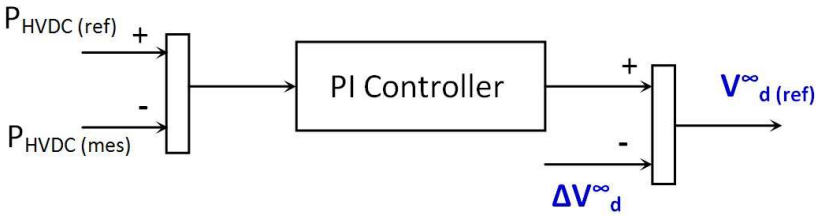

(b) $V_{d_{(ref)}}^{\infty}$ adjustment for POD (damped case).

Figure 4.9: PI controller for SM via VSC-HVDC system with constant P_{HVDC} reference.

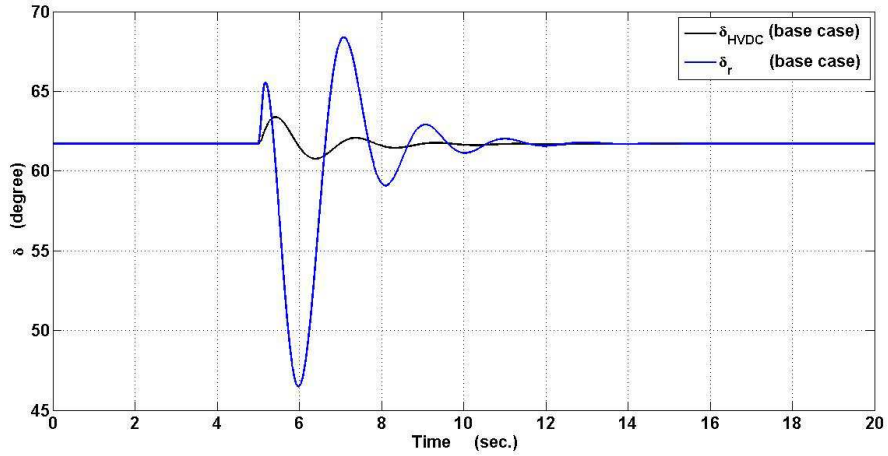

Figure 4.10: Comparison between δ_r and δ_{HVDC} time responses for the base case of SM via VSC-HVDC system in presence of a fault at t=5 seconds (R_{fault}=10 Ω and t_{fault}=120 mseconds).

Moreover, the rotor angle dynamic behavior in the base case of SM via VSC-HVDC has lower overshoot and higher setting time. Consequently, the oscillations are desirably damped when comparing with the SMIB case.

As depicted in Figure (4.10), the dynamic behavior of both δ_{HVDC} and δ_r for the base case of SM via VSC-HVDC system are presented when a fault is considered. The gains of the PI controller (K_p and K_i) used for regulating $V_{d_{(ref)}}^{\infty}$ are chosen as (0.005 and 4) respectively. Clearly, the time response of δ_{HVDC} has lower overshoot and shorter settling time compared to the δ_r time response.

In Figure (4.11), the influence of K_p of the PI controller that governs $V_{d_{(ref)}}^{\infty}$ is demonstrated. The different time responses of δ_{HVDC} verify that the variation of K_p has only a small effect on the dynamic behavior. The behavior's overshoot and its settling time remain almost constant for various K_p. However in Figure (4.12), the effect of K_i of the PI controller on the δ_{HVDC} time response is illustrated taking into account a fault occurrence at t=5 seconds. For constant K_p, greater values of K_i lead to higher overshoot dynamic behavior.

Similarly, Figure (4.13) displays the effect of K_p of the PI controller governing $V_{d_{(ref)}}^{\infty}$ on δ_r dynamic behavior. Insignificant influence of K_p on δ_r dynamic behavior is shown.

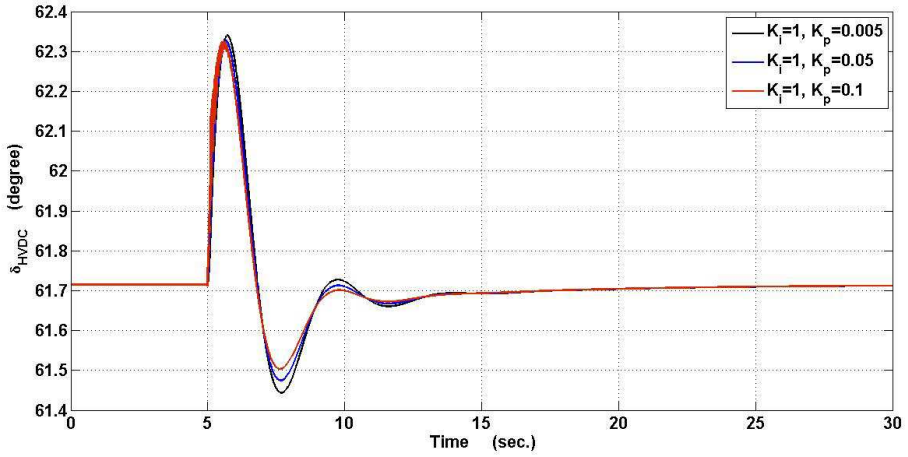

Figure 4.11: Influence of the proportional gain of the PI controller (K_p) on damping δ_{HVDC} oscillations for the base case of SM via VSC-HVDC system in presence of a fault at t=5 seconds (R_{fault}=10 Ω and t_{fault}=120 mseconds).

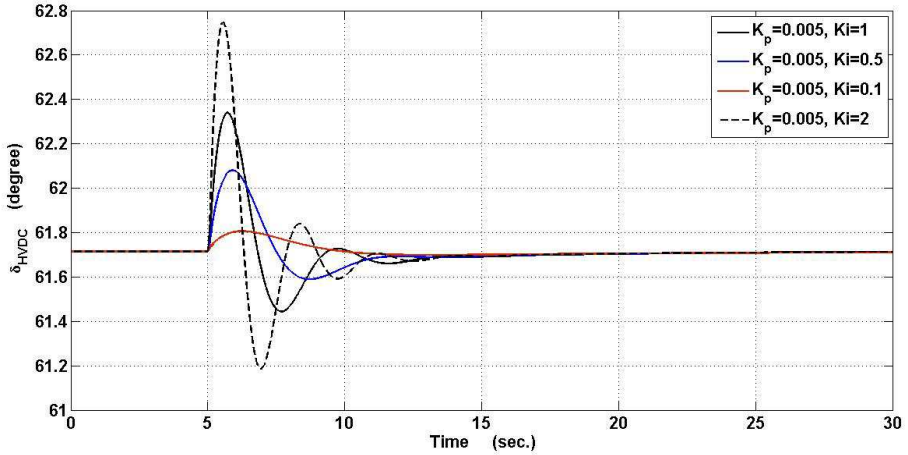

Figure 4.12: Influence of the integral gain of the PI controller (K_i) on damping δ_{HVDC} oscillations for the base case of SM via VSC-HVDC system in presence of a fault at t=5 seconds (R_{fault}=10 Ω and t_{fault}=120 mseconds).

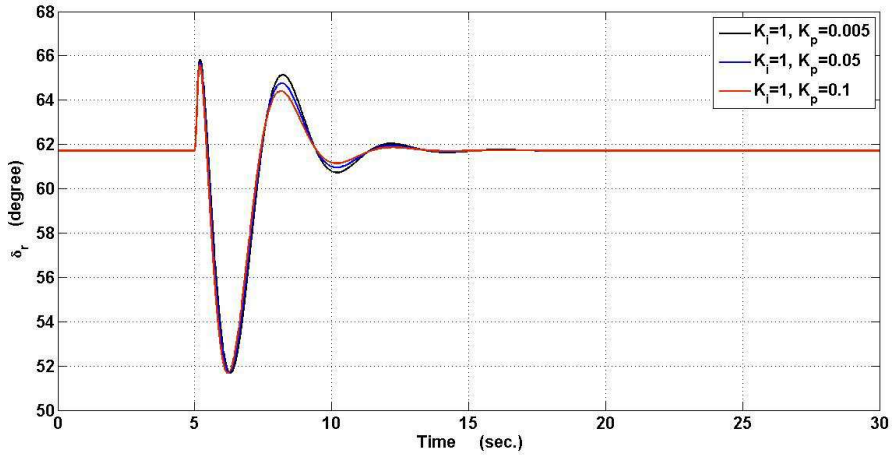

Figure 4.13: The effect of the proportional gain of the PI controller (K_p) on damping δ_r oscillations for the base case of SM via VSC-HVDC system in presence of a fault at t=5 seconds (R_{fault}=10 Ω and t_{fault}=120 mseconds).

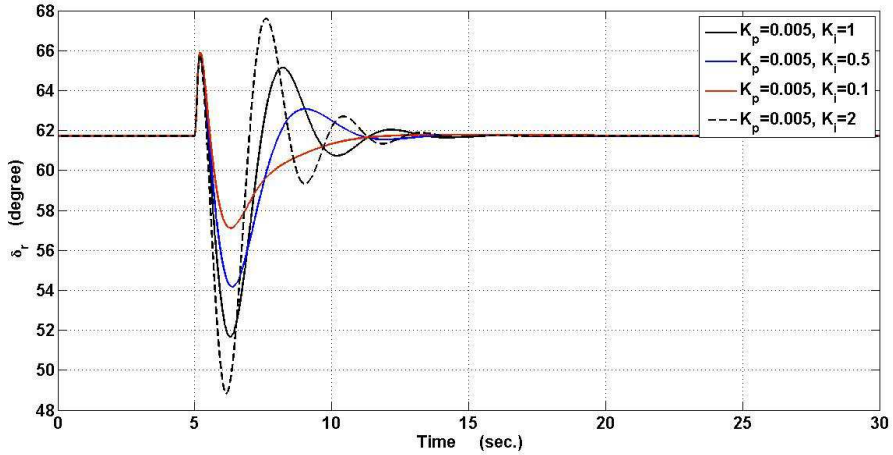

Figure 4.14: The effect of the integral gain of the PI controller (K_i) on damping δ_r oscillations for the base case of SM via VSC-HVDC system in presence of a fault at t=5 seconds (R_{fault}=10 Ω and t_{fault}=120 mseconds).

However for the same K_p, the decrease of K_i of the PI controller provides lower overshoot to δ_r time response as illustrated in Figure (4.14).

Damped Case: $\Delta V_d^{\infty} \neq 0$

From Equation (4.9), ΔV_d^{∞} can be calculated by the following procedure:

$$V_d^{\infty} = V^{\infty} \sin(\delta_{HVDC}) \tag{4.24}$$

$$V_{do}^{\infty} = V^{\infty} \sin(\delta_{HVDCo}) \tag{4.25}$$

As $\delta_{HVDC} = \delta_{HVDCo} + \Delta\delta_{HVDC}$, and, $V_d^{\infty} = V_{do}^{\infty} + \Delta V_d^{\infty}$. Therefore,

$$(V_{do}^{\infty} + \Delta V_d^{\infty}) = V^{\infty} \sin(\delta_{HVDCo} + \Delta\delta_{HVDC}) \tag{4.26}$$

Then,

$$\Delta V_d^{\infty} = V^{\infty} \sin(\delta_{HVDCo} + \Delta\delta_{HVDC}) - V_{do}^{\infty} \tag{4.27}$$

Thus, it can be concluded that:

$$\Delta V_d^{\infty} = V_{do}^{\infty}(\cos(\Delta\delta_{HVDC}) - 1) + V^{\infty} \cos(\delta_{HVDCo}) \sin(\Delta\delta_{HVDC}) \tag{4.28}$$

$\Delta\delta_{HVDC}$ is used to modify $V_{d_{(ref)}}^{\infty}$ in order to damp the electrical power angle oscillation as shown in Figure (4.9b). Thus, $V_{d_{(ref)}}^{\infty}$ can be continuously adjusted by using the PI controller in addition to ΔV_d^{∞} estimated from Equation (4.28).

The damped dynamic behavior of both δ_r and δ_{HVDC}, previously defined in Subsection 4.2.2, is presented in Figure (4.15). At steady state, similar dynamic behavior is illustrated.

Thereafter, Figure (4.16) shows the δ_{HVDC} dynamic behavior by adapting $V_{d_{(ref)}}^{\infty}$ compared to its corresponding behavior of the base case of SM via VSC-HVDC system in presence of a fault. Explicitly, the proposed controller is capable of damping the power angle oscillations appeared in δ_{HVDC} response estimated for the converter's side when ΔV_d^{∞} is taken into account in modifying $V_{d_{(ref)}}^{\infty}$. Lower overshoot during the first swing is occurred. In addition, shorter settling time results. Consequently, improved power angle oscillation behavior for δ_{HVDC} is verified.

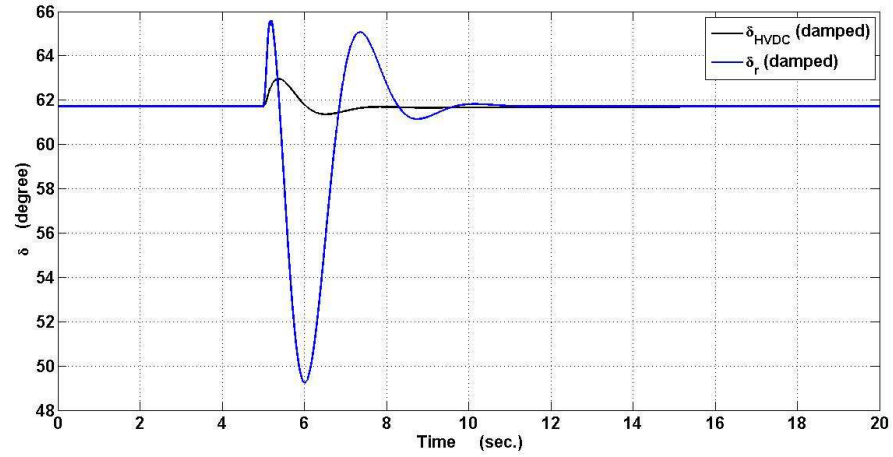

Figure 4.15: Comparison between δ_r and δ_{HVDC} time responses for the damped case of SM via VSC-HVDC system (K_p = 0.005, K_i = 4) in presence of a fault at t=5 seconds (R_{fault}=10 Ω and t_{fault}=120 mseconds).

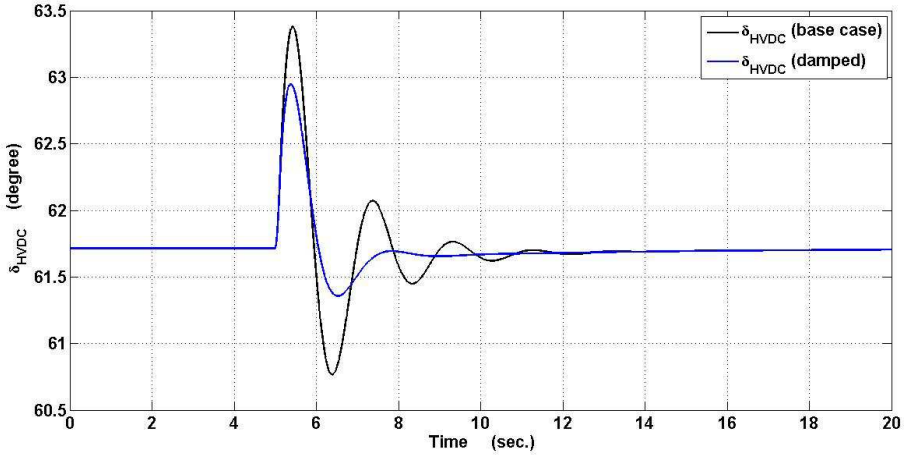

Figure 4.16: δ_{HVDC} dynamic behavior by governing $V_{d(ref)}^{\infty}$ through PI controller with (K_p = 0.005, K_i = 4) considering a fault at t=5 seconds (R_{fault}=10 Ω and t_{fault}=120 mseconds).

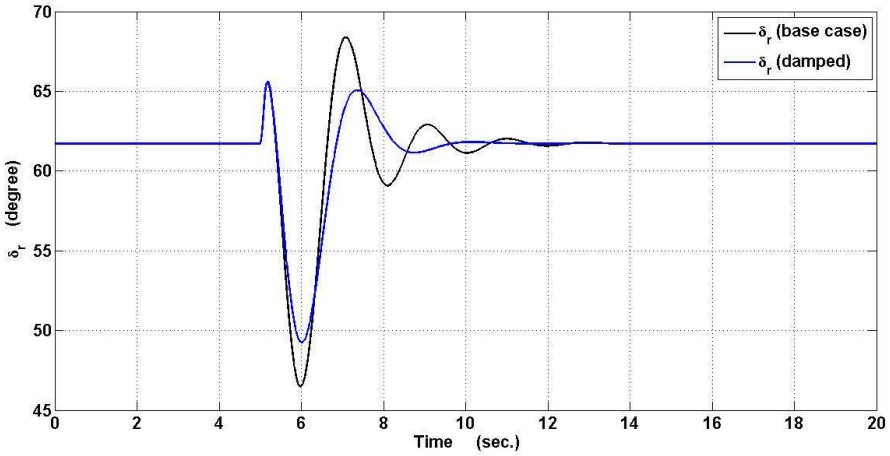

Figure 4.17: The machine rotor angle time response by governing $V_{d_{(ref)}}^{\infty}$ via PI controller with ($K_p = 0.005$, $K_i = 4$) considering a fault at t=5 seconds (R_{fault}=10 Ω and t_{fault}=120 mseconds).

Figure (4.17) illustrates the impact of controlling $V_{d_{(ref)}}^{\infty}$ on the generator rotor angle δ_r dynamic performance. The rotor angle is estimated by integrating the machine rotor angular frequency. The dynamic behavior is studied with and without providing the effect of ΔV_d^{∞} in governing $V_{d_{(ref)}}^{\infty}$.

In favor of the concerned ΔV_d^{∞} used in conjunction with the PI controller, the generator rotor angle oscillations are damped out and slightly enhanced. Explicitly, lower overshoot and shorter settling time are obtained for δ_r dynamic behavior.

In Figure (4.18), the active and reactive power dynamic behavior at the converter's terminal are depicted. Obviously, the system is stable with improved and damped power angle oscillations. Noticeably, oscillations of 50 Hz frequency result after the fault occurrence. These oscillations, which are mainly due to the DC component of the fault current, last about 0.6 seconds. Thereafter, the active and reactive power dynamic behavior track again their steady state values after the fault clearance.

Figure (4.19) presents the effect of governing $V_{d_{(ref)}}^{\infty}$ on the voltages through the system. The voltage on the converter terminal V^{∞} is the one that was greatly influenced by controlling its direct component $V_{d_{(ref)}}^{\infty}$. If ΔV_d^{∞} is considered in calculating $V_{d_{(ref)}}^{\infty}$, damped and enhanced time response of V^{∞} is obtained. However, its influence on V_t and V_{alt} dynamic behavior seems to be negligible.

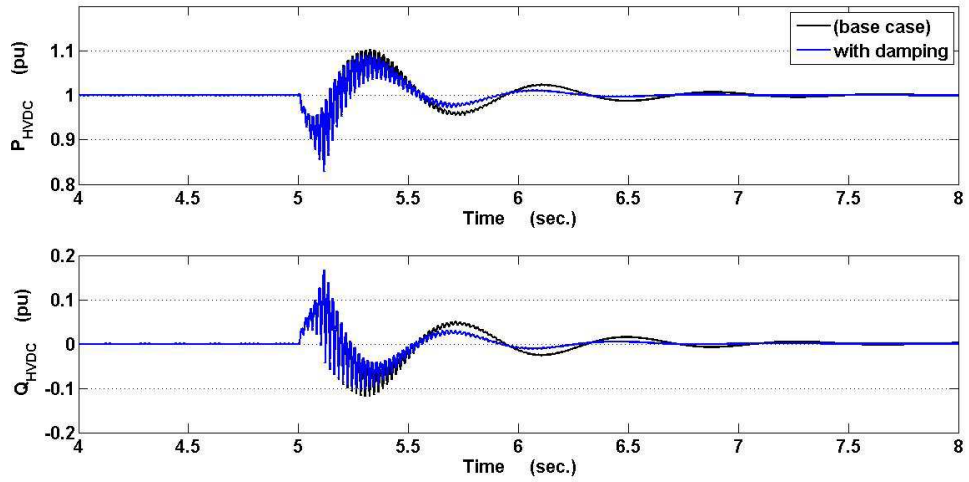

Figure 4.18: Active and reactive power dynamic behavior on the converter's side considering a fault at t=5 seconds (R_{fault}=10 Ω and t_{fault}=120 mseconds).

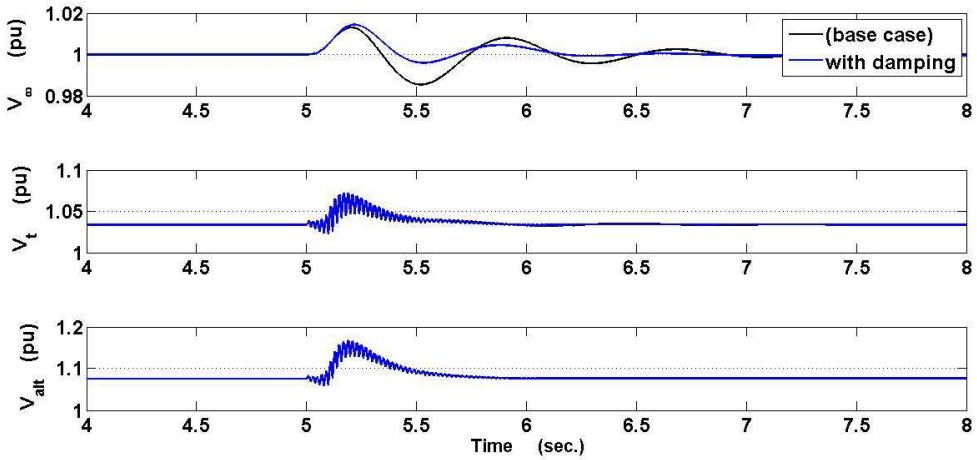

Figure 4.19: V^{∞}, V_t, and V_{alt} time responses under a fault.

4.2.2.2 POD for SM via VSC-HVDC System for changeable P_{HVDC} reference

Another methodology for damping electrical power oscillations and enhancing the dynamic behavior of the proposed SM VSC-HVDC system is to continuously adjust $P_{HVDC_{(ref)}}$ as shown in Figure (4.20). This can be done by taking into account ΔP_{HVDC} signal that depends on $\Delta\delta$.

In Figure (4.20), $P_{HVDC_{(refo)}}$ is the initial signal of the active power reference value on the converter's side that is simply named P_{HVDC} afterward.

To deduce a relation between both ΔP_{HVDC} and $\Delta\delta_{HVDC}$, the forthcoming procedure is followed from Equation (4.29):

$$P_{HVDC} = K_p \sin(\delta_{HVDC}) \tag{4.29}$$

where, K_p proportionally depends on K, such:

$$K = \frac{|V_{alt}||V^{\infty}|}{(X_{tr} + X_{tl})}$$

Therefore, the variation in P_{HVDC} related to δ_{HVDC} variation can be expressed as:

$$\Delta P_{HVDC} = K_p \sin(\Delta\delta_{HVDC}) \tag{4.30}$$

As $\delta_{HVDC} = \delta_{HVDCo} + \Delta\delta_{HVDC}$, and, P_{HVDC}=$P_{HVDC_{(ref)}}$+ΔP_{HVDC}. Therefore,

$$P_{HVDC_{(ref)}} = P_{HVDC} - K_p \sin(\delta_{HVDC} - \delta_{HVDCo}) \tag{4.31}$$

Thus, the new $P_{HVDC_{(ref)}}$ is used to govern V_d^{∞} through a PI controller in order to damp the power angle oscillations of the machine's rotor.

In Figure (4.21), the effect of selecting K_p on improving the dynamic behavior of δ_{HVDC} is analyzed in presence of a fault. An explicit enhancement of the dynamic behavior is attained especially for higher values until $K_p = 25K$. More damped oscillations with reduced overshoot and settling time are obtained rather than that of the base case (with $P_{HVDC_{(ref)}}$ constant). Otherwise, negligible influence on power oscillations damping is noticed for $K_p > 25K$ compared to the case of $K_p = 25K$.

Figure (4.22) demonstrates the impact of governing $P_{HVDC_{(ref)}}$ on enhancing the machine rotor angle time response. For higher values of K_p, better time response with lower overshoot and shorter time response result compared to the base case.

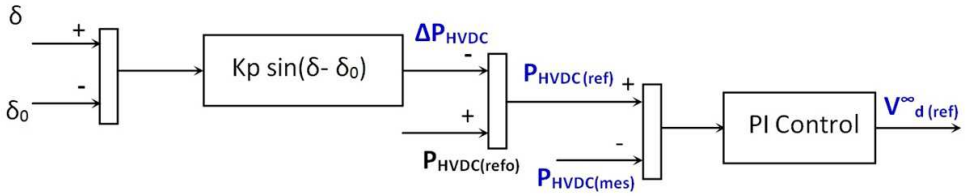

Figure 4.20: $P_{HVDC_{(ref)}}$ adjustment for damping power angle oscillations considering a fault.

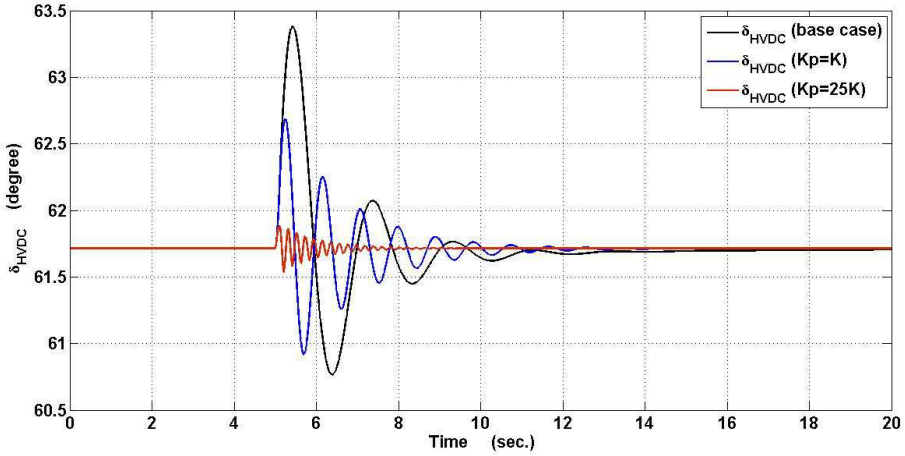

Figure 4.21: Power angle oscillations damping on HVDC side by governing $P_{HVDC_{(ref)}}$ considering a fault at t=5 seconds (R_{fault}=10 Ω and t_{fault}=120 mseconds).

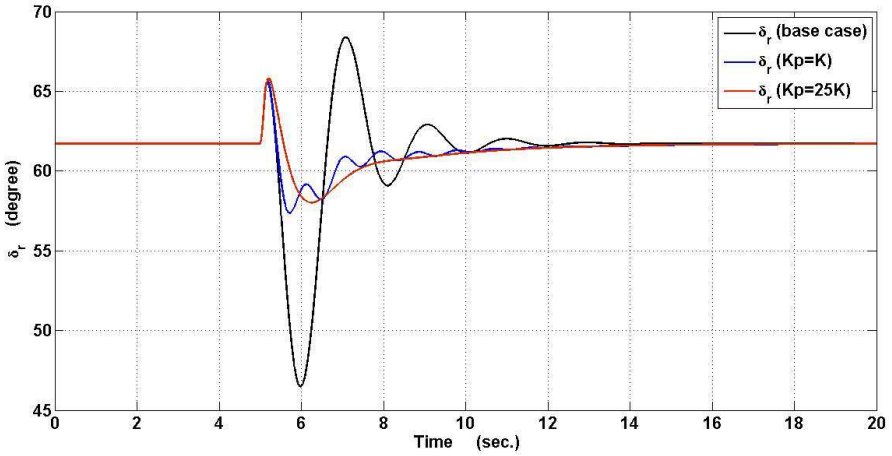

Figure 4.22: The machine rotor angle time response by governing $P_{HVDC_{(ref)}}$ considering a fault at t=5 seconds (R_{fault}=10 Ω and t_{fault}=120 mseconds).

Figure (4.23) verifies that the machine speed dynamic behavior is ameliorated in case of governing $P_{HVDC_{(ref)}}$ rather that considering constant $P_{HVDC_{(ref)}}$.

Figures (4.24) and (4.25) present the effect of adjusting $P_{HVDC_{(ref)}}$ on the dynamic performance of the power supplied by the generator as well as the active and reactive powers on the converter's side in presence of a fault at t=5 seconds.

The performance seems to be enhanced with adjusted $P_{HVDC_{(ref)}}$. After the fault occurrence, oscillations of 50 Hz frequency appear. These oscillations remain less than 1 seconds for re-maintaining the corresponding steady state values after the fault clearance.

Figure (4.25) demonstrates that there is a risk of overcurrent generation in consequence of the fault. This high current may lead to a probable line tripping. Therefore, a control through the *d*-*q* components of the current should be considered to act as a current limiter in order to decrease the line tripping probability.

Figure (4.26) depicts the time response of different voltages through the system taken into account a fault at t=5 seconds. The time responses of V_t and V_{alt} are not influenced by adjusting $P_{HVDC_{(ref)}}$ compared to the base case. V^{∞} is greatly affected because its *d*-component V_d^{∞} depends on $P_{HVDC_{(ref)}}$.

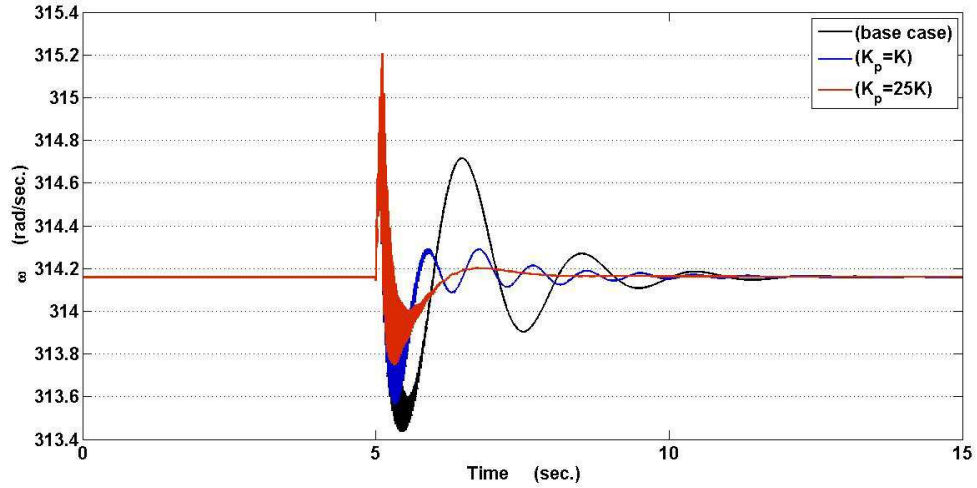

Figure 4.23: The machine speed dynamic behavior assuming a fault at t=5 seconds (R_{fault}=10 Ω and t_{fault}=120 mseconds).

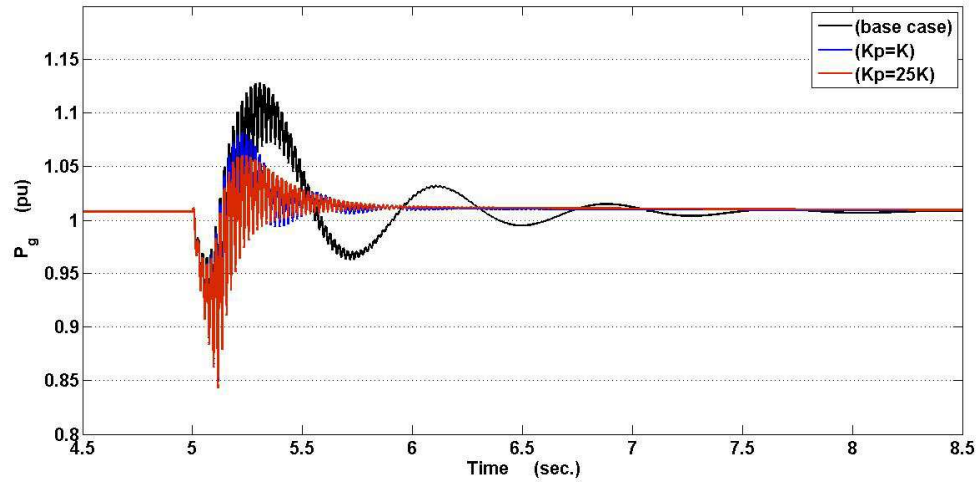

Figure 4.24: Dynamic behavior of the active power delivered by the synchronous generator under a fault at t=5 seconds (R_{fault}=10 Ω and t_{fault}=120 mseconds).

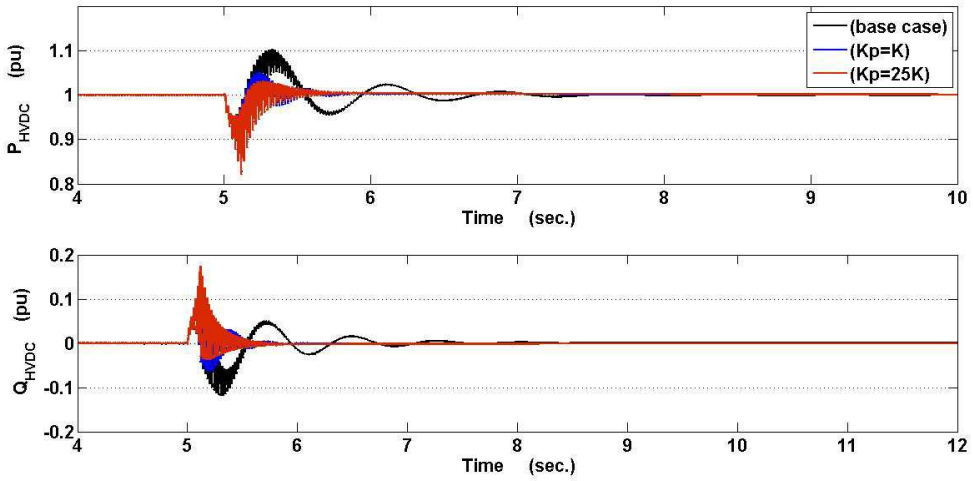

Figure 4.25: Active and reactive power time response on the converter's side under a fault at t=5 seconds (R_{fault}=10 Ω and t_{fault}=120 mseconds).

Obviously, changing $P_{HVDC_{(ref)}}$ due to gain variations leads to different dynamic behavior of V^{∞} compared to the base case. Greater K_p (until $K_p = 25K$) improves V^{∞}'s dynamic performance. The time responses become of lower overshoot and shorter settling time. However, oscillations of 50 Hz that last less than a duration of 1 second may appear after that fault occurrence in case of SM via VSC-HVDC system.

4.3 Conclusions

In this chapter, the conventional PI controller is applied to the converter's side of the SM via VSC-HVDC system in order to damp the power angle oscillations of the synchronous machine. For rotor oscillations enhancement, the system is controlled by either adjusting the phase angle or the voltage magnitude on the VSC converter's side. Thus, the *d-q* components of voltage on the VSC side are governed. Two design approaches based on PI controllers are investigated for this purpose:

The first is to continuously adjust the $V^{\infty}_{d_{(ref)}}$ in case of constant reference power on the converter's side. For doing so, ΔV^{∞}_{d} is calculated while governing $V^{\infty}_{d_{(ref)}}$. The other one aim at governing the $V^{\infty}_{d_{(ref)}}$ in case of varying $P_{HVDC_{(ref)}}$. Hereby, $\Delta P_{HVDC_{(ref)}}$ caused by $\Delta\delta_{HVDC}$ is considered in the PI controller loop.

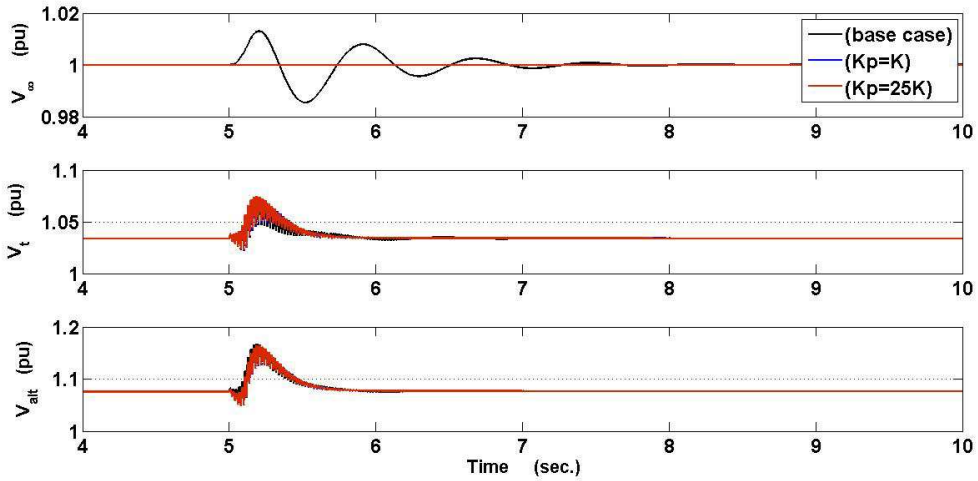

Figure 4.26: V^{∞}, V_t, and V_{alt} time responses under a fault at t=5 seconds (R_{fault}=10 Ω and t_{fault}=120 mseconds).

Simulation results verify that:

- The control of the voltage or the angle on the converter side can achieve better damping for power angle oscillations inside the synchronous machine. Considerable enhanced dynamic performance is demonstrated even under fault;
- The two proposed approaches based on the PI control, which are simple to be implemented, guarantee acceptable dynamic performance enhancement as well as power angle oscillations improvement in presence of faults.

The use of the PI control for governing the $P_{HVDC_{(ref)}}$ reflects more dynamic effects on the system stability. It is more capable of providing POD of the synchronous machine compared to the method of adjusting $V^{\infty}_{d_{(ref)}}$ with constant $P_{HVDC_{(ref)}}$.

Conclusions and Perspectives

IN this chapter, the main conflicting objectives and trade-offs done concerning nonlinear control system design are recalled. The main contributions of this thesis are presented. In addition, some proposals for further research directions are introduced.

Concluding Remarks

Control system analysis and design have to consider the existence of two different classes of properties, *open-loop* and *feedback* properties. Whereas, the former are concerned with the system responses to commands, the later are related to stability and disturbance rejection.

It is well-known that many design methodologies are focused on nonlinear feedback control design. Nevertheless, some approaches are used to simply design a feedback controller but not necessarily provide robust properties. For this reason, If the conventional PI or PID controller is designed, the final achieved feedback properties may not be satisfactory for a wide range of operating condition and parameter uncertainties. Therefore, a trade-off have to be made in order to attain an enhanced system stability and controller robustness.

Additionally, the nonlinear feedback control system is designed in presence of some kind of uncertainty associated with the system model. Effectively, such inherent uncertainty will affect the open-loop and feedback properties. Consequently, the overall system's stability and its dynamic behavior will be influenced. However, uncertain is usually considered as affecting the feedback properties. The reason is obvious: a deterioration of feedback properties may cause more harmful operating conditions than an impairment of open-loop properties, i.e. instability is always undesirable while a deterioration of the command responses may be, in some cases, tolerated.

CONCLUSIONS AND PERSPECTIVES

Throughout the thesis, nonlinear VSC-HVDC transmission links with parameter uncertainties are studied. Therefore, it is necessary to design control strategies which are robust under all possible normal and abnormal situations. In addition to the conventional PI controllers proposed for GL VSC-HVDC transmission systems, different Lyapunov theory-based nonlinear controllers such as AOT and SMC are respectively verified and compared for GG VSC-HVDC ones in presence of parameter uncertainties.

The steady state mathematical models of these systems, whose power flow are respectively unidirectional and bidirectional, are developed based on relatively simple expressions. The proposed nonlinear controllers are then designed to govern the DC link voltages and to control the active and reactive powers on the VSCs' AC terminals to attain unity power factors. The effectiveness of these proposed controllers under normal operating conditions and in presence of parameter uncertainties are investigated. The dynamic behaviors are compared in order to verify which nonlinear control methodology is better adopted to deal with these VSC-HVDC systems considering uncertainties.

For GL VSC-HVDC systems, conventional PI controllers provide an acceptable trade-off among system performance, robustness and simplicity. They show acceptable capability towards tracking the required trajectories, improving the overall system's dynamic behavior and enhancing its stability under parameter uncertainties. However, adequate dynamic behavior can be attained under limited range of uncertainties. For other operating conditions, poor performance may be yielded.

It can be concluded that PI controllers, either considering or not the internal current control loop, are not significantly robust under parameter uncertainties. They can be efficiently used to enhance system behavior during certain operating conditions.

For GG VSC-HVDC transmission systems, nonlinear feedback control laws based on different nonlinear control systems such as AOT and SMC are deduced. These controllers are considered to control active and reactive powers of either converters and to govern the DC link voltage and the reactive power of the other. Indeed, DC link voltage drop, power losses and power flow direction are accounted for. The necessity of significant smooth transitions and chattering-free behavior are highlighted especially for nonlinear SMC design. Thus, chattering phenomena that appear in AOT control are treated proposing two-terms SMC with continuous functions such as saturation and hyperbolic ones instead of the discontinuous sigmoid function.

Both AOT and SMC controller design processes are relatively simple because feedback laws are derived step by step making use of Lyapunov theory. The overall system's performance is enhanced and significant robustness of both designed controllers based on AOT and SMC, under DC cable parameter variations and reference signal changes, are demonstrated. The responses can be further improved by optimizing the controller gains. The main drawback of these controllers are their relative complex implementation compared to conventional PI ones. However, SMC's advantage of chattering-free behavior makes it more desirable than AOT controllers.

Considering networks' parameter uncertainties such as DC cable parameter variations besides reference signal variations, the robustness of the designed controllers based on AOT and SMC is verified and the system's enhanced dynamic performance is illustrated. Moreover, the lack of robustness of these nonlinear controllers against AC line reactance variations is demonstrated.

Obviously, SMC control methodology is efficiently used in favor of its well-damped oscillations, its control flexibility towards improving the system's dynamic behavior and stability, its robustness to certain parameter variations as well as its relative structural simplicity. Still, nonlinear AOT controller's dynamic behavior comprises undesirable chattering. Thus, nonlinear AOT approach is less efficient compared to SMC one towards system stabilization.

In favor of its chattering-free merit and better performance, the superiority of the controller based on two-terms SMC with continuous functions over AOT control and the cascaded conventional PI control with internal current control loop is displayed.

As an important contribution of the thesis, the influence of VSC-HVDC control on enhancing the AC network dynamic performance during faults are verified. After modeling the proposed SM via VSC-HVDC system, the classical PI controller is applied on the VSC side of the system to act on damping the power angle oscillations of the synchronous machine even under a fault. Simulation results verify that the use of the conventional PI control, which are simple to be implemented, for governing the voltage or the angle on the converter side can guarantee acceptable dynamic performance enhancement as well as power angle oscillations damping in presence of faults.

VSC-HVDC, undoubtedly, will continue to provide solutions to challenging issues associated with the modern deregulated powers systems.

Future Work

Future work should explore other possibilities and routes in which this thesis could lead to. Main perspectives should include:

- **Implementation of other nonlinear control algorithms for VSC-HVDC systems:**
  Besides considering nonlinear controllers based on SMC, AOT, and Lyapunov theory based-control in presence of parameter uncertainties, other nonlinear control methodologies could be investigated. Therefore, nonlinear robust controller such as integral SMC, higher order SMC, and H-infinity loop-shaping controller could be considered for trajectory control and stabilization of VSC-HVDC transmission systems under parameter uncertainties. These robust methods aim to achieve robust performance and/or stability in presence of uncertainties.

  Additionally, adaptive control methodologies such as gain scheduling control, nonlinear controllers based on NN or Fuzzy approaches could be used. The adaptive control involves modifying the control law used by a controller to cope with the fact that the parameters of the system being controlled are slowly time-varying or uncertain.

- **Robustness verification and evaluation of SMC and AOT controllers for VSC-HVDC in presence of different fault types:**
  The proposed nonlinear controllers robustness could be verified and assessed for VSC-HVDC systems subjected to different types of faults.

- **Nonlinear control and stabilization of more detailed VSC-HVDC integrated in larger power systems :**
  The design of nonlinear controllers could be considered for a detailed models of VSC-HVDC for larger power systems. Synchronous generators of higher order nonlinear differential equations in addition to comprehensive converter equations would be incorporated in the controller design process. Thus, the system would therefore be larger and its control would be more complex.

- **Optimization of the implemented control algorithms :**
  Various optimization techniques could be incorporated to the implemented control algorithms in order to attain better dynamic performance.

- **Control strategies of an offshore wind farm interconnected to a VSC-HVDC system :**
  Different nonlinear control could be applied and verified for offshore wind farms interconnected to VSC-HVDC systems during normal and abnormal fault conditions.

- **Interaction between PSS model of the AVR and the VSC-HVDC control :**
  The impact of controlling both VSC-HVDC and the PSS model of the AVR on each other could be studied.

Appendix A

VSC-HVDC Operating Conditions and Tuning Gains

GL-HVDC Transmission Systems

Equivalent AC generator and line resistance, R_{L1}= 0.01 Ω
Equivalent AC generator and line inductance, L_{L1}= 40 mH
Rated active power, P_{L1}= 200 MW
Rated DC-voltage, U_{C1}= 300 kV
Load resistance, R= 450 Ω
Load inductance, L= 11.5 mH
DC side capacitor, C_1= 20 μf
Angular frequency, ω_1= 314.16 rad/sec.
Tuning parameters of fast PI controller:
$K_p = 0$, $K_i = 1.6919E{-}4$ (DC voltage control)
$K_p = 1.4264E{-}9$, $K_i = 3.9179E{-}6$ (Reactive power control)
Tuning parameters of slow PI controller:
$K_p = 0$, $K_i = 3.3775E{-}5$ (DC voltage control)
$K_p = 1.9393E{-}10$, $K_i = 1.8486E{-}8$ (Reactive power control) Tuning parameters using cascaded PI controller (with internal current control loop):
Internal current control gains:
$K_p = 50$, $K_i = 0$ (i_{L1d} control)
$K_p = 2.5$, $K_i = 0$ (i_{L1q} control)

Outer control gains:
$K_p = 0.1$, $K_i = 1$ (DC voltage control)
$K_p = 5E{-}6$, $K_i = 100E{-}6$ (Reactive power control)

GG-HVDC Transmission Systems

The overall system's operating conditions and gains are:
Frequency of both AC networks: f_1= 50 Hz, f_2= 60 Hz
Equivalent resistance of AC generator and transmission line and, the equivalent inductance of AC generator and transmission line for both sides:
R_{L1}= 0.01 Ω, L_{L1}= 40 mH and
R_{L2}= 0.01 Ω, L_{L2}= 40 mH
Rated active power of both sides: P_{L1}= P_{L2} =200 MW
Rated DC-voltage on both sides: U_{C1}= U_{C2}=300 kV
DC cable resistances and inductances:
R_{c1}= R_{c1}= 1.95 Ω, and
L_{c1}= L_{c1}= 11.5 mH
Shunt capacitors, C_1= C_2= 20 μf, C_C= 16 μf
Two-Terms SMC controller
Tuning parameters for both sides are:
$K_1 = K_2 = K = 100$
Cascaded conventional PI controller with internal current control loop

- **Side 1**:
  Internal current control gains:
  $K_p = 2.5$, $K_i = 50$ (i_{L1d} control)
  $K_p = 50$, $K_i = 100$ (i_{L1q} control)
  Outer control gains:
  $K_p = 0.2E{-}6$, $K_i = 10E{-}6$ (Active power control)
  $K_p = 0.5E{-}6$, $K_i = 20E{-}6$ (Reactive power control)

- **Side 2**:
  Internal current control gains:
  $K_p = 5$, $K_i = 5$ (i_{L2d} control)

$K_p = 25$, $K_i = 5$ (i_{L2q} control)

Outer control gains:

$K_p = 50E{-}3$, $K_i = 125E{-}3$ (DC voltage control)

$K_p = 0.417E{-}6$, $K_i = 12.5E{-}6$ (Reactive power control)

Equivalent SM via VSC-HVDC System

All data are given in per unit on a base voltage of 500 kV and base power 10 GW, unless otherwise stated.

The synchronous machine parameters are:

X_d=1.5, X_q=1.5, X_{ad}=1.31, X_{aq}=1.29, X_{fd}=1.42, X_{kd}=1.4, X_{kq}=1.34, R_a=0.0015, R_f=0.00063, R_{kd}=0.0153, R_{kq}=0.0207, H=2.62, D=1, f=50 Hz

Transformer parameters:

X_{tr}=0.135, R_{tr}=0.003

Transmission line parameters:

X_{tl}=0.2410, R_{tl}=0.0050

Infinite system active parameters:

V^{∞}=1, P=1, Q=0

Tuning parameters of PI controller (Speed Regulator):

K_p=0.0497, K_i=0.1034

Tuning parameters of PI controller ($V^{\infty}_{d_{(ref)}}$ Regulator):

K_p=0.005, K_i=4

References

[1] D. Velasco, C.L. Trujillo, and R.A. Peña. Power transmission in direct current: Future expectations for Colombia. *Renewable and Sustainable Energy Reviews*, In Press, 2010. xxvi, 2

[2] K. Meah and S. Ula. Comparative evaluation of HVDC and HVAC transmission systems. In *IEEE Power Engineering Society General Meeting*, pages 1–5, 2007. xxvi, 2

[3] N.G. Hingorani. High-voltage DC transmission: a power electronics workhorse. *IEEE Spectrum*, 33(4):63–72, 1996. xxvi, 2

[4] B. Andersen and C. Barker. A new era in HVDC?. *IEE Review*, 46(2):33–39, 2002. xxvi, 2

[5] S. Ruihua, Z. Chao, L. Ruomei, and Z. Xiaoxin. VSCs based HVDC and its control strategy. In *IEEE–PES Transmission and Distribution Conference and Exhibition: Asia and Pacific*, pages 1–6, 2005. xxvi, 2

[6] X.I. Koutiva, T.D. Vrionis, N.A. Vovos, and G.B. Giannakopoulos. Optimal integration of an offshore wind farm to a weak AC grid. *IEEE Transactions on Power Delivery*, 21(2):987–994, 2006. xxvi, 2

[7] I.M. de Alegría, J.L. Martín, I. Kortabarria, J. Andreu, and P.I. Ereŋo. Transmission alternatives for offshore electrical power. *Renewable and Sustainable Energy Reviews*, 13(5):1027–1038, 2009. xxvii, 42, 62

[8] F.O. Rourke, F. Boyle, and A. Reynolds. Marine current energy devices: Current status and possible future applications in Ireland. *Renewable and Sustainable Energy Reviews*, 14(3):1026–1036, 2010. xxvii, 42

[9] W. Zhixin, J. Chuanwen, A. Qian, and W. Chengmin. The key technology of offshore wind farm and its new development in China. *Renewable and Sustainable Energy Reviews*, 13(1):216–222, 2009. xxvii, 42

[10] Z. Chen and F. Blaabjerg. Wind farm–A power source in future power systems. *Renewable and Sustainable Energy Reviews*, 13(6-7):1288–1300, 2009. xxvii, 42

[11] S.Y. Ruan, G.J. Li, L. Peng, Y.Z. Sun, and T.T. Lie. A nonlinear control for enhancing HVDC light transmission system stability. *International Journal of Electrical Power and Energy Systems*, 29(7):565–570, 2007. xxvii, xxviii, xxxi, 2, 3, 6

[12] B.R. Andersen, L. Xu, and P. Cartwright. Topologies for VSC transmission. *Power Engineering Journal*, 16:142–150, 2002. xxvii, 2

[13] G. Venkataramanan and B.K. Johnson. A superconducting DC transmission system based on VSC transmission technologies. *IEEE Transactions on Applied Superconductivity*, 13(2):1922–1925, 2003. xxvii, 2

[14] F. Al Jowder and B.T. Ooi. VSC-HVDC station with SSSC characteristics. *IEEE Transactions on Power Electronics*, 19:1053–1059, 2004. xxvii, 2

[15] L. Weimers. HVDC light: a new technology for a better environment. *IEEE Power Engineering Review*, 18(8):19–20, 1998. xxvii, xxviii, 2, 3, 20, 21, 31, 36

[16] G. Asplund. Application of HVDC Light to power system enhancement. In *IEEE Power Engineering Society Winter Meeting*, volume 4, pages 2498–2503, 2000. xxvii, 2, 62

[17] X.Y. Li. A nonlinear emergency control strategy for HVDC transmission systems. *Electric Power Systems Research*, 67(3):153–159, 2003. xxviii, 3

[18] V.K. Sood, N. Kandil, R.V. Patel, and K. Khorasani. Comparative evaluation of neural-network-based and PI current controllers for HVDC transmission. *IEEE Transactions on Power Electronics*, 9(3):288–296, 1994. xxviii, 3

[19] P. Kundur, N.J. Balu, and M.G. Lauby. *Power system stability and control*, volume 19. McGraw-Hill, New York, 1994. xxviii, 3, 116, 117

[20] X.Y. Li. *Operation and control of HVDC transmission systems*. Science Press, Beijing (Chinese), 1998. xxviii, 3

[21] R.A. Felix, E.N. Sanchez, and A.G. Loukianov. Neural block control for synchronous generators. *Engineering Applications of Artificial Intelligence*, 22(8):1159–1166, 2009. xxix, 1, 4

[22] D. Jovcic, N. Pahalawaththa, and M. Zavahir. Novel current controller design for elimination of dominant oscillatory mode on an HVDC line. *IEEE Transactions on Power Delivery*, 14(2):543–548, 1999. xxix, 4

[23] K. Yamaji, M. Sato, K. Kato, M. Goto, and T. Kawai. Cooperative control between large capacity HVDC system and thermal power plant. *IEEE Transactions on Power Systems*, 14(2):629–634, 1999. xxix, 4

[24] P.K. Dash, A. Routray, and A.C. Liew. Design of an energy function based fuzzy tuning controller for HVDC links. *International Journal of Electrical Power and Energy Systems*, 21(5):337–347, 1999. xxix, xxx, 4, 5

[25] S. Lefebvre, M. Saad, and R. Hurteau. Adaptive control for HVDC power transmission systems. *IEEE Transactions on Power Apparatus and Systems*, (9):2329–2335, 1985. xxix, 4

[26] W.J. Rugh. Analytical framework for gain scheduling. *IEEE Control Systems Magazine*, 11(1):79–84, 2002. xxix, 4

[27] A. Colbia-Vega, J. de Leon-Morales, L. Fridman, O. Salas-Peña, and M.T. Mata-Jiménez. Robust excitation control design using sliding-mode technique for multimachine power systems. *Electric Power Systems Research*, 78(9):1627–1634, 2008. xxix, xxx, 4, 5, 63

[28] J.W. Chapman, M.D. Ilic, C.A. King, L. Eng, and H. Kaufman. Stabilizing a multimachine power system via decentralized feedback linearizing excitation control. *IEEE Transactions on Power Systems*, 8(3):830–839, 1993. xxix, 4

[29] W. Mielczarski and A.M. Zajaczkowski. Nonlinear field voltage control of a synchronous generator using feedback linearization. *Automatica*, 30(10):1625–1630, 1994. xxix, 4

[30] B. Maschke, R. Ortega, and A.J. Van Der Schaft. Energy-based Lyapunov functions for forced Hamiltonian systems with dissipation. *IEEE Transactions on Automatic Control*, 45(8):1498–1502, 2000. xxix, 4

[31] Z. Xi. Non-linear decentralized saturated controller design for multi-machine power systems. *International Journal of Control*, 75(13):1002–1011, 2002. xxix, 4

[32] J. De Leon-Morales, K. Busawon, and S. Acha-Daza. A robust observer-based controller for synchronous generators. *International Journal of Electrical Power and Energy Systems*, 23(3):195–211, 2001. xxix, 4

[33] L.M. Fridman. Singularly perturbed analysis of chattering in relay control systems. *IEEE Transactions on Automatic Control*, 47(12):2079–2084, 2002. xxix, 4

[34] A. Soto-Cota, L.M. Fridman, A.G. Loukianov, and J.M. Canedo. Variable structure control of synchronous generator: singularly perturbed analysis. *International Journal of Control*, 79(1):1–13, 2006. xxix, 4

[35] A.G. Loukianov. Nonlinear block control with sliding mode. *Automation and Remote Control*, 59(7):916–933, 1998. xxix, 4

[36] V.I. Utkin. *Sliding modes in control and optimization*, volume 3. Springer-Verlag, New York, 1992. xxix, 4

[37] K. Ellithy and A. Al-Naamany. A hybrid neuro-fuzzy static var compensator stabilizer for power system damping improvement in the presence of load parameters uncertainty. *Electric Power Systems Research*, 56(3):211–223, 2000. xxx, 5

[38] B. Pal and B. Chaudhuri. *Robust control in power systems*. Springer-Verlag, New York, 2005. xxx, 5

[39] R. Sadikovic, P. Korba, and G. Andersson. Self-tuning controller for damping of power system oscillations with FACTS devices. In *IEEE Power Engineering Society General Meeting*, pages 1–6, 2006. xxx, 5

[40] J. Reeve and M. Sultan. Gain scheduling adaptive control strategies for HVDC systems to accommodate large disturbances. *IEEE Transactions on Power Systems*, 9(1):366–372, 1994. xxx, 5

[41] P.K. Dash, A. Routray, and S. Mishra. A neural network based feedback linearising controller for HVDC links. *Electric Power Systems Research*, 50(2):125–132, 1999. xxxi, 5

[42] J.L. Thomas, S. Poullain, and A. Benchaib. Analysis of a robust DC-bus voltage control system for a VSC transmission scheme. In *the* 7^{th} *International Conference on AC-DC Power Transmission*, pages 119–124, 2001. xxxi, 5, 65, 68, 89

[43] M. Durrant, H. Werner, and K. Abbott. A comparison of current controller designs for VSC-HVDC. In *the* 10^{th} *European Conference on Power Electronics and Applications*, 2003. xxxi, 5, 89

[44] M. Durrant, H. Werner, and K. Abbott. Synthesis of multi-objective controllers for a VSC-HVDC terminal using LMIs. In *the* 43^{rd} *IEEE Conference on Decision and Control*, volume 4, pages 4473–4478, 2004. xxxi, 6, 65, 89

[45] S.Y. Ruan, G.J. Li, X.H. Jiao, Y.Z. Sun, and T.T. Lie. Adaptive control design for VSC-HVDC systems based on backstepping method. *Electric Power Systems Research*, 77(5-6):559–565, 2007. xxxii, 6

[46] D. Jovcic, L. Lamont, and K. Abbott. Control system design for VSC transmission. *Electric Power Systems Research*, 77(7):721–729, 2007. xxxii, 6

[47] R.K. Pandey and A. Ghosh. Design of self-tuning controllers for a two terminal HVDC link. *International Journal of Electrical Power and Energy Systems*, 31(8):389–395, 2009. xxxiii, 7

[48] S. Cole and R. Belmans. Modelling of vsc-hvdc using coupled current injectors. In *Power and Energy Society General Meeting-Conversion and Delivery of Electrical Energy in the* 21^{st} *Century*, pages 1–8, 2008. xxxiii, 7, 116

[49] S. Cole and R. Belmans. A proposal for standard vsc-hvdc dynamic models in power system stability studies. *Electric Power Systems Research*, 2011. xxxiii, 7, 8, 115, 116

[50] L. Zhang and H.P. Nee. Multivariable feedback design of vsc-hvdc connected to weak ac systems. In *IEEE PowerTech, Bucharest*, pages 1–8, 2009. xxxiii, xxxiv, 7, 8

[51] L. Stendius and P. Sandeberg. Large scale offshore wind power energy evacuation by hvdc light. In *European Wind Energy Conference, EWEC'08*, 2008. xxxiv, 9

[52] E. Koldby and M. Hyttinen. Challenges on the road to an offshore hvdc grid. In *Nordic Wind Power Conference*, 2009. xxxiv, 9

[53] G. Verez. System integration of large scale offshore wind power. 2011. xxxiv, 9, 42

[54] Z. Mahi, C. Serban, and H. Siguerdidjane. Direct torque control of a doubly-fed induction generator of a variable speed wind turbine power regulation. In *European Wind Energy Conference, EWEC'07, Milan, Italy*, 2007. xxxv, 10

[55] B. Boukhezzar and H. Siguerdidjane. Nonlinear control with wind estimation of a dfig variable speed wind turbine for power capture optimization. *Energy Conversion and Management*, 50(4):885–892, 2009. xxxvi, 10

[56] S. Wang, G. Li, M. Zhou, and Z. Zhang. Research on vsc-hvdc system to mitigate power output fluctuation caused by wind farms. In *the* 4^{th} *International Conference on Electric Utility Deregulation and Restructuring and Power Technologies, DRPT'11*, pages 314–319, 2011. xxxvi, xxxvii, 10, 11

[57] S.M. Muyeen, R. Takahashi, and J. Tamura. Operation and control of hvdc-connected offshore wind farm. *IEEE Transactions on Sustainable Energy*, 1(1):30–37, 2010. xxxvi, xxxvii, 9, 11

[58] K. Zhao, G. Li, B. Wang, and M. Zhou. Grid-connected topology of pmsg wind power system based on vsc-hvdc. In *the* 4^{th} *International Conference on Electric Utility Deregulation and Restructuring and Power Technologies, DRPT'11*, pages 297–302, 2011. xxxvii, 11

[59] L. Trilla, O. Gomis-Bellmunt, A. Sudria-Andreu, J. Liang, and T. Jing. Control of scig wind farm using a single vsc. In *the* 14^{th} *European Conference on Power Electronics and Applications, EPE'11*, pages 1–9, 2011. xxxvii, 11

[60] MC Nguyen, K. Rudion, and Z.A. Styczynski. Improvement of stability assessment of vsc-hvdc transmission systems. In *the* 5^{th} *International Conference on Critical Infrastructure, CRIS'10*, pages 1–7, 2010. xxxvii, 11

[61] P. Hu, R. Karki, and R. Billinton. Reliability evaluation of generating systems containing wind power and energy storage. *IET Generation, Transmission and Distribution*, 3(8):783–791, 2009. 8, 9

[62] M.S. Lu, C.L. Chang, W.J. Lee, and L. Wang. Combining the wind power generation system with energy storage equipments. In *IEEE Industry Applications Society Annual Meeting, IAS'08*, pages 1–6, 2008. 8, 9

[63] Z. Chen, J.M. Guerrero, and F. Blaabjerg. A review of the state of the art of power electronics for wind turbines. *IEEE Transactions on Power Electronics*, 24(8):1859–1875, 2009. 9, 42

[64] M.P. Bahrman and B.K. Johnson. The ABCs of HVDC transmission technologies. *IEEE Power and Energy Magazine*, 5(2):32–44, 2007. 17, 18, 24, 26, 27, 28, 29, 30, 31, 32, 34

[65] B.R. Andersen. HVDC Transmission–Opportunities and Challenges. *Andersen Power Electronic Solutions Ltd, UK*, 2006. 18

[66] J. Setréus and L. Bertling. Introduction to HVDC technology for reliable electrical power systems. In *the* 10^{th} *IEEE International Conference on Probabilistic Methods Applied to Power Systems*, pages 1–8, 2008. 18, 19, 22, 25, 28

[67] R. Moran. *Executioner's current: Thomas Edison, George Westinghouse, and the invention of the electric chair*. Random House, Inc., 2003. 18

[68] G. Asplund. Electric transmission system in change. In *IEEE Power Electronics Specialists Conference Key Notes*, 2008. 18, 19, 20, 21, 44

[69] SEIMENS. High voltage direct current transmission - proven technology for power exchange. *brochure from SIEMENS, March 2007, Available online: http://www.siemens.com*, 2007. 19, 22, 23

[70] V.F. Lescale. Modern HVDC: state of the art and development trends. In *IEEE International Conference on Power System Technology, POWERCON'98*, volume 1, pages 446–450, 1998. 19

[71] D. Melvold. HVDC Projects Listing. *DC and Flexible AC Transmission Subcommittee of the IEEE Transmission and Distribution Committee by the Working Group on HVDC and FACTS Bibliography and Records*. 19

[72] A. Kumar, M. Weimin, and G. Ruifeng. Three Gorges-Shanghai HVDC: Reinforcing interconnection between central and east China. In *the* 16^{th} *Conference of the Electric Power Supply Industry, CEPSI'06, Mumbai, India*, pages 6–10, 2006. 19

[73] D. Ravemark and B. Normark. Light and invisible; Underground transmission with HVDC Light. *ABB, ABB Review*, pages 25–29, 2005. 20, 21, 22, 23

[74] P.F. de Toledo. *Feasibility of HVDC for city infeed*. Thesis for the degree of Licentiate, Department of Electrical Engineering, KTH, Stockholm, Sweden, 2003. 22

[75] J. Paulinder. *Operation and control of HVDC links embedded in AC systems*. Thesis for the degree of Licentiate, Chalmers University of Technology, Gothenburg, Sweden, 2003. 22, 28

[76] N. Mohan, T.M. Undeland, and W.P. Robbins. *Power electronics*. John Wiley, New York, 2003. 22

[77] M. Wyckmans. Innovation in the Market: HVDC Light, the new technology. In *the* 7^{th} *International Energy T&D Conference, Adelaide, Australia*, 2003. 23

[78] P. Pourbeik, M. Bahrman, E. John, and W. Wong. Modern countermeasurus to blackouts. *IEEE Power and Energy Magazine*, 4(5):36–45, 2006. 24

[79] V.K. Sood. *HVDC and FACTS controllers*. Kluwer Academic Publisher, 2004. 25

[80] A. Von Meier. *Electric power systems: A conceptual introduction*. IEEE Press, John Wiley Inc., 2006. 26

[81] Y.J. Hafner and R. Ottersten. HVDC with voltage source converters–A desirable solution for connecting renewable energies. In *Conference of Large-scale Integration of Wind Power into Power Systems, Germany*, 2009. 31

[82] M.P. Bahrman. HVDC technologies–The right fit for the application. In *ABB Electric Utility Conference, Paper IV–3*, 2002. 35

[83] V.G. Agelidis, G.D. Demetriades, and N. Flourentzou. Recent advances in high-voltage direct-current power transmission systems. In *IEEE International Conference on Industrial Technology, ICIT, India*, pages 206–213, 2006. 35, 37, 40

[84] H. Ambriz-Perez, E. Acha, and C.R. Fuerte-Esquivel. High voltage direct current modelling in optimal power flows. *International Journal of Electrical Power and Energy Systems*, 30(3):157–168, 2008. 37

[85] P. Jiuping, R. Nuqui, K. Srivastava, T. Jonsson, P. Holmberg, and Y.J. Hafner. AC grid with embedded VSC-HVDC for secure and efficient power delivery. In *IEEE Conference of Energy 2030, USA*, pages 1–6, 2008. 40

[86] O. Heyman, L. Weimers, and M.L. Bohl. Hvdc-a key solution in future transmission systems. In *World Energy Congress, WEC*, pages 12–16, 2010. 42, 43

[87] C. Ismunandar. *Control of multi-terminal VSC-HVDC for offshore wind power integration*. PhD thesis, M.Sc. thesis, Delft University of Technology August, 2010. 42

[88] J. Pan, R. Nuqui, K. Srivastava, T. Jonsson, P. Holmberg, and Y.J. Hafner. Ac grid with embedded vsc-hvdc for secure and efficient power delivery. In *IEEE Energy 2030 Conference*, pages 1–6, 2008. 43

[89] A. L'Abbate, G. Migliavacca, U. Hager, C. Rehtanz, S. Ruberg, H. Ferreira, G. Fulli, and A. Purvins. The role of facts and hvdc in the future paneuropean

transmission system development. In *the* 9^{th} *IET International Conference on AC and DC Power Transmission, ACDC*, pages 1–8, 2010. 43

[90] H. Brandtstädter. *Sliding mode control of electromechanical systems.* PhD Thesis, Fakultät für Elektrotechnik und Informationstechnik, Technische Universität München (TUM), Germany, 2009. 46, 53, 54, 56

[91] M. Krstic, I. Kanellakopoulos, and P.V. Kokotovic. *Nonlinear and adaptive control design.* Adaptive and Learning Systems for Signal Processing, Communications and Control, John Wiley, New York, 1995. 46

[92] P. Zlateva. Variable–structure control of nonlinear systems. *Control Engineering Practice*, 4(7):1023–1028, 1996. 46

[93] S.V. Emelianov. *Variable-structure control systems.* Naulo, Moscow (in Russian), 1967. 46

[94] Utkin V. I. *Sliding modes and their applications in variable structure systems.* Mir, Moscow (in Russian), 1978. 46, 95

[95] B. Drazenovic. The invariance conditions in variable structure systems. *Automatica*, 5(3):287–295, 1969. 46, 51, 53

[96] H. Sira-Ramírez. On the dynamical sliding mode control of nonlinear systems. *International Journal of Control*, 57(5):1039–1062, 1993. 46

[97] K.D. Young. *Variable structure control for robotics and aerospace applications.* Elsevier Science Inc. New York, USA, 1993. 46

[98] Y.B. Shtessel, I.A. Shkolnikov, and M.D.J. Brown. An asymptotic second-order smooth sliding mode control. *Asian Journal of Control*, 5(4):498–504, 2003. 46

[99] R.A. De Carlo, S.H. Zak, and G.P. Matthews. Variable structure control of nonlinear multivariable systems: a tutorial. *IEEE Proceedings*, 76(3):212–232, 1988. 46

[100] Z. Lu, L.S. Shieh, G. Chen, and N.P. Coleman. Simplex sliding mode control for nonlinear uncertain systems via chaos optimization. *Chaos, Solitons and Fractals*, 23(3):747–755, 2005. 46

[101] V.I. Utkin. *Sliding modes in optimization and control problems*. Nauka Publishing, Moscow, (in Russian), 1981. 46

[102] V.I. Utkin, J. Guldner, and J. Shi. *Sliding modes in electromechanical systems*. Taylor and Francis, London, 1999. 46, 47, 55, 58, 63

[103] J.J.E. Slotine. Sliding mode controller design for non-linear systems. *International Journal of Control*, 40(2):421–434, 1984. 46, 58

[104] G. Bartolini, A. Ferrara, and E. Usani. Chattering avoidance by second-order sliding mode control. *IEEE Transactions on Automatic control*, 43(2):241–246, 2002. 46, 58

[105] S.V. Emelyanov, S.K. Korovin, and A. Levant. Higher-order sliding modes in control systems. *Differential Equations*, 29:1627–1647, 1993. 46, 58

[106] J.J.E. Slotine and W. Li. *Applied nonlinear control*. Prentice hall Englewood Cliffs, NJ, USA, 1991. 47, 58

[107] C. Edwards and S.K. Spurgeon. *Sliding mode control: theory and applications*. Taylor and Francis, London, 1998. 47, 58

[108] K.J. Aström and T. Hägglund. The future of PID control. *Control Engineering Practice*, 9(11):1163–1175, 2001. 47, 48

[109] A. Anon. Special edition on PID tuning methods. *Computing and Control Engineering Journal*, 10(2), 1999. 47, 48

[110] D.E. Miller. A new approach to adaptive control: no nonlinearities. *Systems and Control Letters*, 49(1):67–79, 2003. 48, 49

[111] I.D. Landau. From robust control to adaptive control. *Control Engineering Practice*, 7(9):1113–1124, 1999. 48, 49

[112] P.O. Gutman. Robust and adaptive control: fidelity or an open relationship?. *Systems and Control letters*, 49(1):9–19, 2003. 48, 49

[113] R. Marino. Adaptive control of nonlinear systems: Basic results and applications. *Annual Reviews in Control*, 21:55–66, 1997. 48, 49

[114] S. Robak. Robust SVC controller design and analysis for uncertain power systems. *Control Engineering Practice*, 17(11):1280–1290, 2009. 50

[115] S.M. Mahmoud, L. Chrifi-Alaoui, V. Van Assche, and P. Bussy. Sliding mode control of nonlinear SISO systems with both matched and mismatched disturbances. *International Journal of Sciences and Techniques of Automatic Control and Computer Engineering STA*, 2(1):350–367, 2008. 51

[116] U. Itkis. *Control systems of variable structure.* John Wiley, New York, 1976. 51

[117] V.I. Utkin. Equations of the slipping regime in discontinuous systems: I. *Automation and Remote Control*, 32:1897–1907, 1971. 51

[118] V.I. Utkin. Equations of the slipping regime in discontinuous systems: II. *Automation and Remote Control*, 33:211–219, 1972. 51

[119] H. Lee and V.I. Utkin. Chattering suppression methods in sliding mode control systems. *Annual Reviews in Control*, 31(2):179–188, 2007. 51

[120] S. Meier. *Novel voltage source converter based HVDC transmission system for offshore wind farms.* PhD thesis, Royal Institute of Technology, Stockholm, Sweden, 2005. 62

[121] K. Eriksson and J. Graham. HVDC Light a transmission vehicle with potential for ancillary services. In *VIISEPOPE Conference, Curitiba, Brazil*, 2000. 62

[122] L. Weimers. New Markets Need Technology. In *POWERCON, Australia*, 2000. 62

[123] D. Smith. Cross Sound HVDC link extends IGBT power. *Modern power systems*, 20(10):31–36, 2000. 62

[124] D.-C. Lee, K.-D. Lee, and G.-M. Lee. Voltage control of PWM converters using feedback linearization. In *IEEE* 33^{rd} *Industry Applications Conference IAS Annual Meeting*, volume 2, pages 1491–1496, 1998. 62

[125] I.-C. Baik, K.-H. Kim, and M.-J. Youn. Robust nonlinear speed control of PM synchronous motor using boundary layer integral sliding mode control technique. *IEEE Transactions on Control Systems Technology*, 8(1):47–54, 2000. 62

[126] J. Cabrera-Vázquez, A.G. Loukianov, J.M. Cañedo, and V.I. Utkin. Robust controller for synchronous generator with local load via VSC. *International Journal of Electrical Power and Energy Systems*, 29(4):348–359, 2007. 63

[127] M.A. Pai. *Energy function analysis for power system stability.* Kluwer Academic Pub, 1989. 63

[128] P.C. Krause, O. Wasynczuk, and S.D. Sudhoff. *Analysis of electric machinery and drive systems.* IEEE press, J. Willey and Sons Inc., 2002. 63

[129] L. Xu, B.R. Andersen, and P. Cartwright. Control of VSC transmission systems under unbalanced network conditions. In *IEEE PES Transmission and Distribution Conference and Exposition*, volume 2, pages 626–632, 2003. 65, 68

[130] H. Cherouat, H. Siguerdidjane, J.-L. Thomas, and S. Poullain. Sliding modes control of VSC-HVDC transmission systems. In *the* 10^{th} *European Conference on Power Electronics and Applications EPE'03, France*, 2003. 65, 68, 89

[131] H.S. Ramadan, H. Siguerdidjane, and M. Petit. Robust nonlinear control strategy for HVDC Light transmission systems technology. In *the* 34^{th} *Annual Conference of IEEE Industrial Electronics, IECON'08, USA*, pages 360–365, 2008. 65, 68, 89

[132] H.S. Ramadan, H. Siguerdidjane, and M. Petit. On the robustness of VSC-HVDC systems controllers under parameters uncertainties. In *IEEE* 40^{th} *North American Power Symposium, NAPS'08*, pages 1–8, 2008. 68, 89

[133] H.S. Ramadan, H. Siguerdidjane, M. Petit, and Kaczmarek R. Robust VSC-HVDC systems based on sliding mode control. In *the* 2^{nd} *Interenational conference, ICEEDT'08, Tunisia*, pages 1–8, 2008. 89

[134] H.S. Ramadan, H. Siguerdidjane, and M. Petit. A robust stabilizing nonlinear control design for VSC-HVDC systems: a comparative study. In *IEEE International Conference of Industrial Technology, ICIT'09, Australia*, pages 1–6, 2009. 89

[135] H.S. Ramadan, H. Siguerdidjane, M. Petit, and R. Kaczmarek. VSC-HVDC systems stabilization and robustness realization using sliding mode controllers. In *International Conference on Renewable Energy: Generation and Applications ICREGA'10, Al Ain, UAE*, pages 1–7, 2010. 94, 95

[136] M. Karimi-Ghartemani and M.R. Iravani. Wide-range, fast and robust estimation of power system frequency. *Electric Power Systems Research*, 65(2):109–117, 2003. 97

[137] M. Karimi-Ghartemani and A.K. Ziarani. Periodic orbit analysis of two dynamical systems for electrical engineering applications. *Journal of Engineering Mathematics*, 45(2):135–154, 2003. 97

[138] M.L. Crenshaw, K.E. Bollinger, R.T. Byerly, R.L. Cresap, L.E. Eilts, and D.E. Eyre. Excitation system models for power system stability studies. *IEEE Transactions on Power Apparatus and Systems*, 100(2):494–509, 1981. 116

[139] R.T. Byerly. Dynamic models for steam and hydro turbines in power system studies. *IEEE Transactions on Power Apparatus and Systems*, (6):1904–1915, 1973. 116

[140] S. Cole and R. Belmans. Transmission of bulk power: the history and applications of voltage-source converter high-voltage direct current systems. *IEEE Industrial Electronics Magazine*, 3(3):19–24, 2009. 116

[141] A. Srujana and J.S.V. Kumar. A novel hvdc control strategy to enhance interconnected power systems: A graphical-based solution. *American Journal of Scientific Research*, (11):35–46, 2010. 116

[142] Y. Guo, D.J. Hill, and Y. Wang. Nonlinear decentralized control of large-scale power systems. *Automatica-Kidlington*, 36(9):1275–1290, 2000. 116

[143] C. Zhu, M. Khammash, V. Vittal, and W. Qiu. Robust power system stabilizer design using h^{∞} loop shaping approach. *IEEE Transactions on Power Systems*, 18(2):810–818, 2003. 117

[144] G.E. Boukarim, S. Wang, J.H. Chow, G.N. Taranto, and N. Martins. A comparison of classical, robust, and decentralized control designs for multiple power system stabilizers. *IEEE Transactions on Power Systems*, 15(4):1287–1292, 2000. 117

[145] R.T.H. Alden and P.J. Nolan. Evaluating alternative models for power system dynamic stability studies. *IEEE Transactions on Power Apparatus and Systems*, 95(2):433–440, 1976. 117

[146] M.A. El-Sharkawi. Choice of model and topology for external equivalent systems. *IEEE Transactions on Power Apparatus and Systems*, (12):3761–3768, 1983. 117

[147] W.J. Wilson and J.D. Aplevich. Dynamic equivalent power system models. *IEEE Transactions on Power Apparatus and Systems*, (12):3753–3760, 1983. 117

[148] M. Dehghani and S.K.Y. Nikravesh. Nonlinear state space model identification of synchronous generators. *Electric Power Systems Research*, 78:926–940, 2000. 117

COMMANDE NON LINEAIRE ET STABILISATION DES SYSTEMES DE TRANSMISSION VSC-HVDC

RESUME : L'intégration des liaisons à courant continu dans les systèmes électriques permet d'accroitre les possibilités de pilotage des réseaux, ce qui permet d'en améliorer la sûreté et de raccorder de nouveaux moyens de production. Pour cela la technologie VSC-HVDC est de plus en plus plébiscitée pour interconnecter des réseaux non synchrones, raccorder des parcs éoliens offshore, ou contrôler le flux d'énergie notamment sur des longues distances au travers de liaisons sous-marines (liaison NorNed).
Les travaux de cette thèse portent sur la modélisation, la commande non-linéaire et la stabilisation des systèmes VSC–HVDC, avec deux axes de travail.
Le premier se focalise sur la conception et la synthèse des lois de commandes non-linéaires avancées basées sur des systèmes de structures variables (VSS). Ainsi, les commandes par modes glissants (SMC) et le suivi asymptotique de trajectoire des sorties (AOT) ont été proposées afin d'assurer un degré désiré de stabilité en utilisant des fonctions de Lyapunov convenables. Ensuite, la robustesse de ces commandes face à des perturbations et/ou incertitudes paramétriques a été étudiée. Le compromis nécessaire entre la robustesse et le comportement dynamique requis dépend du choix approprié des gains. Ces approches robustes, qui sont facile à mettre en œuvre, ont été appliquées avec succès afin d'atteindre des performances dynamiques élevées et un niveau raisonnable de stabilité vis-à-vis des diverses conditions anormales de fonctionnement, pour des longueurs différentes de liaison DC.
Le deuxième vise à étudier l'influence de la commande du convertisseur VSC-HVDC sur l'amélioration de la performance dynamique du réseau de courant alternatif en cas d'oscillations. Après une modélisation analytique d'un système de référence constitué d'un groupe connecté à un convertisseur VSC-HVDC via un transformateur et une ligne, un contrôleur conventionnel simple PI est appliqué au niveau du convertisseur du système pour agir sur les oscillations rotoriques de la machine synchrone. Cette commande classique garantie une amélioration acceptable des performances dynamiques du système; surtout pour l'amortissement des oscillations de l'angle de puissance de la machine synchrone lors de défauts.

Mots clés : VSC-HVDC, Commande non-linéaire, Commande par modes glissants, fonctions de Lyapunov, Incertitudes paramétriques, Robustesse, Amortissement des oscillations, Stabilisation.

NON-LINEAR CONTROL AND STABILIZATION OF VSC-HVDC TRANSMISSION SYSTEMS

ABSTRACT: The integration of nonlinear VSC-HVDC transmission systems in power grids becomes very important for environmental, technical, and economic reasons. These systems have enabled the interconnection of asynchronous networks, the connection of offshore wind farms, and the control of power flow especially for long distances.
This thesis aims the non-linear control and stabilization of VSC-HVDC systems, with two main themes.
The first theme focuses on the design and synthesis of nonlinear control laws based on Variable Structure Systems (VSS) for VSC-HVDC systems. Thus, the Sliding Mode Control (SMC) and the Asymptotic Output Tracking (AOT) have been proposed to provide an adequate degree of stability via suitable Lyapunov functions. Then, the robustness of these commands has been studied in presence of parameter uncertainties and/or disturbances. The compromise between controller's robustness and the system's dynamic behavior depends on the gain settings. These control approaches, which are robust and can be easily implemented, have been applied to enhance the system dynamic performance and stability level in presence of different abnormal conditions for different DC link lengths. The second theme concerns the influence of VSC-HVDC control on improving the AC network dynamic performance during transients. After modeling the Single Machine via VSC-HVDC system in which the detailed synchronous generator model is considered, the conventional PI controller is applied to the converter side to act on damping the synchronous machine power angle oscillations. This simple control guarantees the reinforcement of the system dynamic performance and the power angle oscillations damping of the synchronous machine in presence of faults.

Keywords: VSC-HVDC, Nonlinear control, Sliding mode control, Lyapunov functions, Parameter uncertainties, Robustness, Power oscillations damping, Stabilization.